Axonal mechanisms underlying presynaptic short-term plasticity of dopamine release in striatum

DPhil in Physiology, Anatomy and Genetics

Mark Condon

St Catherine's College, Oxford

Axonal mechanisms underlying presynaptic short-term plasticity of dopamine release in striatum

Mark Condon, St Catherine's College,

DPhil in Physiology, Anatomy and Genetics, Hilary Term 2018

Abstract

Dopamine (DA) signalling plays a central role in the functions of the basal ganglia, supporting behavioural processes such as action selection and reinforcement learning. Consequently, dysfunction of DA release is implicated in a wide range of neurological and psychiatric disorders, including Parkinson's disease and addiction.

DA is released from an extensively-branched axonal arbor in the striatum, but it remains unclear how the characteristics of these complex axons influence the short-term plasticity of DA release. This thesis uses fast-scan cyclic voltammetry and patch-clamp electrophysiology in slices of mouse striatum to study the axonal factors that shape the conversion of firing activity in midbrain DA neurons to DA release in the striatum.

Firstly, short-term plasticity of DA release was shown to be governed by a region-specific hierarchy of mechanisms related to Ca^{2+} dynamics at DA release sites, and to excitability of DA axons in striatum, which was maintained by the dopamine transporter (DAT). Second, tonic background activity in DA neurons was shown to enhance the contrast of DA signals evoked by bursts, in a region-specific manner, and was also regulated by the DAT. Third, release of γ-amino butyric acid (GABA) from DA axons was shown to be insensitive to regulation by the DAT, in contrast to the release of DA.

These data suggest that the characteristics of DA axons, particularly expression of the DAT, can powerfully regulate short-term plasticity of DA release in a region-specific manner. These findings extend our understanding of the regulation of DA signalling and may have implications for the manner in which presynaptic activity in DA neurons is read out as DA release across striatal regions.

Contents

Acknowledgments

First of all, I would like to acknowledge the continual support and encouragement provided by my supervisor, Professor Stephanie Cragg. Steph's tenacious commitment to rigourous science, thoughtful conclusions and correctly-aligned axis labels have helped me get the most out of my time in the lab.

I would also like to thank all members of the Cragg lab who I've worked with over the last three years – I couldn't have asked for a better group. I would particularly like to thank Dr Sarah Threlfell and Dr Katherine Brimblecombe for patiently answering endless stupid questions, teaching me the ways of the voltammetrist, and calling a spade a spade; Dr Richard Exley, for pointing out why my slices kept dying; Dr Yanfeng Zhang, for his crash course in patching; and everyone else who has shared their knowledge, their time, and has helped me cling to sanity. I should also acknowledge Dr Nicola Platt, despite the fact we've never met, for doing so much of the excellent work on which this thesis is based, and for writing it all down in such an eminently readable fashion.

I would like to thank the Medical Research Council for their generous funding, without which none of this would have been possible. The same can be said of the mice, whose contribution cannot be overlooked.

Last, but certainly not least, I would like to thank my parents, family and friends, who have put up with a considerable quantity of science-induced grouchiness. I particularly want to thank Kerry Mellor for her constant love and support, and for doing pretty much all of the cooking in the latter half of 2017.

Abbreviations

1p $[DA]_o$	Dopamine release evoked by a single pulse
5-HT	5-hydroxytryptamine
β2* nAChR	β2-subunit-containing nicotinic acetylcholine receptor
AAV	Adeno-associated virus
ACh	Acetylcholine
aCSF	Artificial cerebro-spinal fluid
ALDH1a1	Aldehyde dehydrogenase type 1a1
AP	Action potential
AP/ML/DV	Anterior-posterior/medial-lateral/dorsal-ventral
AUC	Area under the curve
$[Ca^{2+}]_o$	Extracellular concentration of calcium ions
Calbindin-D28k	28 kilo-Dalton calbindin protein
CFM	Carbon fibre microelectrode
ChI	Cholinergic interneuron
ChR2	Channelrhodopsin-2
CPu	Caudate-putamen
d/iSPN	Direct/indirect-pathway spiny projection neuron
D1/D2-SPN	Dopamine type 1/2 receptor-expressing spiny projection neuron
D1-5R	Dopamine type (1-5) receptor
D2L/S	Long/short splice variant of dopamine type 2 receptor
D-AP5	D-(2R)-amino-5-phosphonopentanoate
DA	Dopamine
$[DA]_o$	Extracellular concentration of dopamine
DAT	Dopamine transporter
DHβE	Dihydro-β-erythroidine
EYFP	Enhanced yellow fluorescent protein
FCV	Fast-scan cyclic voltammetry
FSI	Fast-spiking interneuron
GABA	γ-amino butyric acid
$GABA_{A,slow}$	Slow current mediated by $GABA_A$ receptors
GAT1/4	GABA transporter type 1/4
GEVI	Genetically-encoded voltage indicator
GPe	External segment of the globus pallidus
GPi	Internal segment of the globus pallidus
iGluR	Ionotropic glutamate receptor
I_h	Hyperpolarisation-activated cation current
IPI	Inter-pulse interval
$[K^+]_o$	Extracellular concentration of potassium ions
K_v	Voltage-gated potassium channel
LED	Light-emitting diode
nAChR	Nicotinic acetylcholine receptor
Na_v	Voltage-gated sodium channel
NBQX	2,3-dihydroxy-6-nitro-7-sulfamoyl-benzo[f]quinoxaline-2,3-dione
mAChR	Muscarinic acetylcholine receptor

P2/P1 or PPR	Paired-pulse ratio
PBS	Phosphate-buffered saline
PBS-Tx	Phosphate-buffered saline with 0.5% Triton X-100
PD	Parkinson's disease
P_r	Release probability
PSCs	Post-synaptic currents
PV	Parvalbumin
RRP	Readily-releasable pool of vesicles
S3KO	Synapsin-III knock-out
SEM	Standard error of the mean
SNARE	Soluble N-ethylmaleimide-sensitive factor attachment protein receptor
SNc	Substantia nigra pars compacta
SNr	Substantia nigra pars reticulata
STD	Short-term depression
STF	Short-term facilitation
STN	Sub-thalamic nucleus
STP	Short-term plasticity
TAN	Tonically active neuron
TH	Tyrosine hydroxylase
VGCC	Voltage-gated calcium channel
vGluT2	Vesicular glutamate transporter type 2
VMAT	Vesicular monoamine transporter
VTA	Ventral tegmental area

Chapter 1.
Introduction

In classical studies of neuronal conduction and chemical neurotransmission, the neuronal axon has been described as a high-fidelity cable, faithfully transmitting digital information from the cell body, where dendritic inputs are integrated to generate action potentials, to the axonal boutons or release sites, where action potentials are converted to extracellular chemical signals by the synaptic release machinery. However, more recent work has provided evidence that the function of the axon is not limited to the generation and transmission of all-or-none action potentials. Indeed, axons have been shown to perform a range of computational processes, changing the shape, rate and timing of action potentials, as well as influencing the activity of surrounding projections through axo-axonic interactions (Bucher & Goaillard 2011). Furthermore, in addition to digital encoding of information as action potentials, some mammalian central axons can conduct analogue signals generated by subthreshold excitatory inputs (Alle & Geiger 2006). It is therefore important to investigate the varying structural and functional properties of axons in different neuronal populations to fully understand the processes by which information is encoded and manipulated during neurotransmission.

Dopaminergic neurons of the mammalian midbrain project an extensive axonal arbor to the striatum and other structures. Dopamine neurotransmission in the mesostriatal pathways plays important roles in action selection, behavioural reinforcement and motor function, and dysfunction of this pathway has been implicated in a diverse range of pathological states including Parkinson's disease, addiction, schizophrenia and others. The pattern and rate of action potential generation in the midbrain DA neurons is thought to encode behaviourally-relevant information about the motivational value and/or salience of environmental stimuli; however, it is currently unclear how this signal is altered during propagation through the extensive axonal arbor, and during conversion to dopamine release at striatal release sites. To fully understand DA signalling, it is necessary to describe the synaptic and axonal factors that shape DA release.

In this thesis, I explore specific properties of DA axons that will govern the conversion of presynaptic firing to DA release. These properties, including axonal excitability, intracellular Ca^{2+} dynamics at release sites, and the functions of the DA transporter, interact to shape DA release over a range of frequencies and patterns of presynaptic activity. I also extend this investigation to determine whether GABA release from DA release sites is subject to the same mechanisms of presynaptic regulation.

In this chapter, I will introduce background information that is relevant to the interpretation of this thesis as a whole. Section 1.1 will briefly review existing literature regarding the role of neuronal axons in neurotransmitter release and short-term plasticity (STP), Section 1.2 will discuss the organisation of striatal circuits influenced by DA, and Section 1.3 will describe the regulation and functions of striatal DA signalling.

1.1 The roles of neuronal axons in short-term plasticity

1.1.1 Overview

Synaptic plasticity is the process by which patterns of activity can influence the subsequent strength of neurotransmission at a synapse or neurotransmitter release site. This fundamental mechanism scales synaptic output, maintaining homeostasis of neuronal excitability (Turrigiano 2012); creates a record of prior synaptic activity, which has been suggested to underlie certain memory processes (Morris 2003); and modulates synaptic responses to patterns of presynaptic activity, enabling computational processing of information encoded by the presynaptic neuron (Abbott & Regehr 2004). A diverse range of synaptic mechanisms can modulate plasticity over different timescales, and as such different forms of plasticity are described based on their duration. For example, long-term potentiation at hippocampal CA3-CA1 synapses can be maintained for months (Abraham et al. 2002), while short-term plasticity, which will be the focus of this thesis, operates on the scale of milliseconds to minutes (Zucker & Regehr 2002).

Mechanisms of short-term plasticity can influence signalling either presynaptically, by modulation of neurotransmitter release, or postsynaptically, through changes in neurotransmitter signal detection and transduction. The direction of synaptic plasticity is also variable, with distinct mechanisms contributing to facilitation or depression of subsequent release. Many of the processes underlying presynaptic STP are dependent on the properties of axons and synapses, and therefore mediate powerful computational processing downstream of information encoding at the level of the dendrites, soma and axon initial segment (Abbott & Regehr 2004; Bucher & Goaillard 2011).

However, there are significant technical challenges associated with the study of computational processing in axons and neurotransmitter release sites. The study of short-term plasticity has largely been carried out at large synapses, such as the Calyx of Held in the auditory brainstem, which have sufficient accessible membrane area to permit direct recordings of presynaptic activity with patch-clamp techniques. In other central neurons, direct electrophysiological recordings at presynaptic boutons or axon shafts are rare, although recently-developed techniques have allowed such recordings to be made in certain preparations (Kawaguchi & Sakaba 2015; Hu & Jonas 2014; Sasaki et al. 2012). This section will be review the fundamental processes underlying neurotransmitter release, as well as mechanisms of short-term plasticity described at classically-studied central synapses.

1.1.2 Fundamental mechanisms of neurotransmitter release

Synapses mediate information transfer between neurons, converting presynaptic action potentials into a chemical neurotransmitter signal which can cross the synaptic cleft, bind to postsynaptic receptors and be transduced back to an electrical signal in the postsynaptic cell. The process of Ca^{2+}-dependent exocytosis underlying neurotransmitter release is thought to be conserved across populations of central and peripheral neurons. The fundamental principles were

described by Bernard Katz and colleagues in the mid-20th century, but the underlying physiology remains a topic of intense study.

Neurotransmitter release is a probabilistic process, which is thought to consist of three mechanistically distinct processes; spontaneous, synchronous, and asynchronous release. At rest, release probability (P_r) is low, so release is limited to small spontaneous release events that give rise to miniature postsynaptic potentials (del Castillo & Katz 1954). The arrival of an action potential causes a transient increase in P_r through a mechanism that is dependent on the synchronous opening of voltage-gated Ca^{2+} channels (VGCCs).

Opening of VGCCs at the presynaptic terminal leads to an increase in $[Ca^{2+}]_I$ that is not uniform throughout the intra-terminal space, but instead depends on proximity to open VGCCs. In the immediate vicinity of clusters of open VGCCs, known as Ca^{2+} nanodomains, $[Ca^{2+}]$ may be as high as ~100 µM, decreasing rapidly over 10-100 nm due to diffusion and binding to Ca^{2+} buffers (Naraghi & Neher 1997). In Ca^{2+} microdomains, which extend 100-1000 nm from open VGCCs and which include active zones at which exocytotic neurotransmitter release occurs, peak $[Ca^{2+}]_o$ during VGCC opening at the calyx of Held has been estimated to be in the range of 10-25 µM (Schneggenburger & Neher 2000).

The high local $[Ca^{2+}]$ caused by rapid, synchronous opening of VGCCs activates Ca^{2+}-sensor proteins that trigger the assembly of the exocytotic machinery. Ca^{2+} binding to fast sensors of the synaptotagmin family triggers interaction between soluble N-ethylmaleimide-sensitive factor attachment protein receptor (SNARE) proteins on the synaptic vesicle and on the plasma membrane, leading to fusion and neurotransmitter release (Sudhof 2012). Affinity of Ca^{2+} binding to synaptotagmins is generally low, explaining the requirement for large local increases in $[Ca^{2+}]$. However, the affinity and kinetics of Ca^{2+} binding differ between synaptotagmin isoforms, and expression of different isoforms may be a key mechanism underlying variation in basal P_r between distinct neuronal populations. For example, Syt9 binds Ca^{2+} with a much lower affinity

and triggers release on a slower timescale than Syt1, whereas Syt2 binds Ca^{2+} with a similar affinity to Syt1, but triggers release more rapidly (Xu et al. 2007). Dopamine neurons are thought to express Syt1, Syt4, and Syt7; axonal DA release is reportedly dependent on Syt1, while somatodendritic release is dependent on Syt4 and Syt7 (Mendez et al. 2011).

This rapid synchronous release event is terminated by VGCC closure during repolarisation (Bischofberger et al. 2002; Borst & Sakmann 1996). The Ca^{2+} transient is also amplified by release of Ca^{2+} from intracellular stores through Ca^{2+}-induced Ca^{2+} release (Emptage et al. 2001). Following synchronous release, P_r can remain elevated for up to tens of seconds through a distinct Ca^{2+}-dependent process (Bacaj et al. 2013), giving rise to asynchronous release events which can drive longer-lasting postsynaptic effects (Iremonger & Bains 2007).

In many neurons, neurotransmitter is stored in multiple distinct vesicular pools that are differentiated by their sensitivity to release by presynaptic stimulation. The general organisation that has been described at well-studied synapses consists of a readily-releasable pool (RRP), that is highly sensitive to stimulation, as well as recycling and reserve (or resting) pools that are recruited during prolonged stimulation (Rizzoli & Betz 2005). Vesicles of the readily-releasable pool are docked at release sites, while vesicles of the other pools are largely intermingled (Denker et al. 2009), and vesicles may also be docked but not primed for release (Rettig & Neher 2002). Pools are therefore not thought to be segregated by spatial proximity to the release site, but instead by binding to protein markers that maintain functional separation and regulate mobilisation of vesicles. These markers include synapsins, a family of proteins that bind reserve pool vesicles to actin structures and guide mobilisation of vesicles to the release site (Bykhovskaia 2011).

In DA neurons, vesicles may segregate into at least two pools, since DA axons in rat striatum continue to store dopamine after depletion of DA release in the presence of an inhibitor of synthesis (Ewing et al. 1983). Furthermore, a large proportion of mouse striatal vesicles labelled

with a VMAT-dependent false fluorescent neurotransmitter are not released in response to electrical stimulation up to 15 Hz, but a subset of these can be subsequently released following strong depolarisation (Pereira et al. 2016). Furthermore, segregation of vesicles to the reserve pool is thought to be dependent on synapsin III (Kile et al. 2010; Zaltieri et al. 2015). The role of synapsins in dopamine transporter-mediated regulation of STP will be discussed in Chapters 3 and 4.

1.1.3 Presynaptic short-term plasticity

Classical action potential-dependent neurotransmitter release therefore serves to convert integrated electrical signals encoded at the level of dendrites and soma into an extracellular chemical signal that can activate multiple post-synaptic targets. However, the role of synapses in signalling goes beyond reliable information transfer; the properties of synaptic terminals also permit processing of this information. As a result, neurotransmitter output at a given release site is not necessarily a faithful read-out of somatic action potential firing. Several mechanisms underlying presynaptic STP at central synapses, which may be relevant to the regulation of DA signalling, are described below.

1.1.3.1 Presynaptic short-term facilitation

Mechanisms driving STP influence neurotransmitter signalling over periods of milliseconds to minutes (Zucker & Regehr 2002). Short-term facilitation (STF) is the transient enhancement of neurotransmitter release, acting to increase the magnitude of release events less than 1 second after induction. STF can occur after a single stimulus, and typically modulates transmitter release within trains of high-frequency stimuli. Presynaptically, STF has been suggested to arise primarily due to intra-terminal Ca^{2+} summation (Katz & Miledi 1968; Wu & Saggau 1994). If a subsequent depolarisation occurs before the initial Ca^{2+} transient has fully decayed, a process that can occur over hundreds of milliseconds, residual Ca^{2+} is summated with further Ca^{2+} entry to form an enhanced Ca^{2+} transient (Chen & Regehr 1999). This summated Ca^{2+} transient triggers exocytosis

of a greater population of neurotransmitter-containing vesicles than would occur if a single stimulus is delivered in isolation, leading to short-term enhancement of signalling.

However, it has been suggested that this simple model of intra-terminal Ca^{2+} summation does not explain observed patterns of STF at all synapses. Residual $[Ca^{+}]_o$ following synchronous release is estimated to be <1 μM (Regehr et al. 1994), whereas local $[Ca^{2+}]_o$ required to trigger synchronous release is thought to be at least 10 μM (Schneggenburger & Neher 2000). A nonlinear summation of residual and microdomain $[Ca^{2+}]$ is therefore required to explain STF (Neher 1998).

Such a nonlinear summation may arise from the binding of Ca^{2+} to fast buffers within the presynaptic terminal (Felmy et al. 2003). Following terminal depolarisation and opening of VGCCs, fast Ca^{2+} buffers bind local intracellular Ca^{2+}, reducing the magnitude of the Ca^{2+} transient and the neurotransmitter release event (Hochner et al. 1991; Adler et al. 1991; Ohana & Sakmann 1998). When a subsequent depolarisation arrives at a short interval, buffer capacity is reduced due to incomplete unbinding from intracellular Ca^{2+} evoked by the first stimulus. The second Ca^{2+} transient will therefore saturate the buffer with more Ca^{2+} to spare, resulting in greater neurotransmitter release (Neher 1998; Rozov et al. 2001). This process, known as pseudofacilitation, can occur due to saturation of the endogenous fast calcium buffer calbindin (Blatow et al. 2003). The potential role of calbindin in STP of DA release will be discussed in Chapters 3 and 4 of this thesis.

An alternative mechanism by which residual Ca^{2+} might enhance subsequent release is by binding to and activating a presynaptic Ca^{2+} sensor that can increase P_r. The synaptotagmin 7 (Syt7) isoform has been suggested to perform this function at hippocampal and corticothalamic synapses, since Syt7 knock-out mice display reduced STF at these synapses without any change in initial P_r (Jackman et al. 2016). Such a mechanism could feasibly regulate STF of DA release, since Syt7 is thought to be expressed by DA neurons; however, a role for Syt7 in axonal control of DA release has not been described (Mendez et al. 2011).

1.1.3.2 Presynaptic short-term depression

The strength of synaptic signalling can also be reduced by mechanisms driving short-term depression (STD). Presynaptic mechanisms of STD are typically thought to involve changes in P_r (Zucker & Regehr 2002). At hippocampal excitatory synapses, intense stimulation has been shown to deplete the readily-releasable pool (RRP) of docked vesicles at the release sites, reducing P_r at subsequent stimulation (Dobrunz & Stevens 1997). However, STD has also been described under conditions that are not thought to lead to RRP depletion, such as during paired-pulse stimulation at low frequencies (Xu & Wu 2005). It is therefore probable that multiple synaptic mechanisms contribute to STD in different neuronal populations.

Activity-dependent changes in Ca^{2+} entry can also underlie STD. Ca^{2+}-dependent modulation of VGCC gating has been shown to underlie both facilitation and depression of Ca^{2+} entry and neurotransmitter release (Cuttle et al. 1998; Forsythe et al. 1998; Nanou et al. 2016). Ca^{2+} sensors such as calmodulin can alter the activity of a range of Ca^{2+} channel subtypes, suggesting that the effects of Ca^{2+}-dependent modulation of VGCCs on STP might depend on patterns of channel expression in different neuronal populations (Wykes et al. 2007; Mochida et al. 2008; Lee et al. 1999).

1.1.4 Non-synaptic plasticity

STP does not necessarily arise at the synapse. Mechanisms of STP have also been identified that operate at sites upstream of the synapse, altering the properties of AP propagation in the axon.

Modulation of terminal excitability represents a potential regulator of synaptic efficacy, since canonical mechanisms of neurotransmitter release rely on presynaptic depolarisation to trigger calcium influx and therefore exocytosis. Voltage-gated K^+ (K_v) channels commonly play key roles in tuning of axonal and terminal excitability, due to their diverse channel properties and differential expression and subcellular localisation across neuronal populations (Dodson & Forsythe 2004; Trimmer et al. 2015). Voltage-gated sodium (Na_v) channels are also important in

the regulation of terminal excitability, but due to the relatively small number of Na_v channel subtypes expressed in axons, their effects are less likely to underlie differential patterns of plasticity in distinct neuronal populations (Debanne 2004). As a result of their diversity, K^+ channels can influence neurotransmitter release through modulation of terminal excitability by various mechanisms. K^+ channels typically mediate outward currents, because the reversal potential for K^+ ions is more hyperpolarised than resting membrane potential (RMP). Consistent with this hyperpolarising effect, low-threshold K_v channels at axon terminals in the Calyx of Held have been shown to suppress terminal excitability following action potentials (Dodson et al. 2003; Ishikawa et al. 2003).

Action potential waveforms can also be altered by K^+ channels, such as those mediating fast-inactivating A-type currents, which can support enhancement of neurotransmitter release. Action potential broadening due to use-dependent inactivation of K^+ currents has been shown to increase the total Ca^{2+} entry per action potential and therefore drive facilitation of neurotransmitter release (Geiger & Jonas 2000; Jackson et al. 1991; Shu et al. 2007). Of relevance to the interpretation of findings described in this thesis, the rate of use-dependent inactivation of certain K^+ channels, including some K_v1 channels, can be increased by a reduction in $[K^+]_o$ (Baukrowitz & Yellen 1995). This decrease in total conductance of K^+ would be expected to have a depolarising effect on neuronal membrane potential. Conversely, expression of high-threshold K_v3 channels can ensure reliable fast repolarisation of APs, limiting use-dependent changes in AP waveform (Alle et al. 2011; Rowan et al. 2014; Rudy & McBain 2001). The effects of K^+ currents on terminal excitability therefore depend on the complement of K^+ channels expressed on the axon.

Conduction failures at axonal branch points may also contribute to short-term depression. While action potentials are typically conducted reliably through continuous axons, changes in axon geometry such as branch points and boutons cause a change in impedance which can prevent progression of action potentials where the elevated threshold for conduction is not met

(Swadlow et al. 1980). Neurons which are well-adapted for reliable conduction, such as motor neurons, are myelinated and have low numbers of branch points and therefore infrequent failures; however, many central neurons are unmyelinated and extensively branched, and therefore have higher rates of conduction failure (Ohura & Kamiya 2016; Ofer et al. 2017). Furthermore, use-dependent changes in the rate of conduction failure can alter the pattern of APs reaching presynaptic terminals, influencing the conversion of presynaptic firing to neurotransmitter release. This mechanism has been shown to drive release-independent STD at autaptic contacts on cultured hippocampal neurons (Brody & Yue 2000) and at the neuromuscular junction in crayfish (Hatt & Smith 1976). Conduction failure can therefore represent an additional form of non-synaptic plasticity. Mechanisms underlying use-dependent conduction failure that may operate at DA axons will be discussed in Chapter 3.

These fundamental principles governing neurotransmitter release and STP have been well-defined at specific synapses. However, the regulation of STP varies between neuronal populations, and it remains unclear which particular set of mechanisms operate at DA release sites and therefore define the relationship between presynaptic activity and DA release. This thesis will explore the role of axonal mechanisms in STP of DA release. The following sections in this chapter will describe the organisation of neuronal circuits within the striatum, and the anatomy and physiology of DA projections, to introduce aspects of DA neuron physiology relevant to axonal regulation of STP and outline the importance of local regulation of DA signalling in striatal processing.

1.2 Circuit organisation of the striatum

1.2.1 Overview

The striatum is the main input nucleus of the basal ganglia, a group of sub-cortical nuclei implicated in a diverse range of physiological functions and behaviours, including action selection, associative learning and motor control. Furthermore, disruption of basal ganglia signalling

contributes to the aetiology of many neurological and psychiatric disorders, such as Parkinson's disease, Huntington's disease and addiction (Obeso et al. 2014). As such, understanding of the cellular basis of basal ganglia function is necessary for the design of treatments for these disorders, which represent a considerable societal burden.

The striatum receives excitatory and inhibitory inputs from a large network of functional brain areas, including the thalamus, various cortical regions, and from dopaminergic and GABAergic projections from the ventral midbrain (Wichmann & Delong 2007). These inputs are integrated to activate signalling pathways that project through the basal ganglia nuclei (**Fig. 1.1**) and subsequently form outputs to effector regions such as the hypothalamus, thalamus and superior colliculus, as well as feedback to the cortex and midbrain. The topographic arrangement of projections between each anatomical structure forms a set of parallel loops that each support specific behavioural and cognitive functions (Alexander & Crutcher 1990; Redgrave et al. 2011), although a degree of integration between loops is thought to occur at the level of the striatum (Averbeck et al. 2014) as well as at other points in the signalling pathway (Joel & Weiner 1994).

The striatum therefore mediates both parallel and integrated processing, driven by a complex circuit structure comprising a number of different cellular populations. While the vast majority of striatal neurons are GABAergic spiny projection neurons (SPNs), processing in these cells is locally modulated by a broad array of interneurons with diverse physiological characteristics. Processing is also influenced by neuromodulatory dopaminergic input, which will be discussed further in section 1.3. A significant body of work has described the interplay between striatal interneurons, dopamine and SPNs, which will be briefly reviewed in this section. This will illustrate the potential of short-term plasticity of dopamine release to influence striatal output and therefore behaviour.

1.2.2 Functional regions of the striatum

The striatum is a large and complex structure, with roles in a number of processes and behaviours. Because of the topographic organisation of inputs and outputs (DeLong & Wichmann

2010), the non-uniform distribution of certain neuronal populations (Matamales et al. 2016), and regional differences in the regulation of DA release (Cragg 2003; Threlfell & Cragg 2011) it is important to address functional differences between major striatal regions in order to understand the region-specific roles of striatal processing in learning and behaviour. Throughout this thesis, a distinction is drawn between the dorsal region of the striatum, containing the caudate nucleus and putamen, and the ventral region, containing the nucleus accumbens. The relative positioning of these structures varies considerably between primates and rodents, although the cellular structure and function appears to be largely conserved.

In primates, including humans, the caudate nucleus and putamen of the striatum are structurally and functionally distinct (Gerfen & Bolam 2016). The caudate nucleus is found lateral of the anterior horn of the lateral ventricle, while the putamen sits more caudally, medial to the external capsule and lateral to the globus pallidus. The nuclei are physically separated by the white matter of the internal capsule, although this is not a rigid barrier since there is some overlap in inputs to the two structures. The caudate nucleus is primarily targeted by afferent fibres of the prefrontal cortex, while the putamen receives its main inputs from motor and somatosensory cortex. The nucleus accumbens (NAc) is adjacent to the two regions, but evidently delineated by the ventromedial end of the internal capsule.

In rodents, the striatum is a continuous structure positioned ventrally to the external capsule and lateral to the dorsal horns of the lateral ventricle. The caudate nucleus and putamen are not segregated, and are considered as a single contiguous nucleus known as the caudate-putamen (CPu), although the regional variation in corticostriatal inputs is comparable to that seen in primates. The anatomical boundaries between the CPu and NAc are also less evident, although again the topographic pattern of afferent fibres is similar.

In Chapters 3 and 4 of this thesis, presynaptic regulation of DA release is explored in CPu and NAc, to determine how axonal mechanisms differentially shape DA signalling in these two regions.

1.2.3 Spiny projection neurons

Approximately 95% of the neurons in the striatum are GABAergic spiny projection neurons (SPNs), also known as medium-sized spiny neurons (MSNs), which integrate afferent inputs with local synaptic and neuromodulatory signalling and project to downstream basal ganglia nuclei. SPNs are typically divided into two populations based on their projection targets, which are discussed further below.

SPNs switch between periods of low and high excitability known as up- and down-states (Wilson & Groves 1981; Wilson & Kawaguchi 1996). The resting down-state, characterised by a hyperpolarised membrane resting membrane potential, occurs due to abundant expression of inwardly-rectifying K^+ channels (Nisenbaum & Wilson 1995). These currents inactivate with depolarisation, such that switching between these states is dependent on concurrent activity in excitatory synaptic inputs (Wilson & Kawaguchi 1996), which activate a regenerative Ca^{2+}-dependent process in the distal dendrites of SPNs that maintains the up-state following this concurrent input (Plotkin et al. 2011). Due to rapid desensitisation of glutamate receptors at any given synaptic contact, concurrent inputs from distinct afferent projections produces the greatest excitatory effect on SPN activity, and as such SPNs are well-adapted to integrate excitatory input from multiple sources (Carter et al. 2007).

1.2.3.1 Inputs to SPNs

Excitatory inputs to SPNs arise principally in the cortex and thalamus (Nauta et al. 1974; Somogyi et al. 1981; Guo et al. 2015). Both populations form asymmetric glutamatergic synapses onto SPNs from both pathways (Doig et al. 2010), but differ in terms of their subcellular targets (Dubé et al. 1988; Smith et al. 1994). Projections from other basal ganglia nuclei, including GPe (Bevan et al. 1998; Saunders et al. 2016; Guo et al. 2015), and elsewhere in the brain, such as the hippocampus, amygdaloid complex and the dorsal raphe nuclei (Wall et al. 2013; Voorn et al. 2004; Guo et al. 2015), also form inputs to SPNs.

Corticostriatal projections form synapses principally onto dendritic spines on SPNs, with fewer synapses onto dendritic shafts and soma (Dubé et al. 1988; Xu et al. 1989). Corticostriatal neurons form sparse connections with a large number of SPNs, meaning that these inputs are selective; in other words, activation of a given SPN depends on synchronised activity in a specific set of corticostriatal projections (Zheng & Wilson 2002; Yim et al. 2011). Thalamostriatal projections arise from several distinct thalamic nuclei, and these populations differ in their regional and subcellular targets. The main projections arise from the intralaminar nuclei of the thalamus; specifically, from the centromedian/parafascicular complex (Cm-Pf), and from the central lateral and paracentral nuclei (Berendse & Groenewegen 1990; Castle et al. 2005). The Cm-Pf projection primarily forms synapses onto the dendritic shafts of SPNs, but also onto distal dendrites of cholinergic interneurons (Smith et al. 2004; Ding et al. 2010).

There is a complex pattern of inter-connectivity between striatal SPNs. In addition to their major projections to extra-striatal targets, SPNs also form axon collaterals within the striatum (Somogyi et al. 1981) which branch locally to form an arbor of similar size to the dendritic field. These collaterals mediate a network of inter-inhibition, such that stimulation of a given SPN evokes IPCSs in surrounding SPNs (Tunstall et al. 2002; Guzmán et al. 2003).

SPNs also receive inputs from local interneurons, midbrain DA neurons and surrounding SPNs. Dopaminergic modulation of SPN activity will be discussed in section 1.3, while modulation by local interneurons will be discussed later in this section.

1.2.3.2 Outputs from SPNs

SPNs are thought to integrate synaptic signals from this wide range of inputs to modulate excitatory drive from the cortex and thalamus. This information is then relayed to downstream nuclei within the basal ganglia, which in turn influence cortical processing and behaviour.

According to the classical view of basal ganglia connectivity, SPNs can be classified into one of two projection pathways (Albin et al. 1989). Direct pathway SPNs (dSPNs) send monosynaptic

projections to the output nuclei of the basal ganglia, namely the internal segment of the globus pallidus (GPi) and substantia nigra pars reticulata (SNr). Indirect pathway SPNs (iSPNs) project to the external segment of the globus pallidus (GPe), synapsing with neurons that project to the GPi and SNr. These two populations can also be distinguished by expression of specific DA receptor subtypes and other chemical markers. dSPNs express substance P and D1-type DA receptors, while iSPNs express enkephalin and D2-type DA receptors (Gerfen et al. 1990; Surmeier et al. 1996; Albin et al. 1989). It has been suggested that a subset of SPNs co-express D1 and D2 receptors (Surmeier et al. 1992; Aperia et al. 2000), although it is unclear how far this functional data is influenced by the distribution of dopamine receptors throughout striatal circuits.

SPNs and pallidal projection neurons are GABAergic, forming inhibitory connections in postnatal animals. Output from dSPNs therefore inhibit neurons in the GPi and SNr, which form the output projections of the basal ganglia (Cebrian et al. 2005), and consequently disinhibit activity in the target regions of those outputs. In contrast, GABA release from iSPNs inhibits neurons of the GPe, disinhibiting neurons of the GPi, and consequently inhibiting activity in target regions. Based on this contrasting pattern of connectivity, activity in dSPNs is broadly thought to favour downstream processing in the cortex and other target regions, while activity in iSPNs inhibits such processing (DeLong 1990).

According to this model of SPN connectivity, the two output systems of the striatum perform opposing roles within the general basal ganglia functions of action selection and other cognitive and motor functions. The model suggests that parallel processing within the striatum permits the evaluation and integration of multiple potential actions, and that inter-inhibition between SPNs and other circuit elements allows the selection of favourable options along with the suppression of non-selected possibilities (Alexander & Crutcher 1990; Nelson & Kreitzer 2014). The roles of the direct and indirect pathways are therefore to promote particular actions by disinhibition of the relevant basal ganglia targets, and to inhibit possible or ongoing actions by parallel inhibition

of alternative targets, respectively. In support of this, it has been shown that selective activation of dSPNs promotes continuous movement, while activation of iSPNs causes freezing in rodents (Kravitz et al. 2010), although it is not clear how well such stimulation represents physiological activity in striatal neurons. Furthermore, selective ablation of dSPNs or iSPNs leads to hypolocomotion and hyperlocomotion, respectively, and impaired performance on a motor learning task in both cases (Durieux et al. 2012).

It is generally accepted on the basis of such evidence that SPNs can be divided into at least two sub-populations that contribute differentially to basal ganglia processing. However, additional evidence suggests that the model described above does not fully explain the complexity of striatal processing. Recent evidence shows that dSPNs and iSPNs may be concurrently activated during behaviour, suggesting that the relationship between the two pathways may not be as antagonistic as previously thought (Cui et al. 2013). Furthermore, the model of opposing pathways does not account for the complex regulation of SPN activity by striatal interneurons, or for the roles of other basal ganglia elements such as the 'hyperdirect' pathway, that connects cortical regions to the GPi/SNr via the subthalamic nucleus (Nambu et al. 2002). As such, the roles of the two major SPN output pathways in basal ganglia function are still under investigation.

SPNs also project to the dopaminergic midbrain nuclei (Kalivas et al. 1993), with separate populations thought to target DAergic and GABAergic neurons (Xia et al. 2011; Watabe-Uchida et al. 2012). These projections do not appear to retain the topographical organisation of the mesostriatal projections, with populations of neurons from across striatum projecting to the different midbrain nuclei (Gerfen 1985). This projection may represent a mechanism of feedback control over DA signalling (Rahman & McBride 2001), although this suggestion is based on correlative evidence and has yet to be confirmed.

1.2.4 Cholinergic interneurons

The remainder of the cellular structure of the striatum, approximately 3-5% of the total neuron count, is made up of small populations of interneurons (Tepper & Bolam 2004). The first of these to be described were the cholinergic interneurons (ChIs), identified by their large soma and lack of dendritic spines (Kawaguchi 1993). ChIs are distributed throughout the striatum, with decreasing density along the anterior-posterior axis (Matamales et al. 2016).

In the absence of synaptic input, ChIs generate APs due to an intrinsic pacemaker mechanism, and as such are tonically active in slice preparations (Bennett & Wilson 1999). This firing leads to release of the neurotransmitter acetylcholine (ACh), which activates two classes of receptors to exert its postsynaptic effects. Nicotinic ACh receptors (nAChRs) are fast ligand-gated cation channels, while muscarinic ACh receptors (mAChRs) are modulatory G-protein coupled receptors. It has been suggested that ACh may operate at least partially through non-synaptic volume transmission (Descarries et al. 1997) based primarily on the low frequency of synaptic specialisations and broad distribution of ACh release sites (Contant et al. 1996), although the relative contributions of synaptic and extra-synaptic signalling to ACh transmission remain unclear.

ChIs form direct inputs on SPNs, with symmetric synapses distributed between the soma, dendrites and spines (Izzo & Bolam 1988). Cholinergic input supports long-term depression at corticostriatal synapses (Pakhotin & Bracci 2007) through activation of M_4 muscarinic receptors (Pancani et al. 2014). Cholinergic signalling also drives direct inhibition of SPNs by striatal neurogliaform neurons (English et al. 2011). Cholinergic signalling also exerts powerful control over DA release, which will be discussed in section 1.3.

Due to these wide-ranging effects on striatal processing, the role of striatal ChIs in basal ganglia function is subject of intensive study. ChIs are thought to correspond to the tonically active interneurons (TANs) identified by their physiological properties during *in vivo* single-unit

recordings in primates (Inokawa et al. 2010). In response to certain environmental stimuli, these neurons exhibit a multi-component firing pattern; this consists of an initial increase in firing rate, followed by a pause of variable duration, and subsequently a rebound excitation in some cases. Several different cellular mechanisms have been proposed to underlie this response (Schulz & Reynolds 2013), and it can occur in naïve TANs or be acquired after behavioural conditioning (Apicella 2002). The behavioural role of this response remains unclear, but it is temporally coincident with phasic activity in DA neurons (Morris et al. 2004), and may relieve nAChR-dependent gating of DA release (see section 1.3.3.3) during signalling of reward-related events.

1.2.5 GABAergic interneurons

The small population of inhibitory interneurons in the striatum is highly diverse, comprising several biochemically and physiologically distinct sub-populations. At present, relatively little is known about the consequences of this functional diversity for striatal processing and dopamine release.

The most extensively-characterised population of striatal GABAergic interneurons are the fast-spiking interneurons (FSIs), which express the fast Ca^{2+} buffer parvalbumin (PV) and are consequently also known as PV+ interneurons (Kawaguchi 1993). These neurons receive input from corticostriatal projections (Ramanathan et al. 2002) and as such are thought to mediate rapid feed-forward inhibition of SPNs (Tepper & Koós 1999; Koos et al. 2004). FSIs also receive inhibitory input from PV-expressing projection neurons in the GPe (Saunders et al. 2016; Bevan et al. 1998) and from ChIs (Koós & Tepper 2002; Chang & Kita 1992). Gap junctions with surrounding FSIs allow fast electrical signalling to maintain a high level of synchrony throughout the population (Tepper & Koós 1999; Hjorth et al. 2009; Kita et al. 1990).

A number of other minor populations of GABAergic interneurons have been identified in the striatum, including those that express calretinin, two distinct forms of neuropeptide Y-expressing neurons (Ibáñez-Sandoval et al. 2011), and several types of 5-HT3a receptor-expressing neurons

(Muñoz-Manchado et al. 2014). However, the physiological properties and roles of these populations remain incompletely described, and it is largely unclear how they contribute to striatal function.

1.3 The mesostriatal dopaminergic system

1.3.1 Overview

Midbrain DA neurons form projections to various brain regions, including various cortical areas, striatum, amygdala, hippocampus, septum, lateral habenula and sub-thalamic nucleus, among others (Yetnikoff et al. 2014). DA receptors are expressed throughout the striatum, supporting the wide-ranging actions of DA on striatal function. This section will briefly review the projections and firing of midbrain DA neurons, the regulation of DA signalling in the striatum, and the roles of DA function in behaviour.

1.3.2 The midbrain dopamine nuclei

Populations of dopaminergic neurons are found in several anatomical regions, principally the substantia nigra pars compacta (SNc), ventral tegmental area (VTA) and retrorubal area, all of which send DAergic projections to the striatum (Björklund & Dunnett 2007). The SNc is further subdivided into a dorsal tier, in which DA neurons express the calcium buffer calbindin, and a ventral tier, which is calbindin-negative and more susceptible to degeneration in Parkinson's disease (Yamada et al. 1990). The dorsal tier is continuous with the VTA, in which DA neurons are also calbindin-positive (Lavoie & Parent 1991). Several other proteins are also used as biochemical markers for DA neurons in these anatomical regions. For example, in rats, more mRNA for the DAT is detected in DA neurons in SNc than in VTA (Blanchard et al. 1994).

While the principal cells of the midbrain nuclei are dopaminergic, these regions also contain smaller populations of GABAergic projection neurons (Nair-Roberts et al. 2008). These neurons make local connections within the midbrain (Ciccarelli et al. 2012), as well as projecting to target

structures including the striatum (Van Bockstaele & Pickel 1995). Much less is known about GABAergic projection neurons, although they have been shown to contribute to mesostriatal signalling of reward, specifically the encoding of aversive stimuli (Tan et al. 2012; van Zessen et al. 2012).

1.3.2.1 Anatomy of dopaminergic projections

Dopaminergic neurons of the ventral midbrain nuclei send axonal projections to several targets in the forebrain. These projections are typically described in terms of three major projection pathways: the mesostriatal pathway, projecting to the striatum; the mesolimbic pathway, projecting mainly to the NAc, amygdala, olfactory tubercle and septum; and the mesocortical pathway, projecting mainly to the cingulate, prefrontal and perirhinal cortical areas (Yetnikoff et al. 2014). These projections arise from distinct populations of DA neurons which are differentially distributed between midbrain nuclei, although there is significant overlap in the anatomical locations of these groups. While DA neurons of the SNc and VTA project mainly to CPu and NAc respectively (Ungerstedt 1971), a subset of the projections to CPu arise from neurons in the VTA (Aransay et al. 2015), and similarly some projections to NAc originate in SNc (Björklund & Dunnett 2007). This overlap is partially explained by the diverse projection targets of calbindin-positive projections from dorsal tier SNc, which include both dorsolateral CPu and NAc (Lavoie et al. 1989; Prensa & Parent 2001).

Each dopamine neuron has a single thin, unmyelinated axon that emanates from the shaft of a principle dendrite, rather than from the soma (Tepper et al. 1987). Dopaminergic axons are carried in the dorsal part of the medial forebrain bundle, a loose collection of white matter projecting from the midbrain through the lateral hypothalamus to the olfactory tubercle (Ungerstedt 1971; Nauta et al. 1978; Beckstead et al. 1979), although locally-projecting DA neurons with branched axons have been observed in VTA (Aransay et al. 2015). Within the striatum, DA axons branch extensively to form a dense axonal arbor that has been estimated to

contain up to 25,000 branch points, with a total membrane length up to 780 mm in the rat (Matsuda et al. 2009; Pissadaki & Bolam 2013). However, the size of the axonal arbor varies considerably according to the anatomical location and projection targets of individual DA neurons (Aransay et al. 2015; Pacelli et al. 2015), which may explain the smaller arborisations observed in other studies (Prensa & Parent 2001; Gauthier et al. 1999).

These studies clearly show that axonal arborisation of DA neurons within the striatum is large and highly complex. As described in section 1.1, neuronal axons can play key roles in STP of neurotransmitter release; however, it remains unclear how the complexity of DA axons influences DA release in striatum. Chapter 3 of this thesis will therefore explore the effects of changes in axonal excitability on STP.

1.3.2.2 Firing rates of midbrain DA neurons

At the level of the soma, DA neurons generate relatively broad action potentials at frequencies up to 10 Hz, with an average rate of approximately 4 Hz (Grace & Bunney 1984b; Clark & Chiodo 1988; Lacey et al. 1989). This tonic firing is dependent on an intrinsic ionic pacemaking mechanism, in which Na^+ and Ca^{2+} channels gradually drive membrane to a spiking threshold.

However, the relative roles of these channels differ between sub-populations of DA neurons. In SNc DA neurons, the slow oscillatory potential underlying pacemaking is primarily driven by Ca^{2+} currents (Puopolo et al. 2007; Chan et al. 2007), while in VTA neurons Ca^{2+} channels play a much smaller role, and an additional voltage-insensitive Na^+ current supports slow depolarisation (Khaliq & Bean 2010). A-type K^+ currents (I_A) also regulate pacemaking; in SNc neurons, firing rate is inversely correlated to the amplitude of I_A (Liss et al. 2001), while in VTA neurons, I_A has been shown to limit slow depolarisation to maintain regular low-frequency firing (Khaliq & Bean 2008). The hyperpolarisation-activated cation current I_h has been shown to increase pacemaker firing frequency in a subset of DA neurons (Seutin et al. 2001) which may correspond specifically to calbindin-negative neurons of the SNc (Neuhoff et al. 2002). SK channels maintain regularity of

firing in SNc (Ping & Shepard 1996), and lower expression of these channels results in more irregular firing in VTA neurons (Wolfart et al. 2001).

The firing patterns of DA neurons *in vivo* are considerably more diverse than the regular pacemaker activity observed in *ex vivo* preparations. Regular pacemaker potentials are still observed, which drive slow depolarisation to threshold and hence slow, regular firing at average frequencies up to approximately 8 Hz (Grace & Bunney 1984b). However, basal firing *in vivo* is much less regular, and is interspersed with high-frequency bursts of approximately 2-5 spikes. The limits to the range of firing frequencies that occur during DA neuron bursts remain subject to debate; classically, burst frequencies are described as not typically exceeding 25 Hz (Grace & Bunney 1984a; Freeman et al. 1985; Kiyatkin & Rebec 1998), but more recent reports suggest that while the distribution of instantaneous frequencies peaks at 10-25 Hz, pairs of spikes at instantaneous frequencies up to 100 Hz and above do occur (Hyland et al. 2002).

Burst firing is not thought to occur spontaneously in slice preparations (Grace & Onn 1989), but can be evoked by activation of NMDARs (Johnson et al. 1992) or inhibition of SK channels (Ping & Shepard 1996), and is dependent on intracellular Ca^{2+} (Grace & Bunney 1984a; Mercuri et al. 1994). Accordingly, burst firing *in vivo* is thought to be driven by excitatory synaptic inputs from areas that include the pedunculopontine nucleus (Lokwan et al. 1999; Floresco et al. 2003) and subthalamic nucleus (Smith & Grace 1992; Chergui, Akaoka, et al. 1994). However, bursting activity is not homogenous between all DA neurons; the proportion of all spikes recorded in a given neuron that occur within bursts can range from none to approximately 80% (Mameli-Engvall et al. 2006). Furthermore, burst firing may actively limit synchronisation of firing between DA neurons *in vivo*, by driving somatodendritic DA release and local activation of D2 receptors expressed on surrounding DA neurons which couple to hyperpolarising K^+ currents and will mediate lateral inhibition of DA neuron firing (Beckstead et al. 2004). This mechanism might limit undesirable oscillations in DA release in target structures.

The broad range of reported frequencies of both basal and burst firing *in vivo* may be due in part to differences in experimental approaches. The choice of animal model is likely to influence the average frequency of DA neuron firing as well as the properties of bursting activity; however, studies examining species differences under comparable recording conditions are rare. Where average firing rates in mice and rats have been compared, results have been mixed, with differences reported in both directions, although the amount of bursting as indicated by the proportion of spikes occurring in bursts may be lower in mice (Marinelli & McCutcheon 2014; Panin et al. 2012).

Recordings are also made under a range of different conditions. Animals might be awake or anaesthetised, using any of a variety of different anaesthetic agents at different depths of anaesthesia. These factors are likely to alter the activity of afferent inputs to DA neurons, and consequently influence DA neuron firing, in ways that are difficult to predict. For example, chloral hydrate anaesthesia may dose-dependently reduce the amount of bursting, which may be due to changes in excitatory input to DA neurons (Fà et al. 2003), although average firing rate remains similar to recordings in awake, freely-moving animals (Hyland et al. 2002). Compared to chloral hydrate anaesthesia, urethane anaesthesia may further decrease bursting activity, as well as average firing rate (Pistis et al. 2004), whereas both of these measures may be slightly increased under isoflurane anaesthesia (Panin et al. 2012).

DA neurons *in vivo* can therefore show a wide range of firing rates and patterns, which are determined by complex interactions of afferent inputs. In Chapter 4 of this thesis, DA release has been evoked using patterns of stimulation designed to mimic a generalised pattern of DA neuron firing, in order to determine how the intrinsic short-term regulation of DA release is influenced by ongoing activity in DA axons.

1.3.2.3 Functional diversity of midbrain DA neurons

Study of the conductances underlying firing patterns have revealed extensive functional heterogeneity of DA neurons. Sub-populations have been defined in both SNc and VTA with diverse physiological characteristics driven by differential expression of biochemical markers including ion channels, Ca^{2+} buffers and D2 autoreceptors (Neuhoff et al. 2002; Schiemann et al. 2012; Seutin et al. 2001; Wolfart et al. 2001; Margolis et al. 2008; Lammel et al. 2008; Lerner et al. 2015), challenging the classical model of two distinct populations of midbrain DA neurons delineated by the classical anatomical boundaries.

Diversity in some aspects of DA neuron physiology can be predicted on the basis of projection targets, and as such is highly likely to influence regional differences in DA release in the intact projection pathway. Segregation of VTA DA neurons by projection targets reveals a dorsolateral population projecting to the lateral NAc shell, and a medial population projecting to NAc core and medial shell, as well the prefrontal cortex and amygdala (Lammel et al. 2008). DA neurons projecting to the NAc shell showed similar functional properties to neurons in the SNc, while those projecting to the NAc core were able to maintain a higher rate of evoked firing, displayed a shorter afterhyperpolarisation and had lower dopamine transporter expression (Lammel et al. 2008).

In contrast, projections from SNc to CPu are arranged topographically along the medial-lateral axis, with relatively homogeneous firing properties compared to the diversity observed in the VTA (Lerner et al. 2015). However, a gradient of I_h current amplitude across the midbrain has been observed, ranging from a lack of detectable I_h in medial VTA neurons (Lammel et al. 2011) to an increasing magnitude across the medial-lateral axis in the SNc (Lerner et al. 2015), which may influence pacemaker frequency in some neurons (Neuhoff et al. 2002).

1.3.3 Dopamine release in striatum

The firing frequency of DA neurons at the level of the midbrain is correlated to DA release in the striatum (Suaud-Chagny et al. 1992). Burst firing at an average frequency of 20 Hz in populations of dopamine neurons has been suggested to increase average $[DA]_o$ in striatum approximately 3-10 fold compared to tonic firing alone at an average frequency of 4 Hz, depending on the duration of the burst (Dreyer et al. 2010). However, the exact relationship between somatic firing rates and striatal dopamine release is complex and regionally variable, due to a combination of heterogeneity in the properties of DA neurons and local regulatory mechanisms within the striatum.

1.3.3.1 Dopamine receptors

DA exerts postsynaptic effects by binding and activation of DA receptors. There are five known types of DA receptors, D_1-D_5, all of which are metabotropic G-protein-coupled receptors (GPCRs). These fall into two families; D1-type, comprising D1 and D5, and D2-type, comprising D2, D3 and D4 (Beaulieu & Gainetdinov 2011). The D2 receptor (D2R) is expressed as two functionally distinct splice variants, which are thought to play different roles in DA signalling; the D2S variant is expressed presynaptically and functions as an inhibitory autoreceptor, while the D2L variant mediates postsynaptic effects (Usiello et al. 2000). Splice variants of D3 and D4Rs have also been described (Beaulieu & Gainetdinov 2011), although their roles in striatal DA signalling are less well-defined.

DA neurons express D2 autoreceptors at the level of the soma and at axonal release sites. At the soma, activation of D2Rs leads to opening of G-protein linked inwardly-rectifying K^+ (GIRK) channels, which mediate a hyperpolarising outward current at RMP (Lacey et al. 1988; Beckstead et al. 2004), while at axonal release sites it has been suggested that D2Rs may couple to voltage-gated K^+ channels (Cass & Zahniser 1991; Congar et al. 2002; Martel et al. 2011).

As described in section 2, postsynaptic DA receptors are generally differentially expressed on SPNs, with D1Rs expressed by dSPNs and D2Rs expressed by iSPNs. Key examples of effects of DA on striatal processing, mediated by postsynaptic DA receptors, are described in section 1.3.4.

1.3.3.2 Dopamine uptake

DA signalling events in striatum are terminated by a combination of diffusion and reuptake. Models based on voltammetric data suggest that spillover from the synaptic cleft is regulated primarily by the rate of diffusion away from release sites, while the spatial range at which DA can act, and the time course of extrasynaptic signalling, is limited by uptake at extrasynaptic transporters (Garris et al. 1994; Cragg & Rice 2004). This model is supported by the low transport rates (Povlock & Schenk 2002) and primarily extrasynaptic localisation of the DAT (Hersch et al. 1997). This is in contrast to uptake transporters at fast point-to-point synapses, which limit spillover to low levels through fast rates of uptake and close spatial coupling to release sites (Danbolt 2001).

In addition to DA reuptake, the DAT is thought to play a number of additional roles in DA neuron physiology, which will be discussed in relation to presynaptic STP in Chapter 3.

1.3.3.3 Cholinergic regulation of DA release

The release of acetylcholine from ChIs exerts powerful control of DA release at the level of the striatum. DA axons in the striatum express nAChRs containing the β2 subunit (Jones et al. 2001) which, when activated, promote powerful short-term depression of DA release such that release is almost entirely insensitive to the frequency or duration of presynaptic stimulation (Zhang & Sulzer 2004; Rice & Cragg 2004). When these receptors are inhibited, desensitised or genetically deleted, evoked DA release becomes closely correlated to stimulation frequency. The activation state of nAChRs *in vivo* remains unclear, as these receptors are readily desensitised by agonists; however, blockade of nicotinic receptors has been shown to enhance DA release in response to events predicted to trigger phasic activity in DA neurons, suggesting that nAChRs are tonically

activated rather than desensitised under physiological conditions (Collins et al. 2016). For this reason, it is necessary to occlude cholinergic input in order to study the intrinsic properties of DA release. In Chapters 3 and 4 of this thesis, all experiments have been performed in the presence of an antagonist at β2-subunit-containing nAChRs to remove cholinergic input at DA axons (see sections 3.2 and 4.2 for details).

Furthermore, synchronous genetically-targeted activation of ChIs with optogenetic techniques can evoke DA release events independently of presynaptic activity (Threlfell et al. 2012; Cachope et al. 2012). Under conditions where DA release is evoked simultaneously with ChI activation, for example during local electrical stimulation of striatal tissue, DA release is greater than when nAChRs are blocked (Zhou et al. 2001). While this finding was initially interpreted as control of DA release probability by nAChR activation state, these transients are now thought to be a composite of two release events; an initial event driven by activation of DA terminals, followed by a longer-latency event triggered by synchronous activation of local ChIs (Wang et al. 2014; Shin et al. 2015). It is therefore important to determine how action potential-dependent and ChI-driven DA release events are differentially regulated to understand how behaviourally-relevant DA signals are shaped *in vivo*.

DA release is also regulated by activation of mAChRs. DA neurons in SNc are thought to express M_5-type mAChRs (Vilaro et al. 1990; Weiner et al. 1990), which enhance DA release when activated at the level of striatum (Shin et al. 2015) through a mechanism that may involve changes in Ca^{2+} mobilisation (Foster et al. 2014). mAChRs also mediate feedback onto ChIs through region-specific expression; in dorsal striatum, M_2 and M_4 receptors inhibit ACh release, while in NAc this function is exclusively performed by M_4 receptors (Threlfell et al. 2010). Activation of mAChRs in striatum can therefore promote DA release, or reduce ACh release and therefore limit DA release while enhancing sensitivity to the frequency of presynaptic activity, depending on the pattern of activation (Threlfell & Cragg 2011).

In the work presented in this thesis, cholinergic signalling has been excluded (see Methods) to reveal the intrinsic axonal factors governing STP of DA release. However, the implications of these findings will be discussed in the context of intact cholinergic signalling in Chapter 6.

1.3.4 Modulation of striatal processing by DA

DA receptors are expressed throughout the striatum, and mediate numerous effects on striatal processing depending on the specific receptors subtypes expressed on different neurons, and their subcellular position. This section will briefly describe the roles of DA signalling in regulating excitability of SPNs, activity of local interneurons, and corticostriatal plasticity, to illustrate the potential for changes in the extracellular DA signal to influence basal ganglia function and ultimately behaviour.

1.3.4.1 Regulation of SPN excitability

As implied by the differential expression of DA receptors between the two major populations of SPNs, the effect of DA signalling on striatal processing is to modulate the balance between these parallel processing systems.

At the level of individual SPNs, D1 receptor activation promotes firing activity during up-states by activation of L-type Ca^{2+} channels (Hernández-López et al. 1997; Vergara et al. 2003), while D2 receptors reduce L-type currents and activate hyperpolarising K^{+} currents (Hernandez-Lopez et al. 2000; Perez et al. 2006). Additionally, activation of D1 receptors can prolong up-states in direct-pathway SPNs, while activation of D2 receptors shortens up-states in indirect-pathway SPNs (Plotkin et al. 2011). DA signalling therefore directly and differentially modulates excitability in the two main pathways.

Furthermore, DA can regulate the strength of excitatory synapses onto SPNs. Studies of the effects of DA on corticostriatal plasticity in slice preparations have had mixed results, showing patterns of long-term potentiation and depression that are highly dependent on cell type-specific localisation of DA and ACh receptors (Calabresi et al. 2007; Reynolds & Wickens 2002). However,

the importance of DA-mediated modulation of corticostriatal plasticity has been demonstrated by its roles in learning and motor function (Reynolds et al. 2001; Picconi et al. 2003). This regulation of synaptic plasticity is likely to influence the transitions of SPNs between up- and down-states, providing a further mechanism by which DA can modulate striatal output to downstream basal ganglia nuclei.

1.3.4.2 Regulation of local interneurons

DA release in striatum also regulates the activity of local interneurons. ChIs in both CPu and NAc express inhibitory D2 receptors (Alcantara et al. 2003) that reduce ACh release (Stoof et al. 1987), an effect that appears to be more pronounced in CPu than in NAc (Henselmans & Stoof 1991). Activation of D2 receptors activates a hyperpolarising current in ChIs (Straub et al. 2014), reduces pacemaker frequency by modulation of voltage-gated Na^+ channels (Maurice et al. 2004) and inhibits release by limiting Ca^{2+} entry (Yan et al. 1997). Conversely, activation of D1 receptors appears to increase striatal ACh release (Damsma et al. 1991; Consolo et al. 1999; Imperato et al. 1992), although the mechanism by which this occurs remains unclear, since only a small fraction of ChIs are thought to express D1 receptors (Le Moine et al. 1991). D5 receptors are also expressed on ChIs, and can enhance GABAergic inhibition of ChIs (Yan & Surmeier 1997; Rivera et al. 2002). D5 receptors are widely expressed on striatal GABAergic interneurons, including PV-positive, NPY/somatostatin/NOS-positive, and calretinin-positive neurons (Rivera et al. 2002). A fraction of NPY/somatostatin/NOS-positive neurons are also thought to express D1 receptors (Le Moine et al. 1991).

DA is therefore well-placed to mediate wide-ranging modulation of striatal processing, and determining the factors shaping DA release is of considerable importance in understanding the modulatory actions of dopamine within the striatum.

1.3.4.3 Regulation of corticostriatal plasticity

Long-term plasticity of corticostriatal synapses may play a central role in reinforcement of action selection in the striatum. Selective activation of specific subsets of SPNs from both pathways may bias basal ganglia processing toward selection of specific actions while suppressing alternatives (Cui et al. 2013; Freeze et al. 2013). Changes in the weighting of excitatory inputs to the striatum, through modulation of long-term plasticity at synapses onto SPNs, is therefore thought to support the selection and reinforcement-based learning of actions (Yin et al. 2009).

However, the mechanisms underlying expression of different forms of long-term plasticity at these synapses remain controversial. In both slice and *in vivo* preparations, different forms of plasticity have been induced depending on the preparation, stimulation protocol and manipulations of DA signalling (Reynolds & Wickens 2002; Kreitzer & Malenka 2008). A common factor is the importance of DA signalling (Wang et al. 2006; Kreitzer & Malenka 2007; Calabresi et al. 1997), leading to the suggestion that phasic DA release gates the induction of corticostriatal plasticity which is required for reward-related reinforcement of actions (Reynolds et al. 2001; Fisher et al. 2017). This gating is thought to depend on both the timing and magnitude of DA release in the striatum (Thivierge et al. 2007; Arbuthnott & Wickens 2007).

Determining the factors governing striatal DA release in response to presynaptic activity is therefore important in understanding the complex circuit-level physiology of the striatum, and the role of striatal processing in basal ganglia function.

1.3.5 Release of other primary neurotransmitters from DA axons

In addition to the synthesis and release of DA, some dopaminergic neurons have the capacity to release glutamate (Chuhma 2004; Stuber et al. 2010; Tecuapetla et al. 2010; Adrover et al. 2014) and/or GABA (Tritsch et al. 2012; Nelson et al. 2014; Kim et al. 2015) from axonal release sites. Release of two or more neurotransmitters or neuropeptides from the same neuron has been demonstrated in other neuronal populations (Seal & Edwards 2006; Vaaga et al. 2014), and

appears to contradict the classical view that all release sites on a given neuron release the same neurotransmitter, of which there can be only one (Strata & Harvey 1999). Two distinct phenomena have been described; co-release, which describes simultaneous releases of multiple transmitters from the same synaptic vesicles, and co-transmission, in which different transmitters are released from separate vesicular pools within the same neuron (Vaaga et al. 2014). In the latter case, vesicle pools may be localised to the same release site but differentially regulated, spatially segregated to different subcellular sites within the axon, or possibly a combination of both (Lee et al. 2010).

1.3.5.1 Glutamate co-transmission

Glutamate release from DA neurons has been shown to occur in the ventral striatum (Chuhma 2004; Stuber et al. 2010; Tecuapetla et al. 2010). Within striatum, glutamate co-transmission is thought to be restricted to dopamine neurons projecting to the NAc and olfactory tubercle (Stuber et al. 2010), with no glutamate co-transmission or glutamatergic markers observed in the dorsal striatum (Mingote et al. 2015), although one study has reported glutamatergic EPSCs in SPNs in response to selective stimulation of DA axons (Tritsch et al. 2012). A subset of midbrain DA neurons express a vesicular glutamate transporter (VGluT2), primarily in the VTA (Kawano et al. 2006; Mendez et al. 2008), which may explain the regional selectivity of glutamate co-transmission in striatum. Packaging of glutamate into DA vesicles can promote dopamine storage, through the effects of VGluT2 on the proton gradient that drives DA accumulation through VMAT (Hnasko et al. 2010). However, in adult animals, VGluT2 is localised to vesicle pools in DA axons but spatially segregated from DA release sites (Zhang et al. 2015). These VGluT2-positive axonal segments form asymmetric synapses onto SPN spines separate to the symmetric synapses formed by TH-positive DA release sites, suggesting that glutamate is co-transmitted, rather than co-released, from DA neurons (Descarries et al. 2008; Zhang et al. 2015).

The role of glutamate co-transmission in basal ganglia function remains unclear, although several studies have investigated effects of glutamatergic manipulations on mesostriatal circuits and behaviour. Mice with conditional deletions of VGluT2 in DA neurons have reduced DA release in NAc, as well as reduced hyperlocomotion in response to acute administration of cocaine, supporting a role for glutamate in the maintenance of DA signalling (Hnasko et al. 2010).

1.3.5.2 GABA co-release

GABA release from DA neurons has been more recently discovered, and is less well-described than glutamate co-transmission. Specific activation of DA neurons has been shown to evoke $GABA_A$ receptor-mediated IPSCs in SPNs, in both CPu (Tritsch et al. 2012) and in NAc (Tritsch et al. 2014), supported by ultrastructural data showing localisation of GABA to VMAT- and TH-positive boutons in the striatum (Stensrud et al. 2013). GABA is thought to be co-stored and released from DA vesicles, since GABAergic IPSCs were dependent on the vesicular monoamine transporter (Tritsch et al. 2012). Synthesis of GABA in canonical GABAergic neurons is typically mediated by glutamate decarboxylase, but expression of this enzyme has only been demonstrated in a very small minority of dopamine neurons (Tritsch et al. 2014). Instead, putative GABA co-release in DA neurons is thought to be maintained by a combination of uptake through the plasma membrane GABA transporter and synthesis through an alternative pathway, mediated by aldehyde dehydrogenase (ALDH1a1) (Tritsch et al. 2014; Kim et al. 2015).

Chapter 5 of this thesis will explore the presynaptic regulation of GABA release from DA axons in striatum, to determine whether the mechanisms underlying release and STP are similar for both transmitters.

1.3.6 Behavioural roles of DA neuron activity

Early studies of DA as a neurotransmitter identified its depletion in Parkinson's disease (PD), which involves prominent motor dysfunction (Ehringer & Hornykiewicz 1960). For this reason, the role of DA in behaviour has historically been studied with respect to the control of motor function

in the basal ganglia (Albin et al. 1989). However, other studies have shown key roles for DA in reward-related learning and other fundamental processes, suggesting a more general role for DA in cognitive function. This section will briefly review the roles of DA in motor function and reward-related processes, to underscore the importance of striatal DA signalling in behaviour.

1.3.6.1 Motor function

Post-mortem analysis of midbrain tissue from PD patients reveals a significant, selective loss of DAergic neurons in the ventral tier of the SNc thought to underlie the motor symptoms of the disease (Brichta & Greengard 2014). This suggests a dependence of normal motor function on DA signalling, but the exact role of DA in motor control remains unclear.

Early studies of DA neuron firing identified increases in firing on initiation of movement (Schultz et al. 1983; Romo & Schultz 1990), although this effect was inconsistent and was not replicated in other experiments (DeLong et al. 1983). However, recent studies have renewed the possibility of a specific role for DA signalling in motor control. A subset of DA neurons signal postural adjustments with a pause in firing (Dodson et al. 2016), and activity in DA axons in the striatum can signal the onset of movement (Howe & Dombeck 2016). These studies appear to support a role for DA in the initiation and rapid ongoing modulation of behaviour that is not necessarily related to reward value (Costa 2011; Jin & Costa 2010).

1.3.6.2 Reward signalling

Single-unit recordings of DA neuron activity from awake behaving animals show phasic increases in average firing rate on presentation of an unexpected reward (Romo & Schultz 1990). The increase is associated with an increase in bursting activity, both in the proportion of all spikes occurring in bursts and in the average intra-burst frequency (Hyland et al. 2002). After training, where the reward is paired with a predictive cue such as an auditory tone or visual stimulus, the timing of this phasic increase in firing is shifted such that it occurs not on presentation of the reward itself, but instead on presentation of the cue (Schultz & Romo 1990; Mirenowicz & Schultz

1994). Furthermore, the phasic increase in firing is associated with an increase in extracellular [DA] in the striatum, which also shifts from the presentation of reward to presentation of the predictive cue following training (Phillips et al. 2003; Roitman et al. 2004; Day et al. 2007). The mechanism underlying this shift may involve changes in the synaptic strength of specific excitatory inputs on DA neurons (Stuber et al. 2008).

It has been suggested that the reward-evoked increase in firing is not a single event, but instead consists of two temporally separate components; first, a rapid component which is insensitive to reward value, and secondly a slower, longer-duration component which encodes the subjective value and probability of reward (Fiorillo et al. 2013; Schultz 2016). The first component is not selective for reward-related stimuli, but is instead activated by any salient stimulus of sufficient strength, impact or novelty (Chiodo et al. 1980; Horvitz et al. 1997). This component is invariant to motivational value because it precedes full identification of the stimulus, suggesting that this initial excitation encodes a temporal signal of stimulus detection (Redgrave et al. 2008).

The second component of the DA neuron response co-varies with the subjective value of rewards (Tobler et al. 2005), and is thought to encode the difference between expected and actual outcomes, known as reward prediction error (RPE). RPE permits updating of the subjective calculations of value made by an organism in order to inform cognitive processes such as action selection and associative learning (Schultz et al. 1997). An unexpected reward elicits a positive RPE, which serves to bias the selection of future actions to maximise the chance of further reward (Stopper et al. 2014). Over repeated pairings of a predictive cue and reward, the RPE encoded by DA neuron firing acts as a teaching signal to drive associative learning such that the cue alone can elicit reward-seeking behaviour (Montague et al. 1996; Steinberg et al. 2013). The role of DA neurons in learning is, in this model, to integrate RPE from various inputs, and to feed this value into plasticity mechanisms in their target structures to influence the selection of future behavioural options.

1.3.6.3 Encoding of aversive stimuli

The question of how dopamine neurons signal a negative RPE in response to aversive stimuli remains contentious. Several studies have shown that such stimuli can evoke a rate reduction or pause in DA neuron firing (Ungless et al. 2004; Fiorillo 2013), while others described phasic increases in DA neuron firing, similar to reward responses, in response to aversive stimuli (Joshua et al. 2008; Brischoux et al. 2009; Matsumoto & Hikosaka 2009). It has been argued that studies describing excitation in response to aversive stimuli are simply describing the rapid, reward-invariant component of the phasic DA response, and that findings of DA neuron excitation in response to aversive stimuli are therefore misleading (Fiorillo et al. 2013; Fiorillo 2013; Schultz 2016). However, a recent study has shown that responses to rewarding and aversive events can modulate plasticity in distinct brain regions that are targeted by projections from populations of DA neurons with distinct physiological characteristics, suggesting that functional diversity among DA neurons underlies the signalling of different salient events (Lammel et al. 2011).

1.4 Conclusions

DA signalling has been shown to play an important part in fundamental processes related to action selection and reinforcement learning. Many key studies into the regulation and outcomes of DA signalling have measured rates and patterns of AP firing at DA neuron soma in the ventral midbrain. It is generally accepted that changes in DA neuron firing rate will be reported as changes in DA release in striatum, resulting in modulation of striatal processing.

However, it has also been shown that striatal DA release is locally regulated by both local signalling and intrinsic properties of DA neurons. This means that DA release in the striatum may not necessarily be a faithful read-out of DA neuron firing. It is therefore necessary to fully explore the local factors governing DA release, and how these operate during different rates and patterns of presynaptic activity, in order to understand the effects of DA signalling on striatal processing and behaviour.

In this thesis I have used fast-scan cyclic voltammetry (FCV) and patch-clamp electrophysiology to explore the intrinsic axonal factors governing DA release in acute slice preparations of mouse striatum. In Chapter 2, the selection and use of methods in this thesis will be described in detail. Chapter 3 will describe FCV experiments exploring the relationship between axonal and presynaptic factors in short-term plasticity of DA release. Chapter 4 will explore how these mechanisms operate on a background of ongoing activity to shape differences in the signal contrast of DA release in response to bursts of stimulation. Chapter 5 will explore the presynaptic regulation of GABA signalling by DA neurons, using patch-clamp electrophysiology. The implications of these findings in the wider context of DA signalling will be discussed in Chapter 6.

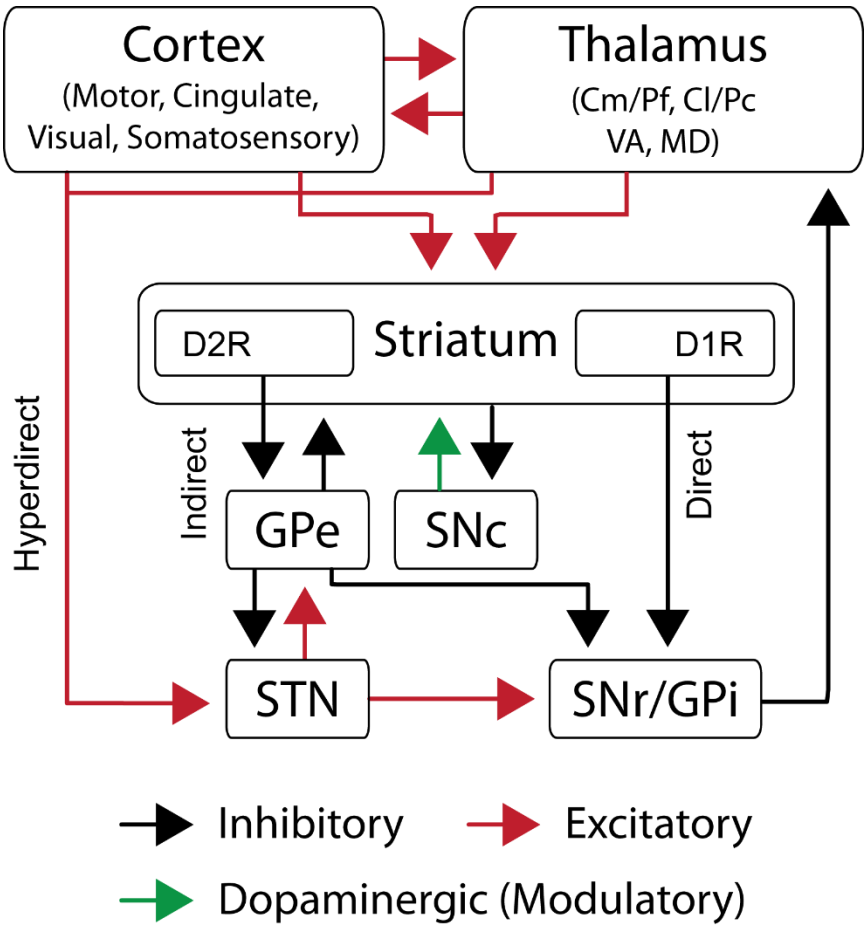

Figure 1.1 Connectivity within the basal ganglia

A simplified representation of major signalling pathways between the cortex, thalamus, and the basal ganglia nuclei. Thalamic nuclei: Cm/Pf, centromedian/parafascicular nuclei; Cl/Pc, central lateral/ paracentral nuclei; VA, ventral anterior nucleus; MD, medial dorsal nucleus. Other nuclei: SNc, substantia nigra pars compacta, GPe, globus pallidus external segment; SNr/GPi, substantia nigra pars reticulata/globus pallidus internal segment; STN, sub-thalamic nucleus.

Chapter 2.
General Methods

In this chapter, I will describe the details of methods and techniques which are used in other chapters in this thesis. This will include a discussion of the animal models and preparations used, as well as a brief overview of and detailed methods for stimulation of DA axons, fast-scan cyclic voltammetry (FCV), patch-clamp electrophysiology, and immunohistochemistry.

2.1 Mice as a model organism for the study of DA signalling

The study of neurotransmission includes work performed in a range of experimental models, from cultured neurons to human subjects. Different approaches are necessary to answer distinct experimental questions. Studies of cultured cells and simpler organisms offer a greater degree of experimental control, while work on more complex organisms such as mammals may more accurately describe the physiology of intact neuronal circuits. Answering a particular experimental question therefore requires careful selection of experimental models.

Rodents are commonly used in the study of neuronal circuits, since they share conserved neuronal properties, organisation of certain circuits and even some behavioural patterns with humans. For this reason, their use is usually preferred over that of non-mammalian animal models such as nematode worms (*Caenorhabditis elegans*) or fruit flies (*Drosophila melanogaster*), which are more suitable for the study of genetics and fundamental properties of cells and synapses.

The use of rodents in place of more complex mammals is primarily driven by both practical and ethical considerations. While the study of the regulation of DA release in human brains would be of the greatest relevance to medical science, the range of experimental techniques that can be performed in humans remains limited. Non-invasive approaches are frequently used to image markers of DA neurotransmission in healthy humans as well as those suffering from DA-related disorders such as PD, but these approaches offer relatively little opportunity for specific manipulations of the DAergic system. Invasive recording techniques and manipulations can be

performed in non-human primates; however, these animals are considered to have a greater capacity to experience pain and suffering than other animals, and as such a strong, specific scientific rationale is required for their experimental use in the UK.

Rodents are therefore an appropriate model for the study of striatal DA release. The experiments described in this thesis were performed in acute sections of striatal tissue from the mouse (*Mus musculus*). Mice are preferable to rats and other rodents for several reasons. Firstly, mice reach maturity more rapidly than rats, and so can be used for experiments at a younger age. This also reduces the cost and time required for breeding of transgenic animals. Secondly, mice are commonly used as experimental models in neuroscience, so a large number of genetically-modified strains are readily available, such as the $DAT^{IRES\text{-}Cre}$ mice used in Chapters 4 and 5. Thirdly, mice are smaller and have a lower energetic demand, so can be housed in larger groups than other rodents such as rats. This is important not only for cost-effectiveness but also for animal welfare, as rodents are highly social animals.

2.1.1 Animals

All procedures were carried out in accordance with a UK Home Office-approved project licence and local guidelines.

Adult wild-type C57Bl/6NCrl (Charles River) were used for most FCV experiments in Chapters 3 and 4. The C57Bl6 strain is commonly used as a background strain for genetically-modified mice, so using this model allows easier comparison of the new data to the existing literature. The C57Bl/6NCrl strain is derived from the commonly-used C57Bl/6J strain, and is useful in the study of DA neurotransmission as it carries a wild-type gene for α-synuclein, a protein important in the regulation of DA release (Abeliovich et al. 2000), unlike some C57Bl/6 strains in which a spontaneous deletion of this gene has been observed (Specht & Schoepfer 2001).

In other experiments in Chapter 4, and in Chapter 5, transgenic mice expressing Cre recombinase under the control of the promoter for the dopamine transporter (DAT) have been used. In these

animals, an internal ribosome entry site-linked Cre (IRES-Cre) recombinase gene has been inserted downstream of the endogenous DAT gene (Bäckman et al. 2006). Heterozygote $DAT^{IRES\text{-}Cre}$ mice, which were used in experiments, were locally bred from homozygote $DAT^{IRES\text{-}Cre}$ mice on a C57Bl/6J background (B6.SJL-*Slc6a3*$^{tm1.1(cre)Bkmn}$/J, stock # 006660, Jackson Laboratories).

2.2 Studying DA neurotransmission in slice preparations

Studies of neuronal circuits in rodent tissue can be conducted in range of different preparations. These include *in vivo* experiments, in which data are collected from living, intact animals; *ex vivo* preparations, in which tissue is collected from animals and studied outside of the body under approximately physiological conditions; and *in vitro* studies, in which biological cells or molecules are studied outside of their physiological context. In the case of DA signalling, approaches range from recordings of DA neuron activity or DA release in freely-moving animals to studies of cultured DA neurons. Similar to choosing animal models, selection of an experimental preparation to answer a particular experimental question necessitates a balance between control over experimental variables and the relevance of findings to physiological conditions.

The experiments described in this thesis have all been conducted in acute coronal sections of mouse striatum. This technique is suitable for the study of axonal factors governing release and plasticity of DA and co-transmitted GABA for several reasons. The advantages of the coronal slice preparation will be described below.

Firstly, slices taken from adult animals preserve the normal connectivity of the striatum, and allow the development of the unique axonal arbor of midbrain DA neurons. This represents a considerable advantage over reduced preparations such as synaptosomes, which may be useful for the study of synaptic machinery present at DA release sites, but do not include intact axonal projections. While DA neurons can be dissected from the midbrain nuclei and used to prepare primary cultures, these cultured neurons lack the diverse neuronal populations and physiological

patterns of synaptic connectivity found in the adult striatum. Although the work in this thesis concerns the intrinsic presynaptic properties of DA axons, key properties such as axonal geometry and ion channel localisation may differ in cultured neurons. DA neurons cultured from induced pluripotent stem cells may represent an important model for the study of DA neuron physiology in the future, but currently do not faithfully replicate the structural and physiological properties of mature DA neurons. Slice preparations are necessary because it is not currently possible to replicate the unique morphology and physiology of DA neurons *in vitro*.

Second, slice preparations allow ready administration of drugs and manipulation of the extracellular environment. Drugs used during *in vivo* experiments are typically administered via peripheral routes, such as intraperitoneal or intravenous injections, or into the brain tissue, through implanted cannulae or by iontophoresis directly onto neurons during recording. While these techniques can permit drug application across different ranges of spatial specificity, the drug concentration reaching the recording site cannot be consistently controlled to the degree that is possible with bath application in a slice preparation. Accurate, sustained changes in the ionic composition of the CSF, as required for many experiments in this thesis, are not feasible in the intact brain. The degree of experimental control required in experiments described in this thesis would therefore not be readily attainable using an *in vivo* approach.

Third, the measurement of extracellular [DA] in slice preparations is more straightforward than it is in intact rodents. The regulation of DA release can be readily studied using FCV in both anaesthetised and freely-moving animals (Millar et al. 1985; Garris et al. 1997). However, data collected in these experiments requires complex analysis to extract DA signals, since these signals are small and are influenced by factors which cannot be easily controlled in the intact brain, such as pH and temperature (Runnels et al. 1999). The choice of anaesthetics for *in vivo* experiments can also be problematic as these can interact with experimental drugs (McFarlane et al. 1995) and alter DA neuron physiology (Marinelli & McCutcheon 2014). By contrast, DA signals collected

using FCV in slice preparations typically have a high signal-to-noise ratio, and extraneous variables can often be easily controlled by manipulation of the extracellular environment. The interpretation of experiments performed in slice preparations is therefore often simpler, and this approach is preferred when the advantages offered by *in vivo* preparations are not considered crucial.

Finally, there are ethical advantages to the use of slices rather than conducting *in vivo* experiments in intact animals. Animals used for experiments in this thesis were killed by cervical dislocation, a method that causes immediate death, with minimal suffering. In addition to this, several striatal slices can be collected from each animal, allowing multiple experiments to be conducted on tissue from the same animal. This is in contrast to *in vivo* experiments, during which animals must typically be anaesthetised for long periods or maintained after invasive surgery.

A key limitation of slice preparations that should also be considered is the loss of DAergic projections from the midbrain to the striatum. Coronal sections preserve the local striatal circuitry and the striatal portion of DA axons, but crucially sever these axons from their cell bodies in the midbrain. This necessitates stimulation of DA axons to evoke DA release (see section 2.3), although this might also be considered an advantage, as the properties of DA axons can be studied in the absence of presynaptic activity.

Preservation of the intact DAergic projection would allow the study of the effects of excitability over the whole range of the axonal arbor. This connectivity is preserved in anaesthetised rodents, but as described above the application of drugs and manipulation of extracellular solution is highly challenging in such preparations. Parasagittal slices that preserve the mesostriatal pathways have been described, in which striatal DA release can be evoked by stimulation of the SNc (Ammari et al. 2009). However, despite the advantage of intact nigrostriatal circuitry, preparation of these slices is associated with a higher failure rate than coronal sections, and only small DA signals could be consistently evoked (Ammari et al. 2009). While a parasagittal

preparation was not used in this thesis, it might be useful for future experiments exploring the differences in STP between populations of midbrain DA neurons.

2.2.1 Slice preparation for FCV

Most FCV experiments described in this thesis used adult (> 35 days) male wild-type (WT) C57Bl/6CNrl mice (Charles River), while some were conducted in adult male heterozygote $DAT^{IRES\text{-}Cre}$ mice conditionally expressing ChR2-EYFP, as described in section 2.3.2.

Mice were killed by cervical dislocation and brains extracted into ice-cold HEPES-based buffer containing in mM: 120 NaCl, 20 $NaHCO_3$, 6.7 HEPES acid, 5 KCl, 3.3 HEPES salt, 2 $CaCl_2$, 2 $MgSO_4$, 1.2 KH_2PO_4, 10 glucose, saturated with 95% O_2/5% CO_2 (carbogen). The calculated osmolarity of this solution was 334.8 mOsm. Acute 300 µm thick coronal striatal slices, containing both dorsal striatum (CPu) and nucleus accumbens core (NAc) were cut in ice-cold HEPES-based buffer using a vibratome (VT1200S; Leica). Slices were kept at room temperature in carbogenated HEPES-based buffer for at least 1 hour before being transferred to the recording chamber.

2.2.2 Slice preparation for patch-clamp electrophysiology

Electrophysiology experiments were conducted in adult male heterozygote $DAT^{IRES\text{-}Cre}$ mice conditionally expressing ChR2-EYFP, as described in section 2.3.2.

Mice were killed by intraperitoneal injection with 0.1 mL sodium pentobarbital (Euthatal) under isoflurane anaesthesia, and intracardially perfused with ice-cold carbogenated cutting solution containing (in mM): 85 NaCl, 25 $NaHCO_3$, 10 glucose, 65 sucrose, 2.5 KCl, 1.25 NaH_2PO_4, 7 $MgCl_2$, 0.5 $CaCl_2$. The calculated osmolarity of this solution was 327.5 mOsm. Acute 300 µm thick coronal striatal slices, containing both dorsal striatum (CPu) and nucleus accumbens core (NAc) were cut in ice-cold cutting solution, then incubated for a minimum of 30 minutes at 32°C in carbogenated

aCSF, which contained (in mM): 130 NaCl, 10 glucose, 2 $MgCl_2$, 2.5 KCl, 1.25 NaH_2PO_4, 26 $NaHCO_3$, 2.5 $CaCl_2$.

2.3 Stimulation of DA release in slice preparations

DA axons in coronal sections of striatum are severed from their cell bodies in the midbrain. DA release cannot therefore be driven by DA neuron firing in this preparation, and is not thought to occur due to spontaneous activity in severed DA axons (Rice et al. 2011). Spontaneous release driven by ACh signalling at nAChRs has been observed, although these events are small in amplitude and occur irregularly (Yorgason et al. 2017). DA release must therefore be evoked in slice preparations by stimulation of DA axons.

Two approaches to stimulation of DA axons have been used in this thesis. Local electrical stimulation was used to evoke DA release in tissue from wild-type C57Bl/6NCrl mice, while optical stimulation was used to evoke DA release and GABA release from DA axons in tissue from heterozygote $DAT^{IRES\text{-}Cre}$ mice selectively expressing a light-sensitive ion channel in DA neurons. The advantages and disadvantages of each method will be briefly considered in this section.

Electrical stimulation has been used to evoke DA release in many studies, both in *ex vivo* tissue and *in vivo*. In slice preparations, a stimulating electrode is placed in contact with the slice, and current pulses of small amplitude and short duration (see section 2.3.1 for details) are passed through the tip of the electrode and into the tissue. In this thesis, local stimulation has been used, although in preparations where the entire DA projection is maintained (see section 2.2) DA release can also be evoked by stimulation of the medial forebrain bundle or midbrain nuclei. When delivered at 22-minute intervals, local electrical stimulation can reliably evoke DA release for 9 hours (Bull et al. 1990). Release is abolished by inhibition of voltage-gated sodium channels with TTX (Cragg 2003) indicating that release sites are predominantly depolarised by action potentials evoked in local axon branches, rather than being directly depolarised by current flow

from the stimulating electrode. DA release that is TTX-insensitive, and therefore thought to arise from direct depolarisation of release sites, can be evoked, but only at very high stimulation intensities (Cragg group, unpublished observations).

Local electrical stimulation is therefore a simple and reliable method to evoke DA release in a slice. However, this method is inherently non-specific, as current flow from the stimulating electrode cannot be limited to a particular neuronal population. Striatal sections preserve the neuronal diversity of the striatum, including SPNs, interneurons and glia, and all of these circuit elements are activated by electrical stimulation. DA release is regulated by GABA (Melchior et al. 2015; Pitman et al. 2014; Schmitz et al. 2002), glutamate (Avshalumov et al. 2003) and acetylcholine signalling (Exley & Cragg 2008), as well as by opioids (Schlösser et al. 1995) and the neuropeptide substance P (Brimblecombe & Cragg 2015), all of which can be released by striatal neurons. Nicotinic ACh receptors can be readily blocked by antagonists such as dihydro-β-erythroidine (DHβE) or desensitised by agonists to exclude cholinergic signalling (Rice & Cragg 2004), and GABA and glutamate release are not thought to influence DA release in response to single pulses or paired pulses at short intervals (Hartung et al. 2011). However, effects of non-selective activation can be difficult to predict, especially where longer and more complex train stimulations are delivered.

Optogenetic techniques offer much greater selectivity than electrical stimulation. This technology, pioneered in the last decade, uses selective genetic markers to drive expression of light-sensitive proteins, known as opsins, in a specific neuronal population (Deisseroth 2015). Opsins undergo conformational changes when exposed to light at a particular wavelength, forming ion channels or pumps (Zhang et al. 2011). Stimulation using light of a specific wavelength can then drive depolarisation or hyperpolarisation of target neurons, depending on the particular opsin used. The selectivity of this approach enables studies of the roles of specific

neuronal populations in the physiology of complex neuronal circuits or behaviours, which are typically infeasible using non-selective electrical stimulation.

In this thesis, channelrhodopsin-2 (ChR2), a cation channel developed from the algae *Chlamydomonas reinhardtii*, was used to depolarise neurons (Nagel et al. 2003). Currents mediated by ChR2 have rapid rise times ($\tau \approx 200$ µs) and recover rapidly from desensitisation (Nagel et al. 2003), permitting reliable light-evoked generation of APs in response to train stimulation up to approximately 20 Hz in DA neuron soma (Tsai et al. 2009). ChR2 has a relatively low single-channel conductance, so in this thesis the H134R variant has been used to reliably evoke DA release, although this comes at the cost of slower channel opening and deactivation kinetics which may limit the frequency at which ChR2-H134R can reliably drive spiking (Nagel et al. 2005).

Selective targeting of opsin expression to target neurons is commonly achieved with very high specificity using site-specific recombinases, a general approach for targeting genetic manipulations to specific cells (Branda & Dymecki 2004). This approach relies on the specific expression of recombinases in transgenic animals, driven by a cell-type specific genetic promoter in target cells. In the $DAT^{IRES\text{-}Cre}$ animals used in this thesis, Cre recombinase expression was driven by the promoter for the DAT (Bäckman et al. 2006). A viral construct containing an inverted gene for ChR2 fused in-frame with a gene encoding enhanced yellow fluorescent protein (EYFP) was injected intracerebrally into heterozygote $DAT^{IRES\text{-}Cre}$ mice. The ChR2-eYFP gene is flanked in the construct by two inverted pairs of short palindromic *lox* sites (see **Fig. 2.1**), which are recognised and inverted by Cre recombinase, resulting in forward orientation and therefore expression of the ChR2-EYFP gene in DAT-positive neurons (Branda & Dymecki 2004). Other recombinases recognising alternative palindromic sites have also been developed, and can be used in intersectional strategies to define neuronal populations by multiple genetic markers (Fenno et al. 2014).

An alternative method for selective targeting uses the Ai32 mouse line, which expresses an inverted gene encoding ChR2-EYFP at the ubiquitous Rosa26 locus (Madisen et al. 2012). This line can be crossed with the $DAT^{IRES\text{-}Cre}$ mouse line to produce mice that display strong, consistent expression of Chr2-EYFP in all DAT-expressing neurons without the need for viral injections. However, during pilot experiments these animals were found to show unusually strong depression of DA release (data not shown), raising questions about the developmental effects of ChR2 expression in DA axons. For this reason, viral approaches were used to drive ChR2 expression throughout this thesis.

Expression of ChR2 under the control of the DAT promoter allows selective activation of DA axons to evoke DA release, excluding the effects of modulatory inputs (Melchior et al. 2015). A further advantage of selective activation is that it can be used to selectively identify the source of signalling events, and to observe such events where they would be occluded by converging inputs activated during non-selective stimulation. Such an approach is necessary to observe GABA-mediated currents evoked by stimulation of DA axons (Tritsch et al. 2012).

However, the optogenetic technique has several disadvantages that make it unsuitable as a sole approach to stimulation of DA neurons. Firstly, the channel kinetics of the available opsins make it unclear whether AP generation in DA neurons can follow repetitive stimulation during long trains or at higher frequencies. More recently-developed opsins can drive firing at higher rates (Gunaydin et al. 2010), but do so at the cost of lower single-channel conductance, and as such do not reliably evoke DA release (Cragg group, unpublished observations). Second, expression of ChR2 may lead to aberrant short-term depression of neurotransmitter release at hippocampal synapses, although this has not yet been demonstrated at DA release sites (Jackman et al. 2014). Third, long-term expression of ChR2 has been shown to lead to the development of abnormal morphological features in cortical axons in the rat, although this effect was more severe following *in utero* electroporation than with the viral transfection method used in this thesis (Miyashita et

al. 2013). Fourth, the transgenic mouse lines used to achieve conditional expression of opsins in specific neuronal populations may display altered physiology that reduces their validity for the study of DA release under normal physiological conditions. For example, the heterozygote $DAT^{IRES-Cre}$ animals used to express ChR2 in DA neurons in this thesis have reduced expression of the DAT compared to wild-type C57Bl/6J mice (Bäckman et al. 2006). Finally, conditional expression of opsins in DA neurons currently require intracerebral injections in transgenic animals, which is likely to cause greater suffering and distress to the animal than in experiments using wild-type mice, where surgery is not required.

In this thesis, both electrical and optical stimulation methods were used to evoke DA release in slice preparations. In FCV experiments in Chapters 3 and 4, optogenetic techniques have been used sparingly, where it is necessary to demonstrate that striatal circuits do not contribute to plasticity. Optogenetic techniques were used in all experiments in Chapter 5, as this approach is currently necessary to evoke detectable GABA co-release in the coronal slice preparation.

2.3.1 Methods for electrical stimulation

As described above, local electrical stimulation is thought to indiscriminately activate all neurons within the spread of the stimulation that are successfully brought to threshold. In the striatum, this will include cholinergic interneurons (Melchior et al. 2015), which are known to exert powerful control over STP of DA release. In order to study the intrinsic axonal and presynaptic factors governing DA release, cholinergic signalling must be excluded. For this reason, throughout this thesis, all experiments using electrical stimulation were carried out in the presence of dihydro-β-erythroidine (DHβE, 1 μM), an antagonist at β2-subunit containing nAChRs, relieving the powerful short-term depression of DA release that is maintained by activation of these receptors (Rice & Cragg 2004). Other receptors, such as GABA and glutamate receptors, are not thought to exert significant control over DA release during single- or paired-pulse stimulation at the intervals used in this thesis, and so were not inhibited (Hartung et al. 2011).

A concentric bipolar Pt/Ir electrode with a 25 µm tip diameter (FHC) was placed on the surface of the striatal tissue, approximately 100 µm from site of the recording electrode. In all experiments, individual pulses consisted of a square 0.6 mA current pulse of 200 µs width. Under drug-free conditions in a striatal slice, a single pulse using these parameters evokes near-maximal $[DA]_o$, and as such is considered a perimaximal stimulation (Cragg 2003). However, in the presence of DHβE, these stimulation parameters are not perimaximal, but were used to allow ready comparison with previous findings.

Stimulations (single, paired-pulse or trains) were delivered at 2.5 minute intervals, during which time release is reliably recovered. At a given site, single-pulse stimulations were delivered until release was stable (less than 10% variation over 3 consecutive stimulations), after which release was typically stable for up to 10 hours. Data were only included for analysis where release remained stable for the duration of the experiment.

2.3.2 Methods for viral transfection

All surgical procedures were performed according to aseptic technique. Mice were deeply anaesthetized with isoflurane (2% w/o). Prior to surgery, meloxicam (Metacam, 5 mg/kg) was administered intraperitoneally for post-operative analgesia. The scalp was shaved and the animal was placed securely in a stereotaxic frame. The scalp was then cleaned with chlorhexidine (HiBi scrub) and bupivacaine hydrochloride with epinephrine (Marcaine, 2 mg/kg) was injected subcutaneously into the scalp for local anaesthesia. A craniotomy was made above the injections site with a hand drill. Injections of 1 µL adeno-associated virus (AAV) serotype 5 construct (pAAV5-double floxed-hChR2(H134R)-EYFP-WPRE-pA) were given either unilaterally or bilaterally in either VTA (co-ordinates from Bregma in mm: AP -3.1, ML ±0.5, DV -4.4) and in the SNc (from Bregma in mm: AP -3.5, ML ±1.2, DV -4.0) using a 2.5 µL 33-gauge Hamilton syringe at 0.2 µL/min with a microinjector. Injection was made at approximately 400 nL/min, followed by a 10 minute delay before retraction of the needle to minimise suction of the vector into the electrode track.

Following wound closure with sterile monofilament suture (Ethicon), animals were allowed to recover in a temperature-controlled cage.

Animals were maintained for at least 3-4 weeks following surgery to allow virus expression.

2.3.3 Methods for optical stimulation

In experiments using optical stimulation in tissue from $DAT^{IRES\text{-}Cre}$ animals injected with an AAV-5 construct encoding ChR2-eYFP (as described above), DHβE was not used, because selective activation of DA axons is not thought to evoke release of ACh (Melchior et al. 2015).

Two different methods of optical stimulation were used. For all experiments using optical stimulation in Chapter 4, and for some experiments in Chapter 5, a 470 nM LED system (OptoLED, Cairn Research) was used to deliver full-field illumination of the field of view, which was a circle of diameter 2.2 mm or 0.55 mm under a 10x or 40x water-immersion objective, respectively (eyepiece field number 22). For other experiments in Chapter 5, a 473 nm diode laser (DL-473, Rapp Optoelectronic) coupled to the microscope by an optic fibre (200 µm multi-mode, numerical aperture 0.22) was used to illuminate a 15 µm spot under a 40x water-immersion objective. In all experiments, activation of the light source was driven by a 2 ms TTL pulse. Optical stimulation of DA release in Chapter 4 was delivered at a perimaximal intensity that was determined at the beginning of each experiment to account for variability in the extent of ChR2 expression.

2.4 Fast-scan cyclic voltammetry

In Chapters 3 and 4 of this thesis, evoked DA release was measured using FCV at carbon fibre microelectrodes (CFMs) inserted into the striatal tissue. This technique is well-suited to the study of transient changes in extracellular [DA] ($[DA]_o$) due to its unique balance of chemical selectivity and sub-second temporal resolution.

Electrochemical detection uses the faradaic current produced by a change in the oxidation state (oxidation or reduction) to quantify the concentration of an electroactive substrate. In

voltammetric methods, the potential difference (voltage) across a working electrode is varied to determine faradaic current as a function of applied voltage, which can be represented by a plot known as a voltammogram. Such detection methods are widely used in analytical chemistry, and have a number of applications in neuroscience. Many biological compounds are susceptible to electrochemical detection, including monoamine neurotransmitters such as dopamine.

FCV is an electrochemical detection technique that employs rapid cycling of the applied potential across a range predicted to oxidise the compound of interest. On the forward sweep, from a negative potential to a positive potential, the substrate is oxidised, and subsequently reduced on the reverse sweep, producing measurable faradaic currents. DA has two readily-oxidised hydroxyl groups, making it suitable for electrochemical detection. In the specific case of DA detection, DA is oxidised to dopamine-*O*-quinone on the forward sweep, at approximately +650 mV, and reduced to DA on the reverse sweep. This cycle is repeated at a frequency of 8 Hz, corresponding to a measurement of faradaic current every 125 ms. Higher sweep frequencies are commonly used, yielding a more accurate representation of the kinetics of $[DA]_o$ transients, but this is achieved at the cost of reduced signal amplitude.

FCV can be used to measure changes in extrasynaptic spillover of DA from a population of release sites, since the diameter of the CFM tip is several orders of magnitude larger than a typical synaptic cleft. This is compatible with the physiological properties of DA signalling, which is thought to occur at least in part through extrasynaptic volume transmission (Gonon et al. 2000). The faradaic current can be converted to DA concentration following calibration of the CFM with a known concentration of DA; a single-point calibration is adequate, since the relationship between faradaic current and $[DA]_o$ is linear over the range of $[DA]_o$ detected in a slice preparation (Bull et al. 1990; Platt 2012). However, only transient changes in $[DA]_o$ can be measured using FCV. This is because a large background signal, produced by the capacitive properties of the electrode and oxidation of functional groups at the electrode surface, must be

subtracted from the total signal to obtain the faradaic current attributable to DA oxidation (Hermans et al. 2008). As a result, continuous FCV recordings are limited to the period over which the background current remains relatively stable, typically less than 1 minute.

The temporal resolution afforded by FCV allows the detection of rapid DA signalling events, but accurate study of the time course of DA release often requires higher rates of detection. A greater temporal resolution is offered by constant-potential amperometry, a similar technique in which the applied potential is maintained at the oxidation potential for the chemical species of interest, providing a continuous signal. However, this approach does not allow distinction of the currents produced by different oxidised species, making it difficult to positively identify the oxidised species as DA. Using FCV, certain monoamine neurotransmitters such as 5-hydroxytryptamine (5-HT), as well as other signalling molecules such as hydrogen peroxide, can be readily distinguished from DA due to their distinct oxidation or reduction potentials. The temporal resolution of FCV is adequate for the detection of DA release events studied in this thesis, and the chemical selectivity of FCV is required to positively identify the oxidised species as DA.

An alternative method for the detection of DA release in the striatum with high temporal resolution is the use of viral constructs to drive expression of DA-activated ion channels in striatal neurons, such that DA evokes fast post-synaptic currents that can be detected with patch-clamp electrophysiology. To date, two methods have been developed to achieve this aim. Firstly, striatal neurons can be transfected with LGC-53, a DA-sensitive ligand-gated ion channel derived from *Caenorhabditis elegans* (Kress et al. 2014). Second, conditional over-expression of G-protein-linked K^+ channels in striatal neurons amplifies D2 receptor-mediated currents to the extent that they can be readily detected in SPNs (Marcott et al. 2014). These techniques allow the study of DA release events with high temporal precision. However, neither construct has not yet been adapted for conditional expression, and the consequences of global expression of DA-activated ion channels throughout the striatum remain unclear. Furthermore, these approaches also

introduce confounding postsynaptic factors such as receptor kinetics and desensitisation, limiting their suitability for the study of presynaptic plasticity. With further development, these approaches have considerable potential for the study of DA transmission; they may be particularly useful for the identification of synaptic DA signalling, since they are likely to be less dependent on DA overflow than existing techniques.

The chemical selectivity of FCV can become inadequate where similar concentrations of multiple different oxidisable species are detected simultaneously, as the peaks on the cyclic voltammogram may begin to overlap. For applications where greater chemical selectivity is required, monoamine neurotransmitters are typically detected using microdialysis. Microdialysis probes are inserted into the tissue and used to collect samples of the extracellular fluid across a semi-permeable membrane, which are then separated using high-performance liquid chromatography coupled to electrochemical detection or an alternative identification method. This technique can powerfully distinguish between chemical species, and furthermore can measure absolute baseline concentrations of neurotransmitters, which is not possible using FCV.

However, with modern microdialysis probes samples can only be collected at a maximum rate of approximately 1 sample/minute, meaning that the temporal resolution of this technique is too low to study individual DA release events on a sub-second timescale. Furthermore, electrical stimulation in striatal tissue is thought to evoke DA release on a much greater scale than other monoamine neurotransmitters, since the resultant FCV signal is enhanced by selective DAT inhibitors but not by blockade or noradrenaline or 5-HT transporters (Bull et al. 1990; Cragg 2003). Under these conditions, release of monoamine transmitters such as noradrenaline, that can confound FCV detection of DA, is limited in the striatum. The chemical selectivity of FCV is therefore considered adequate for the study of DA release in striatal slices.

2.4.1 Methods for fabrication of CFMs

CFMs were produced in-house and each used for a single experiment, since changes in electrode kinetics can occur due to tissue fouling and repeated exposure to DA. Borosilicate capillary tubes (2.0 mm outside diameter, 1.16 mm inside diameter, Harvard Apparatus, UK) were threaded with a single uncoated carbon fibre (7 µm diameter, Goodfellow Cambridge Ltd., UK). Each carbon fibre was filled with acetone, to ease insertion and to clean the carbon fibre, which was subsequently removed by blotting with tissue paper. Following acetone removal, the capillary tube was sealed around the carbon fibre using a PE-2 vertical microelectrode puller (Narishige, Japan). A high heat setting was used to ensure a tight seal between the glass microelectrode and the carbon fibre, as this promotes a high signal-to-noise ratio. The resulting seal is visible under 100x magnification, so can be visually inspected for damage. The carbon fibre is then cut to a length of 50-100 µm from seal to tip, which typically produces a sensitivity within the desired range; shorter electrodes have a reduced sensitivity to DA, while longer electrodes have higher noise levels. A short length of insulated 0.1 mm tinned copper wire was coated with silver conductance paint and inserted into the open end of the capillary tube, in electrical contact with the carbon fibre close to the tip, and secured with cyanoacrylate glue.

2.4.2 Methods for FCV

Slices were transferred to a recording chamber and secured using silver pins placed on the tissue surrounding the striatum. Slices were continuously superfused with carbogenated aCSF which contained (in mM): 124.3 NaCl, 26 $NaHCO_3$, 3.8 KCl, 2.4 $CaCl_2$, 1.3 $MgSO_4$, 1.23 KH_2PO_4, 10 glucose. The calculated osmolarity of this solution was 331.6 mOsm. Superfusion was at a rate of 1.8-2 mL/minute, and aCSF was warmed to a temperature of 31-33^oC. A CFM was connected to the voltammeter headstage and left to cycle in aCSF for approximately 10 minutes, before being inserted into a region of non-striatal tissue (typically cortex or olfactory tubercle) and left to cycle

for a further 30 minutes. These steps allow the electrode to equilibrate to the recording conditions and reduce subsequent baseline drift during the experiment.

The CFM is then inserted at a depth of 100 µm into the recording site. In order to study regional differences in the regulation of DA release, recording sites were either in CPu or NAc. Sites in CPu were in the dorsolateral quadrant of the striatum, while sites in NAc were within 100 µm of the anterior commissure. Following CFM insertion, the full current was inspected to determine whether the microelectrode seal remained intact, and full signal gain was set to provide a working range of 5 V. CFMs with a full signal gain in the range 3-10 mV/nA were considered suitable for recording. The full signal gain was monitored throughout the experiment, as CFMs typically become more sensitive during use, which can result in saturation if left uncorrected.

A biphasic triangular voltage waveform from -700 mV to +1300 mV vs an Ag/AgCl reference electrode (World Precision Instruments, USA) at a rate of 800 V/s was applied to the CFM using a Millar voltammeter (Julian Millar, Barts and the London School of Medicine and Dentistry). The extension of the anodic scan limit beyond +1000 mV has been shown to increase sensitivity to DA at the expense of slower electrode kinetics (Hafizi et al. 1990; Heien et al. 2003). The high scan rate used here further increases the sensitivity to DA, but increases the charging current due to a greater number of adsorption sites (Bath et al. 2000; Keithley et al. 2011). The waveform is delivered at a frequency of 8 Hz, and between sweeps the electrode is held at 0 mV (i.e. switched out of circuit) to limit adsorption (Heien et al. 2003). Background subtraction was performed on-line by the Millar voltammeter, using a baseline recording of the total current stored before each stimulation was delivered. Background-subtracted currents are sampled at 50 kHz and digitised using a Digidata 1440A or 1550A (Molecular Devices, USA).

Data were collected using Axoscope 10.5 (Molecular Devices, USA), and analysed using locally-written scripts in Visual Basic for Applications (Microsoft, USA). The threshold for statistical significance in all analyses $p < 0.05$, adjusted for multiple comparisons where appropriate.

2.5 Patch-clamp electrophysiology

In Chapter 5, whole-cell patch-clamp electrophysiology was used to detect post-synaptic currents in SPNs. This powerful technique is used in a broad range of applications to study electrical signalling in neurons and other excitable cells. The principles of the patch-clamp method will be discussed briefly in this section.

The term 'electrophysiology' describes a range of techniques in which the electrical properties of biological tissues are measured, across a range of spatial scales from single-channel recordings in individual cells to studies of network activity across large brain regions. These approaches often involve measuring changes in voltage across membranes or circuits, or currents passed by ion channels in the membranes of excitable cells.

The electrical properties of cell membranes are primarily determined by their expression of ion channels. Many channels are directly gated by changes in the voltage across the cell membrane, undergoing changes in opening or activation state, at specific potentials. Other channels are gated by the binding of ligands, but may still show some degree of voltage-dependence.

The whole-cell voltage-clamp technique was developed to control membrane potential in order to study the voltage-dependence of electrical processes across cell membranes. Membrane potential, relative to a reference electrode immersed in the extracellular buffer, is measured at an electrode in electrical contact with the interior of the cell, and controlled by passing a continuous current to the intracellular space (Hodgkin et al. 1952). The command voltage can then be altered by increasing or decreasing the current through the intracellular electrode.

Historically, two separate electrodes would be required to maintain voltage clamp in excitable cells; one to detect changes in membrane potential, and the other to pass the current required to maintain the command potential (Guan et al. 2013). The holding current passed by the second electrode is a function of the difference between the command potential and the membrane

potential measured at the first electrode, so the circuit will rapidly compensate for perturbations in the membrane potential by altering the holding current. Because currents carried by ion channels in the cell membrane will alter the membrane potential, the magnitude of these currents can be calculated from changes in the holding current. This technique is used in large cells such as squid giant axons and *Xenopus* oocytes, a common expression system for ion channels, which can be reasonably accessed by two electrodes (e.g. Borre et al. 2014). Discontinuous single-electrode voltage clamp, a variation in which a single sharp electrode is used to monitor voltage and pass current by rapid between the two functions, avoids the traumatic insertion of multiple electrodes, but does so at the cost of greater noise and slower responses to changes in membrane potential compared to two-electrode recordings (Finkel & Redman 1985).

Studies of smaller cells now commonly use the single-electrode patch-clamp technique (Neher et al. 1978). In this approach, a blunt glass microelectrode is attached to the membrane of a target cell, and suction is used to form a high-resistance seal (on the order of gigaOhms) between the electrode tip and the membrane. The patch of membrane covered by the electrode tip is the ruptured, forming a low-resistance junction between the interior of the cell and the interior of the electrode, with minimal leak currents through the seal. Voltage monitoring and passing of the holding current may be performed continuously by the same electrode (Hamill et al. 1981). Voltage-clamp can therefore be performed on cells with an accessible surface of a similar size to the patch electrode, and used to make low-noise recordings of small currents, with the result that single-channel conductances can be studied (Hamill et al. 1981).

Patch electrodes can also be used to record membrane potential when a known current is passed to the interior of the cell. This approach is known as current clamp, although the name is misleading since passing a constant current does not require clamping circuitry. Since the membrane potential is allowed to vary freely, this approach can be used to measure action

potentials and other voltage fluctuations, and to determine how the membrane responds to currents such as those evoked by synaptic inputs.

The patch-clamp is an extremely powerful and flexible technique, since the command potential is not necessarily limited to constant steps in voltage; the membrane voltage can be controlled with sufficient temporal resolution to mimic complex patterns of voltage change, including action potentials (e.g. Yang et al. 2013). Furthermore, in intact brain tissue, patch-clamp recordings can be coupled with electrical or optical stimulation of other neuronal circuit elements to determine whether neurons are functionally connected by synaptic or electrical contacts, and to identify currents activated by synaptic activity.

However, the use of the patch-clamp technique is limited by several key disadvantages. Firstly, inadequate compensation of the resistance through the electrode and the patch can result in inaccurate observations of recorded currents (Marty & Neher 1995). Because voltage recording and clamping are carried out simultaneously by the patch electrode, patch-clamp circuits do not strictly control the voltage at the tip of the electrode; instead, the voltage is clamped at the top of the electrode (i.e. at the headstage wire inside the pipette shaft). This means that current delivered to the interior of the cell is determined as a function of the voltage at the top of the electrode, before passing through the resistance of the electrode and the ruptured patch, known cumulatively as series resistance. Voltage drops across the series resistance can increase the time taken for the membrane potential to reach its new value following a change in the command potential, limiting the temporal resolution of recordings (i.e. the maximum rate of currents that can be accurately resolved) (Sherman et al. 1999). Series resistance can also cause voltage errors (i.e. a mismatch between the membrane potential and the potential at the top of the electrode), which are particularly pronounced when recording large currents (Sigworth 1995).

To decrease the time taken to change the membrane potential, and to accurately clamp it at the desired value, series resistance must be adequately compensated. This can be achieved by

increasing the command voltage proportionally to the holding current, but at high levels of compensation a positive feedback loop is created, increasing the command voltage and hence the holding current until the cell is destroyed (Sigworth 1995). The amplitude and rate of currents that can be measured using patch-clamp techniques is therefore limited by the series resistance of the electrode and the patch.

A second disadvantage of the patch-clamp method is the limited volume that can be successfully clamped; while the voltage at the patch may be well-controlled, the greater access resistance of distal portions of the cell may cause a voltage drop that results in poor voltage control. As a result, these regions may 'escape' the voltage-clamp, altering the time course of recorded currents (Armstrong & Gilly 1992). This means that somatic recordings of currents that are generated in distal regions of the cell, such as dendrites, are not necessarily accurate representations of these currents. This effect limits the recording of currents in distal portions of cells, such as axons or dendrites, where these regions are not accessible to a patch electrode.

In some experiments, the equilibration of the intracellular medium with the recording solution is undesirable, as the dialysis of the cytosolic solutes can disrupt cellular processes such as intracellular signalling pathways. In these cases, inclusion of an antibiotic such as nystatin or gramicidin in the electrode internal solution can partially degrade the membrane, leaving a perforated patch that allows intracellular recording without rupture of the membrane. However, this results in greater access resistance of the patch, reducing the amplitude of measured signals and exacerbating the voltage drop across the series resistance, with its attendant problems.

In Chapter 5 of this thesis, the whole-cell patch-clamp technique was used in voltage-clamp mode to measure the amplitude and kinetics of postsynaptic currents evoked in SPNs by selective stimulation of DA axons. Current clamp recordings were also used to identify recorded neurons. Since postsynaptic currents are routinely detected in SPNs, and the recorded currents were typically <1.5 nA (see Chapter 5), this approach was considered appropriate. The perforated patch

technique was not considered necessary, as these currents appeared to be mediated by ionotropic $GABA_A$ receptors, and therefore should be independent of intracellular signalling.

2.5.1 Methods for Patch-clamp electrophysiology

Slices were transferred to a recording bath, secured using either silver pins or a harp, and continuously superfused with carbogenated aCSF which contained (in mM): 130 NaCl, 10 glucose, 2 $MgCl_2$, 2.5 KCl, 1.25 NaH_2PO_4, 26 $NaHCO_3$, 2.5 $CaCl_2$. The calculated osmolarity of this solution was 286 mOsm. Superfusion was at a rate of 1.8-2 mL/minute, and aCSF was warmed to a temperature of 31-33^oC.

Glass electrodes were prepared using a P-1000 horizontal puller (Sutter Instruments). In voltage-clamp experiments, electrodes were filled with an internal solution containing a high [Cl^-] and Cs^+, a non-selective blocker of K^+ channels, to promote detection of currents carried by Cl^- ions. Internal solution contained (in mM): 120 CsCl, 15 $CsMeSO_3$, 8 NaCl, 0.5 EGTA, 10 HEPES, 2 Mg-ATP, 0.3 Na-GTP, 5 QX-314 and 1% neurobiotin. CsCl-based internal solution was corrected to pH 7.32 and 293 mOsm. Series resistance compensation was not considered necessary, since the amplitudes of recorded currents were <1.5 nA, series resistance in these experiments was typically <15 MΩ, and because statistical comparisons were made between currents recorded under the same conditions.

In current-clamp recordings, electrodes were filled with internal solution containing (in mM): 120 K-gluconate, 10 KCl, 10 HEPES, 4 MgATP, 0.3 NaGTP, 10 Na-phosphocreatine and 0.5% neurobiotin. K-gluconate-based internal solution was corrected to pH 7.09 and 273 mOsm. Membrane potentials were corrected for a ~8 mV liquid junction potential.

Electrodes were rejected if tip resistance in the bath was greater than 5 MΩ. Negative pressure was applied to form a seal with resistance > 1 GΩ, and negative pressure and current pulses were used to rupture the patch. Neurons were selected for recording on the basis of size, low excitability, and lack of a hyperpolarisation-induced sag. During experiments, access resistance

was monitored by measurement of the initial current in response to a delivery of a 1 ms square pulse of +5 mV. Single- or paired-pulse stimulation was delivered at 1 minute intervals, except where otherwise indicated. Cells were held at -70 mV during all recordings.

Recordings were made using a Multiclamp 700B amplifier (Molecular Devices), filtered at 10 kHz using a low-pass Bessel filter and digitised at 10-20 kHz using a Digidata 1550A acquisition board (Axon Instruments). Data were collected using Clampex and offline analysis performed using Clampfit (pClamp10). The threshold for statistical significance in all analyses $p < 0.05$, adjusted for multiple comparisons where appropriate.

2.6 Immunohistochemistry

Immunohistochemistry was used to confirm the localisation of the AAV construct to midbrain DA neurons. As described above, the ChR2 gene was fused to a gene for enhanced yellow fluorescent protein (eYFP), so neurons expressing the construct were fluorescent without any need for immunostaining. Slices from injected $DAT^{IRES\text{-}Cre}$ mice were stained for tyrosine hydroxylase (TH), the rate-limiting enzyme in DA synthesis, or the DAT, both of which are considered to be selective markers for DA neuron identity in the midbrain (Lammel et al. 2015).

During preparation of striatal sections for electrophysiology, the midbrain was collected and fixed in paraformaldehyde (4% in phosphate-buffered saline) for at least 3 days at 4°C. After fixing, midbrains were washed in phosphate-buffered saline (PBS) and 40 µm thick coronal sections containing SNc and VTA were cut on a vibratome room-temperature PBS. Slices were then stored overnight at 4°C in PBS.

Prior to staining, slices were washed 5 times in PBS, then incubated in PBS with 0.5% Triton X-100 (PBS-Tx) with 10% normal goat serum (NGS) and 10% bovine serum (BS) for 30 minutes at room temperature. Slices were then incubated overnight at 4°C in PBS-Tx with 1% NGS and 1% BS with either 1:2000 rabbit anti-TH (T8700, Sigma) or 1:1000 rat anti-DAT (ab5990, Abcam). After

removal of the primary antibody, slices were washed 5 times in PBS, and then incubated in PBS-Tx with 1% NGS and 1% BS with either 1:1000 Dylight 594 goat anti-rabbit (111-515-047, Jackson ImmunoResearch), or 1:500 AlexaFluor 594 goat anti-rat (112-585-003, Jackson ImmunoResearch) for 2 hours at room temperature. Finally, slices were washed a further 5 times in PBS, then dried and mounted onto poly-D-lysine-coated slides and coverslipped using Vectashield Hardset mounting medium (Vector Labs). Slides were imaged using an Olympus BX51WI fluorescence microscope, and images were captured using a QClick cooled-CCD camera and QCapture software (QImaging).

Expression of the ChR2-eYFP construct in midbrain slices was observed only within the boundaries of the dopaminergic nuclei (Franklin & Paxinos 2008), and overlapped at low magnification with staining for TH and DAT (**Fig. 2.3, 2.4**). At higher magnification, eYFP-positive neurons were observed that were also positive for TH or DAT, although not all TH- or DAT-positive neurons expressed eYFP. It is possible that toxicity associated with long-term ChR2-eYFP expression could limit total TH expression or the number of detectable cells expressing both TH and eYFP, but since staining was not conducted in wild-type animals no comparison was available. During visual inspection, no eYFP-positive neurons were observed that did not express TH or DAT, although a formal stereological analysis was not conducted. Since the ChR2-EYFP construct migrates to axons over time, midbrain tissue collected from animals used for FCV experiments, which had sufficient ChR2-EYFP expression in the axonal compartment to drive optically-evoked DA release, showed weaker expression in the DA neuron soma.

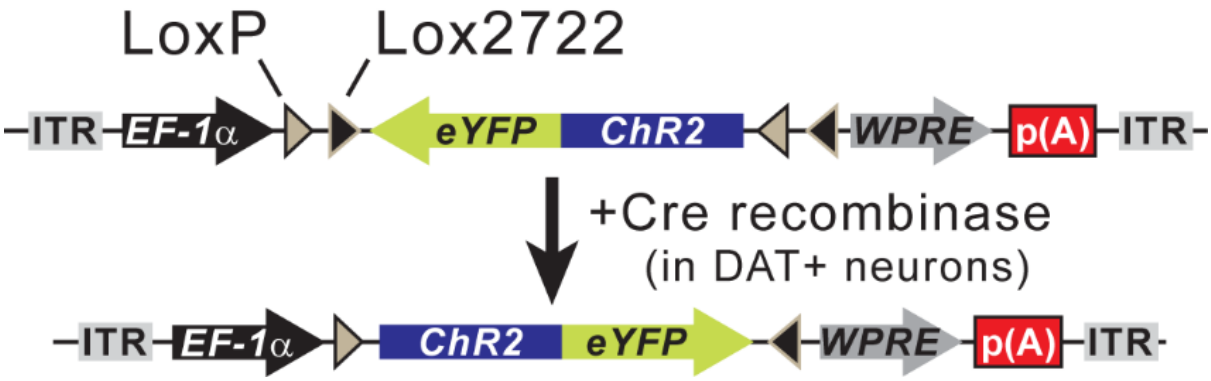

Fig. 2.1 Cre-dependent recombination of virally-delivered ChR2-EYFP construct

Simplified representation of the Cre-dependent construct packaged into AAV5 and injected into $DAT^{IRES\text{-}Cre}$ mice (adapted from Threlfell et al. 2012). The inverted ChR2-EYFP gene is flanked by two pairs of incompatible inverted *lox* sites (*lox*P and *lox*2722). In Cre-expressing neurons, recombination of *lox* sites results in forward orientation of the ChR2-EYFP gene, such that expression can be driven by the EF-1α promoter. The woodchuck hepatitis virus post-transcriptional regulatory element (WPRE) is included to increase mRNA stability.

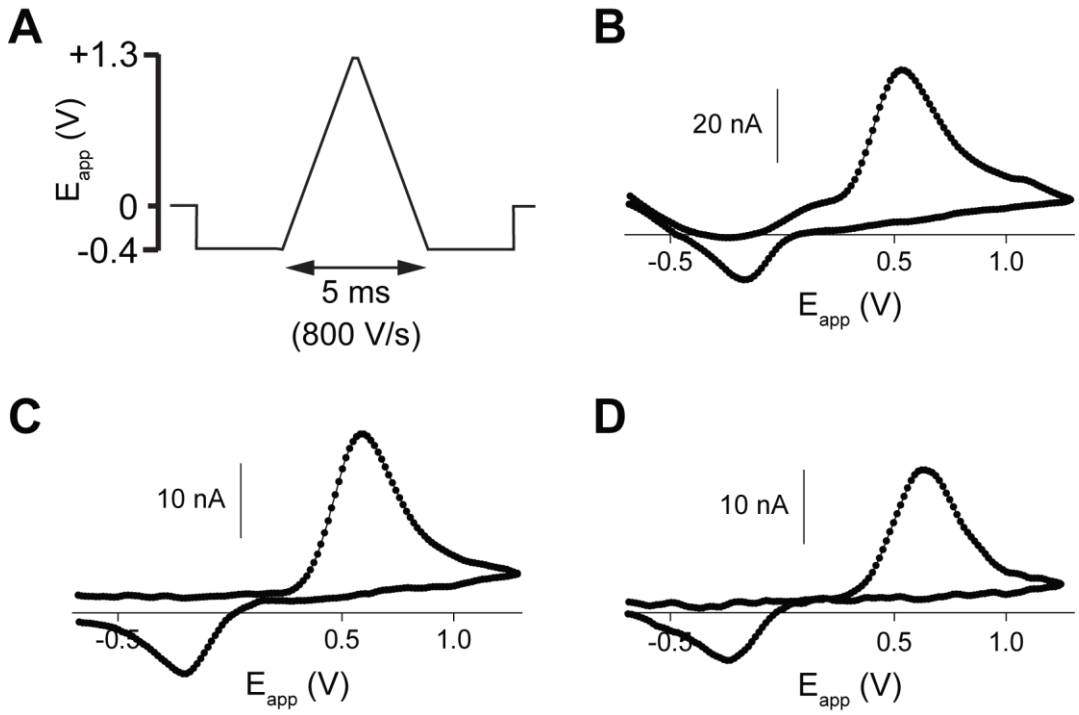

Fig. 2.2 The applied voltage waveform and resulting cyclic voltammograms

(A) Representation of the voltage waveform applied every 125 ms during FCV experiments. The triangular waveform scans from -0.4 V to + 1.3 V and back again at 800 V/s, with a duration of 5 ms for each scan. Note that the electrode rests at 0 V between scans. **(B-D)** Typical background-subtracted cyclic voltammograms recorded during application of the voltage waveform depicted in (A). Each voltammogram shows faradaic current generated by the oxidation (positive peak at approximately +650 mV) and reduction (negative peak at approximately -200 mV) of DA during a single sweep. Cyclic voltammograms were recorded during application of 2 µM DA **(B)**, or evoked DA release with electrical **(C)** or optical **(D)** stimulation.

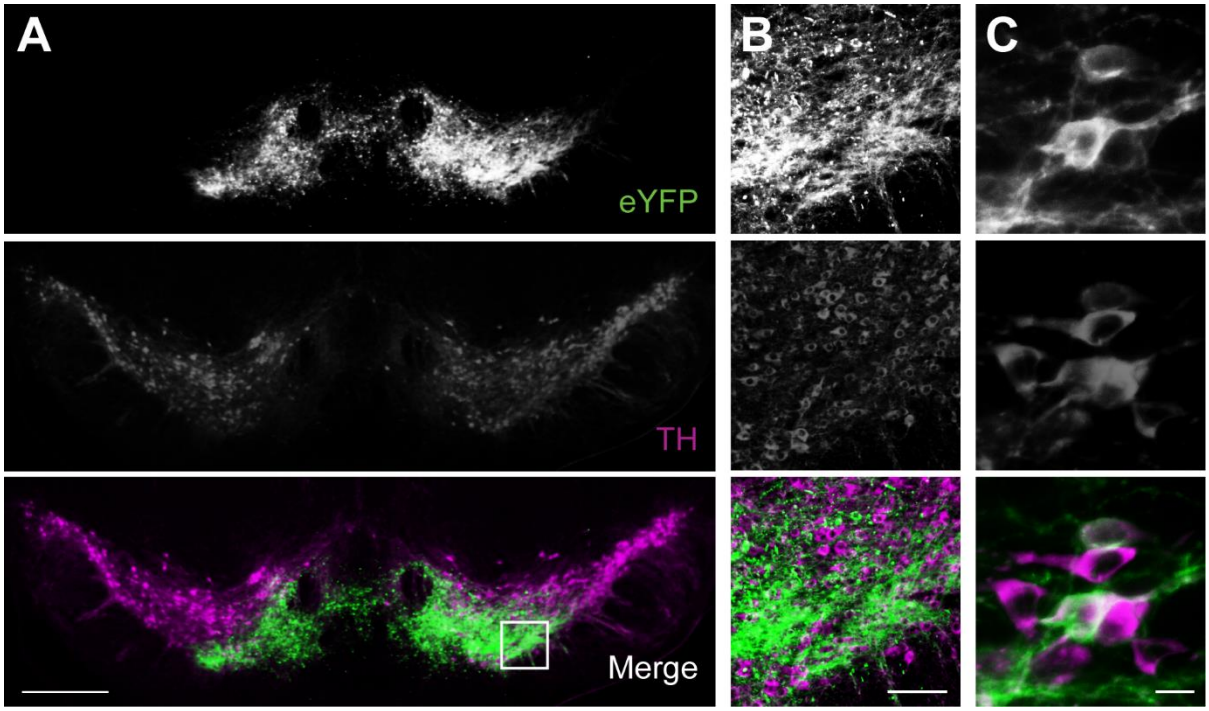

Figure 2.3 eYFP is co-localised with tyrosine hydroxylase (TH) in midbrain neurons

(A) Immunohistochemistry in midbrain sections from a heterozygote $DAT^{IRES\text{-}Cre}$ mouse injected bilaterally with a viral construct encoding ChR2-EYFP (green). Sections were stained for tyrosine hydroxylase (TH, magenta). **(B)** Higher magnification image of the boxed area in (**A**). **(C)** Higher magnification image of neuronal soma expressing both EYFP and TH. Scale bars: 500 µm (**A**), 100 µm (**B**), 10 µm (**C**).

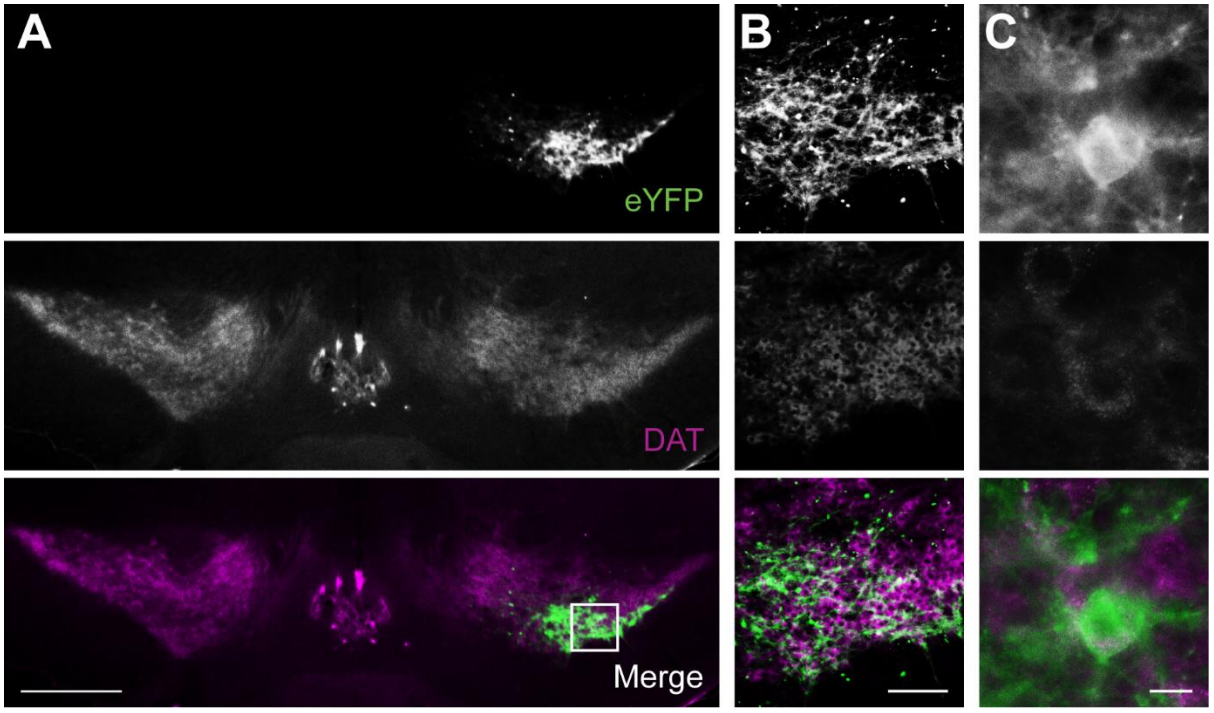

Figure 2.4 eYFP is co-localised with the DAT in midbrain neurons

(A) Immunohistochemistry in midbrain sections from a heterozygote $DAT^{IRES\text{-}Cre}$ mouse injected unilaterally with a viral construct encoding ChR2-EYFP (green). Sections were stained for the DAT (magenta). **(B)** Higher magnification image of the boxed area in (**A**). **(C)** Higher magnification image of neuronal soma expressing both EYFP and DAT. Scale bars: 500 µm (**A**), 100 µm (**B**), 10 µm (**C**).

Chapter 3.

Dopamine transporter function underlies region-specific control of STP

3.1 Introduction

DA neurons encode behaviourally-relevant information about the salience and/or motivational value of environmental stimuli in dynamic patterns of action potential (AP) firing (Schultz 1986; Ljungberg et al. 1992; Hyland et al. 2002; Redgrave et al. 2008; Matsumoto & Hikosaka 2009). However, the manner in which this information is conveyed to target neurons by DA signalling in the striatum remains unclear, since DA release is regionally variable (Brown et al. 2011) and subject to local regulation (Sulzer et al. 2016).

Despite classical accounts of axons as simple high-fidelity cables, neurotransmitter release from CNS axons is shaped by factors that regulate AP conduction such as axonal morphology, ion channel expression, and presynaptic receptors as well as intrinsic mechanisms regulating neurotransmitter release probability and its short-term plasticity (STP) (Debanne 2004; Bucher & Goaillard 2011). Previous work has identified how STP is governed in a region-specific manner by Ca^{2+}-dependent changes in release probability (P_r) , K^+-dependent processes related to axonal excitability and repolarisation, and by the function of the dopamine transporter (DAT) on DA axons (Platt 2012).

It remains unclear how these mechanisms operating at DA axons interact and limit one another to govern STP of DA release. In this chapter I explore how the interactions between release probability, axonal excitability, and DAT function shape re-release of DA at short intervals. Furthermore, this chapter will investigate how the interactions between axonal mechanisms underlying STP differ between the caudate-putamen (CPu) and nucleus accumbens (NAc), two major functional regions of the striatum, to show how axonal mechanisms shape region-specific patterns of STP.

3.1.1 Ca^{2+} handling in DA neurons

As described in Chapter 1, classical studies of fast glutamatergic synapses show a strong inverse relationship between initial P_r and subsequent release; release sites with high initial P_r tend to undergo short-term depression (STD), while sites with low initial P_r tend toward short-term facilitation (STF) (Dobrunz & Stevens 1997; Thomson 2000). However, it remains unclear whether these principles also govern STP of DA release in the striatum. Previous work suggests that STP is weakly related to initial DA release (Jennings et al. 2015), and that paired-pulse facilitation of DA release is only observed at very short inter-pulse intervals, regardless of changes in P_r elicited by varying extracellular [Ca^{2+}] (Platt 2012).

It may be that the relationship between P_r and STP is fundamentally weaker at DA release sites than at fast glutamatergic synapses, possibly because P_r of DA release is thought to be very low (Rooney & Wallace 2015). Alternatively, it may be that another presynaptic mechanism governing STP masks a stronger relationship between P_r and STP. For example, changes in axonal AP waveforms, regulated by K^+ currents, can alter Ca^{2+} entry at presynaptic boutons (Geiger & Jonas 2000; Sabatini & Regehr 1997), and the electrogenic properties of the DAT can alter Ca^{2+} channel activity (Cameron et al. 2015). In this chapter I therefore investigate the effects of K^+-dependent gating and DAT inhibition on the relationship between P_r and STP.

3.1.2 K+ channels in DA neurons

STP of DA release is gated by K^+ conductances operating at DA axons. It has been shown that changes in extracellular [K^+] can gate STP of DA release; increases in $[K^+]_o$ promote STD, while decreasing $[K^+]_o$ relieves STD (Platt 2012). However, the mechanism underlying this relationship remains unclear. A decrease in $[K^+]_o$ might be expected to increase the Nernstian driving force for outward K^+ currents, hyperpolarising the axon and increasing the rate of repolarisation following an action potential. This might in turn limit refractoriness of DA release sites and promote re-release, relieving STD. On the other hand, decreases in $[K^+]_o$ have been shown to promote use-

dependent inactivation of K^+ channels (Baukrowitz & Yellen 1995), which might lead to depolarisation of the axon at the second pulse in a pair, increasing Na^+ channel recruitment and promoting re-release. It is not currently possible to distinguish between these possible mechanisms, due to a lack of experimental techniques capable of measuring short-term changes in action potential dynamics in intact fine axons, so both potential mechanisms will be discussed in this thesis. Either case suggests a strong dependence of STP on currents carried by axonal K^+ channels, which regulate axonal excitability and shape the AP waveform (Kress & Mennerick 2009; Ohura & Kamiya 2016).

At the level of the soma, DA neurons have been shown to express a diverse array of K^+ channels involved in the regulation of excitability and AP generation. It is much less clear which of these channels are also expressed in the axonal compartment, due to the relative inaccessibility of the axon to direct electrophysiological recordings. GIRK channels, which hyperpolarise DA soma in response to D2 autoreceptor activation (Beckstead et al. 2004), are not thought to be typically expressed in the axonal compartment (Liao et al. 1996; Drake et al. 1997), although these channels have been reported at presynaptic sites in some non-DAergic neurons (Ponce et al. 1996; Fernández-Alacid et al. 2009; Grosse et al. 2003). Instead, terminal D2Rs have been suggested to reduce terminal excitability by activating K_v1 channels in rats and mice (Cass & Zahniser 1991; Fulton et al. 2011; Martel et al. 2011) and K_{ATP} channels in rats (Neusch et al. 2000; Tanaka et al. 1995) to provide feedback control of axonal excitability by activating hyperpolarising K^+ currents in DA axons.

It should be noted, however, that these studies do not exclude the effect of local cholinergic input, so it is difficult to determine whether the effects of K^+ channel antagonists on DA release reflect changes in the excitability of DA axons or of cholinergic interneurons. It is therefore necessary to confirm the role of axonal K^+ channels in the regulation of DA release in the absence of cholinergic input. Furthermore, since K^+-dependent gating of DA release is likely to reflect

changes in axonal excitability and AP waveform, it is unclear how the electrogenic properties of the DAT might interact with these processes. This chapter will explore the involvement of voltage-gated K^+ channels and the dependence of K^+-dependent gating on DAT function.

3.1.3 DAT functions at DA axons

The DAT also regulates STP; DAT inhibition limits paired-pulse facilitation at short intervals, and relieves STD at longer intervals (Platt 2012). Classically, the role of the DAT in DA neurotransmission has been considered purely as an uptake transporter, coupling DA transport from the extracellular space to the Na^+ gradient across the axonal membrane. However, the DAT has also been shown to regulate other aspects of DA neuron physiology, which may be relevant to its role in STP.

DA transport mediated by the DAT is electrogenic; each transport cycle transfers one DA molecule, two Na^+ ions and one Cl^- ion into the cell (McElvain & Schenk 1992; Gu et al. 1994). In addition to this electrogenic stoichiometry, the DAT also mediates a transport-coupled current that results in a total current greater than that predicted by transport stoichiometry alone (Sonders et al. 1997). This depolarising current is carried by movement of Cl^- ions out of the cell, is also blocked by cocaine, and can be large enough to depolarise the membrane potential of DA neurons in acute midbrain slices (Ingram et al. 2002; Sonders et al. 1997). Studies in *C. elegans* have demonstrated that the DAT can mediate channel-like activity underlying this Cl^- conductance (Carvelli et al. 2004), and that enhancement of this current by mutation of regulatory elements of the transporter can increase DA release and trigger pathological behaviour (Carvelli et al. 2008). Uptake of dopamine via the DAT can therefore depolarise DA neurons, and inhibition of the DAT may hyperpolarise these neurons. Given that the subcellular distribution of the DAT in DA neurons is weighted toward axonal and dendritic processes (Nirenberg et al. 1996), it may be that the local effects of DAT activity on membrane potential are larger in these compartments than those measured at the soma.

In addition to its roles in DA uptake and regulation of membrane potential, the DAT is thought to regulate the mobilisation of DA vesicles at release sites. Inhibition of the DAT with cocaine increases DA release independently of reduced uptake (Stamford et al. 1989; Lee et al. 2001; Hoffman et al. 2016), and this effect is maintained when the readily-releasable pool of DA vesicles is depleted (Venton et al. 2006). The cocaine-induced increase in release is absent in mice lacking synapsins, a family of vesicle proteins that support segregation of and movement between vesicle pools (Venton et al. 2006; Kile et al. 2010). Relief of STD, as observed during DAT inhibition, has also been observed in other central neurons following genetic deletion of synapsins (Pieribone et al. 1995; Hilfiker et al. 1998). This suggests that cocaine increases DA release by mobilising vesicles from a reserve pool of vesicles, and implies that an interaction between the DAT and synapsins is required to maintain vesicle pool segregation. It has been suggested that only the synapsin III isoform is expressed in DA neurons (Bogen et al. 2006), and the cocaine-induced increase in DA release is similarly reduced in synapsin III knock-out (S3KO) as in mice lacking all known synapsin isoforms (Kile et al. 2010). However, the effects of DAT inhibition on STP are maintained in S3KO animals (Platt 2012) suggesting either that the role of the DAT in STP is not synapsin-dependent, or that DA axons express additional redundant synapsin isoforms that also interact with the DAT. In support of the latter possibility, co-immunoprecipitation of the DAT with synapsin Ib in mouse brain homogenates has been reported (Maiya et al. 2007).

These diverse roles in DA neuron physiology suggest that the DAT is well-placed to shape presynaptic STP, and previous evidence shows that DAT inhibition alters the frequency-dependence of DA release (Platt 2012; Zhang et al. 2009). The DAT regulates aspects of Ca^{2+}-dependent vesicular release, and is likely to influence axonal excitability. This chapter will explore the effects of DAT inhibition on sensitivity to changes in P_r and K^+-dependent gating of STP.

3.1.4 Hypotheses

In this chapter I will therefore investigate the following hypotheses:

1. A stronger relationship between P_r and STP of DA release is masked by mechanisms underlying STD
2. K^+-dependent gating of STP is mediated by axonal K^+ channels
3. The DAT regulates STP and interacts with both Ca^{2+}-dependent and K^+-dependent mechanisms

3.2 Methods

Experiments described in this chapter were carried out according to the general methods laid out in Chapter 2. Variations and further details are described below.

3.2.1 Slice preparation

All experiments in this chapter were performed in slices from adult wild-type C57Bl/6NCrl mice, and were conducted in accordance with a UK Home Office-approved project license and local guidelines.

Slices were prepared as described in Chapter 2.

3.2.2 Fast-scan cyclic voltammetry (FCV)

FCV was carried out as described in Chapter 2.

In each experiment in this chapter, the ionic composition of aCSF was altered. To manipulate $[Ca^{2+}]_o$, $[CaCl_2]$ was reduced or increased accordingly. Where $[K^+]_o$ was reduced, KCl was replaced with NaCl and KH_2PO_4 was replaced with NaH_2PO_4. As a result, 5 mM $[K^+]_o$ contained (in mM) 3.77 KCl, 124.3 NaCl and 1.23 KH_2PO_4, while 1 mM $[K^+]_o$ contained 1.00 KCl, 127.1 NaCl and 1.23 NaH_2PO_4. This small increase in $[Na^+]$ (4 mM total), relative to the high concentration of NaCl in control aCSF (150.3 mM total), was not considered likely to interfere with our findings. Concentrations of all other ions remained unchanged.

3.2.3 Stimulation & experimental design

$[DA]_o$ transients were evoked by electrical stimulation using 200 µs pulses of 0.6 mA current, as described in Chapter 2.

A paired-pulse paradigm was used to investigate STP. Single pulse (1p) and paired pulse (2p) stimulations with inter-pulse intervals of 10-100 ms (corresponding to instantaneous frequencies of 10-100 Hz) were applied at 2.5 minute intervals, with paired pulses at each IPI applied in

pseudorandom order and in triplicate. IPIs of 40-100 ms, corresponding to instantaneous frequencies of 10-25 Hz, were chosen because they fall within the range of frequencies most commonly observed during burst firing in DA neurons *in vivo* (Grace & Bunney 1984a; Hyland et al. 2002). Spike pairs at 10 - 25 ms IPIs, corresponding to 40 – 100 Hz instantaneous frequency, have been rarely observed during burst firing in DA neurons (Hyland et al. 2002; Cohen et al. 2012) but allow investigation of the mechanisms underlying short-term facilitation and changes in P_r (Rice & Cragg 2004; Jennings et al. 2015).

Extracellular DA in response to a single pulse (1p $[DA]_o$) was interpreted as a measure of average P_r across a population of DA release sites (Cragg 2003). Paired-pulse ratios were used as a measure of STP, defined by the ratio P2/P1 where P1 is peak $[DA]_o$ following initial stimulation and P2 is peak $[DA]_o$ attributable to the second stimulation. Since the IPIs used in these experiments do not exceed the time between successive FCV sweeps at 8 Hz (i.e. 125 ms), the $[DA]_o$ transients evoked by each stimulation appear summated and cannot be separately resolved. To determine P2, the average of 1p $[DA]_o$ transients measured 2.5 minutes before and 2.5 minutes after the paired pulse stimulation was subtracted from the summated 2p transient (**Fig. 3.1**).

Where $[Ca^{2+}]_o$ and $[K^+]_o$ were varied concurrently, $[Ca^{2+}]_o$ was varied within each experiment, while $[K^+]_o$ was varied between subjects. In these experiments, $[Ca^{2+}]_o$ was varied in the following pattern (in mM): 2.4, 1.2, 2.4, 3.6, 2.4, with all stimulations performed in triplicate at each stage. Data from repeat stimulations at 2.4 mM $[Ca^{2+}]_o$ were pooled to control for the effects of signal run-down during the experiment. In other experiments, the order of changes in ion concentration was varied. Measurements in control conditions were always collected after 1p $[DA]_o$ was stable and before the application of drugs.

Each individual experiment was conducted in a single site, one site per animal (n = number of animals). Sites in CPu were located in the dorsal half of the striatum, while sites in NAc were within 100 µm of the anterior commissure (NAc core).

3.2.4 Drugs

All drugs were diluted to their final concentration in carbogenated aCSF and bath-applied. All experiments in this chapter were conducted in the presence of dihydro-β-erythroidine (DHβE, 1 µM) to block cholinergic signalling via β2-subunit-containing nicotinic acetylcholine receptors. Where 'control conditions' are referred to, the presence of 1 µM DHβE is assumed.

DHβE and UK78282 were obtained from Tocris Biosciences. Cocaine hydrochloride and 4-aminopyridine (4-AP) were obtained from Sigma. Drugs were dissolved in deionised water or dimethyl sulphoxide (UK78282) to prepare stock aliquots at 1,000-10,000x final concentration.

3.2.5 Data analysis

Data were analysed as described in Chapter 2. Means were compared using unpaired t-test or two-way ANOVA with post-hoc Sidak's tests using Graphpad Prism 6.

3.3 Results

3.3.1 K+-dependent gating does not alter release-dependence of STP

Previous work in this laboratory has demonstrated that a decrease in $[K^+]_o$, thought to alter membrane excitability and repolarisation, can relieve presynaptic STD of DA release (Platt 2012). Since changes in action potential waveform can influence presynaptic Ca^{2+} entry (Sabatini & Regehr 1997), it is possible that limiting STD by reducing $[K^+]_o$ will relieve a clamp on the sensitivity of STP to changes in P_r, driven by variation in $[Ca^{2+}]_o$. I investigated whether the $[K^+]_o$-dependent gating of STP could limit the sensitivity of STP to changes in $[Ca^{2+}]_o$.

An interaction between the effects of changes in $[Ca^{2+}]_o$ and $[K^+]_o$ on STP was investigated firstly in CPu. Evoked $[DA]_o$ was strongly dependent on $[Ca^{2+}]_o$ (**Fig. 3.2A, B**), as previously demonstrated (Bull et al. 1990; Chen & Rice 2001; Cragg 2003). Axonal K_v1 channels have been shown to limit excitability in hippocampal neurons (Rama et al. 2017), and if K^+ channels perform a similar function at DA axons then lowering $[K^+]_o$ might be expected to reduce initial release. However, despite a slight tendency toward higher 1p $[DA]_o$ in 1 mM vs 5 mM $[K^+]_o$, consistent with previous findings (Platt 2012), no significant difference was observed (**Fig. 3.2C**; Unpaired t-test; $p > 0.05$; $n = 10$). The sensitivity of 1p $[DA]_o$ to changes in $[Ca^{2+}]_o$ was also not significantly altered by a reduction in $[K^+]_o$ (**Fig. 3.2D**; Two-way ANOVA; $p > 0.05$; $n = 10$).

When paired-pulse stimulation was delivered, STF was observed at 10 ms IPI and STD at 100 ms IPI in both 5 mM $[K^+]_o$ (**Fig. 3.2E**) and 1 mM $[K^+]_o$ (**Fig. 3.2F**). To test the possibility that reducing $[K+]_o$ may enhance the sensitivity of P2/P1 to $[Ca^{2+}]_o$ in a IPI-dependent manner, we looked for an interaction between $[Ca^{2+}]_o$ and $[K^+]_o$ at each IPI. However, no significant interaction was observed at either 10 ms or 100 ms IPI (**Fig. 3.2G, H**; Two-way ANOVA; $p > 0.05$, $n = 10$), suggesting that K^+-dependent modulation of STP does not significantly enhance the sensitivity of STP to initial release in CPu.

In NAc, $[DA]_o$ was dependent on $[Ca^{2+}]_o$ (**Fig. 3.3A, B**). 1p $[DA]_o$ in 2.4 mM $[Ca^{2+}]_o$ was not significantly different in 1 mM vs 5 mM $[K^+]_o$ (**Fig. 3.3C**; Unpaired t-test; $p > 0.05$; $n = 7$), and the sensitivity of 1p $[DA]_o$ to changes in $[Ca^{2+}]_o$ was not significantly altered by a reduction in $[K^+]_o$ (**Fig. 3.3D**; Two-way ANOVA; $p > 0.05$; $n = 7$). Similar to CPu, STF was observed at 10 ms IPI and STD at 100 ms IPI in both 5 mM $[K^+]_o$ (**Fig. 3.3E**) and 1 mM $[K^+]_o$ (**Fig. 3.3F**). No significant interaction between $[K^+]_o$ and $[Ca^{2+}]_o$ was observed at either IPI (**Fig. 3.3G, H**; Two-way ANOVA; $n = 7$). Modulation of STP by a K^+-dependent mechanism is therefore unlikely to mask sensitivity to variability in initial release driven by changes in $[Ca^{2+}]_o$.

3.3.2 DAT inhibition enhances release-dependence of STP

The dopamine transporter (DAT) is a key regulator of the frequency dependence of STP, promoting short-term facilitation at short intervals and short-term depression at longer intervals (Platt 2012). The DAT may also limit the sensitivity of STP to P_r, since cocaine appears to increase P2/P1 at longer IPIs to a greater extent in low $[Ca^{2+}]_o$ (Platt 2012).

I explored whether inhibition of the DAT with cocaine could increase the sensitivity of STP to changes in $[Ca^{2+}]_o$ in CPu. Cocaine (5 µM) increased the magnitude and decreased the rate of decay of $[DA]_o$ transients, and peak $[DA]_o$ was lower when $[Ca^{2+}]_o$ was reduced in both control conditions and in the presence of cocaine (**Fig. 3.4A, B**). The effect of cocaine on 1p $[DA]_o$ was dependent on $[Ca^{2+}]_o$ (**Fig. 3.4C**; Two-way ANOVA, $[Ca^{2+}]_o$ x cocaine interaction; $F_{1, 12} = 4.791$; $p = 0.049$; $n = 4$). In cocaine, 1p $[DA]_o$ normalised to control was significantly greater in 1.2 mM vs 2.4 mM $[Ca^{2+}]_o$ (*post-hoc* Sidak's test; $p = 0.019$), consistent with previous observations (Kile et al. 2010).

In control conditions, P2/P1 was not significantly altered by a reduction in $[Ca^{2+}]_o$, as observed previously (**Fig. 3.4D**; Two-way ANOVA; $p > 0.05$; $n = 4$). In the presence of cocaine, there was a significant IPI-dependent effect of $[Ca^{2+}]_o$ (**Fig. 3.4E**; Two-way ANOVA, $[Ca^{2+}]_o$ x IPI interaction; $F_{3,}$

$_{24}$ = 3.415; p = 0.034; n = 4); P2/P1 was increased in 1.2 mM vs 2.4 mM $[Ca^{2+}]_o$ at 10, 25 and 40 ms IPI but not 100 ms IPI (*post-hoc* Sidak's test; p < 0.05).

To determine whether the effect of changes in $[Ca^{2+}]_o$ on STP was greater in the presence of cocaine, the presence of an interaction was investigated at each IPI. At 10 ms IPI, decreasing $[Ca^{2+}]_o$ significantly enhanced STF (**Fig. 3.4F**; Two-way ANOVA, main effect of $[Ca^{2+}]_o$; $F_{1, 12}$ = 11.78; p = 0.005; n = 4) but this effect was not altered in the presence of cocaine, suggesting that sensitivity to $[Ca^{2+}]_o$ is similar in the presence and absence of DAT inhibition at this interval. At 25 ms IPI, reducing $[Ca^{2+}]_o$ increased P2/P1 to a greater extent in cocaine than in control conditions (**Fig. 3.4G**; Two-way ANOVA, $[Ca^{2+}]_o$ x cocaine interaction; $F_{1, 12}$ = 17.02; p = 0.001; n = 4); P2/P1 was significantly greater in cocaine vs control at 1.2 mM but not 2.4 mM $[Ca^{2+}]_o$ (*post-hoc* Sidak's test; p < 0.001). At 40 and 100 ms IPI, there was no significant effect of $[Ca^{2+}]_o$ in the presence or absence of cocaine (**Fig. 3.4I**; Two-way ANOVA; p > 0.05; n = 4). These data suggest that DAT inhibition enhances the release-dependence of STP at 25 ms IPI, but has smaller effects at longer intervals. The DAT can therefore limit the relationship between P_r, as controlled by $[Ca^{2+}]_o$, and STP in an IPI-dependent manner.

3.3.3 DAT inhibition does not reveal a modulatory effect of K^+-dependent gating on release-dependence

Since inhibition of the DAT appears to relieve a clamp on release-dependence of STP, I explored whether this might also reveal an interaction between K^+-dependent gating and release-dependence that was not present under control conditions (**Fig. 3.2**).

In CPu, $[Ca^{2+}]_o$ was varied in either 1 mM or 5 mM $[K^+]_o$, in the presence of 5 µM cocaine (**Fig. 3.5A, B**). In 5 mM $[K^+]_o$, decreasing $[Ca^{2+}]_o$ promoted facilitation (5 mM $[K^+]_o$, **Fig. 3.5C**; Two-way ANOVA, main effect of $[Ca^{2+}]_o$; $F_{2, 24}$ = 15.57; p > 0.001; n = 5); P2/P1 was significantly increased in 1.2 mM vs 2.4 mM $[Ca^{2+}]_o$ at 10 ms but not 100 ms IPI (*post-hoc* Sidak's test; p < 0.05). In 1 mM $[K^+]_o$, decreasing $[Ca^{2+}]_o$ also promoted facilitation (**Fig. 3.5D**; Two-way ANOVA, $[Ca^{2+}]_o$ x IPI

interaction; $F_{2, 24} = 13.64$; $p > 0.001$; n = 5); P2/P1 was significantly increased in 1.2 mM vs 2.4 mM $[Ca^{2+}]_o$ at 10 ms but not 100 ms IPI (*post-hoc* Sidak's test; $p < 0.05$). However, no significant interaction between the effects of $[Ca^{2+}]_o$ and $[K^+]_o$ was observed at either IPI (**Fig. 3.5E, F**; Two-way ANOVA; n = 10). While corroborating the effect of DAT inhibition on release-dependence, inhibition of the DAT combined with K^+-dependent relief of STD does not reveal a greater relationship between P_r and STP than DAT inhibition alone.

3.3.4 K^+-dependent gating is dependent on DAT function

Since the effect of changing $[K^+]_o$ appeared weaker in the presence of cocaine than in control conditions (compare **Figs. 3.1 & 3.4**), the relationship between the DAT and K^+-dependent gating of STP was also investigated by varying $[K^+]_o$ in control conditions and in the presence of 5 µM cocaine.

In CPu, changes in $[K^+]_o$ did not appear to alter the shape or magnitude of DA transients, while cocaine increased the magnitude and decreased the rate of decay, as expected (**Fig. 3.6A, B**). 1p $[DA]_o$ was significantly increased by the presence of cocaine, but not altered by a reduction in $[K^+]_o$ in either control conditions or the presence of cocaine (**Fig. 3.6C**; Two-way ANOVA, main effect of cocaine; $F_{1, 12} = 307.1$; $p < 0.001$; n = 4). With paired-pulse stimulation, P2/P1 was significantly modulated by $[K^+]_o$ in control conditions, but not in cocaine (Control, **Fig. 3.6D**; Two-way ANOVA, main effect of $[K^+]_o$; $F_{1, 18} = 20.47$; $p < 0.001$; n = 4; Cocaine, **Fig. 3.6E**; Two-way ANOVA; n = 4); in control conditions, P2/P1 was significantly increased in 1 mM vs 5 mM $[K^+]_o$ at 25 ms IPI (*post-hoc* Sidak's test; $p = 0.003$).

An interaction between the effects of $[K^+]_o$ and cocaine on STP in CPu varied depending on IPI. At 10 ms IPI, P2/P1 was altered in the presence of cocaine, but was not affected by $[K^+]_o$ (**Fig. 3.6F**; Two-way ANOVA, main effect of cocaine; $F_{1, 12} = 430.6$; $p < 0.001$; n = 4); P2/P1 was significantly decreased in cocaine vs control in both 5 mM and 1 mM $[K^+]_o$ (*post-hoc* Sidak's test; $p > 0.001$). At 25 ms IPI, cocaine prevented the effects of a reduction in $[K^+]_o$ on P2/P1 (**Fig. 3.6G**; Two-way

ANOVA, cocaine x $[K^+]_o$ interaction; $F_{1, 12} = 7.686$; $p = 0.017$; $n = 4$); P2/P1 was significantly increased in 1 mM vs 5 mM $[K^+]_o$ in control conditions but not in cocaine (*post-hoc* Sidak's test; $p = 0.007$). At 100 ms IPI, P2/P1 was significantly altered by a reduction in $[K^+]_o$, not by cocaine (**Fig. 3.6H**; Two-way ANOVA, main effect of $[K^+]_o$; $F_{1, 12} = 5.815$; $p = 0.03$; $n = 4$); P2/P1 was significantly increased in 1 mM vs 5 mM $[K^+]_o$ in control conditions but not in cocaine (*post-hoc* Sidak's test; $p = 0.03$).

The relationship between the effects of cocaine and $[K^+]_o$ were also investigated in NAc. As in CPu, varying $[K^+]_o$ did not alter the magnitude of DA transients (**Fig. 3.7A, B**). 1p $[DA]_o$ was not significantly altered by changes in $[K^+]_o$ or by cocaine, although there was a tendency toward greater mean $[DA]_o$ in cocaine (**Fig. 3.7C**; Two-way ANOVA; $n = 3$). P2/P1 was significantly increased by decreasing $[K^+]_o$ in control conditions, but not in the presence of cocaine (Control, **Fig. 3.7D**; Two-way ANOVA, main effect of $[K^+]_o$; $F_{2, 12} = 151.8$; $p < 0.001$; $n = 3$; Cocaine, **Fig. 3.7E**; Two-way ANOVA; $n = 3$); in control conditions, P2/P1 was significantly increased in 1 mM vs 5 mM $[K^+]_o$ at 25 ms IPI (*post-hoc* Sidak's test; $p = 0.027$).

In NAc, the interaction between $[K^+]_o$ and cocaine was also dependent on IPI, according to a pattern that was similar to that observed in CPu. At 10 ms IPI, P2/P1 was decreased in cocaine but was not affected by $[K^+]_o$ (**Fig. 3.7F**; Two-way ANOVA, main effect of cocaine; $F_{1, 8} = 412.6$; $p < 0.001$; $n = 3$); P2/P1 was significantly decreased in cocaine vs control in both 5 mM and 1 mM $[K^+]_o$ (*post-hoc* Sidak's test; $p > 0.001$). At 25 ms IPI, cocaine prevented the increase in P2/P1 evoked by a decrease in $[K^+]_o$ (**Fig. 3.7G**; Two-way ANOVA, cocaine x $[K^+]_o$ interaction; $F_{1, 8} = 6.756$; $p = 0.03$; $n = 3$); P2/P1 was significantly increased in control conditions but not in cocaine (*post-hoc* Sidak's test; $p = 0.040$). At 100 ms IPI, there was no significant effect of either cocaine or $[K^+]_o$ (**Fig. 3.7H**; Two-way ANOVA; $n = 3$). These findings confirm that the DAT maintains STF at short IPIs, and that DAT function is required for K^+-dependent gating of STP in both CPu and NAc.

3.3.5 K^+-dependent gating of STP requires voltage-gated K^+ channels

The role of voltage-gated K^+ (K_v) channels in K^+-dependent gating of STP was also investigated. As described above, the complement of K^+ channels at DA axons has not been extensively studied, making it difficult to attribute K^+ dependent-gating to a specific group of channels. However, since K_v channels are frequently expressed on neuronal axons and regulate axonal excitability and AP waveform, they are a promising candidate to underlie the regulation of DA release by K^+ currents.

$[K^+]_o$ was varied in the presence and absence of the non-selective K_v channel blocker 4-aminopyridine (4-AP). In CPu, 100 µM 4-AP increased the magnitude but did not appear to alter the rate of decay of DA transients (**Fig. 3.8A, B**). 1p $[DA]_o$ was significantly increased in the presence of 4-AP, and while this effect appeared larger in 1 mM vs 5 mM $[K^+]_o$, an interaction did not reach statistical significance (**Fig. 3.8C**; Two-way ANOVA, main effect of 4-AP; $F_{1, 3} = 33.63$; $p = 0.010$; $n = 4$). In control conditions, decreasing $[K^+]_o$ from 5 mM to 1 mM promoted STF at short IPIs and relieved STD at longer IPIs, as previously described (**Fig. 3.8D**; Two-way ANOVA, main effect of $[K^+]_o$; $F_{1, 24} = 47.13$; $p < 0.001$; $n = 4$); P2/P1 was significantly increased in 1 mM vs 5 mM $[K^+]_o$ at 10, 25 and 40 ms but not at 100 ms IPI (*post-hoc* Sidak's test; $p < 0.01$). In the presence of 4-AP, there was no significant effect of $[K^+]_o$ on P2/P1 (**Fig. 3.8E**; Two-way ANOVA; $n = 4$). A significant interaction between $[K^+]_o$ and 4-AP was detected at every IPI, confirming that 4-AP prevented the K^+-dependent modulation of STP (Two-way ANOVA, $[K^+]_o$ x 4-AP interaction: 10 ms IPI, **Fig. 3.8F**; $F_{1, 12} = 5.95$; $p = 0.031$; 25 ms IPI, **Fig. 3.8G**; $F_{1, 12} = 6.00$; $p = 0.031$; 40 ms IPI, **Fig. 3.8H**; $F_{1, 12} = 10.01$; $p = 0.008$; 100 ms IPI, **Fig. 3.8I**; $F_{1, 12} = 26.89$; $p < 0.001$; $n = 4$).

To exclude the possibility that the lack of K^+-dependent gating in the presence of 4-AP was caused by a ceiling effect, the effects of 4-AP on STP were also explored in increased $[K^+]_o$ in CPu, to show that 4-AP could also block a $[K^+]$-dependent decrease in P2/P1. In 7.5 mM $[K^+]_o$, 4-AP similarly increased the magnitude of $[DA]_o$ transients at all IPIs (**Fig. 3.9A, B**). 4-AP significantly increased 1p $[DA]_o$ (**Fig. 3.9C**; Two-way ANOVA, main effect of 4-AP; $F_{1, 8} = 8.811$; $p = 0.018$; $n = 3$) at 5 mM

but not at 7.5 mM $[K^+]_o$ (*post-hoc* Sidak's test; p = 0.040). In control conditions, the effect of $[K^+]_o$ on STP varied between IPIs (**Fig. 3.9D**; Two-way ANOVA, $[K^+]_o$ x IPI interaction; $F_{3, 16} = 5.994$; p = 0.006; n = 3); P2/P1 was significantly decreased in 7.5 mM vs 5 mM $[K^+]_o$ at 10, 25 and 40 ms IPI but not at 100 ms IPI (*post-hoc* Sidak's test; p < 0.05).

In 4-AP, there was no significant effect of $[K^+]_o$ on STP (**Fig. 3.9E**; Two-way ANOVA; n = 3). At 10, 25 and 40 ms IPI, 4-AP significantly reduced the effect of changing $[K^+]_o$ (Two-way ANOVA, $[K^+]_o$ x 4-AP interaction: 10 ms IPI, **Fig. 3.9F**; $F_{1, 12} = 5.951$; p = 0.031; 25 ms IPI, **Fig. 3.9G**; $F_{1, 12} = 6.003$; p = 0.031; 40 ms IPI, **Fig. 3.9H**; $F_{1, 12} = 10.01$; p = 0.008; n = 3). There was no significant interaction at 100 ms IPI (**Fig. 3.9I**; Two-way ANOVA; n = 3). 4-AP therefore prevents K^+-dependent modulation of STP in both directions, suggesting that blockade of K_v channels does not simply limit increases in P2/P1.

In NAc, the effect of 4-AP on the magnitude of DA transients was much less marked, and at some IPIs mean peak $[DA]_o$ was lower in the presence of 4-AP (**Fig. 3.10A, B**). In contrast to CPu, 1p $[DA]_o$ in NAc was not significantly altered in the presence of 4-AP, at either 1 mM or 5 mM $[K^+]_o$ (**Fig. 3.10C**; Two-way ANOVA; n = 3). There was no significant effect of $[K^+]_o$ on P2/P1 in control conditions or in 4-AP (**Fig. 3.10D**, **E**; Two-way ANOVA; n = 3), and 4-AP did not significantly alter the relationship between $[K^+]_o$ at any IPI. However, despite the lack of K^+-dependent modulation, 4-AP did enhance STD at all IPIs (Two-way ANOVA, main effect of 4-AP: 10 ms IPI, **Fig. 3.10F**; F (1, 8) = 85.05; p < 0.001; 25 ms IPI, **Fig. 3.10G**; $F_{1, 8} = 360.4$; p < 0.001; 40 ms IPI **Fig. 3.10H**; $F_{1, 8} = 108.0$; p < 0.001; 100 ms IPI, **Fig. 3.10I**; $F_{1, 8} = 53.67$; p < 0.001; n = 3); P2/P1 was significantly decreased in both 1 mM and 5 mM $[K^+]_o$ at all IPIs (*post-hoc* Sidak's test; p < 0.01).

3.3.6 Axonal Kv1.3/1.4 channels contribute to K^+-dependent gating of STP

The extent to which STD is gated by K^+ currents carried by specific channel subtypes remains unclear. I explored a role for the channels expressing the K_v1.3 or K_v1.4 α-subunits. Both channel subtypes are thought to contribute to the control of axonal excitability in other neurons; K_v1.3

channels support presynaptic STD of GABA release from cultured Purkinje cells (Kawaguchi & Sakaba 2015), while K_v1.4 channels mediate an axonal A-type current in hippocampal neurons (Cooper et al. 1998). The K_v1.4 subunit is strongly expressed in the SNc, but not in the VTA (Luján et al. 2003), and is expressed in the CPu (Sheng et al. 1992; Rhodes et al. 1997). K_v1.4 subunit mRNA has also been detected in the axonal compartment of DA neurons in primary culture (Fulton et al. 2011).

In CPu, the K_v1.3/1.4 blocker UK78282 increased evoked $[DA]_o$ in both 5 mM and 1 mM $[K^+]_o$ (**Fig. 3.11A, B**). In the presence of 5 µM UK78282, 1p $[DA]_o$ was increased in the presence of UK78282 in a manner that did not depend on $[K^+]_o$ (**Fig. 3.11C**; Two-way ANOVA, main effect of UK78282; $F_{1, 8} = 17.59$; $p = 0.003$; $n = 3$). In contrast, the effects of UK78282 on P2/P1 were dependent on $[K^+]_o$ (**Fig. 3.11D**; Two-way ANOVA, UK78282 x $[K^+]_o$ interaction; $F_{1, 8} = 21.73$; $p = 0.002$; $n = 3$); P2/P1 was significantly lower in 5 mM vs 1 mM $[K^+]_o$ in control conditions, but not in the presence of UK78282 (*post-hoc* Sidak's test; $p < 0.05$). This may indicate that K^+-dependent gating of STP is partly mediated by the activation of K_v1.3 and/or K_v1.4 channels on DA axons. However, it is difficult to draw strong conclusions from this finding regarding the subunit composition of K_v channels involved in the regulation of STD due to the relatively weak selectivity of UK78282 for K_v1.3 and K_v1.4 at the concentration used here, which would also be expected to block ~50% of the current mediated by K_v1.2 channels (Hanson et al. 1999).

A-type currents in neuronal axons can also be mediated by K_v3.4 channels, which can regulate repolarisation rate at individual boutons in cerebellar neurons (Rowan et al. 2014; Rowan et al. 2016) and support presynaptic STP at corticostriatal synapses (Meneses et al. 2016). Pilot data ($n = 1$) suggest that BDS-I, a specific blocker of K_v3.4 channels, can limit K^+-dependent gating in a similar manner to UK78282, but does not alter peak $[DA]_o$ (**Fig. 3.12**). K^+-dependent gating may therefore arise from the combined actions of multiple axonal K_v channel subtypes with different effects on DA release.

3.4 Discussion

In this chapter I have explored the interactions between P_r, axonal excitability and DAT function in shaping STP of DA release. The relationship between P_r and STP was limited principally by the DAT, but not by K^+-dependent gating, which was dependent on voltage-gated K^+ channels and supported by the DAT. The channels supporting K^+-dependent gating appeared to include axonal $K_v1.3/1.4$ channels. This section will summarise and discuss these findings, highlighting the key role of the DAT in maintaining region-specific patterns of STP.

3.4.1 Release-dependence of STP

Previous work in this group has identified characteristic mechanisms underlying STP of DA release. Firstly, classical release-dependent STF was shown to occur only at short IPIs in NAc (10 - 25 ms), with no significant modulation in CPu. Second, changes in $[K^+]_o$, thought to alter excitability and/or repolarisation of the axonal membrane following AP propagation, were inversely correlated to P2/P1 across a range of IPIs, with more prominent effects in CPu than in NAc. Third, pharmacological inhibition of the DAT limited STF at short IPIs in both regions, and relieved STD at longer IPIs in CPu but not NAc. I have extended these findings by investigating the interactions between these mechanisms to shape DA release.

The weak sensitivity of STP to variation in initial release driven by changes in $[Ca^{2+}]_o$ might be explained by an alternative mechanism clamping the relationship between initial release and STP. I investigated whether reducing $[K^+]_o$ to relieve the powerful STD that dominates DA release would reveal a stronger modulation of STP by changes in initial release. STD is relieved by a reduction in $[K^+]_o$, which might release a clamp on the release-dependence of STP and render P2/P1 sensitive to changes in initial release.

Reducing $[K^+]_o$ relieved STD more readily in CPu than in NAc, and the effect of changing $[Ca^{2+}]_o$ appeared stronger in NAc, consistent with previous findings, However, changing $[K^+]_o$ did not

significantly increase sensitivity of STP to changes in Ca^{2+}. This suggests that relief of STD may slightly increase sensitivity of plasticity to initial release, but that this does not reveal a release-dependent mechanism like that observed at glutamatergic synapses in the hippocampus or calyx of Held. This raises two main possibilities; that release-dependent mechanisms of plasticity do not play a key role in STP of DA release, or that an alternative mechanism operating at DA release sites acts to limit release-dependence of STP.

3.4.2 DAT function limits release-dependence

The role of the DAT in STP represents a second candidate mechanism for masking a stronger relationship between initial release and plasticity at DA release sites. The DAT appears to contribute to mechanisms underlying both STF and STD of DA release. Inhibition of the DAT reduced PPR at short IPIs, probably because initial release is increased during DAT block (Lee et al. 2001) and STP at these short intervals is release-dependent. At longer intervals, DAT inhibition relieves STD, suggesting that, under drug-free conditions, the DAT limits release-dependence while promoting a $[K^+]$-sensitive mechanism underlying STD. DAT function might therefore mask a stronger relationship between initial release and STP at DA release sites. We investigated whether inhibition of the DAT with cocaine could increase the sensitivity of STP to changes in initial release in CPu. A reduction in $[Ca^{2+}]_o$ increased P2/P1 to a significantly greater extent in the presence of cocaine than in control conditions, suggesting that the DAT acts to limit the release-dependence of STP. The DAT might therefore limit a relationship between initial DA release and STP through several possible candidate mechanisms.

The DAT is thought to limit dopamine release by supporting the function of synapsins. Synapsins are synaptic vesicle proteins which regulate the segregation of different release pools within neurotransmitter release sites (Greengard et al. 1993). In their dephosphorylated state, synapsins direct vesicles away from the active zone, into the reserve pool, while activity-dependent phosphorylation triggers transfer to the readily-releasable pool (RRP) and vesicle docking

(Bykhovskaia 2011). It is unclear how the DAT interacts with this process, but the increase in DA release following DAT inhibition appears to be synapsin-dependent, and may therefore involve mobilisation of vesicle from the reserve pool to the RRP (Venton et al. 2006; Kile et al. 2010). Expansion of the RRP enhances release (Dobrunz & Stevens 1997), and may therefore promote a release-dependent mechanism underlying the relationship between initial P_r and STP. The DAT also interacts with the SNARE protein syntaxin 1A, supporting a role in the regulation of synaptic release machinery (Lee et al. 2004).

Alternatively, the DAT might interact with VGCCs to regulate Ca^{2+} entry. Cocaine enhances DA release with greater potency in reduced $[Ca^{2+}]_o$ (see Fig. 3.4C), and can increase release even in the absence of synapsins when $[Ca^{2+}]_o$ is sufficiently low (Kile et al. 2010), supporting a synapsin-independent effect of cocaine on Ca^{2+} entry. Using optical detection of Ca^{2+}-sensitive dye in rat cortical tissue *in vivo*, cocaine has been shown to increase $[Ca^{2+}]_I$ on a population level, suggesting that cocaine might enhance Ca^{2+} entry in neurons (Du et al. 2006). Furthermore, in mice lacking the $Ca_v2.3$ VGCC α-subunit, which is thought to contribute to the high-threshold R-type Ca^{2+} current (Ertel et al. 2000), the locomotor response to cocaine is blunted (Han et al. 2002). However, $[DA]_o$ was not measured on an appropriate timescale to determine whether release was differentially influenced by cocaine (Han et al. 2002), and the role of the R-type Ca^{2+} current in DA release remains unclear due to a lack of suitable pharmacological inhibitors (Brimblecombe et al. 2015). DAT inhibitors may therefore promote Ca^{2+} entry via VGCCs, increasing DA release and enhancing the sensitivity of STP to changes in $[Ca^{2+}]_o$.

In contrast, other findings suggest that DAT inhibitors might reduce Ca^{2+} entry, since they block a DAT-mediated depolarising conductance that can activate VGCCs. A recent study in non-neuronal cultured cells transfected with human DAT, the depolarising DAT-mediated conductance associated with DA uptake promoted activation of the L-type current mediated by $Ca_v1.2$ and $Ca_v1.3$ channels (Cameron et al. 2015). DAT-dependent depolarisation has also been shown to

activate VGCCs in cultured neurons from cortex, midbrain, and hippocampus; although the specific Ca^{2+} current involved was not conclusively identified, inhibitors of the L-type current reduced the Ca^{2+} signal (Vaarmann et al. 2010). By inhibiting VGCCs, including those mediating L-type currents, DAT inhibitors might force DA release sites into a low-$[Ca^{2+}]_I$ state, which has been suggested to promote a steeper relationship between initial release and STP (Brimblecombe et al. 2015).

Taken together, these data suggest that the regulation of Ca^{2+} availability in DA terminals by the DAT is likely to be complex. The findings in this chapter suggest that there is a strong relationship between DAT function and Ca^{2+} entry, and as a result drugs such as cocaine that inhibit DAT function will shift STP of DA release to a more classical release-dependent state. Further experiments using optical detection of intracellular Ca^{2+} transients will be required to determine whether the net effect of DAT function is to increase or decrease Ca^{2+} entry, and which channel subtypes mediate the subsequent effects on DA release.

3.4.3 Axonal excitability underlies STD

In contrast to the weak influence of P_r, STP of DA release is powerfully modulated by changes in $[K^+]_o$, especially in CPu (Platt 2012). However, the mechanism underlying this K^+-dependent gating of STP remains unclear. The findings in this chapter reveal a key role of voltage-gated K^+ channels in K^+-dependent gating, which may include specific roles for Kv1.3/1.4 and Kv3.4 channels. In light of these findings, candidate mechanisms underlying K^+-dependent gating of STP will be discussed below.

Increasing the driving force for K^+ currents by decreasing $[K^+]_o$ should increase the charge transfer mediated by voltage-gated K^+ channels, but should also hyperpolarise the axonal membrane by potentiating K^+ leak, reducing overall excitability (Balestrino et al. 1986). Fast-activating K^+ currents, such as A-type and D-type currents (Connor & Stevens 1971; Storm 1990), are thought to contribute to rapid repolarisation following APs, since their cumulative inactivation contributes

to the broadening of APs during repetitive stimulation (Saviane et al. 2003; Shu et al. 2007; Geiger & Jonas 2000). Control of repolarisation rate is particularly associated with high-threshold K^+ channels, which activate late in the rising phase of the AP (Dodson & Forsythe 2004). Reducing $[K^+]_o$ may enhance these currents, due to the increased driving force, and possibly also because axonal A-type channels are thought to become de-inactivated at hyperpolarised membrane potentials (Debanne et al. 1997). Enhanced K^+ currents might mediate more rapid repolarisation following the first pulse, reducing refractoriness and enabling greater DA release at the second pulse, resulting in K^+-dependent gating of STD.

However, changes in $[K^+]_o$ are also thought to influence the rate of inactivation of K^+ channels, which might produce distinct effects on K^+ currents in DA axons. The rate of inactivation of certain K^+ channels, including K_v1 channels, is inversely related to $[K^+]_o$, such that use-dependent inactivation develops most rapidly after channel opening in the absence of extracellular K^+ (Baukrowitz & Yellen 1995; Baukrowitz & Yellen 1996). The range of $[K^+]_o$ over which this effect has been observed suggests that a decrease in $[K^+]_o$ from 5 mM to 1 mM might promote use-dependent inactivation (Baukrowitz & Yellen 1995), decreasing the conductance of some K^+ channels at the second pulse. In this case, the membrane potential at the second pulse would be depolarised, resulting in a greater recruitment of voltage-gated Na^+ channels. This increase in excitability could lead to increase DA release at the second pulse, explaining the increase in PPR in reduced $[K^+]_o$.

It is difficult to determine whether in DA axons the net effect of a reduction in $[K^+]_o$ will favour hyperpolarisation, due to an increase in the driving force for K^+ currents, or depolarisation, due to decreased conductance of K^+ channels and greater Na^+ channel recruitment. Nonetheless ,the importance of axonal K^+ currents in STP of DA release is demonstrated by the finding that K^+-dependent gating in CPu is prevented by 4-AP, a non-selective blocker that binds fast-activating voltage-gated K^+ channels with high affinity (Gutman et al. 2005). 4-AP has been shown to

broaden APs at DA neuron soma (Nedergaard 1999), and therefore might enhance STD at DA release sites, and prevent K^+-dependent gating, by prolonging repolarisation and refractoriness following an initial AP. Alternatively, 4-AP might prevent K^+-dependent gating because blocking K_v channels precludes the effect of changes in use-dependent activation.

K^+-dependent gating was also limited by UK78282, a blocker of $K_v1.4$ channels (Wulff & Zhorov 2008), which mediate a fast A-type current and are localised to the axonal compartment of neurons in the rat hippocampus and basal ganglia (Cooper et al. 1998; Sheng et al. 1992; Gutman et al. 2005). Pilot data also suggest that blocking $K_v3.4$ channels, which can also form A-type channels in axons and contribute to fast repolarisation (Rowan et al. 2016), can limit K^+-dependent gating. It should be noted that in both cases, blockade of specific K_v channel subunits increased P2/P1 in 5 mM $[K^+]_o$, but had no discernible effect in 1 mM $[K^+]_o$. This observation appears to be consistent for a prominent role of use-dependent K^+ channel inactivation in mediating the effects of changes in $[K^+]_o$ on P2/P1. In this model, K^+ conductance would be expected to be higher in 5 mM $[K^+]_o$ than in 1 mM $[K^+]_o$, explaining the greater effect of K^+ channel block in the former condition.

These findings might corroborate a role for fast-activating K^+ currents in K^+-dependent gating, although it should be noted that UK78282 also blocks $K_v1.3$ channels with similar efficacy, and would be expected to block a significant proportion of $K_v1.2$ channels at the concentration used here (Hanson et al. 1999). Expression of $K_v1.3$ channels has not been frequently described at neuronal axons, and there is currently no evidence to suggest that these channels are expressed by DA neurons. On the other hand, $K_v1.2$ channels are commonly expressed on axons (Sheng et al. 1994; Rhodes et al. 1997), and implicated in the control of terminal excitability. This lack of selectivity raises the possibility that delayed rectifier currents mediated by these channels also participate in the control of STD.

In NAc, K^+-dependent gating was not observed under control conditions, a regional distinction which will be discussed further in section 3.4.5. Nonetheless, 4-AP still potentiated STD across the full range of IPIs observed, despite the lack of an increase in 1p $[DA]_o$, in contrast to the effect observed in CPu. This demonstrates that the effects of K_v channel block on STP are dissociable from a change in initial release, consistent with the weak release-dependence described previously.

Other K^+-dependent mechanisms are also likely to be involved in regulation of STD. As well as control of repolarisation following APs, K^+ channels control longer-term changes in excitability. Since K^+ channels primarily carry outward hyperpolarising currents, axonal K^+ currents are typically thought to suppress terminal excitability (Dodson & Forsythe 2004). This would appear to contrast with the findings in this chapter, which suggest that promoting K^+ currents relieves STD. However, the effects of K^+ currents on excitability can also alter the rate of axonal conduction failures. In crayfish neurons, hyperpolarisation of the axonal membrane evoked by a decrease in $[K^+]_o$ has been shown to favour more reliable conduction of APs (Smith 1980). Failures of AP conduction have been shown to drive powerful STD at intervals up to 100 ms at glutamatergic autapses in hippocampal cultures (Brody & Yue 2000), suggesting that this could represent a candidate mechanism to underlie STD at DA release sites. Furthermore, changes in repolarisation and in excitability could interact to shape DA release, since increased refractoriness may reduce the safety factor for AP conduction (Swadlow et al. 1980). K^+-dependent gating of STP might therefore reflect a combination of changes in refractoriness and axonal conduction.

3.4.4 DAT supports K^+-dependent gating of STD

STD is modulated by changes in $[K^+]_o$ that will affect membrane polarisation and excitability, particularly in CPu. However, I have shown in this chapter that this effect is abolished when the DAT is inhibited; in both CPu and NAc, reducing $[K^+]_o$ increased P2/P1 in control conditions but not in cocaine. This suggests that DAT function might support K^+-dependent gating of STD.

It is not clear how the DAT might determine the effects of K^+ currents on STP. As described above, K^+-dependent gating is dependent on voltage-gated K^+ channels; however, a functional interaction between the DAT and K^+ channels has not been described. In a study of mouse brain homogenates, DAT was found to co-immunoprecipitate with $K_v2.1$ channels and a number of other axonal proteins (Maiya et al. 2007), suggesting that the DAT might form a protein complex at DA release sites to promote interactions with synaptic proteins and ion channels. In SPNs, somatic $K_v2.1$ channels are co-localised with sites of intracellular Ca^{2+} release (Mandikian et al. 2014), so it is possible that the DAT proteome interacts with sites of Ca^{2+} entry. Further study of the DAT proteome will be necessary to determine whether such interactions occur at the level of DA release sites.

Alternatively, the dependence of K^+-dependent gating on DAT function might represent an indirect effect via membrane excitability. DAT blockade is likely to hyperpolarise axonal membranes and reduce excitability, due to inhibition of electrogenic transport of DA and the depolarising transport-coupled anion conductance (Sonders et al. 1997; Ingram et al. 2002). Axonal hyperpolarisation has been shown to limit conduction failure at axonal branch points in crayfish neurons (Smith 1980). If conduction failure is limited or prevented during DAT inhibition, the influence of small changes in $[K^+]_o$ on axonal conduction failure rate might be sufficiently reduced to prevent significant K^+-dependent gating. If DAT inhibition does reduce the rate of AP failure, it might be expected to relieve STD at longer intervals, an effect which has been observed in previous studies of DA release (Platt 2012).

3.4.5 STP across striatal regions

This chapter has determined a functional hierarchy of mechanisms underlying STP of DA release, and shown that this hierarchy differs subtly between functional regions of the striatum. In the CPu, STP is insensitive to changes in $[Ca^{2+}]_o$ over intervals of 10-100 ms, while in NAc STP is inversely related to $[Ca^{2+}]_o$ at short IPIs. Inhibition of the DAT enhanced sensitivity to Ca^{2+} in CPu,

demonstrating that DAT function regulates Ca^{2+} handling at DA release sites. As a result, Ca^{2+} sensitivity in the two regions appeared more similar, although a formal comparison was not conducted. STP in both regions was sensitive to changes in $[K^+]_o$ under control conditions, but the inverse relationship between P2/P1 and $[K^+]_o$ appeared stronger in CPu than in NAc under control conditions. During DAT inhibition, K^+-dependent gating was absent in both regions, again suggesting that STP across the functional regions of the striatum had become more homogenous.

It is therefore possible that the differences in DAT function underlie the distinct patterns of STP in the two major functional regions of the striatum. DAergic projections to these two regions differ in terms of their Ca^{2+} handling and axonal morphology, with large, complex, calbindin-negative axons typically projecting to the CPu, and less extensively-branched, calbindin –positive neurons projecting to NAc. The roles of the DAT in VGCC function, vesicle handling and excitability may promote the contributions of these distinct characteristics to STP.

These data raise the intriguing possibility that a difference in the properties of DA axons projecting to separate functional regions of the striatum might underlie distinct patterns of STP and hence specialised information processing. Axons projecting to the dorsal striatum are thought to have a greater average terminal arborisation than those projecting to the ventral striatum and NAc (Prensa & Parent 2001; Aransay et al. 2015; Pacelli et al. 2015), and consequently form large numbers of axonal branch points and boutons (Matsuda et al. 2009; Bolam & Pissadaki 2012). The complex geometry at sites such as these create an impedance mismatch that can underlie AP conduction failure (Lüscher & Shiner 1990; Grossman et al. 1979b; Grossman et al. 1979a). Differential conduction fidelity in axons projecting to distinct functional regions of the striatum might therefore promote stronger STD in CPu which is readily tuned by modulation of K_v channel activity, as compared to less frequency-sensitive plasticity in NAc which is instead more sensitive to classical release-dependent mechanisms.

There are differences in DAT function between CPu and NAc that lend support to this argument. Levels of DAT expression, as measured using uptake assays in synaptosomes and autoradiography, appear approximately 3-fold higher in CPu than in NAc (Marshall et al. 1990), and in Michaelis-Menten models the maximal rate of DA uptake in CPu is higher than in NAc, suggesting a greater number of uptake sites (Jones et al. 1995). If DAT expression is higher in DA axons projecting to CPu, it might be expected that these axons will be more strongly depolarised by channel activity mediated by the DAT, and therefore more sensitive to changes in the threshold for conduction failure (Smith 1980). This might also explain why STD is relieved by DAT inhibition at 2.4 mM $[Ca^{2+}]_o$ in CPu, but not in NAc (Platt 2012). Furthermore, DAT inhibition will increase the size of the readily-releasable vesicle pool in both regions by disruption of synapsin function, limiting the difference in sensitivity to changes in $[Ca^{2+}]_o$ due to the altered intra-terminal Ca^{2+} summation associated with fast buffering in NAc but not CPu. Again, if DAT expression is greater in CPu, it seems likely that the increase in Ca^{2+} sensitivity would be greatest in this region; while the effect of cocaine on Ca^{2+} sensitivity was not tested in this chapter, previous evidence suggests that the effect may indeed be greater in CPu than in NAc.

3.4.6 Summary and implications

In this chapter I have shown that diversity in the properties of DA axons projecting to striatum underlie distinct patterns of frequency-dependent presynaptic plasticity in CPu and NAc. Specifically, I have shown that membrane excitability, modulated by currents through voltage-gated K^+ channels, underlies release-independent STD of DA release. Furthermore, sensitivity of STP to changes in initial release is limited by the DAT, but not by K^+-dependent gating, and K^+-dependent gating is dependent on DAT function. This defines a region-specific hierarchy of mechanisms controlling STP, with the DAT as a master regulator underlying regional specificity of frequency-dependent STP.

The findings presented in this chapter and elsewhere (Rice & Cragg 2004; Platt 2012) suggest that STP of DA release may be optimised to enhance contrast between high-frequency and low-frequency bursts, due to STF at very short IPIs and powerful STD at relatively longer IPIs. Furthermore, the range of frequency filtering differs between the major functional regions of the striatum; STF in the CPu is limited to shorter IPIs than in NAc, suggesting that release in CPu is optimised to enhance contrast at higher frequencies than in NAc. This regionally specialised frequency filtering may contribute to the different responses of DA release to presynaptic stimulation across striatal regions (Brown et al. 2011), and to the differing roles of these regions in behaviour.

The findings presented in this chapter also suggest that the specialisation of frequency filtering between striatal regions is dependent on differences in the properties of DA axons projecting to each region. However, the roles of these mechanisms in STP appeared to be entirely dependent on the function of the DAT. When the DAT is inhibited, patterns of STP in the two regions appear to become more similar, suggesting that the specialisation of frequency filtering may be disrupted. This may have important implications for the effects of DAT inhibitors on behaviour. Studies of the development of addiction suggest that the progression from voluntary goal-directed behaviour to pathological habitual reward-seeking is associated with a shift in dependence on striatal function from the NAc core to the dorsolateral striatum, with a key role for the DMS during training, in a manner that is dependent on intact DA innervation (Everitt & Robbins 2013). By limiting the specialisation of DA release properties between these regions, DAT inhibitors might promote the conditions for this shift to occur, contributing to their addictive properties. However, it is worth noting that not all DAT inhibitors are addictive; further work will be required to determine whether different drugs in this class inhibit particular aspects of DAT function, providing a basis for this diversity of dependence liability.

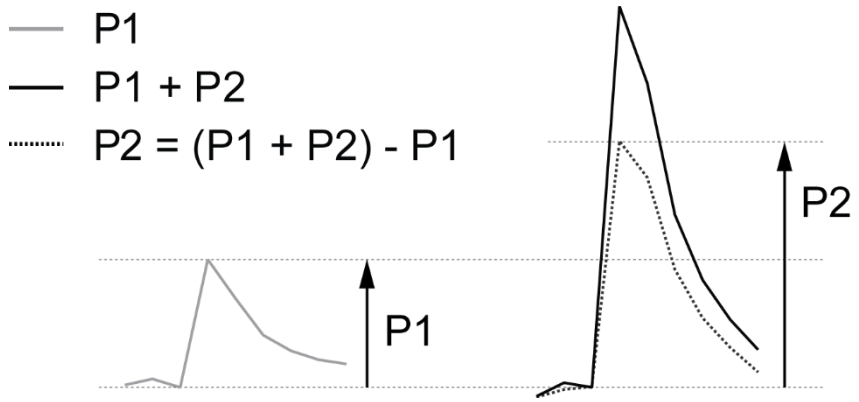

Fig. 3.1 Method of subtraction to determine P2/P1

Where paired-pulse stimulation is delivered at subsecond intervals, $[DA]_o$ from each pulse summates to form a single transient. In order to determine release attributable to the second pulse (P2, dotted line), the transient evoked by a single pulse (P1, grey) is subtracted from the summated transient (P1 + P2, black). The ratio of peak $[DA]_o$ attributable to each pulse (P2/P1) is then calculated as a measure of STP.

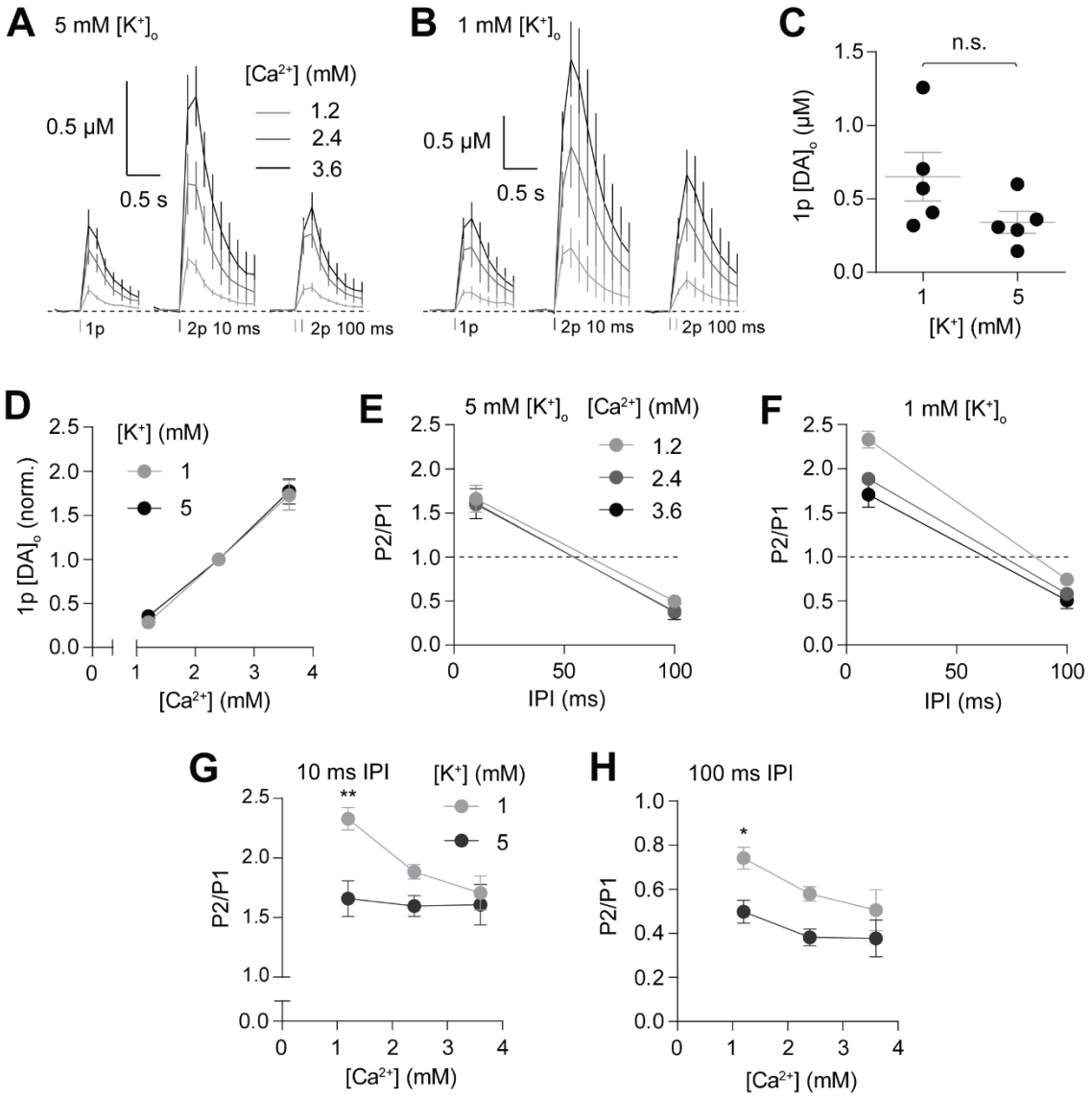

Fig. 3.2 K^+-dependent relief of STD does not enhance release-dependence of STP in CPu

(A, B) Average profiles of $[DA]_o$ transients (mean $[DA]_o$ ± SEM) elicited by single or paired pulses in 1.2 - 3.6 mM $[Ca^{2+}]_o$ in either 5 mM $[K^+]_o$ (**A**, n = 5) or 1 mM $[K^+]_o$ (**B**, n = 5) in CPu. **(C)** Mean peak 1p $[DA]_o$ ± SEM at 2.4 mM $[Ca^{2+}]_o$. Changing $[K^+]_o$ did not significantly alter 1p $[DA]_o$. **(D)** Mean peak 1p $[DA]_o$ normalised to 2.4 mM $[Ca^{2+}]_o$. Changing $[K^+]_o$ did not significantly alter the sensitivity of 1p $[DA]_o$ to $[Ca^{2+}]_o$. **(E, F)** Mean P2/P1 ± SEM against IPI in 1.2 - 3.6 mM $[Ca^{2+}]_o$ in 5 mM $[K^+]_o$ (**E**) or 1 mM $[K^+]_o$ (**F**). Changing $[Ca^{2+}]_o$ modulated STP at 10 ms IPI in 1 mM but not 5 mM $[K^+]_o$. **(G, H)** Mean P2/P1 ± SEM at 10 ms IPI (**G**) and 100 ms IPI (**H**). Reducing $[K^+]_o$ did not significantly increase sensitivity of P2/P1 to $[Ca^{2+}]_o$. *p < 0.05, **p < 0.01.

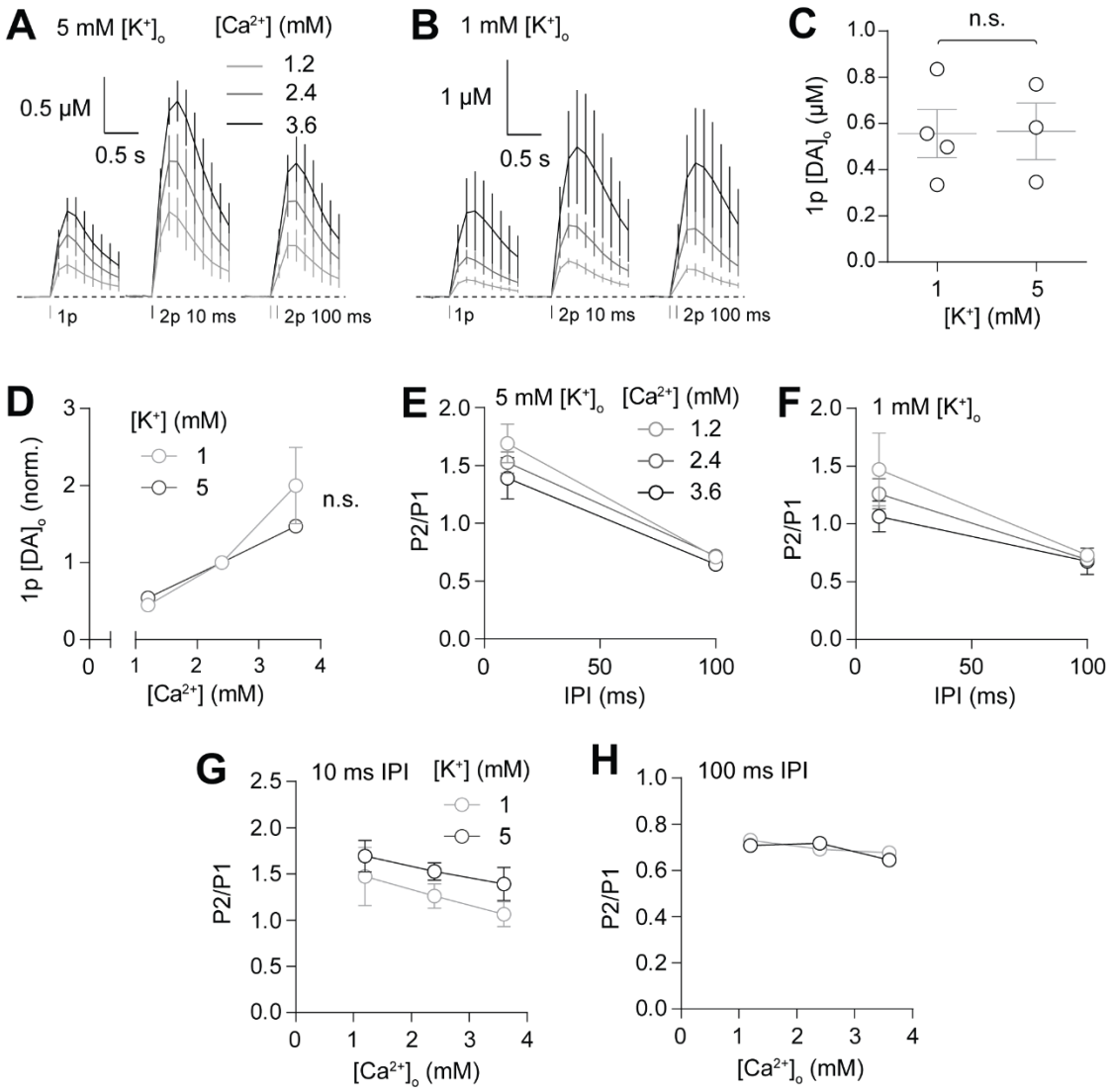

Fig. 3.3 K^+-dependent relief of STD does not enhance release-dependence of STP in NAc

(A, B) Average profiles of $[DA]_o$ transients (mean $[DA]_o$ ± SEM) elicited by single or paired pulses in 1.2 - 3.6 mM $[Ca^{2+}]_o$ in either 5 mM $[K^+]_o$ (**A**, n = 4) or 1 mM $[K^+]_o$ (**B**, n = 3) in NAc. **(C)** Mean peak 1p $[DA]_o$ ± SEM at 2.4 mM $[Ca^{2+}]_o$. Changing $[K^+]_o$ did not significantly alter 1p $[DA]_o$. **(D)** Mean peak 1p $[DA]_o$ normalised to 2.4 mM $[Ca^{2+}]_o$. Changing $[K^+]_o$ did not significantly alter the sensitivity of 1p $[DA]_o$ to $[Ca^{2+}]_o$. **(E, F)** Mean P2/P1 ± SEM against IPI in 1.2 - 3.6 mM $[Ca^{2+}]_o$ in 5 mM $[K^+]_o$ (**E**) or 1 mM $[K^+]_o$ (**F**). Changing $[Ca^{2+}]_o$ did not modulate STP in either 1 mM or 5 mM $[K^+]_o$. **(G, H)** Mean P2/P1 ± SEM at 10 ms IPI (**G**) and 100 ms IPI (**H**). Reducing $[K^+]_o$ did not significantly increase sensitivity of P2/P1 to $[Ca^{2+}]_o$.

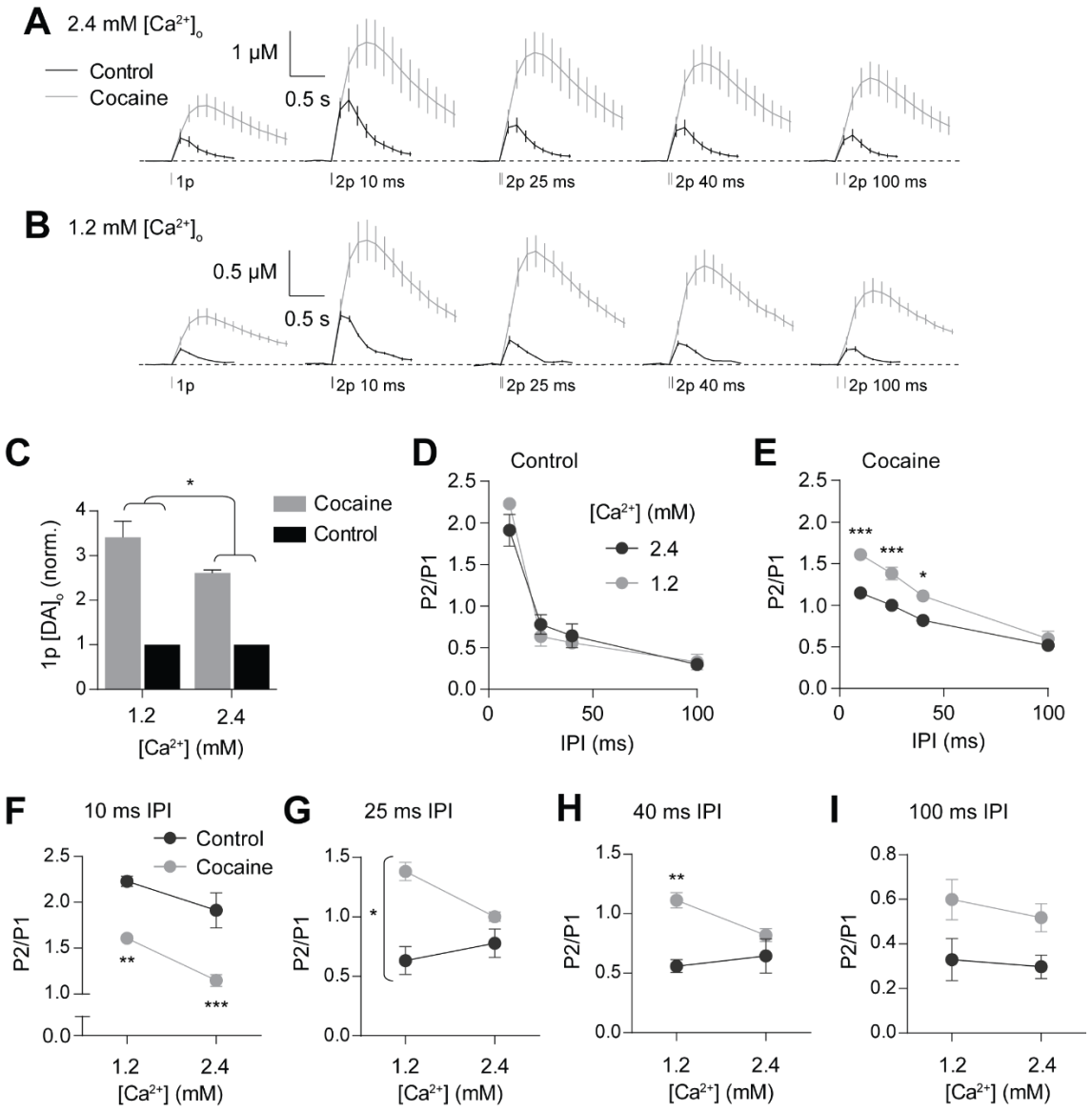

Fig 3.4 DAT inhibition enhances release-dependence of STP in CPu

(A, B) Average profiles of $[DA]_o$ transients (mean $[DA]_o$ ± SEM) elicited by single- or paired-pulses in control conditions or in cocaine in either 2.4 mM $[Ca^{2+}]_o$ (**A**) or 1.2 mM $[Ca^{2+}]_o$ (**B**) in CPu (n = 4). **(C)** Mean peak 1p $[DA]_o$ ± SEM at in control conditions or in cocaine. The cocaine-induced increase in 1p $[DA]_o$ was greater at low $[Ca^{2+}]_o$. **(D, E)** Mean P2/P1 ± SEM against IPI in 1.2 mM and 2.4 mM $[Ca^{2+}]_o$ in control conditions (**D**) or in cocaine (**E**). Reducing $[Ca^{2+}]_o$ significantly increased P2/P1 in cocaine but not control. **(F, G, H, I)** Mean P2/P1 ± SEM at 10 ms (**F**), 25 ms (**G**), 40 ms (**H**) and 100 ms (**I**) IPI. Cocaine significantly enhanced the sensitivity of STP to $[Ca^{2+}]_o$ at 25 ms IPI. *p < 0.05, **p < 0.01, *** < 0.001.

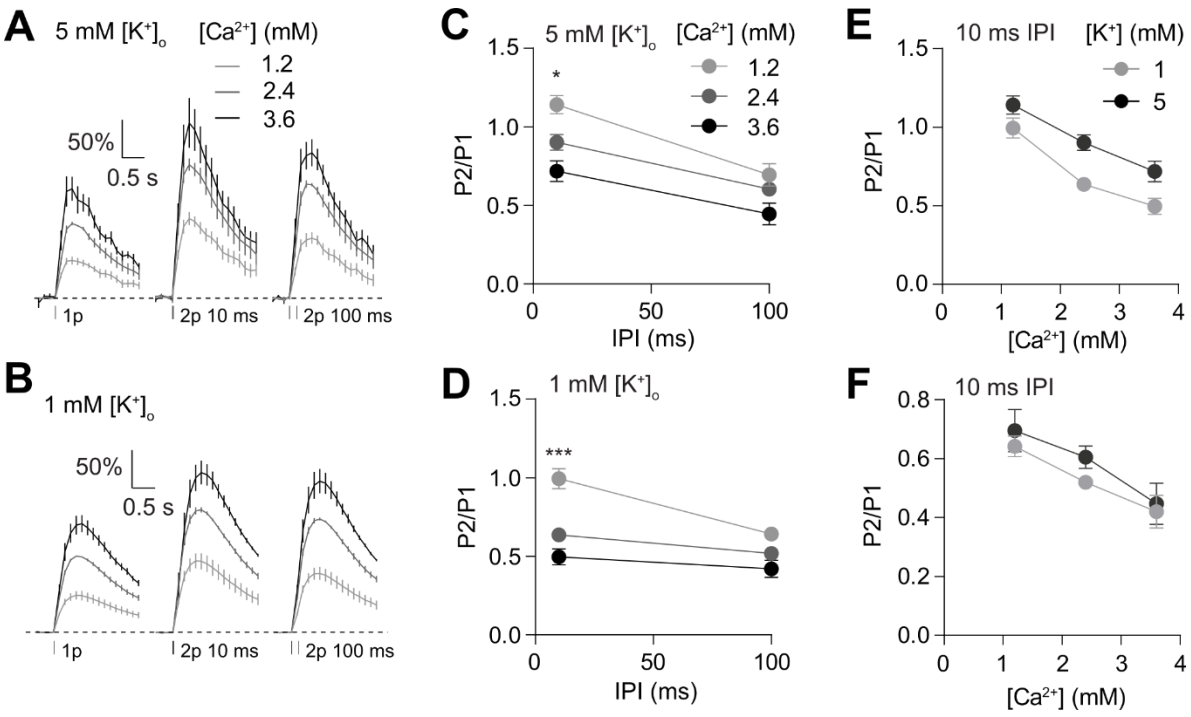

Fig. 3.5 DAT inhibition does not relieve a K+-dependent clamp on release-dependence in CPu

(A, B) Average profiles of $[DA]_o$ transients (mean $[DA]_o$ ± SEM) elicited by single- or paired-pulses in 1.2 mM - 3.6 mM $[Ca^{2+}]_o$ in either 5 mM $[K^+]_o$ (**A**, n = 5) or 1 mM $[K^+]_o$ (**B**, n = 5) in CPu. **(C, D)** Mean P2/P1 ± SEM against IPI in 1.2 mM - 3.6 mM $[Ca^{2+}]_o$ in 5 mM $[K^+]_o$ (**C**) or 1 mM $[K^+]_o$ (**D**). Changing $[Ca^{2+}]_o$ significantly modulated STP at 10 ms IPI in both 5 mM and 1 mM $[K^+]_o$. **(E, F)** Mean P2/P1 ± SEM at 10 ms IPI (**E**) and 100 ms IPI (**F**) in 5 mM and 1 mM $[K^+]_o$. Reducing $[K^+]_o$ did not significantly increase sensitivity of P2/P1 to $[Ca^{2+}]_o$. *p < 0.05, *** < 0.001.

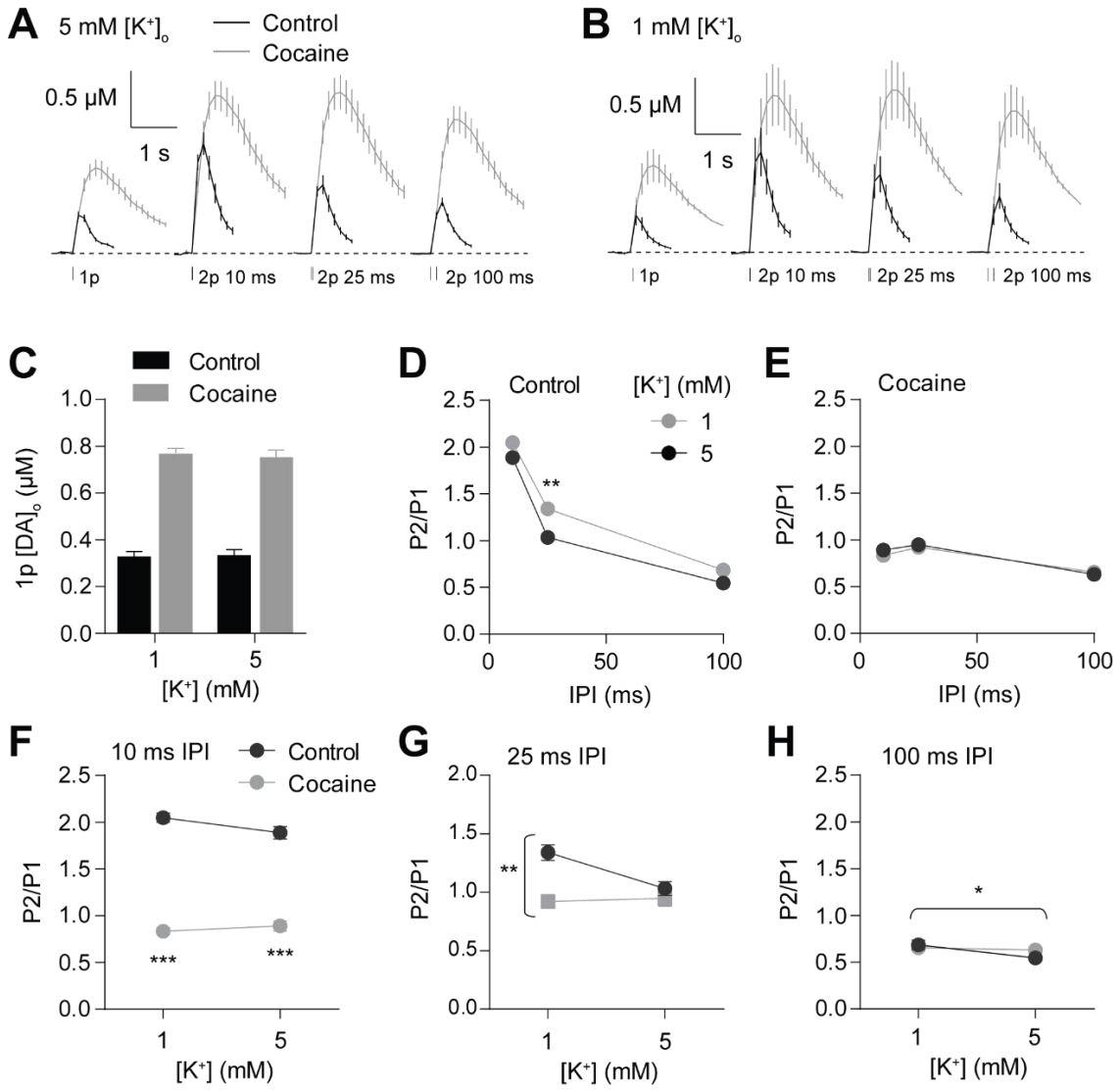

Fig. 3.6 DAT inhibition prevents K^+-dependent gating in CPu

(A, B) Average profiles of $[DA]_o$ transients (mean $[DA]_o$ ± SEM) elicited by single- or paired-pulses in control conditions or in cocaine in either 5 mM $[K^+]_o$ (**A**) or 1 mM $[K^+]_o$ (**B**) in CPu, n = 4. **(C)** Mean peak 1p $[DA]_o$ ± SEM at in control conditions or in cocaine. The cocaine-induced increase in 1p $[DA]_o$ was not affected by a change in $[K^+]_o$. **(D, E)** Mean P2/P1 ± SEM against IPI in 1 mM and 5 mM $[K^+]_o$ in control conditions (**D**) or in cocaine (**E**). A reduction in $[K^+]_o$ relieved STD at 25 ms IPI in control conditions but not in cocaine. **(F, G, H)** Mean P2/P1 ± SEM against $[Ca^{2+}]_o$ at 10 ms (**F**), 25 ms (**G**) and 100 ms (**H**) IPI. Cocaine prevented K^+-dependent relief of STD at 25 ms IPI. *p < 0.05, **p < 0.01, *** < 0.001.

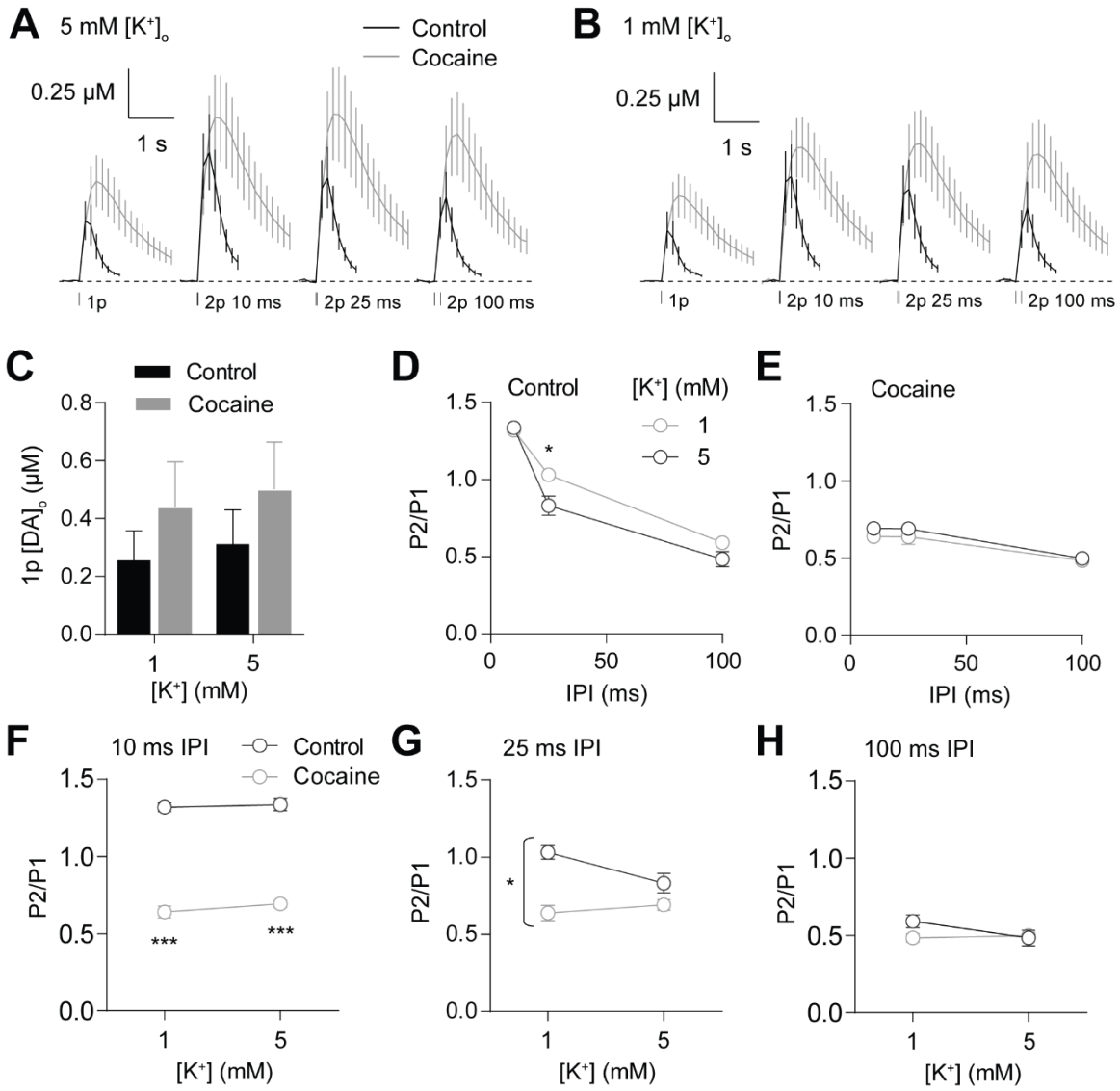

Fig. 3.7 DAT inhibition prevents K^+-dependent gating in NAc

(A, B) Average profiles of $[DA]_o$ transients (mean $[DA]_o$ ± SEM) elicited by single- or paired-pulses in control conditions or in cocaine in either 5 mM $[K^+]_o$ (**A**) or 1 mM $[K^+]_o$ (**B**) in NAc, n = 3. **(C)** Mean peak 1p $[DA]_o$ ± SEM at in control conditions or in cocaine. The cocaine-induced increase in 1p $[DA]_o$ was not affected by a change in $[K^+]_o$. **(D, E)** Mean P2/P1 ± SEM against IPI in 1 mM and 5 mM $[K^+]_o$ in control conditions (**D**) or in cocaine (**E**). A reduction in $[K^+]_o$ relieved STD at 25 ms IPI in control conditions but not in cocaine. **(F, G, H)** Mean P2/P1 ± SEM against $[Ca^{2+}]_o$ at 10 ms (**F**), 25 ms (**G**) and 100 ms (**H**) IPI. Cocaine prevented K^+-dependent relief of STD at 25 ms IPI. *p < 0.05, *** < 0.001.

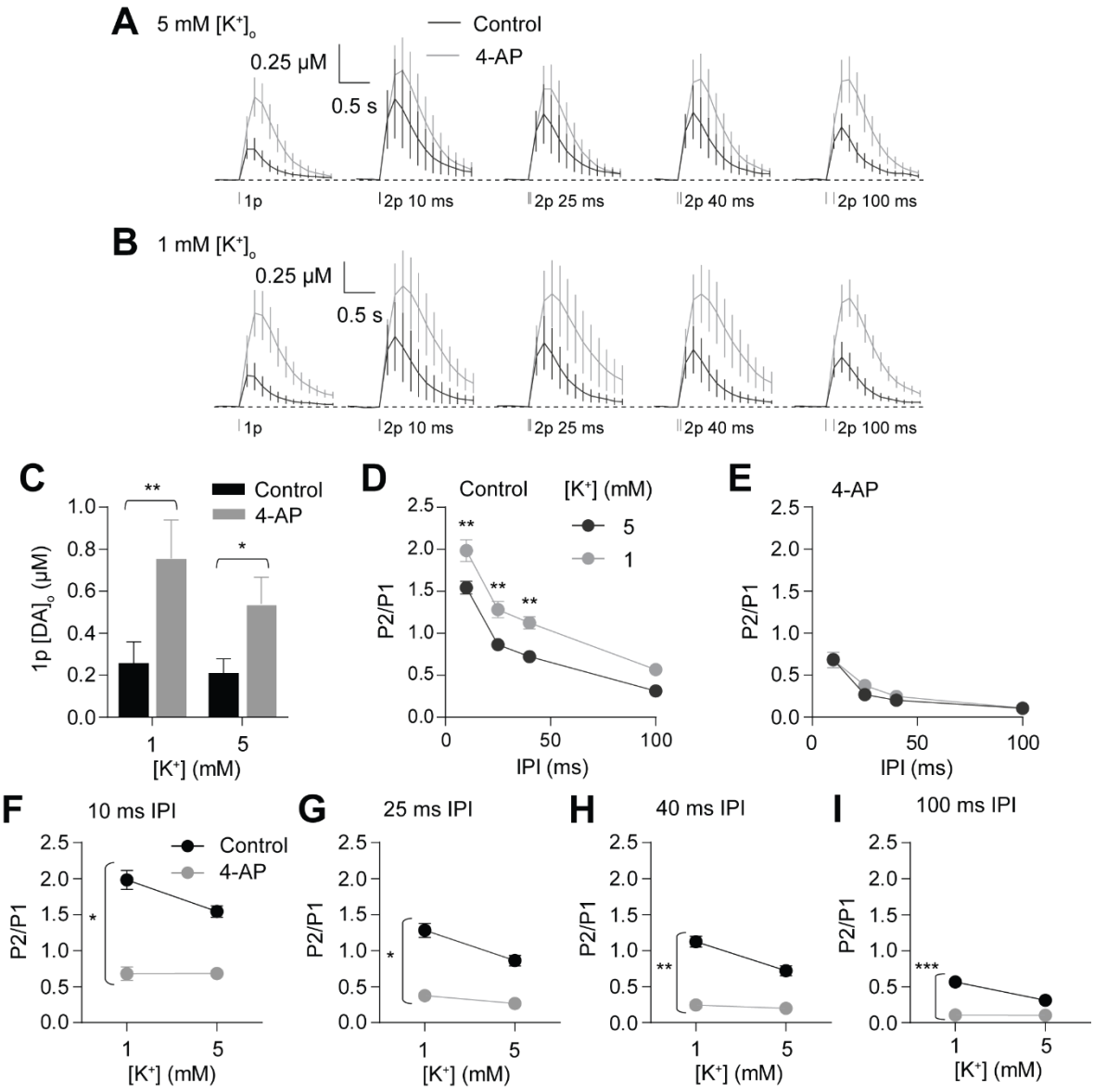

Fig. 3.8 Voltage-gated K^+ channels are required for K^+-dependent gating in CPu

(A, B) Average profiles of $[DA]_o$ transients (mean $[DA]_o$ ± SEM) elicited by single- or paired-pulses in control conditions or in 4-AP in either 5 mM $[K^+]_o$ (**A**) or 1 mM $[K^+]_o$ (**B**) in CPu, n = 4. **(C)** Mean peak 1p $[DA]_o$ ± SEM at in control conditions or in 4-AP. 4-AP significantly increased 1p $[DA]_o$ in both 1 mM and 5 mM $[K^+]_o$. **(D, E)** Mean P2/P1 ± SEM against IPI in 1 mM and 5 mM $[K^+]_o$ in control conditions (**D**) or in 4-AP (**E**). A reduction in $[K^+]_o$ significantly relieved STD in control conditions, but not in 4-AP. **(F, G, H, I)** Mean P2/P1 ± SEM against $[K^+]_o$ at 10 ms (**F**), 25 ms (**G**), 40 ms (**H**) and 100 ms (**I**) IPI. 4-AP reduced P2/P1 and prevented K^+-dependent relief of STD at all IPIs. *p < 0.05, **p < 0.01, *** < 0.001.

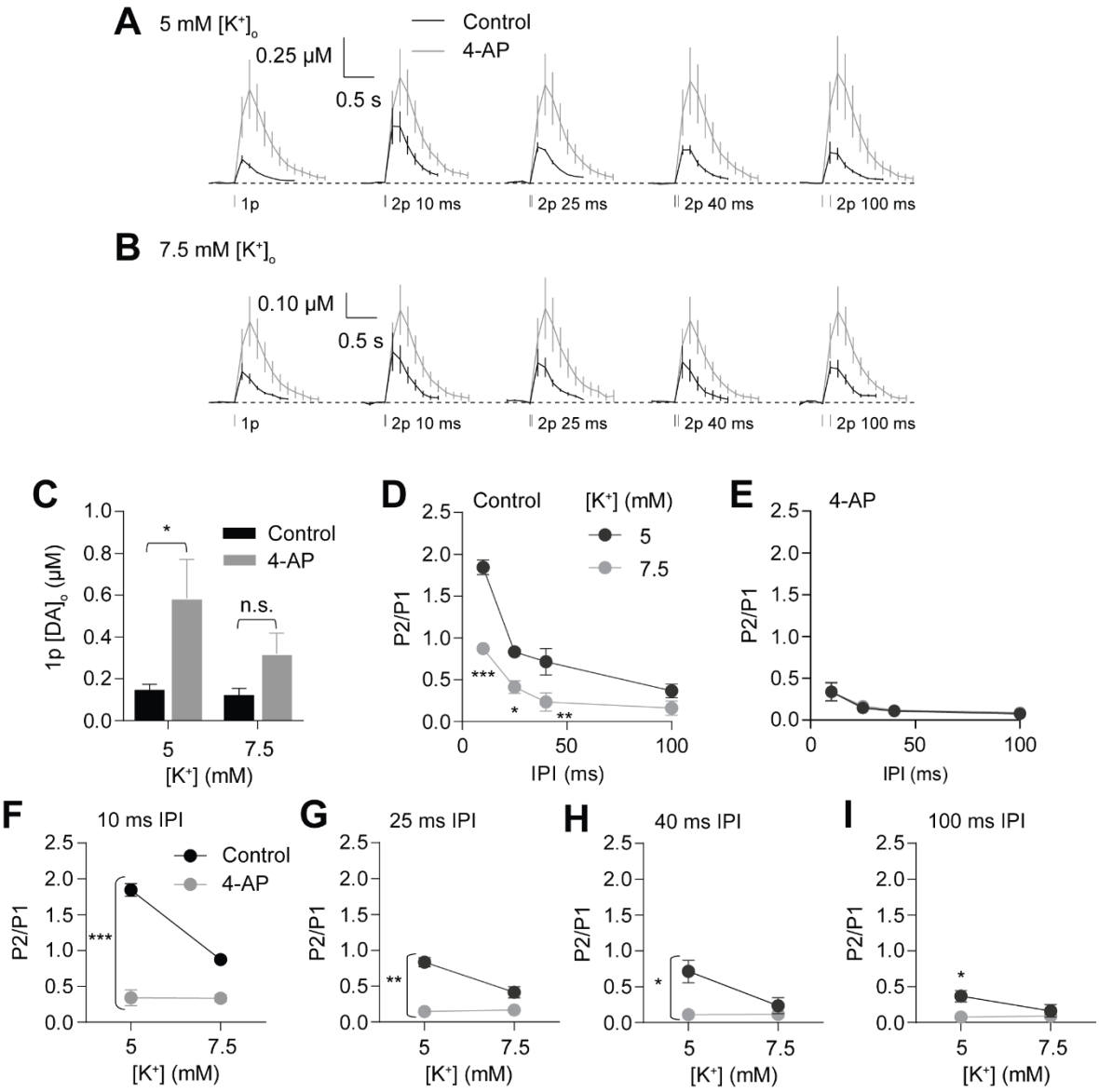

Fig. 3.9 Prevention of K^+-dependent gating is not due to a ceiling effect in CPu

(A, B) Average profiles of $[DA]_o$ transients (mean $[DA]_o$ ± SEM) elicited by single- or paired-pulses in control conditions or in 4-AP in either 5 mM $[K^+]_o$ (**A**) or 7.5 mM $[K^+]_o$ (**B**) in CPu, n = 3. **(C)** Mean peak 1p $[DA]_o$ ± SEM at in control conditions or in 4-AP. 4-AP significantly increased 1p $[DA]_o$ in 5 mM, but not in 7.5 mM $[K^+]_o$. **(D, E)** Mean P2/P1 ± SEM against IPI in 5 mM and 7.5 mM $[K^+]_o$ in control conditions (**D**) or in 4-AP (**E**). A reduction in $[K^+]_o$ significantly enhanced STD in control conditions, but not in 4-AP. **(F, G, H, I)** Mean P2/P1 ± SEM against $[K^+]_o$ at 10 ms (**F**), 25 ms (**G**), 40 ms (**H**) and 100 ms (**I**) IPI. 4-AP reduced P2/P1 at all IPIs and prevented K^+-dependent relief of STD at 10 ms, 25 ms and 40 ms IPI. *p < 0.05, **p < 0.01, *** < 0.001.

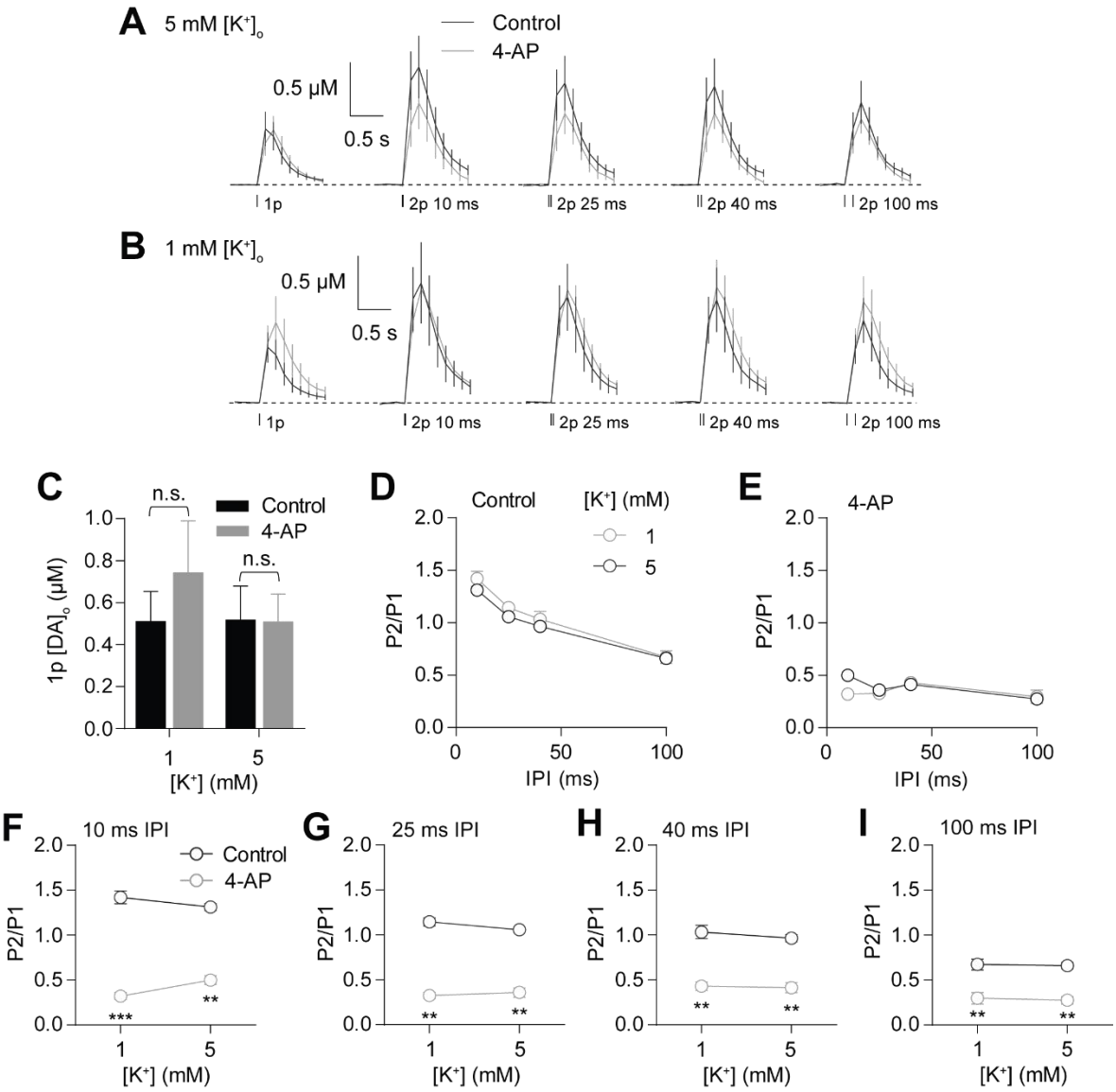

Fig. 3.10 Voltage-gated K^+ channels support STP but not K^+-dependent gating in NAc

(A, B) Average profiles of $[DA]_o$ transients (mean $[DA]_o$ ± SEM) elicited by single- or paired-pulses in control conditions or in 4-AP in either 5 mM $[K^+]_o$ (**A**) or 1 mM $[K^+]_o$ (**B**) in NAc, n = 3. **(C)** Mean peak 1p $[DA]_o$ ± SEM in control conditions (black) or in 4-AP (grey). 4-AP did not significantly increase 1p $[DA]_o$ in either 1 mM or 5 mM $[K^+]_o$. **(D, E)** Mean P2/P1 ± SEM against IPI in 1 mM and 5 mM $[K^+]_o$ in control conditions (**D**) or in 4-AP (**E**). Changing $[K^+]_o$ did not significantly modulate STP in either control conditions or in 4-AP **(F, G, H, I)** Mean P2/P1 ± SEM against $[K^+]_o$ at 10 ms (**F**), 25 ms (**G**), 40 ms (**H**) and 100 ms (**I**) IPI. 4-AP reduced P2/P1 at all intervals but did not alter the effect of $[K^+]_o$. **p < 0.01, *** < 0.001.

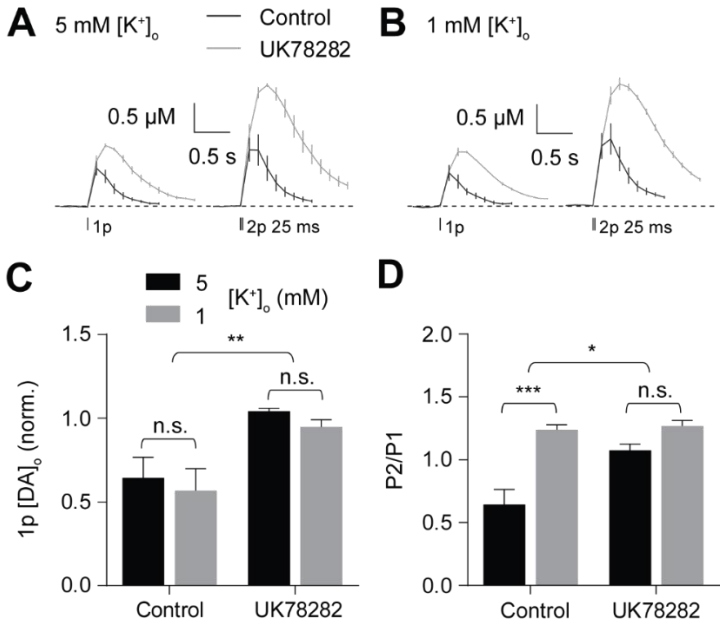

Fig. 3.11 K^+-dependent gating involves axonal $K_v1.4$-subunit-containing channels in CPu

(A, B) Average profiles of $[DA]_o$ transients (mean $[DA]_o$ ± SEM) elicited by single- or paired-pulses in control conditions (black) or in 5 µM UK78282 (grey) in either 5 mM $[K^+]_o$ (**A**) or 1 mM $[K^+]_o$ (**B**) in CPu, n = 3. **(C)** Mean peak 1p $[DA]_o$ ± SEM in 5 mM $[K^+]_o$ (black) or 1 mM $[K^+]_o$ (grey). UK78282 increased 1p $[DA]_o$ in both 5 mM and 1 mM $[K^+]_o$. **(D)** Mean P2/P1 ± SEM at 25 ms IPI in 5 mM $[K^+]_o$ (black) or 1 mM $[K^+]_o$ (grey). The effect of a reduction in $[K^+]_o$ was significantly decreased in the presence of UK78282. Statistical tests are two-way ANOVA with Bonferroni's test for post-hoc comparisons.

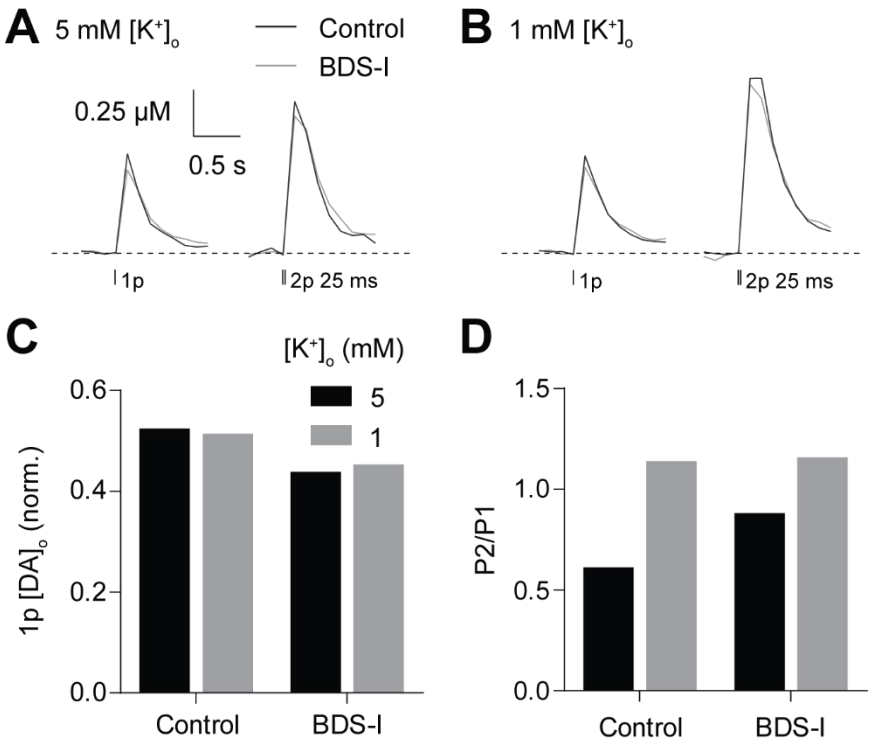

Fig. 3.12 Pilot data suggests a potential role for $K_v3.4$ channels in K^+-dependent gating in CPu

(A) Profiles of $[DA]_o$ transients elicited by single- or paired-pulses in control conditions (black) or in 500 nM BDS-I (grey) in either 5 mM $[K^+]_o$ (**A**) or 1 mM $[K^+]_o$ (**B**) in CPu, n = 1. **(C)** Mean peak 1p $[DA]_o$ in 5 mM $[K^+]_o$ (black) or 1 mM $[K^+]_o$ (grey). **(D)** Mean P2/P1 at 25 ms IPI in 5 mM $[K^+]_o$ (black) or 1 mM $[K^+]_o$ (grey).

Chapter 4.

Ongoing background of tonic activity in DA neurons increases signal contrast of DA release

4.1 Introduction

In this chapter, the axonal mechanisms of STP described in the previous chapter will be studied in the context of stimulation paradigms that more closely mimic firing patterns in intact rodent DA neurons. I explore the regulation of DA release in response to burst stimulation on a background of low-frequency activity, including the roles of Ca^{2+} handling and the DAT in STP under these conditions.

4.1.1 Firing frequencies in rodent DA neurons

DA neurons display multiple overlapping modes of firing. In the absence of synaptic inputs in a slice preparation, DA neurons fire regularly due to their intrinsic pacemaker mechanism, at frequencies up to approximately 10 Hz (Surmeier et al. 2005). However, *in vivo* studies with preserved synaptic inputs to DA neurons have demonstrated more complex patterns of activity.

In contrast to basal firing in slice preparations, DA neurons in anaesthetised rats display irregular firing at frequencies up to approximately 8 Hz, with an average at approximately 4 Hz (Grace & Bunney 1984b; McCutcheon et al. 2012), although the average rate can vary depending on the anaesthetic used (Pistis et al. 2004). These low-frequency firing patterns are interspersed with bursts at higher frequencies, typically comprising 2-6 spikes at average frequencies up to approximately 25 Hz (Grace & Bunney 1984a) which are thought to be dependent on glutamatergic input via NMDA receptors (Overton & Clark 1997). There may be species differences in the average firing rate of DA neurons; however, studies comparing basal firing in rats and mice have had mixed results, reporting small differences in both directions (Panin et al. 2012; Marinelli & McCutcheon 2014).

In awake, freely-moving rats, similar basal rates of firing have been observed, with a mean frequency of approximately 6 Hz (Hyland et al. 2002; Pan et al. 2005; Kiyatkin & Rebec 1998; Freeman et al. 1985). Resting firing rates recorded in awake head-fixed mice also fall within this

range (Dodson et al. 2016). Average intra-burst firing frequencies in freely-moving rats appear similar to those observed under anaesthesia (Hyland et al. 2002; Kiyatkin & Rebec 1998; Cohen et al. 2012), although an analysis of over 20,000 spike pairs has detected instantaneous frequencies above 100 Hz (Hyland et al. 2002).

Beyond these general patterns, the diverse firing patterns of different subpopulations of DA neurons remain incompletely described. Broad anatomical distinctions have been explored, showing that the baseline firing rate of DA neurons in the SNc and VTA are similar (Clark & Chiodo 1988; Panin et al. 2012), although some studies have shown slightly greater average basal firing rates in VTA than SNc (Zhang et al. 2008; Marinelli & McCutcheon 2014). A higher proportion of spikes in VTA DA neurons occur in bursts (Clark & Chiodo 1988; Panin et al. 2012), and bursts in VTA have been shown to include a slightly greater number of spikes on average than in SNc (Tong et al. 1996), although the significance of the relative prominence of bursting activity for basal ganglia function remains unclear.

4.1.2 The role of tonic activity in DA signalling

Tonic firing is an energetically-demanding process, especially given the size of the axonal arbor of midbrain DA neurons, due to the frequent perturbation of the axonal membrane potential (Pissadaki & Bolam 2013). Energetic demand has been proposed as a key determinant of the vulnerability of DA neurons to oxidative stress and neurotoxic substances (Bolam & Pissadaki 2012; Pacelli et al. 2015). In this light, it seems probable that tonic firing is maintained in spite of its energetic burden to serve an indispensable function in DA signalling.

Higher rates of firing in DA neurons results in increased DA release in striatum (Chergui, Suaud-Chagny, et al. 1994; Suaud-Chagny et al. 1992). However, the extent to which short- and long-term changes in DA release are attributable to different firing patterns in DA neurons is not clear. It has been suggested that tonic or basal extracellular [DA] is maintained by low-frequency firing in large populations of DA neurons (Floresco et al. 2003), although this may reflect an increase in

the number of phasic DA transients, which are thought to be driven by synchronous or coincident burst firing in DA neurons (Sombers et al. 2009; Tsai et al. 2009; Zweifel et al. 2009), have been suggested to determine extracellular [DA] though extracellular summation over timescales of seconds (Owesson-White et al. 2012). Ramping increases in striatal [DA] observed during reward-seeking in a maze (Howe et al. 2013) and may be also driven by population-level increases in firing over and above basal rates (Fiorillo et al. 2003). DA signalling on different timescales is therefore sensitive to changes in the firing patterns of populations of DA neurons, but it is not clear how switching between tonic and burst firing in individual neurons influences this process.

In addition to a role in tonic DA release, tonic background activity might also influence the signal contrast of DA release in response to subsequent burst firing. Low-frequency background stimulation of DA release in slices of mouse striatum has been previously shown to decrease DA release, but to increase the ratio between release in response to bursts and in response to individual low-frequency stimuli (Zhang et al. 2009). However, it is unclear whether this effect is caused by local synaptic inputs or by the intrinsic properties of DA axons. Findings presented in Chapter 3 and in previous studies have shown that DA release in the absence of local inputs is subject to powerful STP, the direction and strength of which is highly sensitive to the intervals between APs (Rice & Cragg 2004; Platt 2012). During tonic background activity, DA release might also be influenced by release-dependent factors such as changes in vesicle pool content, intra-terminal Ca^{2+} summation and autoreceptor activity, which do not appear to influence STP in the paired-pulse paradigm employed in Chapter 3.

This chapter will therefore explore the possibility that tonic background activity in DA axons controls the signal contrast of DA transients evoked by bursts due to intrinsic axonal mechanisms governing STP.

4.1.4 Hypotheses

In this chapter I will aim to test the following hypotheses, in order to determine how tonic background activity in DA axons can influence subsequent DA release:

1) Tonic background activity in DA axons increases contrast between release in response to bursts and low-frequency stimuli

2) Enhancement of frequency contrast is due to intrinsic properties of DA axons

3) Changes in the frequency of tonic activity can alter its effect on signal contrast

4) The dopamine transporter limits frequency contrast through uptake and presynaptic STP

4.2 Methods

Experiments described in this chapter were carried out according to the general methods laid out in Chapter 2. Variations and further details are described below.

4.2.1 Animals & slice preparation

Experiments in this chapter were performed in slices from either adult wild-type C57Bl/6NCrl mice or heterozygote $DAT^{IRES\text{-}Cre}$ mice intracerebrally injected with AAV5-ChR2-EYFP. All experiments were conducted in accordance with a UK Home Office-approved project license and local guidelines.

4.2.2 Fast-scan cyclic voltammetry (FCV)

In some experiments in this chapter, the concentration of Ca^{2+} ions in aCSF was reduced. To reduce $[Ca^{2+}]_o$, $[CaCl_2]$ was decreased accordingly. The change in divalent cation concentration was not compensated by ionic substitution (See section 3.2.2). Concentrations of all other ions remained unchanged.

4.2.3 Stimulation and experimental design

DA release was evoked by electrical stimulation (0.6 mA, 200 µs pulse) in experiments using tissue from wild-type C57Bl6 mice, and by optical stimulation (2 ms flash) in experiments in slices from $DAT^{IRES\text{-}Cre}$ mice, as described in Chapter 2. Optical stimulation was delivered using full-field illumination of the slice with a blue LED. In every experiment using optical stimulation, a stimulation-response curve was prepared to determine peri-maximal stimulation intensity. This accounted for variability in the expression of ChR2-EYFP in different animals following viral transfection.

In experiments in this chapter, the ratio between $[DA]_o$ evoked by a short train (a burst) and single pulses was used to investigate the sensitivity of DA release to bursts under different conditions. For the sake of brevity, this ratio is referred to as signal contrast ratio throughout this

chapter. In some experiments, signal contrast ratio was measured for bursts delivered on a background of low-frequency tonic stimulation and for bursts delivered in isolation (i.e. in the absence of background activity). Tonic stimulation consisted of a 3 s stimulation train at a frequency of either 2 or 6 Hz delivered immediately before the burst. Bursts delivered both alone and following tonic background stimulation had a frequency of 25 Hz (i.e. 40 ms IPI) in all experiments.

In some experiments, both peak $[DA]_o$ and area under the curve (AUC) of $[DA]_o$ transients were measured. This was because peak $[DA]_o$ is less sensitive to the effects of uptake and to signal-to-noise ratio, but may underestimate release where stimulation is distributed across multiple FCV sweeps, while AUC gives a better estimation of release in response to longer trains, but is more sensitive to uptake and noise. Peak $[DA]_o$ and AUC evoked by bursts after tonic stimulation were obtained by subtraction of a transient evoked by tonic stimulation alone.

In order to calculate the burst contrast ratio, peak $[DA]_o$ or AUC evoked by the burst were normalised to peak $[DA]_o$ or AUC evoked by a single stimulation, respectively. In the case of bursts delivered alone, normalisation was to 1p stimulation delivered alone. In the case of bursts delivered after tonic stimulation, normalisation was to the final pulse of tonic stimulation (**Fig. 4.1**). Peak $[DA]_o$ and AUC of the final pulse were obtained by subtraction of a transient evoked by a train of a number of pulses that was one less than the number used for tonic stimulation (i.e. 5 pulses where 6 pulses at 2Hz were used for tonic stimulation, or 17 pulses where 18 pulses at 6 Hz were used for tonic stimulation) from a transient evoked by tonic stimulation delivered alone. These values were collected for two stimulations delivered before and after the burst and averaged.

Measurements in control conditions were always collected before bath application of drugs. Where $[Ca^{2+}]_o$ was varied, concentrations were applied in pseudorandom order before and after drug application. Each individual experiment was conducted in a single site, one site per animal (n

= number of animals). Sites in CPu were located in the dorsal half of the striatum, while sites in NAc were within 100 µm of the anterior commissure (i.e. NAc core).

4.2.4 Drugs

All experiments in this chapter were conducted in the presence of dihydro-β-erythroidine (DHβE, 1 µM) to block cholinergic signalling via β2-subunit-containing nicotinic acetylcholine receptors. 'Control conditions' indicates the presence of DHβE and the absence of other drugs.

DHβE was obtained from Tocris Biosciences. Cocaine hydrochloride was obtained from Sigma. Drugs were dissolved in deionised water to prepare stock aliquots at 1,000-10,000x final concentration. All drugs were diluted to their final concentration in carbogenated aCSF and bath-applied.

4.2.5 Data analysis and statistics

The recordings in this chapter were longer in duration than those collected in the previous chapter; data were collected continuously for up to 7 seconds due to the length of the tonic stimulation paradigm. Because of their length these recordings were more sensitive to baseline drift during recording. To correct for this, the average of the current at two time points on each background-subtracted FCV sweep was subtracted from the peak DA current. This resulted in a more stable baseline during these recordings.

In many experiments, the slope of the relationship between burst length and either normalised peak $[DA]_o$ or normalised AUC was compared between conditions. Slopes were obtained by fitting with a linear regression model, and compared using an F-test for comparison of models or with Two-way ANOVA using GraphPad Prism 6. A runs test for deviation from linearity produced a non-significant result ($p > 0.05$) for all curve fits.

4.3 Results

4.3.1 Tonic background activity enhances contrast between single stimulations and bursts

First, I investigated the effect of tonic stimulation on the responsiveness of DA release to bursts of varying length. To mimic tonic activity in DA neurons, six pulses of electrical stimulation at a frequency of 2 Hz (IPI = 0.5 s) were delivered, followed 0.5 s after the final pulse by a burst of 2, 4 or 6 pulses at 25 Hz.

In both CPu and NAc, release in response to each pulse initially declined during tonic stimulation, before reaching a steady state of $[DA]_o$ on which stable responses to individual pulses could be observed. This steady state was reached after a duration of approximately 1.5 s (3 pulses). Burst stimulation evoked greater peak $[DA]_o$ when delivered in isolation than after tonic background stimulation, and peak $[DA]_o$ increased as a function of the number of pulses in the burst in both the presence and absence of tonic background stimulation (**Fig. 4.2A, 4.3A**).

To determine the contrast between $[DA]_o$ evoked by bursts and by single pulses, peak $[DA]_o$ in response to bursts delivered alone was normalised to peak $[DA]_o$ evoked by single pulses delivered alone, while peak $[DA]_o$ in response to bursts delivered after tonic stimulation was normalised to peak $[DA]_o$ evoked by the final pulse of tonic stimulation (see section 4.2.3, **Fig. 4.1**). The slope of the relationship between burst length (the number of pulses in the burst) and normalised peak $[DA]_o$ was then compared. In CPu, the slope of the relationship between burst length and normalised peak $[DA]_o$ was significantly greater when the burst was delivered after tonic stimulation, resulting in an approximately 2.5-fold increase in peak $[DA]_o$ between 2 and 10 pulses, compared to an approximately 1.6-fold increase when the burst was delivered in isolation (**Fig. 4.2B**; Linear regression; Burst only: $\beta = 0.134$ [95% CI: 0.022 to 0.246], $R^2 = 0.73$, vs Tonic stim: $\beta = 0.647$ [95% CI: 0.343 to 0.951], $R^2 = 0.90$; $F_{1,8} = 19.357$; $p = 0.002$; $n = 4$). In NAc, the

relationship between burst length and normalised peak $[DA]_o$ appeared generally stronger than in CPu, and was also significantly greater for a burst after tonic stimulation than for a burst alone, resulting in an approximately 5.5-fold increase in peak $[DA]_o$ between 2 and 10 pulses for a burst after tonic stim compared to an approximately 2.8-fold increase for a burst alone (**Fig. 4.3B**; Linear regression; Burst only: $\beta = 0.456$ [95% CI: 0.356 to 0.557], $R^2 = 0.98$ vs Tonic stim: $\beta = 2.018$ [95% CI: 0.734 to 3.302], $R^2 = 0.83$; $F_{1,8} = 11.326$; $p = 0.010$, $n = 3$).

Peak $[DA]_o$ provides a relatively conservative assessment of differences in DA signalling compared to the area under the curve (AUC) of the [DA] transient, since it is less sensitive to differences in the rate of uptake between striatal regions and compartments (Salinas et al. 2016). However, peak $[DA]_o$ is also likely to underestimate release in response to longer bursts, where stimulation is distributed across a period spanning multiple FCV sweeps (i.e. total stim duration > 125 ms). In these cases, AUC provides a more accurate measure of total DA release in response to the burst, albeit one that that also incorporates differences in uptake. To fully explore the relationship between burst length and signal contrast, AUC of release in response to bursts with and without tonic background stimulation was compared, where AUC in response to bursts was normalised to AUC in response to single pulses as described above.

In CPu, the slope of the relationship between burst length and normalised AUC was greater for a burst after tonic background stimulation than for a burst alone, with an approximately 4.3-fold increase in $[DA]_o$ evoked by 10 vs 2 pulses after tonic background stimulation compared to an approximately 2.4-fold increase for a burst alone (**Fig. 4.2C**; Linear regression; Burst only: $\beta = 0.409$ [95%CI: 0.262 to 0.555], $R^2 = 0.94$, vs Tonic stim: $\beta = 1.954$ [95% CI: 1.378 to 2.529], $R^2 = 0.96$; $F_{1,8} = 52.209$; $p < 0.001$; $n = 4$). In NAc, there was an approximately 8.1-fold increase in AUC evoked by 10 vs 2 pulses after tonic background stimulation, compared to an approximately 4.9-fold increase for a burst alone (**Fig. 4.3C**; Linear regression; Burst only: $\beta = 1.318$ [95% CI: 1.222 to

1.414], R^2 = 0.99, vs Tonic stim: β = 4.860 [95% CI: 2.897 to 6.823], R^2 = 0.92; $F_{1,8}$ = 25.033; p = 0.001; n = 3).

These findings suggest that tonic stimulation enhances the contrast between single pulses and bursts in both regions, but particularly in NAc. This effect was observed when comparing the relationship between burst length and either peak $[DA]_o$ or AUC of the $[DA]_o$ transient, suggesting that the difference between regions is not wholly caused by previously-described differences in uptake rates (Hersch et al. 1997; Marshall et al. 1990). These findings raise the possibility that short-term plasticity of DA release mediates the promotion of burst contrast by tonic background activity.

4.3.2 Contrast enhancement is not due to activation of modulatory inputs

It remains unclear whether enhancement of burst signal contrast following tonic background stimulation is caused by the intrinsic properties of DA axons or by the concurrent activation of striatal circuits that regulate DA release. Unlike the paired-pulse stimulation paradigm used to investigate STP in Chapter 3, the tonic background stimulation used in this chapter is likely to promote release of neuromodulators and inputs to DA axons. To exclude the possibility that the effect of tonic stimulation on burst contrast is caused by the effects of local signalling on DA axons, DA release was selectively evoked by optical stimulation in heterozygote $DAT^{IRES\text{-}Cre}$ animals conditionally expressing ChR2-EYFP in DA axons (see Chapter 2). This approach limits release of other neurotransmitters and neuromodulators, limiting the local modulation of DA release by striatal circuits (Melchior et al. 2015).

In CPu, as observed for electrical stimulation, optical stimulation at 2 Hz caused a decline in evoked DA release that stabilised after approximately 3 pulses (**Fig. 4.4A**). When peak $[DA]_o$ evoked by burst stimulation was normalised to single-pulse release, as described above, tonic stimulation did not significantly increase the slope of the relationship between burst length and normalised peak $[DA]_o$ (**Fig. 4.4B**; Linear regression; p > 0.05; n = 4). The slope of the relationship

between burst length and normalised AUC was also not significantly altered by tonic stimulation (**Fig. 4.4C**; Linear regression; $p > 0.05$; $n = 4$).

In NAc, release during tonic background stimulation appeared to form a plateau at a higher basal level of $[DA]_o$ than in CPu (**Fig. 4.5A**). The relationship between burst length and normalised peak $[DA]_o$ was stronger than in CPu, and the slope was significantly increased by tonic stimulation (**Fig. 4.5B**; Linear regression; Burst only: $\beta = 0.429$ [95% CI: 0.299 to 0.560], $R^2 = 0.95$, vs Tonic stim: $\beta = 3.445$ [95% CI: 3.033 to 3.858], $R^2 = 0.99$; $F_{1,8} = 374.18$; $p < 0.001$; $n = 3$). The relationship between burst length and normalised AUC was even steeper, with an approximately 20.5-fold increase between 2 and 10 pulses after tonic stim compared to an approximately 7-fold increase for a burst delivered alone (**Fig. 4.5C**; Linear regression; Burst only: $\beta = 1.911$ [95% CI: 1.210 to 2.612], $R^2 = 0.93$, vs Tonic stim: $\beta = 11.85$ [95% CI: 8.794 to 14.90], $R^2 = 0.97$; $F_{1,8} = 77.519$; $p < 0.001$; $n = 3$).

The effects of selective optical stimulation of DA axons on signal contrast therefore differed between the functional regions of the striatum. There was no increase contrast between bursts and single stimulations in CPu, but burst contrast appeared much greater in response to optical compared to electrical stimulation in NAc. These findings might therefore suggest that enhancement of burst contrast following tonic stimulation is not due to local modulation, and presynaptic mechanisms operating in NAc promote greater burst contrast than observed in CPu. Alternatively, the optogenetic technique might introduce other factors which alter the effect of tonic background stimulation on burst signal contrast. In either case, these findings do not suggest that enhancement of signal contrast following tonic background stimulation is caused by activation of local inputs.

4.3.3 Contrast enhancement is maintained at a higher tonic stimulation frequency

All experiments described so far in this chapter have used 2 Hz stimulation to mimic the effects of tonic background activity in DA neurons. If the enhancement of signal contrast following tonic

background stimulation is driven by frequency-dependent mechanisms of STP operating at DA axons, the magnitude of contrast enhancement should be dependent on the frequency of tonic background stimulation. The effects of tonic stimulation at 6 Hz on burst signal contrast were therefore investigated.

In CPu, the decline in [DA] evoked by each pulse during 6 Hz tonic stimulation reached a steady state after approximately 1.5 s (9 pulses), similar to the time taken to reach steady-state during 2 Hz stimulation. The steady-state level of $[DA]_o$ appeared higher than that observed during 2 Hz stimulation (see Fig. 4.1), and responses to individual stimuli were not readily identifiable (**Fig. 4.6A**). The slope of the relationship between burst length and normalised peak $[DA]_o$ was steeper after tonic stimulation than when bursts were delivered alone (**Fig. 4.6B**; Linear regression; Burst only: $\beta = 0.115$ [95% CI: 0.033 to 0.198], $R^2 = 0.79$, vs Tonic stim: $\beta = 0.270$ [95% CI: 0.175 to 0.365], $R^2 = 0.94$; $F_{1,8} = 11.66$; $p = 0.009$; $n = 5$). Tonic stimulation also significantly increased the slope of the relationship between burst length and normalised AUC (**Fig. 4.6C**; Linear regression; Burst only: $\beta = 0.252$ [95% CI: 0.177 to 0.328], $R^2 = 0.96$, vs Tonic stim: $\beta = 1.421$ [95% CI: 0.822 to 2.019], $R^2 = 0.92$; $F_{1,8} = 28.881$; $p < 0.001$; $n = 5$).

In NAc, $[DA]_o$ evoked by 6 Hz stimulation did not reach a steady state within 3 s. Release initially decreased, but after approximately 1 s began to increase again (**Fig. 4.7A**). The slope of the relationship between burst length and normalised peak $[DA]_o$ was significantly steeper after tonic stimulation compared to bursts delivered alone (**Fig. 4.7B**; Linear regression; Burst only: $\beta = 0.527$ [95% CI: 0.419 to 0.634], $R^2 = 0.98$, vs Tonic stim: $\beta = 0.792$ [95% CI: 0.683 to 0.900], $R^2 = 0.99$; $F_{1,8} = 23.193$; $p = 0.001$; $n = 5$). There was also a significantly steeper relationship between burst length and normalised AUC (**Fig. 4.7C**; Linear regression; Burst only: $\beta = 1.083$ [95% CI: 0.998 to 1.167], $R^2 = 0.997$, vs Tonic stim: $\beta = 3.407$ [95% CI: 2.956 to 3.858], $R^2 = 0.991$; $F_{1,8} = 197.86$; $p < 0.001$; $n = 5$).

In both regions, the slope of the relationship between burst length following tonic stimulation and peak $[DA]_o$ or AUC were slightly less than observed after 2 Hz tonic stimulation. However, the slope of the relationship between burst length and peak $[DA]_o$ or AUC for bursts delivered alone were similar between the two experiments. These findings therefore suggest that the contrast-enhancing effect of tonic stimulation is maintained, but is weaker at this higher tonic background frequency.

4.3.4 Steady-state $[DA]_o$ is not correlated with signal contrast enhancement

When tonic background stimulation was delivered at a higher frequency, steady-state $[DA]_o$ during tonic background stimulation was increased, but the magnitude of signal contrast enhancement was decreased. If signal contrast enhancement following tonic background stimulation is driven by a release-dependent mechanism such as vesicle pool depletion or activation of D2 autoreceptors, there should be a significant negative correlation between steady-state $[DA]_o$ and burst signal contrast across a population of release sites.

To exclude this possibility, average steady-state $[DA]_o$ was plotted against burst signal contrast ratio for a 4-pulse burst following tonic stimulation at each site recorded for experiments in this chapter. This includes recordings at different frequencies of tonic background stimulation, in different $[Ca^{2+}]_o$, and in the presence and absence of cocaine, driving a wide range of steady-state $[DA]_o$. Linear curves were fit to data from both CPu and NAc (**Fig. 4.8**). No significant correlation between steady-state $[DA]_o$ and burst signal contrast was observed in either region, and there was no significant difference between the slopes of the two curves, suggesting that enhancement of signal contrast following tonic background stimulation is not driven by a release-dependent mechanism such as D2 autoreceptor activation or depletion of readily-releasable vesicle pools.

4.3.4 $[Ca]^{2+}$-driven changes in release probability regulate signal contrast

As discussed in Chapter 3, presynaptic plasticity of DA release is only weakly enhanced by decreases in P_r driven by a reduction in $[Ca^{2+}]_o$, as shown in Chapter 3 and in previous work (Platt

2012). In this chapter, the relationship between burst contrast and $[Ca^{2+}]_o$ was investigated, to determine whether burst contrast is differentially sensitive to changes in P_r.

To explore the effect of changes in P_r on burst contrast, 25 Hz bursts of 2, 4 or 6 pulses were delivered either in isolation or on a background of 2 Hz stimulation in 1.2 and 2.4 mM $[Ca^{2+}]_o$. In CPu, a similar decline of $[DA]_o$ to steady state was observed during tonic stimulation in either 1.2 or 2.4 mM $[Ca^{2+}]_o$, producing stable responses after approximately 1 s. Mean steady-state $[DA]_o$ in 1.2 mM $[Ca^{2+}]_o$ was approximately 50% of steady-state $[DA]_o$ in 2.4 mM $[Ca^{2+}]_o$ (**Fig. 4.9A**). Linear regression curves were fit to plots of burst length against normalised AUC to determine the slope of the relationship in 1.2 mM and 2.4 mM $[Ca^{2+}]_o$ when bursts were delivered alone (**Fig. 4.9B**) or following tonic background stimulation (**Fig. 4.9C**). The slope of the relationship was increased by tonic stimulation, and decreasing $[Ca^{2+}]_o$ increased the slope to a greater extent following tonic stimulation (**Fig. 4.9D**; Two-way ANOVA, background stimulation x $[Ca^{2+}]_o$ interaction; $F_{1, 16} = 5.47$; $p = 0.033$; $n = 5$). This suggests that, while changing P_r did not alter signal contrast when a burst was delivered in isolation, a reduction in P_r can enhance signal contrast in the presence of tonic background stimulation.

In NAc, decline to steady state during tonic background stimulation was similar both 1.2 and 2.4 mM $[Ca^{2+}]_o$, and steady state $[DA]_o$ was lower when $[Ca^{2+}]_o$ was reduced (**Fig. 4.10A**). Linear regression curves were fit in all conditions to obtain the slope of the relationship between burst length and normalised AUC for bursts delivered alone (**Fig. 4.10B**) or following tonic background stimulation (**Fig. 4.10C**). Tonic stimulation increased signal contrast but, unlike in CPu, did not alter the effect of $[Ca^{2+}]_o$ (**Fig. 4.10D**; Two-way ANOVA, main effect of background stimulation; $F_{1, 16} = 83.20$; $p < 0.001$; $n = 5$). Tonic background stimulation therefore appears to promote a stronger dependence of signal contrast on P_r in CPu, but not in NAc.

4.3.5 The DAT limits signal contrast in CPu

In Chapter 3 it was demonstrated that, in a paired-pulse paradigm, inhibition of the dopamine transporter (DAT) promotes the modulation of STP by changes in P_r (section 3.3.2). To determine whether a DAT-mediated clamp on release-dependence also underlies the weak modulation of burst contrast by changes in P_r, the effect of a decrease in $[Ca^{2+}]_o$ on burst contrast was explored in the presence and absence of cocaine.

In CPu, cocaine increased the amplitude of DA release events, and also promoted extracellular summation due to inhibition of DA uptake. As a result, DA release did not reach a steady state during tonic background stimulation at 2 Hz (**Fig. 4.11A**), in contrast to background stimulation during normal DAT function, demonstrating the role of the DAT in limiting extracellular summation. Linear regression curves were fit to the relationship between normalised AUC and burst length in the presence (**Fig. 4.11B**) and absence of cocaine (**Fig. 4.11C**). The slope of this relationship was significantly increased in the presence of cocaine, and when $[Ca^{2+}]_o$ was reduced, but the effect of lowering $[Ca^{2+}]_o$ was not altered by cocaine (**Fig. 4.11D**; Two-way ANOVA, main effect of cocaine; $F_{1, 12} = 84.94$; $p < 0.001$; main effect of $[Ca^{2+}]_o$; $F_{1, 12} = 59.68$; $p > 0.001$; $n = 4$); reducing $[Ca^{2+}]_o$ from 2.4 mM to 1.2 mM increased the slope in both control conditions and in the presence of cocaine (*post-hoc* Sidak's test; $p < 0.001$). This suggests that DAT function and P_r both regulate signal contrast in CPu, but the DAT does not govern the effects of P_r.

In NAc, release in response to tonic stimulation also reached a steady state in control conditions but not in cocaine (**Fig. 4.12A**). Linear regression curves were fit to the relationship between normalised AUC and burst length in the presence (**Fig. 4.12B**) and absence of cocaine (**Fig. 4.12C**). The slope of this relationship was altered by a change in $[Ca^{2+}]_o$ (**Fig. 4.12D**; Two-way ANOVA, main effect of $[Ca^{2+}]_o$; $F_{1, 12} = 16.07$; $p = 0.002$; $n = 4$); reducing $[Ca^{2+}]_o$ from 2.4 mM to 1.2 mM increased the slope in the presence of cocaine, but not in control conditions (*post-hoc* Sidak's test, $p = 0.004$). There was also a trend toward a steeper relationship in the presence of cocaine,

but this did not reach significance ($p = 0.08$), suggesting that DAT-mediated control of signal contrast in NAc is weak.

These findings therefore suggest that a decrease in P_r enhances signal contrast of DA release in response to bursts in both CPu and NAc, and this dependence on P_r was not limited by the DAT. However, the DAT does appear to limit signal contrast in CPu but not in NAc.

4.4 Discussion

In this chapter, I have explored the effects of tonic background activity on $[DA]_o$ evoked by bursts of varying lengths. I have also explored the roles of Ca^{2+} handling and DAT function in control of burst contrast, in order to determine whether the mechanisms governing STP of DA release can influence the signal contrast of DA transients in response to bursts during ongoing activity. Tonic background activity increases the signal contrast of DA release in response to bursts, to a greater extent in NAc than in CPu, while contrast in CPu was more readily increased by changes in P_r and DAT function.

4.4.1 Effects of tonic stimulation on burst contrast across striatal regions

At rest, DA neurons fire APs at low frequency, interspersed with higher-frequency bursts that are thought to encode reward-related information about salient environmental stimuli. The role of tonic firing in the physiological functions of DA signalling remains unclear. It has been suggested that this low-frequency activity evokes DA release, maintaining a basal level of $[DA]_o$ that will activate high-affinity D2 receptors at rest (Floresco et al. 2003). However, other reports indicate that tonic [DA] is primarily maintained by summation of release in response to burst events (Owesson-White et al. 2012) and phasic increases in DA neuron firing (Fiorillo et al. 2003). In this chapter, I show that tonic activity in DA axons can also increase the contrast of DA transients in response to bursts of varying lengths, and that the magnitude of this effect is markedly different between the CPu and NAc.

During low-frequency regular stimulation (referred to as tonic background stimulation), DA release depressed rapidly then reached a steady state, resulting in $[DA]_o$ transients that were much smaller than those evoked by single-pulse stimulation. However, release evoked by a higher-frequency burst increased more steeply as a function of burst length after tonic stimulation than when bursts were delivered alone (i.e. separated by 2.5 minutes from any previous stimulation). This suggests that the DA release machinery is more sensitive to the

number of pulses in a burst when the burst arrives on a background of low-frequency activity. Signal contrast of bursts delivered alone was much greater in NAc than in CPu, as has been previously demonstrated (Cragg 2003; Zhang et al. 2009; Exley et al. 2008). In addition to this, tonic stimulation preceding the burst had a much greater effect on burst contrast in NAc, producing a steeper relationship between burst length and DA release than in CPu. This is consistent with a role for presynaptic STP of DA release in shaping signal contrast, since PPR of DA release is low at stimulation intervals corresponding to frequencies of approximately 10 Hz or less, and higher in NAc than in CPu at instantaneous frequencies of 25-40 Hz (Platt 2012). However, several other presynaptic factors could contribute to the regional difference in burst contrast, which will be discussed below.

It has previously been suggested that the greater sensitivity of DA release in NAc can be attributed to differences in expression of nicotinic acetylcholine receptor (nAChR) subtypes (Zhang et al. 2009). However, the present experiments were conducted in the presence of an antagonist at β2*-nAChRs, which are expressed on DA axons (Jones et al. 2001) and powerfully control STP (Rice & Cragg 2004), excluding this possibility.

DA neurons projecting to the CPu are thought to express more DAT protein than those projecting to NAc, resulting in faster DA uptake in synaptosomes prepared from CPu than from NAc (Marshall et al. 1990). Furthermore, Michaelis-Menten models fit to DA uptake kinetics obtained using FCV in striatal tissue show a greater maximal rate of uptake at a saturating $[DA]_o$ in CPu than in NAc, implying a greater number of uptake sites in CPu (Jones et al. 1995). This raises the possibility that the greater burst contrast ratio in NAc is caused by a slower rate of uptake and hence greater summation of extracellular DA during burst stimulation. However, in this chapter, burst contrast remained greater in NAc than in CPu in the presence of cocaine, suggesting that a slower rate of uptake does not fully explain greater burst contrast in NAc.

The difference in burst contrast between CPu and NAc could also arise due to differences in D2 autoreceptor function. Activation of D2 autoreceptors by DA release might inhibit subsequent release to a greater extent in CPu, resulting in a weaker sensitivity to the length of bursts. However, since DA release is required to activate D2 receptors, if the weak enhancement of signal contrast by tonic activity in CPu were explained by greater D2 autoreceptor activation there should be a stronger correlation between steady-state $[DA]_o$ and signal contrast ratio in CPu than in NAc. However, no significant difference in the slope of this relationship was observed between the two regions, suggesting that the stronger enhancement of signal contrast by tonic background activity in NAc compared to CPu is not due to regional differences in D2 autoreceptor function.

These findings suggest that DA release in NAc is inherently more sensitive to burst stimulation than release in CPu. Furthermore, tonic stimulation preceding burst stimulation increases the contrast between bursts of different lengths, to a greater extent in NAc than in CPu. These effects are not adequately explained by differences in nAChR expression, rate of uptake or regional differences in D2 autoreceptor function. Notably, paired-pulse stimulation of DA release at 25 Hz, the frequency of burst stimulation in this chapter, results in a paired-pulse ratio (PPR) of approximately 0.5 (indicating STD) in CPu and approximately 1 in NAc (Platt 2012). Weaker burst contrast in CPu may therefore be due to greater STD during the burst. Tonic firing in DA neurons may therefore enhance burst contrast through a presynaptic mechanism.

4.4.2 Stimulation-dependent increase and regional differences are due to intrinsic properties of DA neurons

Burst contrast is enhanced by tonic activity preceding the burst, but it is unclear whether this occurs due to the intrinsic axonal mechanisms governing STP of DA release, or due to activation of other circuit elements in the striatum (e.g. SPNs, interneurons and glial cells). The longer stimulation trains used in the present experiments are more likely to evoke the release of

neurotransmitters and other neuromodulators that may modulate DA release than the paired-pulse stimulation paradigm used in Chapter 3.

If enhancement of signal contrast following tonic background stimulation is caused by non-selective activation of local modulatory inputs, then this effect should be absent where DA axons conditionally expressing ChR2-EYFP are selectively activated using optical stimulation. In CPu, the significant difference between contrast ratio of bursts delivered alone and after tonic background stimulation, which was observed under control conditions, was not observed when DA release was evoked using optical stimulation. In contrast, the difference observed in NAc was even greater than that observed in control conditions. This may indicate that the enhancement of burst contrast in CPu but not NAc is promoted by non-selective activation of striatal neurons.

However, it is also possible that the properties of optically-evoked DA release differ between CPu and NAc, and that this difference underlies the contrasting region-specific effect of optical stimulation on burst contrast. The possibility that differences in ChR2 properties lead to the lack of an effect of tonic stimulation in CPu are supported by the observation that AUC of DA transients in response to bursts of 2, 4 and 6 pulses are similar for electrical and optical stimulation (compare Figs. 4.1C and 4.3C), while AUC for bursts of 8 and 10 pulses are lower for optical than for electrical stimulation. Artificially strong STD has previously been reported where ChR2 is virally expressed in unmyelinated axons in hippocampus, and this depression is more pronounced in response to longer stimulation trains (Jackman et al. 2014). This may suggest that ChR2 in CPu DA axons promotes greater STD than observed with electrical stimulation. Given that optical stimulation produced a higher contrast ratio in NAc, it is difficult to conclude whether the weaker effect in CPu is caused by the selective activation of DA axons or by aberrant effects of ChR2 expression on STP at DA release sites in CPu.

Enhancement of burst contrast by tonic stimulation is therefore not caused, and may even be inhibited, by non-selective activation of local circuits in NAc. In CPu, the effect of local circuits is

less clear, but burst contrast is still elevated by low-frequency stimulation when selective activation of DA axons is used. It is therefore likely that the enhancement of burst contrast by tonic stimulation is not wholly caused by activation of local inputs to DA axons.

4.4.3 Dependence of burst contrast on tonic stimulation frequency

Tonic firing of DA neurons *in vivo* is distributed across a range of frequencies, with the mean frequency at approximately 6 Hz (see section 4.1.1). At a higher stimulation frequency, the steady-state level of $[DA]_o$ on which bursts occur will be greater, which may limit contrast between DA release in response to single stimulations and in response to bursts. To explore this possibility, burst contrast was measured using a tonic stimulation frequency of 6 Hz (3 s, 18 pulses) followed by a 25 Hz burst.

When tonic stimulation preceding the burst was delivered at a frequency of 6 Hz, the steady-state $[DA]_o$ was increased. Under these conditions, estimates of burst contrast ratio were subject to greater error, as the release events attributable to individual pulses during regular stimulation were smaller than those at 2 Hz. Nonetheless, the contrast ratio of bursts delivered after regular 6 Hz stimulation was still greater than that of bursts delivered alone. This effect was observed in both CPu and NAc, although again contrast ratios were higher under all conditions in NAc.

Enhancement of burst contrast by preceding regular stimulation was maintained but was weaker at a higher frequency of regular stimulation. This could be attributed to a higher steady-state $[DA]_o$, or to smaller burst events. Comparison of mean peak $[DA]_o$ evoked by burst events after regular stimulation at 2 and 6 Hz suggests that transients evoked by bursts were approximately 50% lower in the latter case, while normalised AUC was decreased by a smaller amount. This suggests that a combination of increased steady state $[DA]_o$ and decreased $[DA]_o$ in response to bursts underlies the weaker effect observed at higher regular stimulation frequency.

Increasing the frequency of tonic stimulation therefore both increased steady-state [DA] during tonic stimulation and decreased the ratio between release in response to tonic stimulation and

bursts. This could indicate that tonic firing in DA neurons has distinct functions at different frequencies. Changes in the frequency of tonic firing of DA neurons *in vivo* might therefore shift the role of tonic activity from promoting contrast to driving long-term increases in extracellular [DA] in striatum and consequently limiting phasic increases in $[DA]_o$ driven by burst firing.

4.4.4 Weak effects of Ca^{2+}-dependent modulation on burst contrast

The effect of tonic stimulation on burst contrast was not prevented by selective stimulation or higher regular stimulation frequency, and as described above is unlikely to be due to differences in uptake, D2AR function or nAChR expression. Axonal mechanisms of STP might therefore shape the contrast ratio between bursts and single stimuli during ongoing activity. As described in Chapter 3, STP in a paired-pulse paradigm was more sensitive to changes in $[Ca^{2+}]_o$ in NAc than in CPu. This might be explained by pseudofacilitation, the process by which saturation of an intra-terminal Ca^{2+} buffer such as calbindin during initial stimulation increases the proportion of the Ca^{2+} transient evoked by a subsequent stimulation available to drive neurotransmitter release (Blatow et al. 2003, see section 1.1.3.1), which might occur in NAc due to greater expression of calbindin in DA neurons projecting to that region. However, in this chapter, signal contrast on a background of tonic stimulation was enhanced by a decrease in initial P_r in CPu but not in NAc, suggesting that high P_r relative to NAc contributes to the more limited signal contrast in CPu. The regional difference in sensitivity to changes in $[Ca^{2+}]_o$ is therefore reversed on a background of tonic stimulation, with greater sensitivity in CPu than in NAc.

It is unclear why higher P_r limits signal contrast in CPu relative to NAc. An intuitive explanation might be that tonic background stimulation in CPu results in depletion of the readily releasable vesicle pool, but since greater release would be expected to lead to more extensive depletion, this explanation is inconsistent with the finding that signal contrast is not correlated with steady-state $[DA]_o$. Instead, this regional difference is likely to be due in part to a regional difference in a DAT-mediated clamp on sensitivity to P_r, as described below.

4.4.5 The DAT limits burst contrast and dependence on P_r

Data presented in Chapter 3 also demonstrated that the relationship between P_r and PPR was stronger when the DAT was inhibited with cocaine (see section 3.3.2), suggesting the DAT mediates a clamp on the dependence of STP on P_r. In this chapter, I have investigated whether inhibition of the DAT also enhances the effect of $[Ca^{2+}]_o$ on signal contrast.

Inhibition of the DAT with cocaine increased signal contrast in CPu, but not in NAc, suggesting that the DAT limits contrast in CPu. This is likely to reflect a faster rate of uptake in CPu, which is thought to contain more DA uptake sites (Marshall et al. 1990), reflected by a higher maximal rate of uptake (Jones et al. 1995). The DAT is therefore likely to limit extracellular summation over the course of the burst to a greater extent in CPu than in NAc, limiting the dependence of DA release on burst length.

The effects of changing $[Ca^{2+}]_o$ during DAT inhibition were region-specific. In CPu, the slope of the relationship between signal contrast and burst length was increased by a reduction in $[Ca^{2+}]_o$, in both the presence and absence of cocaine, but the magnitude of the effect was not dependent on DAT inhibition. This suggests that signal contrast in CPu is dependent on P_r, regardless of DAT function. However, in NAc, signal contrast was enhanced by low P_r when the DAT was inhibited, but not under control conditions, suggesting that DAT-mediated clamping of P_r-dependence plays a significant role in shaping the response to bursts in this region. As described in section 3.4.2, the DAT might limit a relationship between initial P_r and STP by altering the dynamics of Ca^{2+} influx through presynaptic VGCCs, or by tuning vesicle mobility at DA release sites through an interaction with synaptic vesicle proteins. However, the exact mechanism remains undetermined.

On a background of tonic activity, the DAT therefore appears to limit dependence of signal contrast on P_r in NAc but not in CPu. Inhibition of the DAT might therefore reduce the regional specialisation of DA release, resulting in a more consistent pattern of DA signalling across the functional regions of the striatum.

4.4.6 Summary and implications

These findings could suggest that low-frequency activity in DA neurons maintains contrast between basal extracellular [DA] and larger release events in response to bursts that encode information about salient stimuli.

Experiments described in this chapter have shown that tonic activation of DA axons increases the strength of the relationship between burst length and DA release, and therefore may represent a mechanism to enhance postsynaptic responses to bursting activity in DA neurons. These findings support the hypothesis that tonic low-frequency firing promotes release events in response to higher-frequency bursts. Tonic firing in DA neurons may promote fast, high-contrast DA signals in striatum, that may be necessary to accurately signal reward prediction errors, with integration of release events over time encoding motivation (Hamid et al. 2015).

Furthermore, this may indicate a regional specialisation of the properties of DA volume transmission in striatum, driven by presynaptic STP. Modelling of dopamine receptor occupancy suggests that high-contrast phasic DA release in response to bursting promotes activation of D1Rs and limits activation of D2Rs (Dreyer et al. 2010). In NAc, high-affinity DA receptors are more readily saturated by large DA release events than in CPu (Dreyer & Hounsgaard 2013), which could indicate that release in NAc is well-adapted for rapid switching between postsynaptic reporting of tonic and phasic events at D2R- and D1R-expressing SPNs, respectively, while release in CPu is adapted for more graded changes in postsynaptic response. In this chapter, inhibition of the DAT with cocaine made the relationship between burst length and DA release more similar across the two regions, which might contribute to the transfer of behavioural control from NAc to dorsolateral CPu (Everitt & Robbins 2013). Acute exposure to cocaine *in vivo* promotes bursting by increasing NMDAR input to DA neurons (Creed et al. 2016), so it is likely that the cocaine-mediated enhancement of burst contrast will be even greater under these conditions. Increased

reporting of burst events through contrast enhancement may be an important factor in development of addiction.

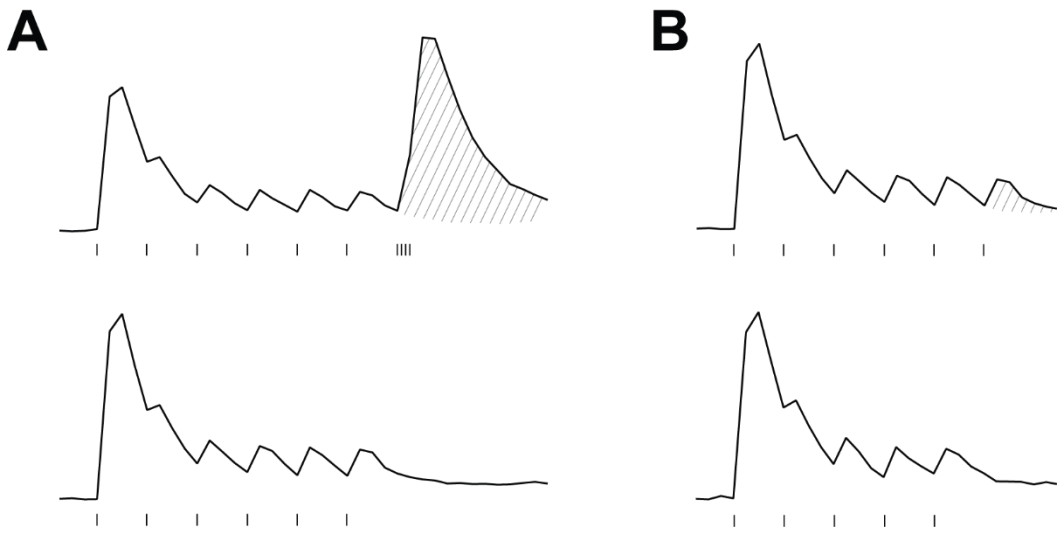

Fig. 4.1 Method of subtraction to determine $[DA]_o$ for normalisation

A) Determination of $[DA]_o$ attributable to a burst following tonic background stimulation. A DA transient evoked by tonic background stimulation delivered alone (6 pulses at 2 Hz, lower panel) subtracted from a transient evoked by tonic background stimulation followed by a burst (upper panel) gives $[DA]_o$ attributable to the burst (hashed area). **B)** Determination of $[DA]_o$ attributable to the final pulse of tonic background stimulation. A DA transient evoked by tonic background stimulation with the final pulse omitted (5 pulses at 2 Hz, lower panel) subtracted from a transient evoked by tonic background stimulation delivered alone (6 pulses at 2 Hz, upper panel) gives $[DA]_o$ attributable to the final pulse (hashed area). The peak or AUC of the transient attributable to the burst (hashed area in **A**) is then normalised to the peak or AUC, respectively, of the transient attributable to the final pulse of tonic background stimulation (hashed area in **B**).

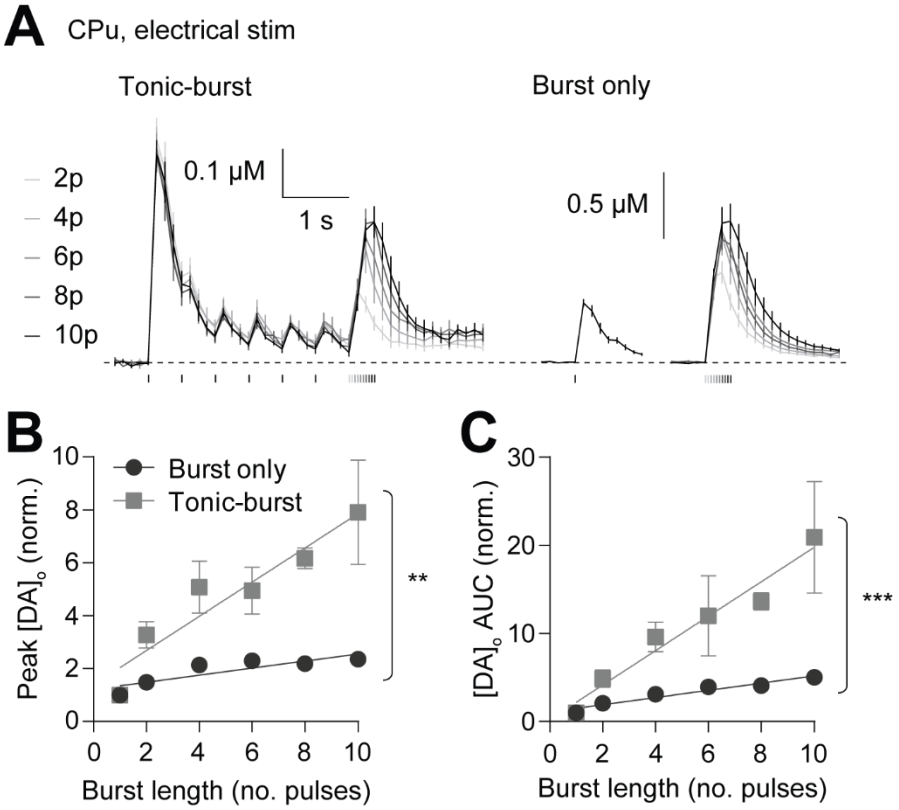

Fig. 4.2 Tonic background stimulation increases signal contrast of electrically-evoked bursts in CPu

A) Average profiles of $[DA]_o$ transients (mean $[DA]_o$ ± SEM) evoked by bursts of 2-10 electrical pulses at 25 Hz delivered alone (black) or after tonic stimulation at 2 Hz (grey) in CPu (n = 4). **B)** Mean peak $[DA]_o$ (±SEM) evoked by bursts delivered alone (black) or after tonic stimulation at 2 Hz (grey) normalised to single pulse delivered alone or during tonic stimulation, respectively. Slope of the linear regression curve was significantly greater after tonic stimulation. **C)** Mean AUC of $[DA]_o$ (±SEM) evoked by bursts delivered alone (black) or after tonic stimulation at 2 Hz (grey) normalised to single pulse delivered alone of during tonic stimulation, respectively. Slope of the linear regression curve was significantly greater after tonic stimulation. **p < 0.01, ***p < 0.001.

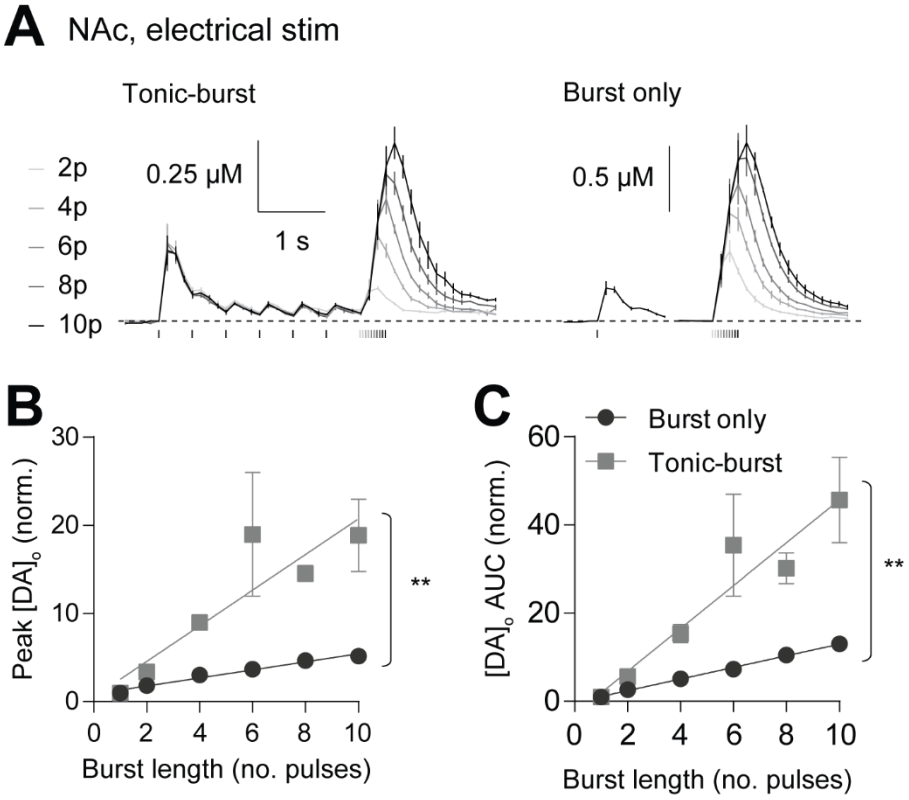

Fig. 4.3 Tonic background stimulation increases signal contrast of electrically-evoked bursts in NAc

A) Average profiles of $[DA]_o$ transients (mean $[DA]_o$ ± SEM) evoked by bursts of 2-10 electrical pulses at 25 Hz delivered alone (black) or after tonic stimulation at 2 Hz (grey) in NAc (n = 3). **B)** Mean peak $[DA]_o$ (±SEM) evoked by bursts delivered alone (black) or after tonic stimulation at 2 Hz (grey) normalised to single pulse delivered alone or during tonic stimulation, respectively. Slope of the linear regression curve was significantly greater after tonic stimulation. **C)** Mean AUC of $[DA]_o$ (±SEM) evoked by bursts delivered alone (black) or after tonic stimulation at 2 Hz (grey) normalised to single pulse delivered alone of during tonic stimulation, respectively. Slope of the linear regression curve was significantly greater after tonic stimulation. **$p < 0.01$.

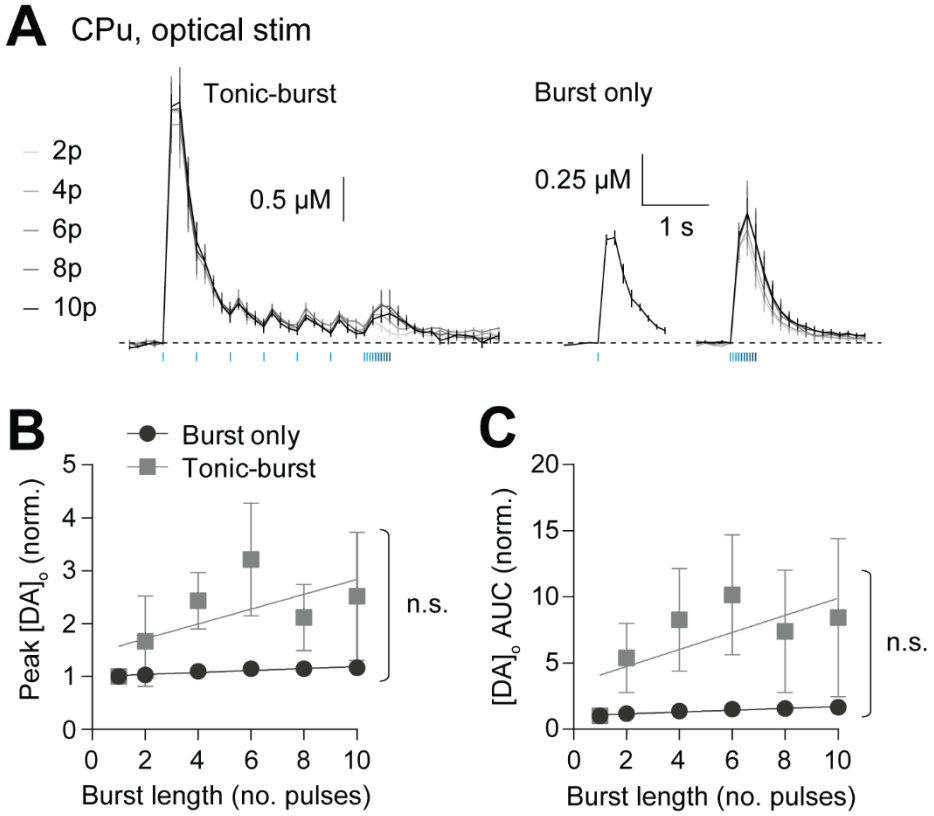

Fig. 4.4 Tonic background activity does not affect signal contrast of optically-evoked bursts in CPu

A) Average profiles of $[DA]_o$ transients (mean $[DA]_o$ ± SEM) evoked by bursts of 2-10 optical pulses at 25 Hz delivered alone (black) or after tonic stimulation at 2 Hz (grey) in CPu (n = 4). **B)** Mean peak $[DA]_o$ (±SEM) evoked by bursts delivered alone (black) or after tonic stimulation at 2 Hz (grey) normalised to single pulse delivered alone or during tonic stimulation, respectively. **C)** Mean AUC of $[DA]_o$ (±SEM) evoked by bursts delivered alone (black) or after tonic stimulation at 2 Hz (grey) normalised to single pulse delivered alone of during tonic stimulation, respectively.

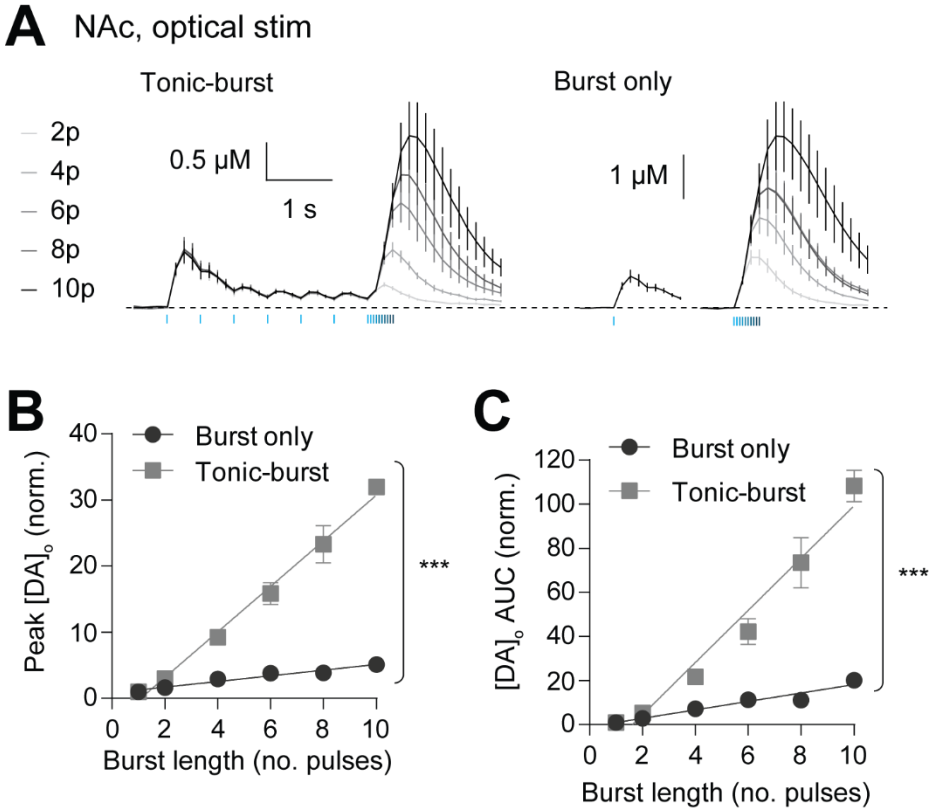

Fig. 4.5 Tonic background activity increases signal contrast of optically-evoked bursts in NAc

A) Average profiles of $[DA]_o$ transients (mean $[DA]_o$ ± SEM) evoked by bursts of 2-10 optical pulses at 25 Hz delivered alone (black) or after tonic stimulation at 2 Hz (grey) in CPu (n = 3). **B)** Mean peak $[DA]_o$ (±SEM) evoked by bursts delivered alone (black) or after tonic stimulation at 2 Hz (grey) normalised to single pulse delivered alone or during tonic stimulation, respectively. Slope of the linear regression curve was significantly greater after tonic stimulation. **C)** Mean AUC of $[DA]_o$ (±SEM) evoked by bursts delivered alone (black) or after tonic stimulation at 2 Hz (grey) normalised to single pulse delivered alone of during tonic stimulation, respectively. Slope of the linear regression curve was significantly greater after tonic stimulation. ***$p < 0.001$.

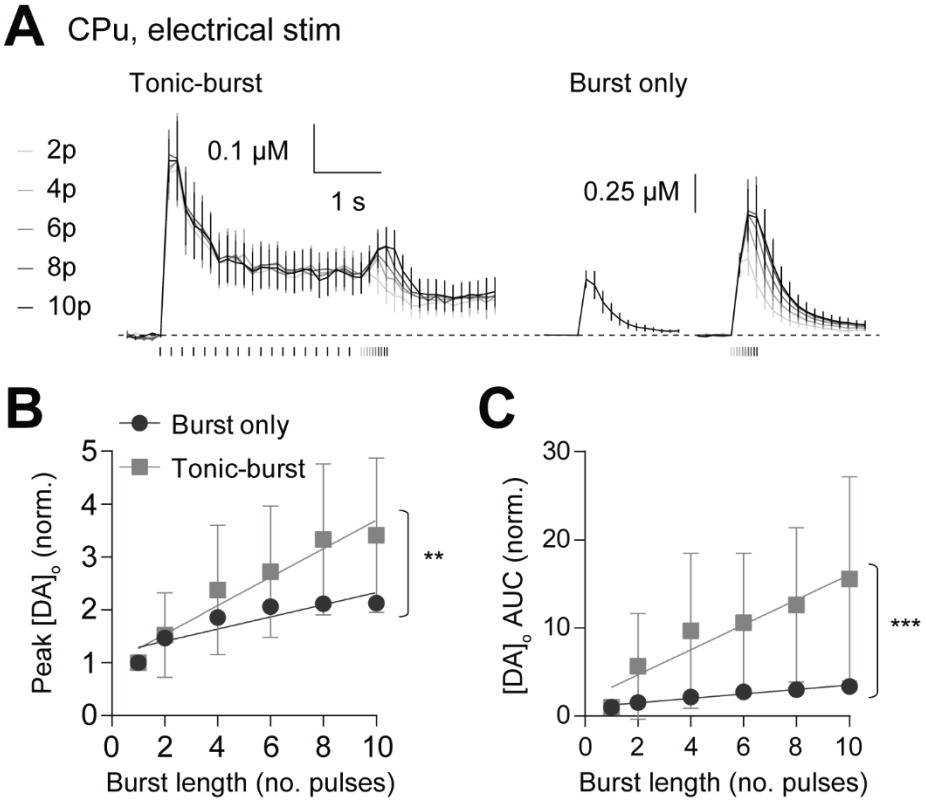

Fig. 4.6 Tonic background stimulation at 6 Hz increases signal contrast of bursts in CPu

A) Average profiles of $[DA]_o$ transients (mean $[DA]_o$ ± SEM) evoked by bursts of 2-10 electrical pulses at 25 Hz delivered alone (black) or after tonic stimulation at 6 Hz (grey) in CPu (n = 4). **B)** Mean peak $[DA]_o$ (±SEM) evoked by bursts delivered alone (black) or after tonic stimulation at 6 Hz (grey) normalised to single pulse delivered alone or during tonic stimulation, respectively. Slope of the linear regression curve was significantly greater after tonic stimulation. **C)** Mean AUC of $[DA]_o$ (±SEM) evoked by bursts delivered alone (black) or after tonic stimulation at 6 Hz (grey) normalised to single pulse delivered alone of during tonic stimulation, respectively. Slope of the linear regression curve was significantly greater after tonic stimulation. **p < 0.01, ***p < 0.001.

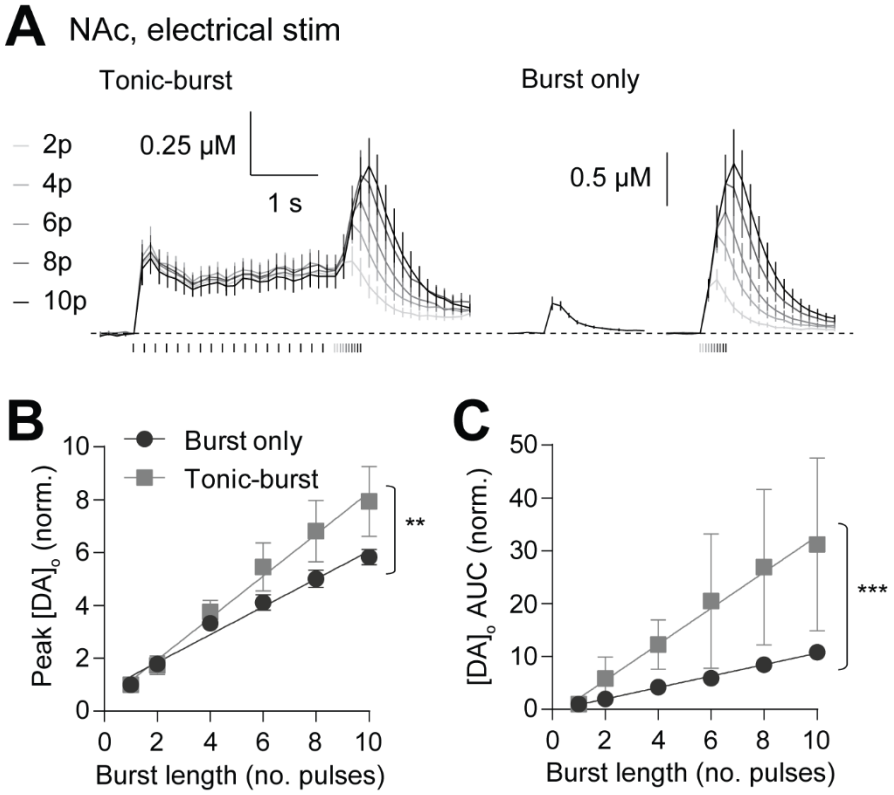

Fig. 4.7 Tonic stimulation at 6 Hz increases signal contrast of bursts in NAc

A) Average profiles of $[DA]_o$ transients (mean $[DA]_o$ ± SEM) evoked by bursts of 2-10 electrical pulses at 25 Hz delivered alone (black) or after tonic stimulation at 6 Hz (grey) in NAc (n = 3). **B)** Mean peak $[DA]_o$ (±SEM) evoked by bursts delivered alone (black) or after tonic stimulation at 6 Hz (grey) normalised to single pulse delivered alone or during tonic stimulation, respectively. Slope of the linear regression curve was significantly greater after tonic stimulation. **C)** Mean AUC of $[DA]_o$ (±SEM) evoked by bursts delivered alone (black) or after tonic stimulation at 6 Hz (grey) normalised to single pulse delivered alone of during tonic stimulation, respectively. Slope of the linear regression curve was significantly greater after tonic stimulation. **p < 0.01, ***p < 0.001.

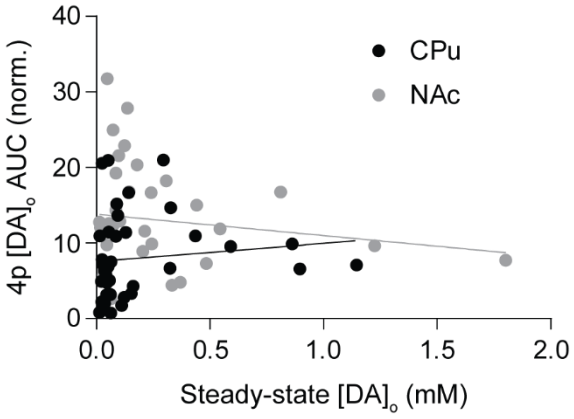

Fig. 4.8 Steady-state $[DA]_o$ is not correlated to burst signal contrast

Steady-state $[DA]_o$ plotted against signal contrast ratio of a 4-pulse burst following tonic stimulation at a population of recording sites in CPu (black) and NAc (grey). Plots were fitted with a linear regression model. No significant correlation was observed in either region, and there was no significant difference between the slopes of the two curves.

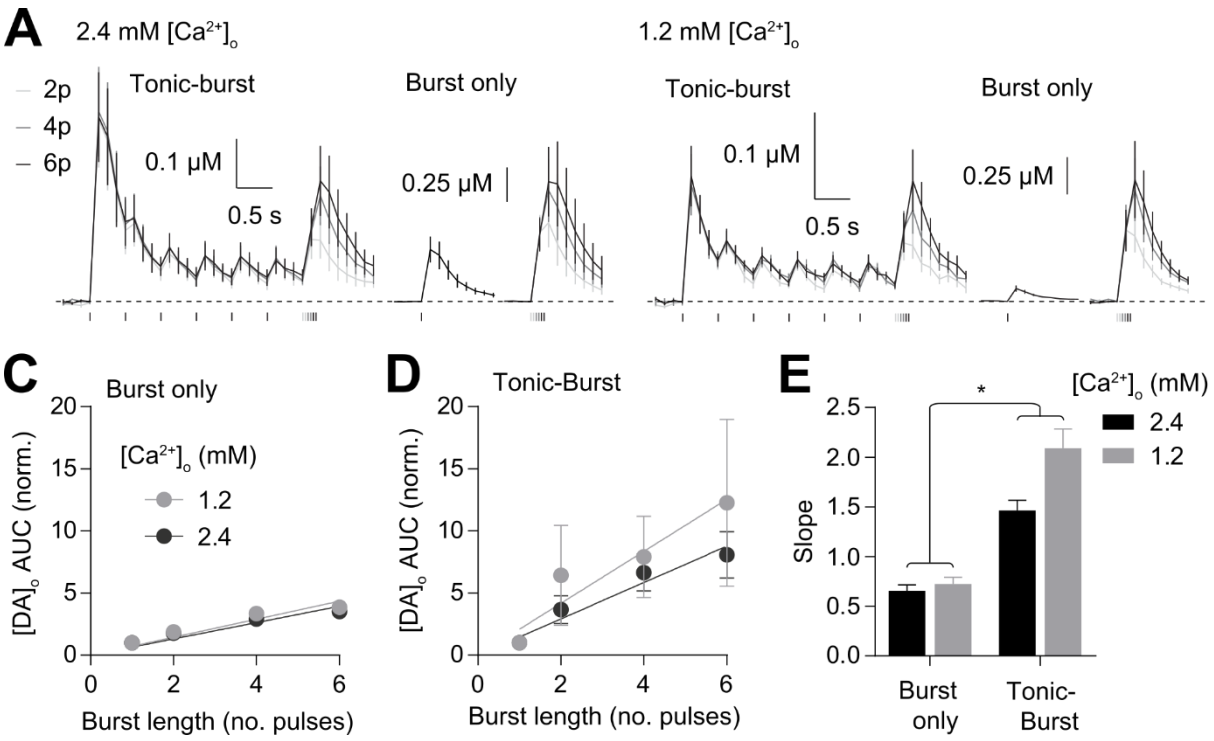

Fig. 4.9 Reducing P_r promotes signal contrast after tonic stimulation in CPu

A) Average profiles of $[DA]_o$ transients (mean $[DA]_o$ ± SEM) evoked by bursts of 2-6 electrical pulses at 25 Hz delivered alone (black) or after tonic stimulation at 2 Hz (grey) in 2.4 mM (left) or 1.2 mM $[Ca^{2+}]_o$ (right) in CPu (n = 5). **B)** Mean AUC of $[DA]_o$ (±SEM) evoked by bursts delivered alone in 2.4 mM (black) or 1.2 mM $[Ca^{2+}]_o$ (grey) normalised to single pulse delivered alone. **C)** Mean AUC of $[DA]_o$ evoked by bursts delivered after tonic stimulation at 2 Hz in 2.4 mM (black) or 1.2 mM $[Ca^{2+}]_o$ (grey) normalised to single pulse delivered during tonic stimulation. **D)** Mean slope (±SEM) of the relationship between burst length and normalised AUC evoked by bursts delivered alone or after tonic stimulation at 2 Hz in 2.4 mM (black) or 1.2 mM $[Ca^{2+}]_o$ (grey). Tonic stimulation significantly increased slope, but changing $[Ca^{2+}]_o$ did not significantly alter slope in either condition. **p < 0.01.

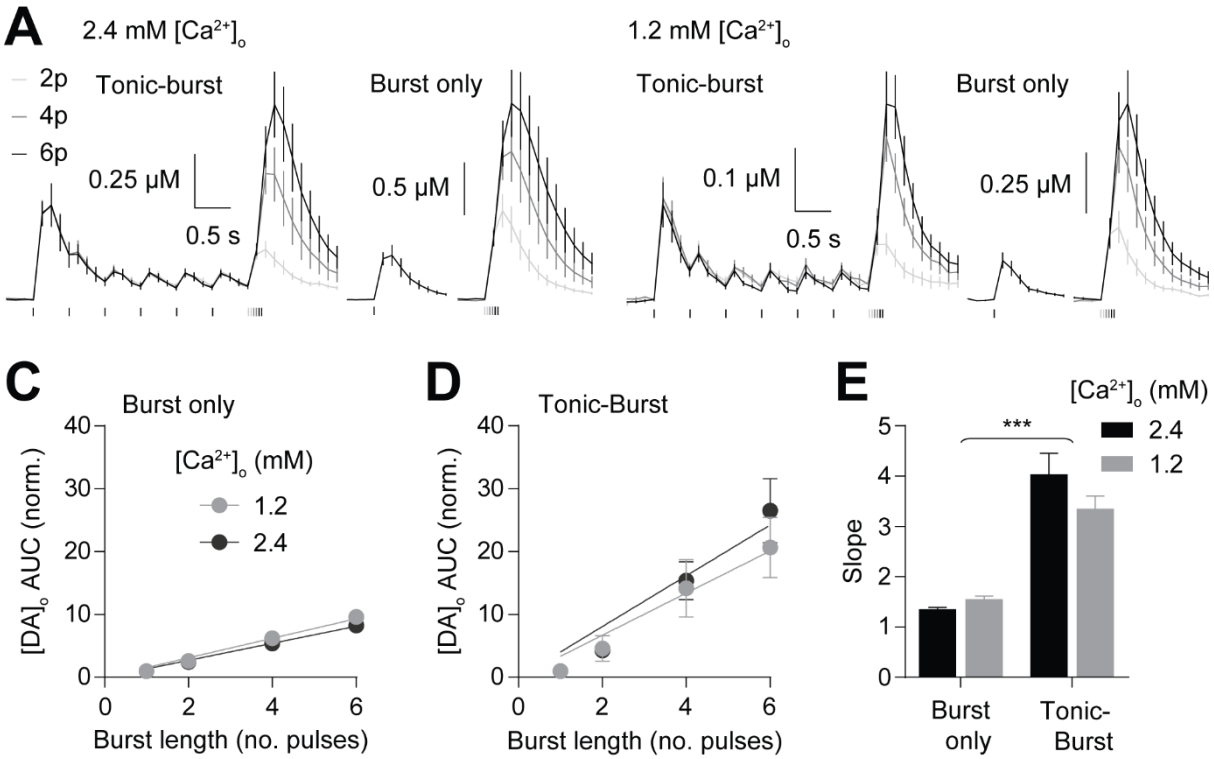

Fig. 4.10 Reducing P_r does not promote signal contrast after tonic stimulation in NAc

A) Average profiles of $[DA]_o$ transients (mean $[DA]_o$ ± SEM) evoked by bursts of 2-6 electrical pulses at 25 Hz delivered alone (black) or after tonic stimulation at 2 Hz (grey) in 2.4 mM (left) or 1.2 mM $[Ca^{2+}]_o$ (right) in NAc (n = 5). **B)** Mean AUC of $[DA]_o$ (±SEM) evoked by bursts delivered alone in 2.4 mM (black) or 1.2 mM $[Ca^{2+}]_o$ (grey) normalised to single pulse delivered alone. Slope of the linear regression curve was significantly greater in 1.2 mM than in 2.4 mM $[Ca^{2+}]_o$. **C)** Mean AUC of $[DA]_o$ evoked by bursts delivered after tonic stimulation at 2 Hz in 2.4 mM (black) or 1.2 mM $[Ca^{2+}]_o$ (grey) normalised to single pulse delivered during tonic stimulation. Slope of the linear regression curve was significantly greater in 2.4 mM than in 1.2 mM $[Ca^{2+}]_o$. **D)** Mean slope (±SEM) of the relationship between burst length and normalised AUC evoked by bursts delivered alone or after tonic stimulation at 2 Hz in 2.4 mM (black) or 1.2 mM $[Ca^{2+}]_o$ (grey). Tonic stimulation significantly increased slope, and a reduction in $[Ca^{2+}]_o$ decreased slope after tonic stimulation. **$p < 0.01$.

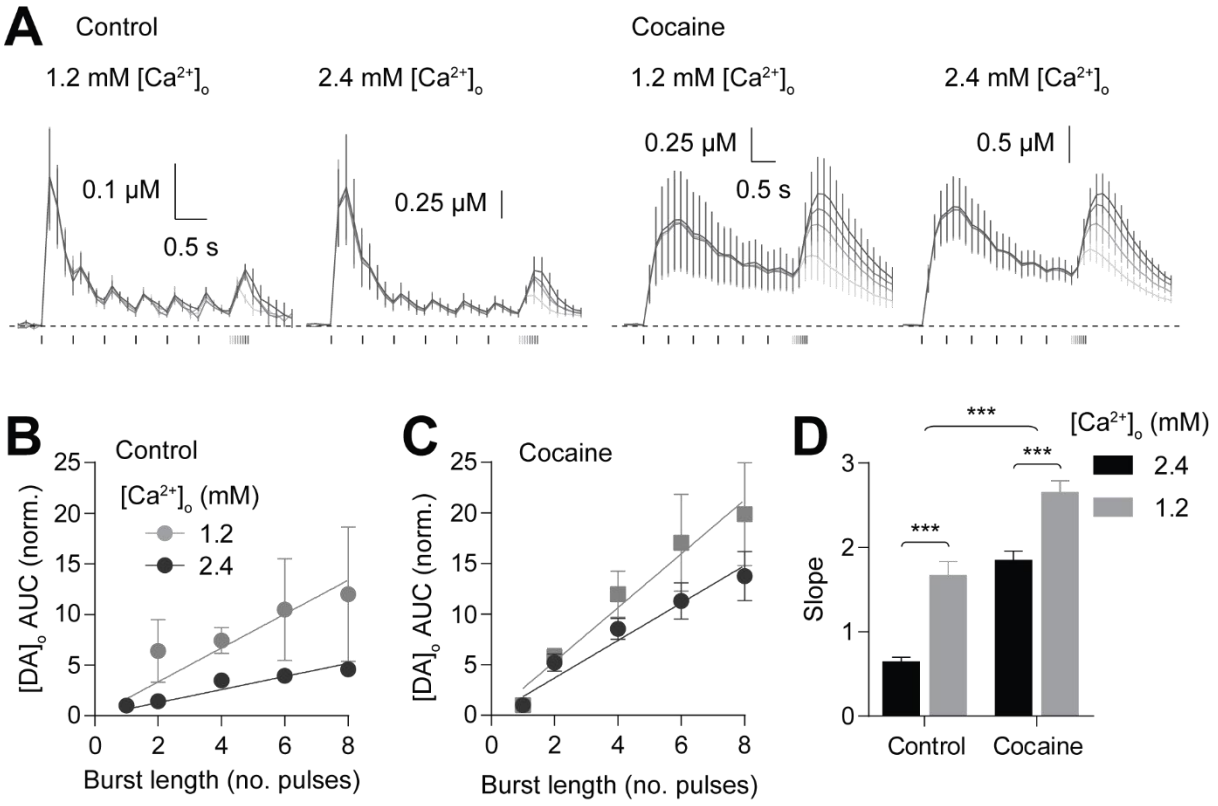

Fig. 4.11 DAT limits signal contrast and dependence on P_r in CPu

A) Average profiles of $[DA]_o$ transients (mean $[DA]_o$ ± SEM) evoked by bursts of 2-8 electrical pulses at 25 Hz in 2.4 mM (black) or 1.2 mM $[Ca^{2+}]_o$ (grey) in control conditions (left) or in cocaine (right) in CPu (n = 4). **B)** Mean AUC of $[DA]_o$ (±SEM) evoked by bursts in 2.4 mM (black) or 1.2 mM $[Ca^{2+}]_o$ (grey) in control conditions, normalised to single pulse delivered during tonic stimulation. Slope of the linear regression curve was significantly greater in 1.2 mM than in 2.4 mM $[Ca^{2+}]_o$. **C)** Mean AUC of $[DA]_o$ (±SEM) evoked by bursts in 2.4 mM (black) or 1.2 mM $[Ca^{2+}]_o$ (grey) in cocaine normalised to single pulse delivered during tonic stimulation. Slope of the linear regression curve was significantly greater in 1.2 mM than in 2.4 mM $[Ca^{2+}]_o$. **D)** Mean slope (±SEM) of the relationship between burst length and normalised AUC evoked by bursts in control conditions or cocaine in 2.4 mM (black) or 1.2 mM $[Ca^{2+}]_o$ (grey). Cocaine significantly increased slope, and a reduction in $[Ca^{2+}]_o$ increased slope in the presence and absence of cocaine. *$p < 0.05$, **$p < 0.01$, ***$p < 0.001$.

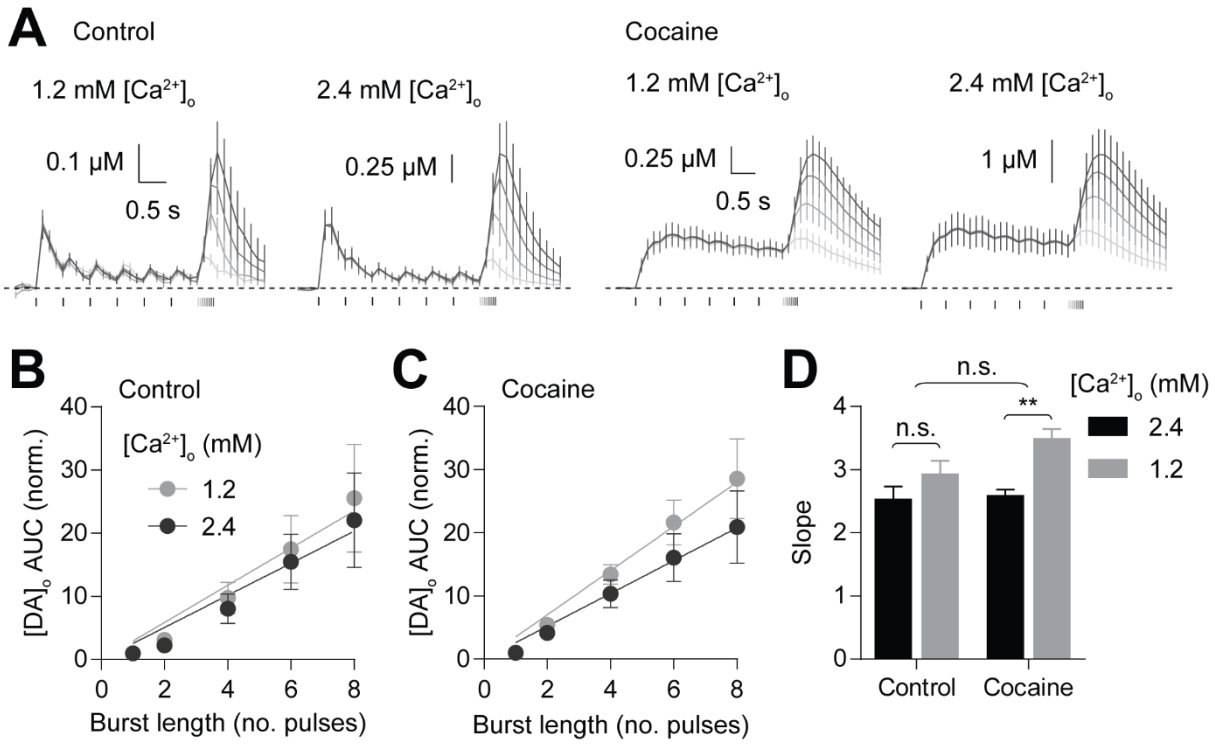

Fig. 4.12 DAT does not limit signal contrast in NAc

A) Average profiles of $[DA]_o$ transients (mean $[DA]_o$ ± SEM) evoked by bursts of 2-8 electrical pulses at 25 Hz in 2.4 mM (black) or 1.2 mM $[Ca^{2+}]_o$ (grey) in control conditions (left) or in cocaine (right) in NAc (n = 4). **B)** Mean AUC of $[DA]_o$ (±SEM) evoked by bursts in 2.4 mM (black) or 1.2 mM $[Ca^{2+}]_o$ (grey) in control conditions, normalised to single pulse delivered during tonic stimulation. **C)** Mean AUC of $[DA]_o$ (±SEM) evoked by bursts in 2.4 mM (black) or 1.2 mM $[Ca^{2+}]_o$ (grey) in cocaine normalised to single pulse delivered during tonic stimulation. Slope of the linear regression curve was significantly greater in 1.2 mM than in 2.4 mM $[Ca^{2+}]_o$. **D)** Mean slope (±SEM) of the relationship between burst length and normalised AUC evoked by bursts in control conditions or cocaine in 2.4 mM (black) or 1.2 mM $[Ca^{2+}]_o$ (grey). Cocaine significantly increased slope, and a reduction in $[Ca^{2+}]_o$ increased slope in the presence but not in the absence of cocaine. *p < 0.05, **p < 0.01, ***p < 0.001.

Chapter 5.

GABAergic signalling by DA neurons is not regulated by the DAT

5.1 Introduction

In this chapter I explore the properties of GABA transmission evoked by selective stimulation of DA axons, aiming to determine whether co-released GABA is regulated by the DAT in a similar manner to DA release.

Co-transmission from DA axons

Historically, it has been thought that individual neurons can release only a single neurotransmitter at all release sites, and that neuronal identity is defined by the released transmitter (Strata & Harvey 1999). However, it has since become clear that numerous neuronal populations are capable of the release of multiple primary neurotransmitters (Vaaga et al. 2014). The degree of spatial separation between release sites for different neurotransmitters in co-releasing neurons can vary; transmitters might be released from segregated sites in the axonal arbor, released from distinct vesicle pools at common release sites, or co-stored and released from a common vesicle pool (Tritsch et al. 2016).

Optogenetic tools have been used to demonstrate that DA neurons are also capable of both GABAergic (Tritsch et al. 2012; Kim et al. 2015; Tritsch et al. 2014) and glutamatergic signalling (Chuhma 2004; Chuhma et al. 2009; Stuber et al. 2010; Tecuapetla et al. 2010). GABA is thought to be co-released from vesicles that also store and release DA, since GABA release is prevented by inhibition of the vesicular monoamine transporter (VMAT) (Tritsch et al. 2012), and electron microscopy for immunogold-labelled GABA shows a high degree of co-localisation with tyrosine hydroxylase (TH) and VMAT (Stensrud et al. 2014). GABA co-release has been identified in both CPu and NAc (Tritsch et al. 2014; Tritsch et al. 2012).

The function of GABA co-release from DA neurons remains unclear. In the CNS, GABA frequently acts as a fast point-to-point transmitter, in contrast to the slow modulatory transmission mediated by DA, although GABA can also act via volume transmission (Isaacson et al. 1993). This

raises the possibility, as suggested for glutamate co-transmission (Chuhma 2004), that GABA co-release represents a mechanism for fast signalling between DA neurons and postsynaptic targets, complementing the slow modulatory transmission mediated by DA release. Ultrastructural studies have shown GABA storage in approximately 10% of striatal boutons expressing VMAT or TH (Stensrud et al. 2014) and that 30-40% of striatal DA-positive varicosities appear to form symmetric synaptic contacts (Descarries et al. 1996), although it remains unclear to what extent these two populations overlap. In support of a role for GABA in inhibitory signalling, loss of the ubiquitin ligase Ube3a limits GABA co-release and appears to increase motivation in mice to respond for self-stimulation of mesolimbic DA neurons (Berrios et al. 2016).

Presynaptic regulation of GABA co-release

While functional and anatomical evidence suggest that GABA is co-released from vesicles that store DA, it remains unclear whether the mechanisms of presynaptic regulation that shape DA release also apply to co-released GABA. If GABA and DA are indeed released from the same pool of vesicles, it might be expected that the presynaptic mechanisms outlined in Chapter 3, and in previous work (Platt 2012), would regulate the release of both transmitters in a similar manner. Given that the dopamine transporter (DAT) is thought to promote segregation of synaptic vesicle pools and therefore limit release (Venton et al. 2006; Kile et al. 2010), it seems probable that GABA release would also be limited by DAT function, and conversely enhanced by DAT inhibition.

However, a recent report suggested that DAT inhibition with the selective inhibitor GBR12935 did not change the amplitude of currents evoked by activation of DA axons in DAT^{Cre};Ai32 mice (Kim et al., 2015, Supplementary Figure 4). This may indicate that GABA release is not regulated by DAT function, although it has not yet been demonstrated that application of GBR12935 increases DA release in a similar manner to other DAT inhibitors. In light of this finding, this chapter will explore the regulation of GABA release from DA neurons, to determine whether the DAT can limit the release of GABA in a similar manner to DA.

In addition, the mechanisms governing presynaptic short-term plasticity (STP) of DA release would be expected to regulate STP of GABA release, if these transmitters are released from the same vesicle pool. It has been shown that IPSCs evoked in striatal SPNs by optical activation of DA neurons are subject to strong STD at a 5 s IPI, showing a similar paired-pulse ratio to DA transients at the same IPI (Adrover et al. 2014), supporting the hypothesis that STP of DA and GABA release is similarly regulated. However, as described above, GABA release may not be regulated by the DAT (Kim et al. 2015). It is unclear whether STP of GABA release will be regulated by DAT function. If DA and GABA release are similarly regulated, DAT inhibition should relieve STD of GABA release at IPIs of 25-100 ms, at which DAT inhibition has been observed to relieve STD in Chapter 3 and in previous work (Platt 2012). This chapter will also explore whether STP of GABA release is regulated by DAT function.

Hypotheses

In this chapter I aim to test the following hypotheses, in order to determine whether co-released GABA is regulated similarly or differentially to DA.

1) DA axons in striatum can release GABA, which activates $GABA_A$ receptors to trigger fast post-synaptic currents in SPNs.

2) GABA release, and therefore the magnitude of post-synaptic currents in SPNs, is limited by DAT function.

3) DAT function supports STD of GABA release.

5.2 Methods

Experiments described in this chapter were carried out according to the general methods laid out in Chapter 2. Variations and further details are described below.

Slice preparation

Experiments described in this chapter were conducted in striatal slices prepared from adult heterozygote DAT-internal ribosome entry site-Cre ($DAT^{IRES\text{-}Cre}$) mice conditionally expressing ChR2 in DA neurons. Methods for breeding and AAV5-ChR2 transfection are described in Chapter 2. All experiments were conducted in accordance with a UK Home Office-approved project licence and local guidelines.

Animals were anaesthetised with isoflurane and killed by intraperitoneal injection of sodium pentobarbital (Euthatal) before being intracardially perfused with ice-cold cutting solution saturated with carbogen (95% O_2/5% CO_2). Cutting solution contained (in mM): 85 NaCl, 25 $NaHCO_3$, 10 glucose, 65 sucrose, 2.5 KCl, 1.25 NaH_2PO_4, 7 $MgCl_2$, 0.5 $CaCl_2$.

Brains were extracted and slices were prepared as described in Chapter 2. Slices were incubated for a minimum of 30 minutes at 32°C in carbogenated aCSF, which contained (in mM): 130 NaCl, 10 glucose, 2 $MgCl_2$, 2.5 KCl, 1.25 NaH_2PO_4, 26 $NaHCO_3$, 2.5 $CaCl_2$.

Whole-cell electrophysiology

For recording, slices were transferred to a recording bath under continuous perfusion at a rate of approximately 2 mL per minute with carbogenated aCSF warmed to 31-33°C. Whole-cell voltage- and current-clamp recordings were performed on striatal SPNs, as described in Chapter 2.

Stimulation and experimental design

Post-synaptic currents were evoked by whole-field or local illumination with an LED or laser system, respectively, as described in Chapter 2. In some experiments, laser output was reduced to

a sub-maximal stimulation intensity (approximately 70% of control) to limit saturation of the post-synaptic response.

Drugs

Cocaine hydrochloride was obtained from Sigma. AP-5 was obtained from Insight Biotechnology. NBQX was obtained from Abcam. Bicuculline was obtained from Tocris Biosciences. Drugs were dissolved in deionised water or dimethyl sulphoxide (NBQX, bicuculline) to prepare stock aliquots at 1,000-10,000x final concentration. All drugs were diluted to their final concentration in oxygenated aCSF and bath-applied. Following drug application, PSCs were monitored for at least 3 sweeps and data were collected for analysis once the change in amplitude between sweeps did not differ from basal run-down.

Data analysis & statistics

Cells were recorded in dorsolateral and dorsomedial CPu, and in NAc core. Due to the low numbers of cells recorded in each region, all cells were pooled for analysis. Amplitude data have been colour-coded in Figs. 5.2-5 to indicate whether the data were collected in CPu or NAc, although no formal analysis was conducted to examine differences between currents recorded in in the two regions.

Data were analysed as described in Chapter 2, using the Wilcoxon signed rank test for non-parametric data, and t-tests (paired or unpaired) and two-way ANOVA for parametric data. Data are presented as means ± SEM unless otherwise stated.

In all experiments, average values of IPSC amplitude, onset and rise times and decay constants were measured from an average of 3 replicate traces recorded after drug wash-on in each condition. To obtain decay time constants of PSCs, single exponential curves were fit to the falling phase of average PSCs.

5.3 Results

5.3.1 Optical stimulation of DA axons evokes PSCs in striatal SPNs

In slices from $DAT^{IRES\text{-}Cre}$ mice injected unilaterally or bilaterally with AAV5-ChR2-EYFP, cells expressing EYFP in midbrain sections also expressed tyrosine hydroxylase (see Chapter 2). Recordings were made in striatal neurons that matched the reported electrophysiological properties of SPNs (**Fig. 5.1A**) (Planert et al. 2013; Cepeda et al. 2008). Brief (2 ms) blue light flashes evoked rapid outward post-synaptic currents (PSCs) in striatal SPNs in drug-free conditions (**Fig. 5.1B**). PSCs had peak amplitudes of -539.1 ± 102.1 pA (range -40.6 to -1595.0 pA, n = 26 cells). As previously described (Tritsch & Sabatini 2012; Kim et al. 2015), the kinetics of PSCs were slow, with a mean rise time of 5.49 ± 0.41 ms and an average decay time constant (τ_{decay}) of 62.74 ± 5.29 ms. Mean onset latency was 2.06 ± 0.07 ms, which is thought to be consistent with monosynaptic transmission (Tritsch et al. 2012; Sabatini & Regehr 1996).

When evoked at 1-minute intervals, PSCs were subject to run-down which was less pronounced where stimulation was delivered at intervals of 2 minutes (**Fig. 5.1C**). For this reason, all subsequent experiments were performed using intervals of 2 minutes between successive stimulations.

5.3.2 Optically-evoked PSCs are not mediated by ionotropic glutamate receptors

Postsynaptic currents in striatal SPNs mediated by both glutamate and GABA released from DA axons have been described, and at a holding potential of -70 mV both are expected to activate outward currents in SPNs (Tritsch et al. 2014; Stuber et al. 2010). To identify the contribution of glutamate release to PSCs evoked by optical stimulation of DA axons, antagonists at ionotropic glutamate receptors (iGluRs) were applied. In the presence of the AMPA receptor antagonist NBQX (5 µM) and the NMDA receptor antagonist D-AP5 (50 µM), optical stimulation readily evoked PSCs (**Fig. 5.2A**). Following application of iGluR antagonists, PSCs had a mean amplitude of

-414.3 ± 90.5 pA, which was significantly less than the mean amplitude in drug-free conditions (**Fig. 5.2B;** Wilcoxon matched-pairs rank test; W = 139.0; p = 0.001; n = 18). This difference could be due to inhibition of an iGluR-mediated component of the PSC, or alternatively could be caused by current run down, since data were collected at different time points following break-in due to differences in the time taken for drug wash-on.

To explore the cause of this decrease in peak amplitude, peak currents were compared 10 minutes after break-in, normalised to the amplitude of the first evoked current, in the presence or absence of iGluR antagonists. Cells in which wash-on was not complete after 10 minutes were excluded. When amplitude was compared at a constant time-point, no significant differences were observed (**Fig. 5.2C;** Unpaired t-test; n = 15), suggesting that use-dependent run-down contributed to the decrease in PSC amplitude. However, in the presence of iGluR antagonists, the rise time of optically evoked PSCs was significantly longer than observed in drug-free conditions, which is consistent with the inhibition of a fast glutamatergic component of the PSC (**Fig. 5.2D**; Paired t-test; t = 2.139; p = 0.047; n = 18). To explain this discrepancy, it should be noted that cells recorded in both CPu and NAc were pooled for this analysis; glutamatergic currents have been reported in NAc but not CPu (Stuber et al. 2010), so it is probable that a glutamatergic component may be present in some recordings that is not evident in the pooled amplitude data. To exclude the confounding effects of any glutamatergic currents, all subsequent experiments were performed in the presence of iGluR antagonists.

The residual PSCs evoked by optical stimulation of DA axons are not mediated by ionotropic glutamate receptors. Since metabotropic glutamate receptors are not likely to mediate rapid currents, it seems probable that the currents observed are mediated by another ionotropic receptor class.

5.3.3 PSCs are dependent on $GABA_A$ receptors

PSCs mediated by $GABA_A$ receptors have been previously demonstrated following selective activation of DA axons (Tritsch et al. 2012). To test the involvement of these receptors, PSCs were evoked in the presence of the $GABA_A$ receptor antagonist bicuculline (10 µM, **Fig. 5.3A**). The amplitude of PSCs was significantly reduced following application of bicuculline (**Fig. 5.3B**; Wilcoxon matched-pairs rank test; W = 36; p = 0.008; n = 8) and this reduction was significantly greater than that caused by the run-down of PSCs in control conditions (**Fig. 5.3C**; Two-way RM-ANOVA, bicuculline x time interaction; $F_{7, 84}$ = 9.147; p < 0.001; n = 7), suggesting that PSCs are primarily mediated by activation of $GABA_A$ receptors, consistent with previous findings (Tritsch et al. 2012).

5.3.4 PSCs are unaffected by DAT inhibition

GABA currents evoked by optical stimulation of DA axons are dependent on the vesicular monoamine transporter (Tritsch et al. 2012), the transporter responsible for loading of synaptic vesicles at DA release sites. This suggests that GABA is co-released from vesicles that also contain DA, which is corroborated by localisation of GABA to DA-containing vesicles in striatal tissue (Stensrud et al. 2014). If this is the case, it might be expected that DAT inhibitors such as cocaine would increase the amplitude of $GABA_A$-mediated PSCs. Since cocaine increases DA release partly through a mechanism involving synaptic vesicle mobilisation that is dependent on synapsins (Venton et al. 2006; Kile et al. 2010), cocaine may also increase evoked GABA release.

Contrary to expectation, PSCs appeared significantly smaller following application of cocaine (5 µM, **Fig. 5.4A, B**; Wilcoxon matched-pairs rank test; W = 55; p = 0.002; n = 10). This decrease was due to the rapid run-down of PSCs, since normalised amplitude of PSCs in cocaine was not significantly different from run-down in control conditions (**Fig. 5.4C**; Paired t-test; p > 0.05; n = 14). GABA is not thought to be a substrate for the DAT, and instead is accumulated in DA neurons through uptake via the plasma membrane GABA transporter (Tritsch et al. 2014) and through

aldehyde dehydrogenase 1a1 (ALDH1a1)-mediated synthesis (Kim et al. 2015). Consistent with this, cocaine did not significantly alter rise time (**Fig. 5.4D;** Paired t-test; $p > 0.05$; $n = 10$), and τ_{decay} of PSCs was significantly decreased (**Fig. 5.4E**; Paired t-test; $t = 2.89$; $p = 0.018$; $n = 10$) in contrast to the effect that would be expected if cocaine inhibited GABA uptake, since inhibitors of GABA uptake have been shown to slow the decay of PSCs in SPNs (Tritsch et al. 2014). To exclude the possibility that a super-maximal stimulation intensity prevented further increases in PSC amplitude through saturation of the GABA release process or postsynaptic receptor activation, stimulation intensity was decreased to 70%, resulting in a marked decrease in PSC in amplitude (**Fig. 5.4F**). Following cocaine application, at reduced stimulation intensity, there was no significant change in PSC amplitude (**Fig. 5.4G**; Paired t-test; $p > 0.05$; $n = 3$), suggesting that the lack of increased GABA release following cocaine treatment is not due to super-maximal stimulation intensity. This suggests that DAT inhibition does not increase co-release of GABA from DA axons, as suggested by findings in a previous report (Kim et al. 2015).

5.3.5 PSCs are subject to STD that is not relieved by DAT inhibition

The role of the DAT in regulation of STP of PSCs was also investigated, to determine whether this mirrors the regulation of STP of DA release. Furthermore, since the amplitude of PSCs was not affected by DAT inhibition, this might show whether the role of the DAT in STP is dissociable from the regulation of STP.

Paired pulses were delivered at an inter-pulse interval (IPI) of 100 ms, in control conditions and in the presence of cocaine (5 µM). Under all conditions, PSCs were subject to STD (**Fig. 5.5A**). PPR was not significantly altered in the presence of cocaine (**Fig. 5.5B**; Unpaired t-test; $p > 0.05$; $n = 3$), suggesting that STP of $GABA_A$-mediated currents is not regulated by the DAT.

5.4 Discussion

In this chapter, I have explored the role of the DAT in the regulation of GABA co-release from DA axons, to determine whether similar DAT-mediated mechanisms govern the release and presynaptic plasticity of both DA and GABA.

5.4.1 Postsynaptic currents evoked by stimulation of DA axons

Release of both GABA and glutamate from DA axons has been demonstrated previously (Chuhma 2004; Tritsch et al. 2012). The IPSCs observed in this chapter were evoked by selective optical stimulation of DA axons in striatum, and were not sensitive to inhibition of ionotropic glutamate receptors, but were almost completely abolished by competitive antagonism of the $GABA_A$ receptor. These findings suggest that these currents arise are attributable to GABA release from DA neurons, and corroborate the previously-reported characteristics of currents driven by co-release (Tritsch et al. 2012; Tritsch et al. 2014; Kim et al. 2015). These characteristics include a short onset latency and relatively slow decay. It has been suggested that GABA co-release could mediate fast inhibitory signalling by DA neurons (Tritsch et al. 2012). However, the slow decay of these currents may suggest that they are better adapted for modulatory volume transmission than fast point-to-point signalling.

In this chapter, IPSCs had a decay phase time constant of 66.9 ± 8.2 ms in drug-free conditions. This is consistent with the reported characteristics of currents activated by GABA co-release, which have reported a decay constant of 56 ± 4 ms (Tritsch et al. 2012), but not glutamate co-transmission, which has reported time constants of 12.1 ± 1.4 ms (Chuhma 2004) and 6.0 ± 0.3 ms (Tecuapetla et al. 2010). The reason for this slow decay is unclear; GABAergic IPSCs evoked in SPNs by stimulation of synaptically-connected SPNs or FSIs have been reported to decay faster, with time constants of 12.4 ± 9.5 ms and 11.4 ± 2.1 ms, respectively (Koos et al. 2004). This effect is likely to be partly due to the high internal $[Cl^-]$ used in this study, which will increase the decay time of $GABA_A$-mediated IPSCs due to an intracellular effect of Cl^- ions on the receptor kinetics

(Houston et al. 2009). However, in cerebellar Purkinje cells a 15-fold increase in [Cl^-] increased decay constant approximately 2-fold (Houston et al. 2009), suggesting either that this effect is considerably more prominent in striatal SPNs, or that it cannot explain the large decay constant of optically-evoked IPSCs. The slow kinetics might also be due to dendritic filtering caused by inadequate space-clamp of the distal dendritic spines. However, the high [Cs^+] internal solution used in recordings in this chapter decreases electrotonic distance between dendrites and soma (Wilson 1995), and fast IPSCs evoked by stimulation of local SPNs, which also form synapses onto distal dendrites, have been recorded under similar conditions (Koos et al. 2004).

In other neuronal populations, a slow $GABA_A$-mediated current ($GABA_{A,slow}$) has been identified. $GABA_{A,slow}$ has been described to show decay constants of more than 30-70 ms (Pearce 1993; Karayannis et al. 2010; Szabadics et al. 2007), consistent with the properties of the currents observed in this chapter. The kinetics of $GABA_{A,slow}$ are thought to arise from long-duration, low-concentration extracellular GABA transients (Szabadics et al. 2007; Karayannis et al. 2010). Such transients can be evoked in cortex by stimulation of neurogliaform cells (NGFCs), which mediate GABAergic volume transmission (Oláh et al. 2009). NGFCs, similar to DA neurons, are characterised by an extensive arborisation of fine axon branches forming small *en passant* boutons, structural features which are thought to favour GABAergic volume transmission (Armstrong et al. 2012). Furthermore, the decay of $GABA_{A,slow}$ in hippocampal neurons is prolonged by inhibition of GABA uptake transporters, while the decay of $GABA_{A,fast}$ is unaffected (Banks et al. 2000); the decay of IPSCs evoked in striatal SPNs by stimulation of DA axons is also sensitive to uptake inhibition (Tritsch et al. 2014). SPNs also receive tonic GABAergic input (Ade et al. 2008; Kirmse et al. 2008) mediated by extrasynaptic $GABA_A$ receptors (Luo et al. 2013). These findings might indicate that co-released GABA from DA neurons is well-adapted for volume transmission, and mediates a current similar to $GABA_{A,slow}$ at striatal SPNs, which is distinct from the fast inhibitory currents mediated by GABA release from FSIs and surrounding SPNs.

The IPSCs observed in this chapter match the characteristics of currents mediated by GABA co-release from DA neurons. However, there is also a possibility that $GABA_A$ receptors on SPNs could be activated by GABA released from non-DA neurons under these experimental conditions. Indeed, in addition to DAergic projections, GABAergic neurons have also been shown to project from the midbrain to striatum, although it is unclear whether these projections form significant synaptic contacts onto SPNs (Brown et al. 2012). In order for these neurons to be activated, they would have to express the light-sensitive ion channel ChR2. This might occur through non-specific expression of Cre recombinase in non-DA neurons, leading to ectopic expression of the optogenetic construct. However, previous studies using similar surgical protocols and viral vectors suggest that only 1-4% of transfected neurons in the midbrain of $DAT^{IRES\text{-}Cre}$ mice do not express TH (Stuber et al. 2010; Lammel et al. 2015; Tritsch et al. 2012), and in another study only 0.7% of transfected neurons contained mRNA for GAD65, a synthetic enzyme for GABA (Straub et al. 2014). This suggests that ectopic expression of ChR2 in GABAergic midbrain neurons is rare in $DAT^{IRES\text{-}Cre}$ animals.

5.4.2 Co-release of GABA is not regulated by DAT function

The various primary transmitters that can be released by DA neurons are thought to be localised to distinct sites within the axonal arbor. Glutamate is thought to be localised to axonal regions that do not contain DA, but are continuous with regions containing DA release sites (Zhang et al. 2015) in midbrain DA neurons projecting to the NAc but not CPu (Stuber et al. 2010; Tecuapetla et al. 2010). On the other hand, GABA is thought to be stored in and released from synaptic vesicles that also contain DA (Tritsch et al. 2012; Stensrud et al. 2014).

If DA and GABA are stored and released by the same pool of vesicles, it might be expected that DAT function should limit release of GABA in a synapsin-dependent manner, as it does for DA (Kile et al. 2010). However, I have shown in this chapter that DAT inhibition does not increase the amplitude of optically-evoked IPSCs. Furthermore, this is corroborated by a small data set

included in a recent report, which showed that the selective DAT inhibitor GBR12935 also does not increase amplitude of optically-evoked IPSCs (Kim et al. 2015). Glutamate co-transmission, which is thought to occur through glutamate release from axonal segments that do not release DA, is similarly not enhanced by cocaine (Adrover et al. 2014). These findings suggest that release of DA and GABA may be differentially regulated, which would appear to challenge the model of co-storage and co-release of DA and GABA from a common vesicle pool.

However, it remains possible that DA and GABA are co-released from a common vesicle pool, but only in a subset of DA release sites or by a specific sub-population of DA neurons with distinct regulation of synaptic vesicle mobilisation. This would explain the dependence of GABA co-release on VMAT, and also why GABA release does not appear to be regulated by DAT function. Not every DA release site is thought to store and release GABA; in a study using electron microscopy and immunogold labelling, approximately 10% of axonal boutons positive for tyrosine hydroxylase and 13% of boutons positive for VMAT were also positive for GABA (Stensrud et al. 2014). It may be that the release of vesicles from release sites containing GABA is regulated differently from those that do not, such that DAT is able to specifically limit release of DA but not GABA.

The argument that GABA-releasing DA axons may represent a biochemically-distinct subpopulation that display different vesicular properties may be supported by the patterns of synthetic enzymes and transporters in the striatum and midbrain. ALDH1a1, which has been shown to participate in a synthetic pathway that accounts for approximately 70% of GABA turnover in DA neurons (Kim et al. 2015), is not uniformly expressed throughout striatum, but instead is enriched in areas including the rostral NAc shell, dorsal parts of the CPu, and the caudal region of the dorsolateral striatum (McCaffery & Dräger 1994; Sgobio et al. 2017). In dorsolateral striatum, ALDH1a1 is specifically enriched in the striosomal compartment relative to matrix (Sgobio et al. 2017). Membrane GABA transporters (GAT1 and GAT4), which also contribute to the

maintenance of GABA co-release, appear to be expressed preferentially in SNc and lateral VTA relative to other midbrain regions (Tritsch et al. 2014), although their pattern of expression in the striatum has not been systematically studied. Expression of the transporters and synthetic enzymes thought to be required for GABA co-release are therefore restricted to specific sub-populations of neurons.

Since proteins involved in the synthesis and transport of GABA are differentially expressed by subsets of DA neurons, it may be that the expression of synaptic machinery for the regulation of vesicle mobilisation at striatal DA release sites could also vary. It has been suggested that specific synapsin isoforms mediate the effects of cocaine on DA release (Kile et al. 2010); if vesicles that store and release GABA interact with different synapsin isoforms, DAT inhibition may not affect mobilisation in this way. Further investigation of the physiological and biochemical properties of co-releasing neurons will be necessary to explore this possibility.

There are also methodological considerations that could affect the interpretation of these findings. Due to variability in the degree of ChR2 expression attained with viral transfection methods, the intensity of light stimulation required to evoke IPSCs of maximal amplitude differs between slices prepared from different animals, and between recording sites in a given slice. To control for this, a stimulation intensity-output relationship can be established for each experimental replicate. However, due to the rapid run-down of IPSCs, it was not possible to establish this relationship for each cell, and each experimental replicate was conducted using a constant stimulation intensity. This raises the possibility that GABA release from DA axons was maximally evoked in all experiments, such that the effects of cocaine on vesicle mobilisation were limited by an inability to evoke further release. However, this interpretation appears unlikely, since reducing stimulation intensity to a level that evoked IPSCs of smaller amplitude did not reveal a cocaine-induced increase, although this experiment was only conducted in a small subset of the complete sample.

Desensitisation of $GABA_A$ receptors may also influence the magnitude of currents reported in this chapter, and potentially the ability of these experiments to detect increased GABA release in response to cocaine. $GABA_A$ receptors have been shown to rapidly enter a desensitised state following activation (Jones & Westbrook 1995); it may be that $GABA_A$ receptor desensitisation enforces a ceiling effect on postsynaptic responses detected in SPNs, preventing postsynaptic detection of increased GABA release following cocaine application. Experiments permitting direct measurement of extrasynaptic GABA transients, or postsynaptic detection following pre-treatment with GABA agonists may be useful in determining the effects of receptor desensitisation on the postsynaptic response.

5.4.3 GABA co-release is subject to STD that is not DAT-dependent

In this chapter I have shown that GABA IPSCs are subject to strong short-term depression at an IPI of 100 ms. The extent of this STD is similar to that observed with DA release, as demonstrated in Chapter 3 and in previous reports (Rice & Cragg 2004; Platt 2012), and for glutamate co-transmission (Adrover et al. 2014). While this chapter does not address the relationship between STP and IPI, a previous report shows that PPR of GABA IPSCs remains low (approximately 0.5) at a 5 s IPI, suggesting that the recovery of IPSCs from STD occurs on a similar timescale to that of DA release (Adrover et al. 2014). However, in the present work this STD of GABA PSCs was not relieved by inhibition of the DAT, further corroborating the suggestion that GABA co-release is not regulated by the same mechanisms that govern DA release.

As shown in Chapter 3, STP of DA release is regulated in a region-specific manner by axonal mechanisms related to P_r and axonal excitability. Determining whether these mechanisms regulate STP of GABA release may provide some insight into the relationship between release of DA and GABA from DA axons. If GABA is released from specific sites on DA axons, it might be expected that STP of GABA release will be similarly sensitive to changes in $[K^+]_o$, which are likely to alter excitability of DA axons. However, the sensitivity of STP of GABA release to P_r, and the

complement of VGCCs that support GABA release and STP, may differ between sites. Furthermore, with regard to STP of DA release, these mechanisms are themselves regulated by the DAT; it is unclear whether this would be the case for STP of GABA release. Further experiments will therefore be required to fully characterise the differential hierarchy of mechanisms governing STP of GABA compared to DA release.

STD of GABA PSCs is also likely to be regulated by postsynaptic mechanisms, such as desensitisation of $GABA_A$ receptors. $GABA_A$ receptors are readily desensitised, as described above, and desensitisation is thought to be enhanced by long exposure to GABA (Karayannis et al. 2010). If the slow IPSCs observed in this chapter are driven by prolonged extracellular GABA transients that favour receptor desensitisation, then this may be a significant mechanism contributing to STD. Receptor desensitisation and other potential postsynaptic mechanisms of STD will therefore have to be excluded before a thorough comparison to STP of DA release can be made.

5.4.4 Summary and implications

In this chapter, I have explored the presynaptic regulation of GABA co-release by the DAT. DA neurons release GABA in a manner that is better adapted for volume transmission than fast point-to-point signalling. While GABA is thought to be co-stored and released with DA from a common pool of vesicles, release and STP of GABA IPSCs were unchanged by DAT inhibition, suggesting that mobilisation of GABA-containing vesicles is regulated in a manner that is not dependent on the DAT.

Accumulating evidence suggests that selective activation of DA axons leads to release of a neurotransmitter that binds and activates $GABA_A$ receptors on striatal SPNs, producing measurable IPSCs. It has been suggested that GABA is released in concert with dopamine from a common vesicle pool, and mediates fast inhibitory point-to-point transmission at synapses formed by dopamine axons which might modulate or shunt excitatory input onto SPNS (Tritsch et

al. 2014). However, several factors suggest that co-released GABA may be poorly adapted for fast signalling.

The kinetics of the IPSCs recorded in this chapter are slow compared to those detected at classical synaptic connections onto SPNs. The kinetics and sensitivity of these currents to GABA reuptake blockers suggests a dependence on the time course of the extracellular GABA transient that is characteristic of GABAergic volume transmission. Furthermore, the data presented in this chapter, as well as in other work (Tritsch et al. 2014), suggest that these currents run down rapidly during low-frequency stimulation. While these currents have not been recorded *in vivo*, and may be more stable under physiological conditions, this degree of run down suggests that the amplitude of IPSCs is likely to be small during the tonic firing of DA neurons, reducing the probability that such currents could significantly perturb membrane potential beyond a localised shunting effect in the dendritic arbor.

Furthermore, I have presented data suggesting that the release of GABA is not regulated by the DAT, in contrast to DA release. This raises the possibility that GABA and DA are co-stored and released from distinct vesicle pools within DA release sites, or alternatively that GABA is released by a specialised subset of DA release sites with distinct regulation of vesicle mobilisation and exocytosis.

Taken together, these findings suggest that GABA release from DA neurons might be released from specialised sites on DA axons to exert modulatory effects at synaptic and/or extrasynaptic receptors on SPNs. It has been suggested that slow modulatory GABAergic signalling is well-placed to play key role in regulating plasticity of excitatory inputs in the hippocampus (Capogna & Pearce 2011), which is consistent with the position of symmetric synapses formed by DA neurons onto SPNs at dendritic spines that receive excitatory input from glutamatergic projections. Release of GABA from DA axons may therefore have important modulatory effects on network activity within the striatum.

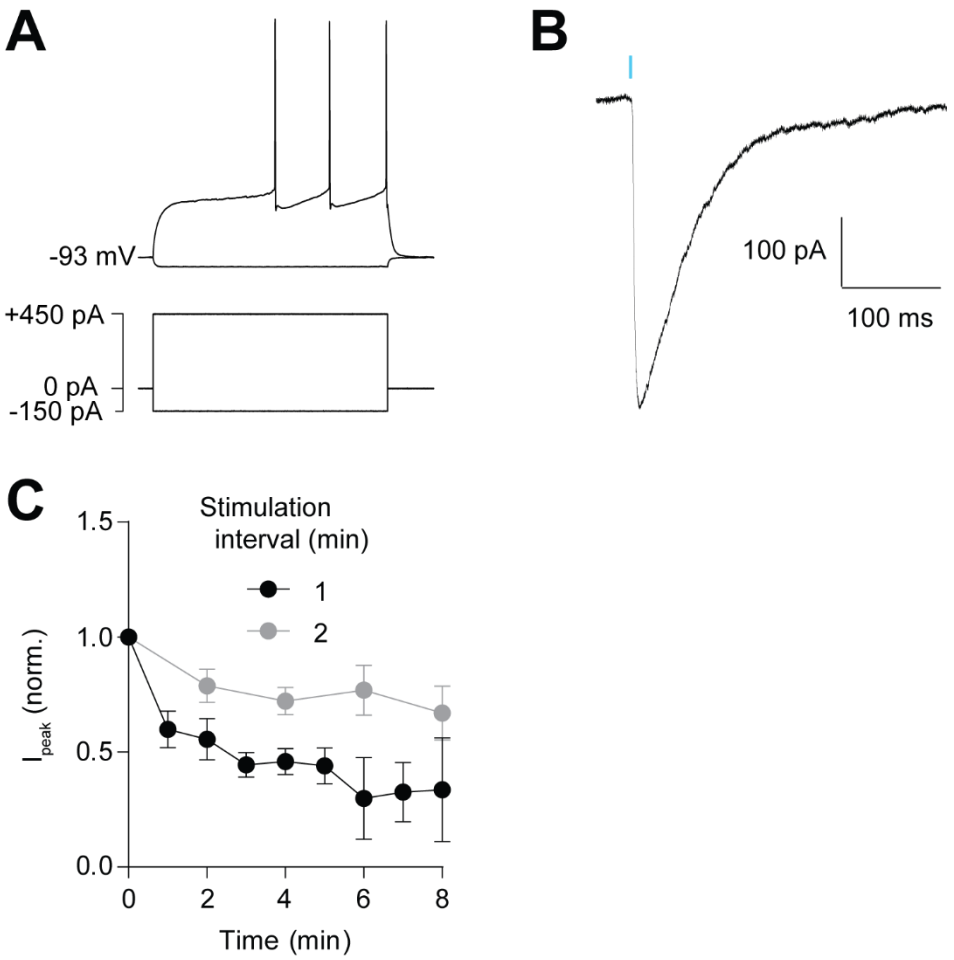

Fig. 5.1 Optical activation of DA axons evokes outward PSCs in SPNs

(A) Current clamp recording of a striatal neuron typical of neurons recorded in this chapter. Note the delayed discharge and absence of a hyperpolarisation-induced sag. **(B)** Optically-evoked PSC recorded under voltage clamp, in drug-free conditions. Neurons were held at -70 mV. **(C)** Mean evoked peak current normalised to amplitude of the first response. Optical stimulation was delivered at 1 minute (black) or 2 minute intervals (grey).

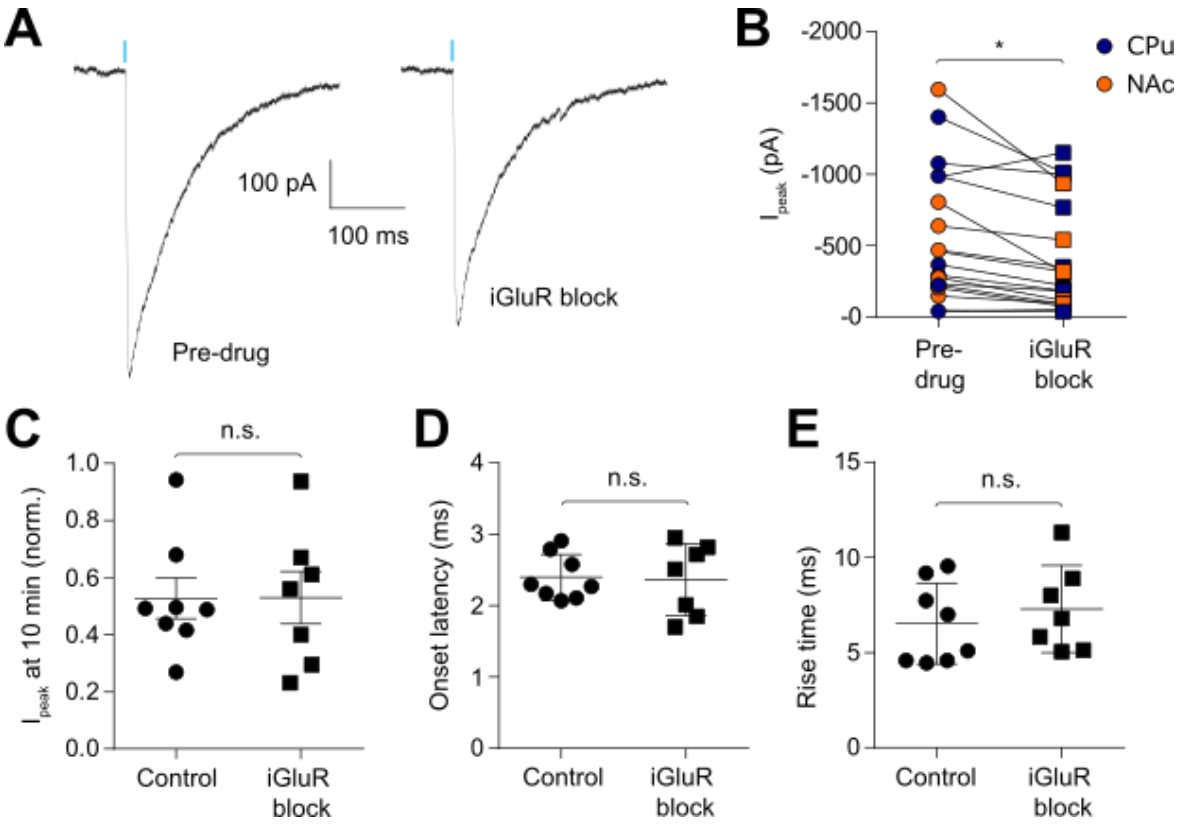

Fig. 5.2 PSCs are maintained in the presence of iGluR antagonists

(A) Optically-evoked PSCs recorded in control conditions and in the presence of iGluR antagonists (NBQX, 5 µM and AP5, 50 µM). **(B)** Peak PSC amplitude in control conditions and in the presence of iGluR antagonists, in cells in CPu (blue) and NAc (orange). Mean amplitude was significantly lower in iGluR block than in control conditions. **(C)** Mean peak PSC amplitude (±SEM) 10 minutes after break-in, normalised to the amplitude of the first response, in control conditions (n = 7) and in iGluR block (n = 8). The decrease in amplitude in iGluR block was not significantly different from basal run-down in control conditions. **(D)** Rise time of PSCs recorded in control conditions and in the presence of iGluR antagonists. Mean rise time was significantly longer in iGluR block. *p < 0.05.

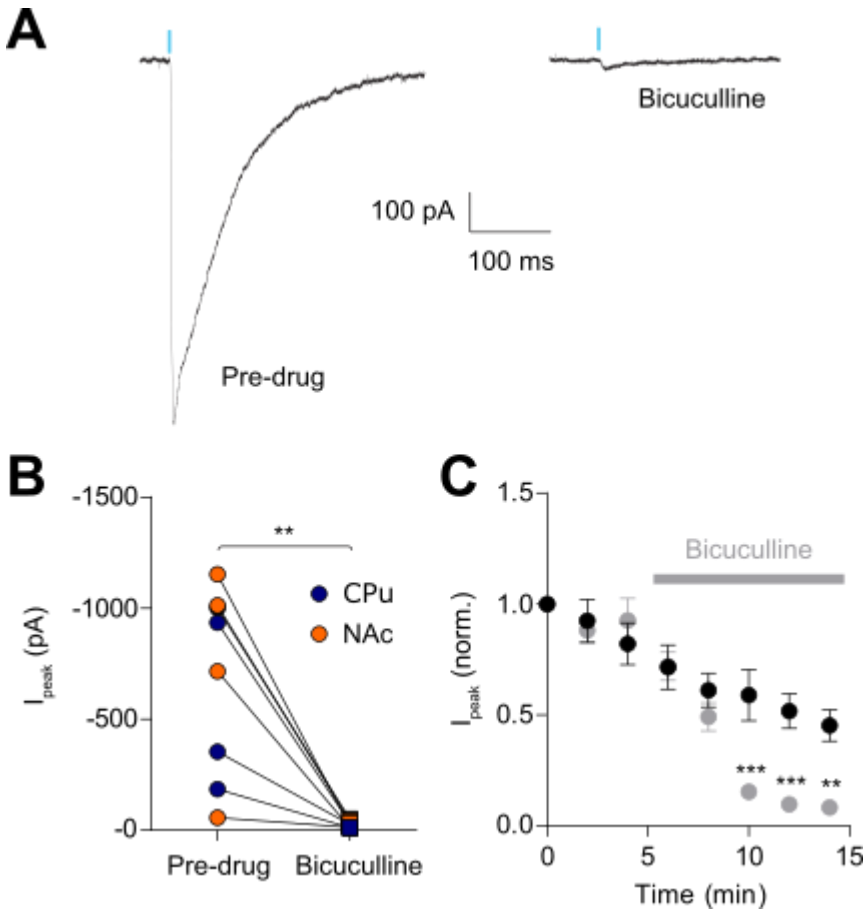

Fig. 5.3 PSCs are dependent on $GABA_A$ receptors

(A) Optically-evoked PSCs recorded in control conditions and in the presence of bicuculline (10 µM). **(B)** Peak PSC amplitude in control conditions and in the presence of bicuculline, in cells in CPu (blue) and NAc (orange). Mean amplitude was significantly lower in the presence of bicuculline. **(C)** Mean peak amplitude (±SEM) over time in control conditions (n = 7) and in the presence of bicuculline (n = 7). Mean peak amplitude during application of bicuculline (grey bar) was significantly lower than basal run-down. **p < 0.01, ***P < 0.001.

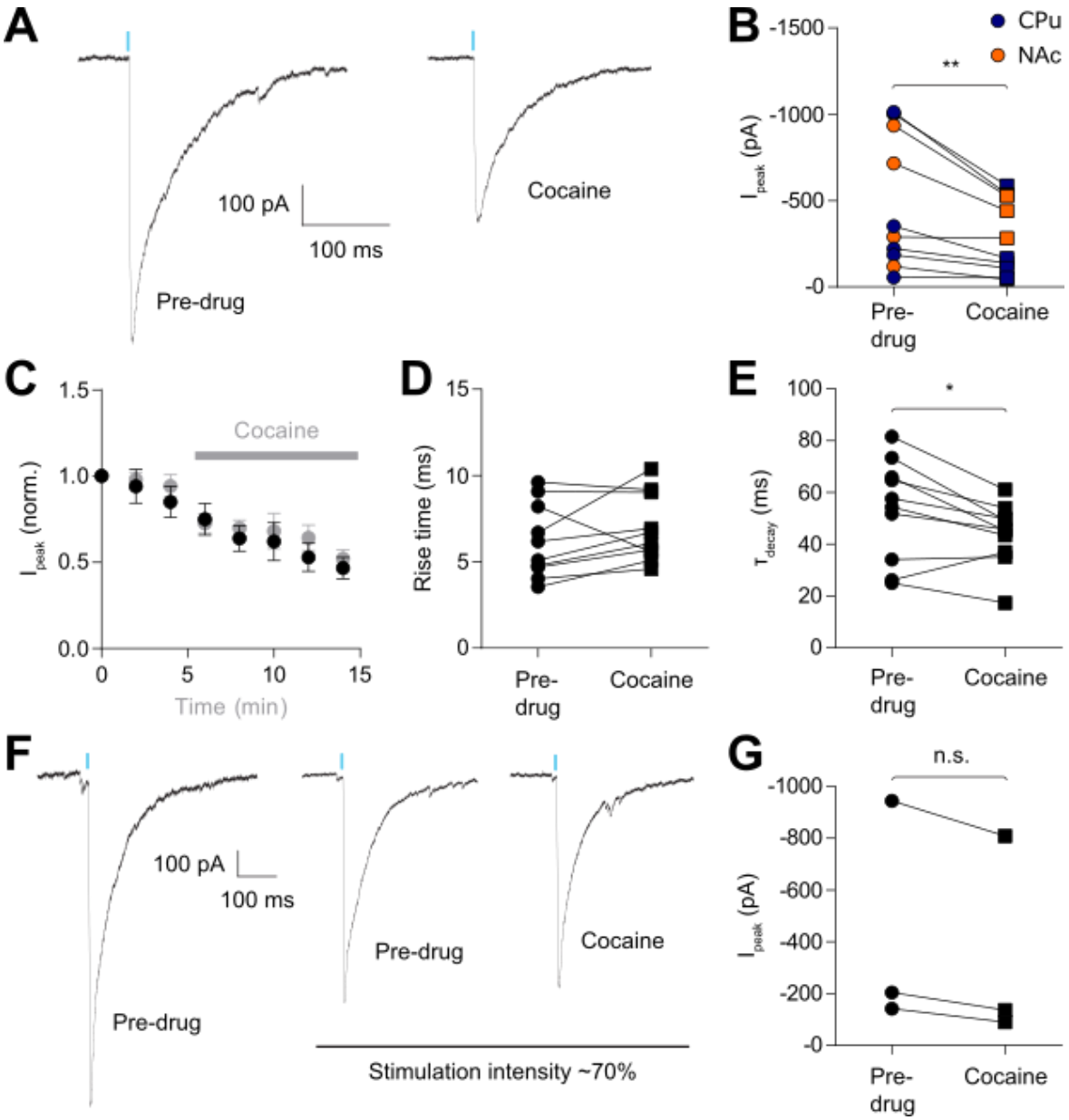

Fig. 5.4 PSCs are unaffected by DAT inhibition

(A) Optically-evoked PSCs recorded in control conditions and in the presence of cocaine (5 µM). **(B)** Peak PSC amplitude in control conditions and in the presence of cocaine, in cells in CPu (blue) and NAc (orange). Mean amplitude was significantly lower in the presence of cocaine. **(C)** Mean peak amplitude (±SEM) over time in control conditions (n = 7) and in the presence of cocaine (n = 7). The decrease in amplitude during cocaine application (grey bar) was not significantly different from basal run-down in control conditions. **(D)** Rise time of PSCs recorded in control conditions and in the presence of cocaine. **(E)** Decay constant of PSCs recorded in control conditions and in

the presence of cocaine. Mean decay constant was significantly lower in cocaine. **(F)** Optically-evoked PSCs recorded in control conditions at maximal laser intensity (left), and in control conditions and the presence of cocaine after laser intensity was reduced to ~70% (middle and right). **(G)** Peak PSC amplitude at 70% laser intensity in control conditions and in the presence of cocaine. At 70% laser intensity, mean amplitude was not significantly altered in the presence of cocaine.

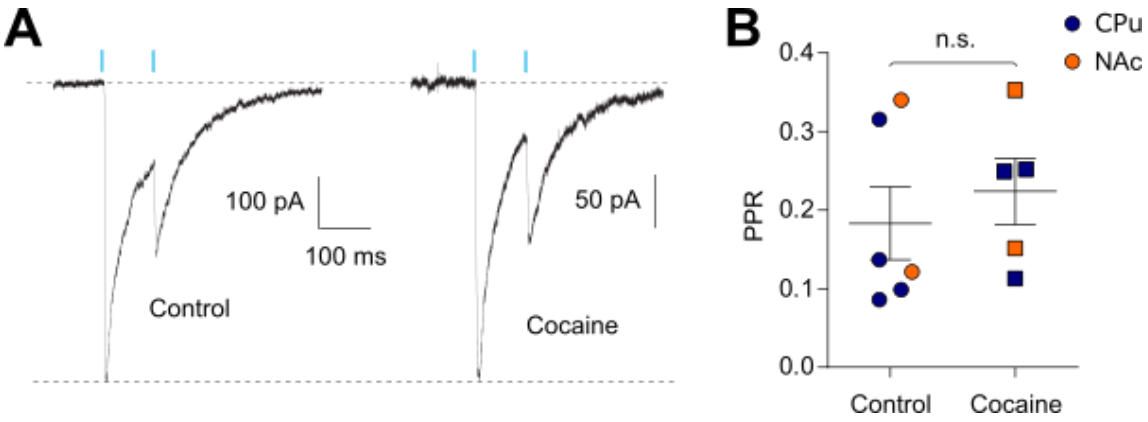

Fig. 5.5 PSCs are subject to short-term depression that is not relieved by DAT inhibition

(A) PSCs evoked by paired-pulse stimulation at 100 ms IPI in control conditions and in the presence of cocaine (5 µM). **(B)** Mean paired-pulse ratio (±SEM) at 100 ms IPI in control conditions (n = 6) and in the presence of cocaine (n = 5), in cells in CPu (blue) and NAc (orange). Mean PPR was not significantly altered in the presence of cocaine.

Chapter 6.

General Discussion

Activity patterns in midbrain DA neurons encode behaviourally-relevant information about the motivational value of salient stimuli. However, it remains unclear how local regulation and axonal properties regulate the conversion of firing patterns into DA release in the striatum. The regulation of DA release is important, because DA is the extracellular signal that mediates transfer of information from DA neurons to postsynaptic targets, and therefore influences subsequent downstream activity in the basal ganglia and consequently shapes behaviour. In order to understand how DA neurons regulate and modify behaviour, it will be necessary to fully understand how somatic firing patterns are converted into postsynaptic DA signals.

The central aim of this thesis was to explore the regulation of short-term plasticity of DA release by intrinsic axonal factors, to provide a better understanding of how these factors shape the conversion of presynaptic firing in DA neurons to DA release in the striatum. Chapter 3 identified interactions and regional differences between mechanisms that shape DA release. Chapter 4 further explored these mechanisms in the context of tonic background activity, to determine their role in shaping signal contrast of DA signalling in response to high-frequency bursts. Chapter 5 examined the distinction between presynaptic STP of DA and of GABA that is thought to be co-released from DA axons. In this final chapter, I will consider these findings in the wider context of DA signalling, and their implications for the understanding of DA-dependent behaviour and pathology.

6.1. A mechanistic hierarchy of presynaptic STP in striatum

In Chapter 3, I examined the interactions between presynaptic mechanisms of STP of DA release that have been identified in previous work (Platt 2012), in order to determine how these mechanisms act in concert to shape DA release. Three candidate mechanisms were considered: K^+-sensitive changes in axonal excitability, the function of the dopamine transporter (DAT) in DA axons and release sites, and Ca^{2+}-sensitive changes in release probability (P_r).

6.1.1 Axonal excitability regulates STP of DA release

Excitability of neuronal membranes is governed by their relative conductances and the electrochemical driving force for movement of ions between the intracellular compartment and extracellular medium. Typically, intracellular $[K^+]$ ($[K^+]_i$) is high, while extracellular $[K^+]$ ($[K^+]_o$) is low, resulting in a strongly negative reversal potential for K^+ ions. The magnitude of currents is determined by the driving force for the carrier ion, and the driving force (at rest) is defined as the difference between the reversal potential for that ion and the resting membrane potential (RMP). Reducing $[K^+]_o$ even further therefore results in a more negative reversal potential for K^+, and a greater driving force for K^+ currents. The neuronal membrane should become hyperpolarised, and the amplitude of currents carried by K^+ ions will be greater.

Alternatively, changes in $[K^+]_o$ might alter the total conductance of K^+ channels at DA axons. Certain K^+ channels undergo use-dependent inactivation which is dependent on a conformational change in the channel, and shows limited voltage-dependence but is strongly inhibited by an increase in $[K^+]_o$ (Baukrowitz & Yellen 1995; Hoshi et al. 1991). This $[K^+]_o$-dependence is thought to arise because binding of K^+ to a site near the outer opening of channel pore inhibits the required conformational changes, so inactivation is promoted by reduced extracellular K^+ availability (Baukrowitz & Yellen 1996). The range of $[K^+]_o$ over which use-dependent activation is promoted suggests that an decrease from 5 mM to 1 mM $[K^+]_o$ could significantly increase the rate of inactivation, and prolong the period over which K^+ channels continue to inactivate following repolarisation (Baukrowitz & Yellen 1995). As a result, in a paired-pulse paradigm, a greater proportion of K^+ channels could be in an inactivated state at the second pulse, reducing the total K^+ current.

Reducing $[K^+]_o$ might therefore have two opposing effects on membrane potential in DA axons. Firstly, a Nernstian increase in K^+ current could hyperpolarise the membrane and promote fast repolarisation. Second, an increase in the rate of K^+ channel inactivation could result in use-

dependent depolarisation. It is difficult to determine, based on the indirect evidence available, whether either or both of these effects occurs following a decrease in $[K^+]_o$, and if both, which is more prominent in shaping STP of DA release.

A reduction in $[K^+]_o$ has been shown to increase paired-pulse ratio (PPR) of DA release across inter-pulse intervals (IPIs) of 10-200 ms, while an increase in $[K^+]_o$ decreases PPR across the same range of IPIs (Platt 2012). In Chapter 3, I demonstrated that the K^+-dependent gating of PPR was dependent on voltage-gated K^+ (K_v) channels, since K^+-dependent gating was absent in the presence of the non-selective K_v channel blocker 4-aminopyridine (4-AP). Axonal K_v channels are therefore required to shape STP of DA release; however, identifying a specific mechanism underlying the regulation of STP by $[K^+]_o$ is challenging, due to the inaccessibility of individual DA axons to electrophysiological recording techniques, uncertainty regarding the specific K^+ channels expressed at DA axons, and variability in the selectivity of pharmacological antagonists for particular K^+ channel subtypes. Several potential mechanisms will be discussed below.

One potential mechanism that might underlie K^+-dependent gating of STP is the rate of repolarisation at DA axons and release sites. Inactivation of axonal K_v channels decreases the rate of repolarisation, broadening the action potential waveform (Marsh & Brown 1991). Repetitive stimulation can lead to depolarisation of the membrane, due to accumulation of K^+ ions in the extracellular space around the axon, resulting in AP broadening (Foust et al. 2011; Kole et al. 2007). Low $[K^+]_o$ conditions, where the axonal membrane is hyperpolarised and the driving force for currents carried by K^+ ions is high, are therefore likely to promote fast repolarisation and narrow APs. Since repolarisation rate can be determined by K^+ channel activity at the level of individual release sites (Rowan et al. 2016), promoting K^+-mediated currents may result in a greater population of non-refractory release sites able to release DA in response to the second pulse in a pair, increasing PPR. The range of IPIs over which changes in refractoriness might modulate PPR is unclear, as the duration of the refractory period in DA axons is unknown,

although extracellular recordings in the medial forebrain bundle suggest it may be less than 10 ms (Yeomans et al. 1988). If this is the case at striatal release sites, additional K^+-dependent mechanisms are likely to contribute to gating of STP.

Alternatively, an increase in the rate of K^+ channel inactivation in low $[K^+]_o$ could also enhance re-release. Changes in $[K^+]_o$ might alter use-dependent inactivation of K^+ channels, as described above, leading to a change in the recruitment of voltage-gated Na^+ channels. If use-dependent inactivation of K^+ channels leads to depolarisation of the axonal membrane, this depolarisation might in turn promote recruitment of Na_v channels at the second pulse. By this mechanism, reduced $[K^+]_o$ could promote stronger depolarisation during the second AP and hence greater DA release, increasing P2/P1.

Another mechanism by which changes in $[K^+]_o$ might influence STP is by altering the rate of AP conduction failure in DA axons. APs in DA neurons might be particularly susceptible to conduction failure, due to the structure of the extensive axonal arbor (Kopysova & Debanne 1998). The axons of DA neurons are thin and extensively branched, which might be expected to result in a high impedance to AP conduction (Debanne 2004). In crayfish axons, it has been shown that depolarisation of fine actions can result in conduction block at branch points, which is relieved by hyperpolarisation or a reduction in $[K^+]_o$ (Smith 1980). Increases in $[K^+]_o$ also lead to conduction block in rat cerebellar axons (Kocsis et al. 1983) and to branch point failure in lobster axons (Grossman et al. 1979b). In the experiments described in Chapter 3, decreasing $[K^+]_o$ may limit the rate of conduction failure, increasing DA release at the second pulse. However, a global decrease in the rate of conduction failure should affect DA release in a uniform manner, so it is unclear why PPR would increase as a result unless a use-dependent mechanism contributes to the failure rate. Conduction failure has been shown to develop progressively during repetitive stimulation in hippocampal neurons in culture (Brody & Yue 2000) and in slices prepared from juvenile animals (Muñoz-Cuevas et al. 2004). It may be that the safety factor for AP conduction in DA neurons is

sufficiently low that paired-pulse stimulation significantly increases the probability of conduction failure at the second pulse in a given axonal branch, particularly when $[K^+]_o$ is elevated.

There might also be effects of altering $[K^+]_o$ on the activation state of voltage-gated Na^+ (Na_v) channels, which could further influence AP conduction in DA axons. Cumulative voltage-dependent inactivation of Na_v channels during repetitive activity reduces the amplitude of APs and the reliability of conduction (Fleidervish et al. 1996; Carr et al. 2003; Kawaguchi & Sakaba 2015). Depolarisation of axonal membranes in higher $[K^+]_o$ may therefore promote use-dependent inactivation of Na_v channels and attenuation of axonal APs, which has been suggested to drive STD (He et al. 2002; Prakriya & Mennerick 2000). Conversely, enhanced recruitment of Na_v channels due to inactivation of K^+ channels at low $[K^+]_o$ could enhance conduction fidelity in a use-dependent manner.

STD of DA release is therefore likely to be caused by a combination of mechanisms relating to excitability and AP waveform in DA axons. In particular, refractoriness of DA release sites, conduction failures at branch points in the axonal arbor, and possibly Na^+-dependent attenuation of axonal APs, are likely to limit re-release of DA in a paired-pulse paradigm.

6.1.2 The role of axonal A-type channels in STP

The data described in Chapter 3 may also suggest a role for fast-inactivating A-type K+ channels. At the concentration used here, 4-AP is more potent in blocking K^+ channels that carry fast-inactivating A-type currents, including $K_v1.4$ and members of the K_v3 and K_v4 subfamilies (Gutman et al. 2005). Furthermore, K^+-dependent gating was limited by the $K_v1.3/1.4$ blocker UK78282, and pilot data suggests that a similar effect is observed in the presence of BDS-1, a selective inhibitor of $K_v3.4$ channels. A-type K^+ currents may therefore operate either alone or in concert with other K^+ currents to maintain STD of DA release.

Axonal A-type channels have been suggested to play key roles in both repolarisation and the regulation of AP conduction at branch points. In hippocampal neurons, axonal K^+ channels

carrying A-type currents are thought to be inactivated at RMP (Storm 1990). When the membrane is hyperpolarised, these channels become de-inactivated. Where K_v channels carrying A-type currents are clustered at axonal branch points, this current can prevent AP conduction in hippocampal axons (Kopysova & Debanne 1998; Debanne et al. 1997). However, de-inactivation of A-type currents is unlikely to underlie K^+-dependent gating of STP, because de-inactivation should be promoted when $[K^+]_o$ is low, and the axonal membrane is thought to be hyperpolarised. Under these conditions, enhanced A-type currents should increase the rate of conduction failure, limiting re-release and reducing PPR. However, in this thesis and in previous work (Platt 2012), PPR is increased in low $[K^+]_o$. An alternative interpretation is that A-type currents promote conduction failure and reduce release at the first pulse, then become inactivated and do not limit DA release in response to the second pulse, increasing PPR (Debanne et al. 1999). However, we do not observe a decrease in single-pulse $[DA]_o$, which is again consistent with previous findings (Platt 2012). De-inactivation of A-type K^+ currents in low $[K^+]_o$ is therefore unlikely to underlie K^+-dependent gating of STP.

The role of A-type currents in STD may instead relate to repolarisation. Channels carrying A-type currents, particularly the K_v3 subfamily, are thought to enable faithful axonal conduction of APs at high frequencies by maintaining a high rate of repolarisation (Rudy & McBain 2001). K_v3 channels activate at a high threshold, and so are activated late in the depolarising phase of the AP, and carry large outward currents to drive rapid repolarisation (Alle et al. 2011). It may be that A-type currents in DA axons act as part of a repertoire of K^+ channels controlling repolarisation, and their inhibition by 4-AP reduces PPR by slowing repolarisation, resulting in a greater population of refractory release sites at the second pulse. However, if A-type currents support rapid repolarisation, it is unclear why inhibition of specific axonal K_v subunits increased PPR in 5 mM $[K^+]_o$, where K^+ currents are expected to be smaller. This effect could be explained if use-dependent inactivation of K^+ channels is promoted by reduced $[K^+]_o$, as described above. In this case, blockade of specific K_v channels would be expected to depolarise the axon and enhance Na^+

channel recruitment in 5 mM $[K^+]_o$, but would have a limited effect in 1 mM $[K^+]_o$ where a greater proportion of K_v channels would already be inactivated.

These findings suggest a role for axonal A-type currents in the regulation of STP of DA release. However, these data may reflect a specific function of A-type currents in regulating the fidelity of AP propagation in DA axons, or a more general role of voltage-dependent K^+ currents in governing refractoriness. Experiments exploring the effects of a wider range of K^+ channels in STP, and characterisation of the complement and distribution of K^+ channel expression at DA axons, would be necessary to comprehensively define the specific channels and currents involved in shaping DA release.

6.1.3 The DAT as a master regulator of STP

The DAT is thought to regulate multiple aspects of DA neuron physiology. First of all, the DAT terminates signalling events (Garris et al. 1994), and limits the spatial range at which DA can act on its targets (Cragg & Rice 2004), through reuptake of DA from the extracellular space. Second, the DAT is thought to limit DA release by maintaining segregation between vesicle pools at DA release sites, since some DAT inhibitors increase DA release in a manner that is dissociable from uptake (Lee et al. 2001), and dependent on synapsins (Kile et al. 2010; Venton et al. 2006). Finally, the DAT can depolarise neuronal membranes through a channel conductance associated with substrate binding that mediates an inward current (Sonders et al. 1997; Ingram et al. 2002; Carvelli et al. 2004). The DAT has been shown to regulate STP, as DAT inhibitors limit STF of DA release at short IPIs and relieve STD at longer IPIs in CPu but not NAc (Platt 2012). Given these roles in excitability and DA release, the DAT is well-placed to govern other mechanisms driving STP of DA release.

Relieving STD by reducing $[K^+]_o$ did not alter the dependence of STP on P_r, as manipulated by varying $[Ca^{2+}]_o$. Since the DAT also supports STD at IPIs of 25-40 ms in CPu (Platt 2012), I investigated whether DAT function might mask a dependence of STP on P_r at these intervals.

Inhibition of the DAT in CPu increased PPR at 25-40 ms IPIs and potentiated the effect of a reduction in $[Ca^{2+}]_o$ at 25 ms IPI. This suggests that the DAT limits the release-dependence of STP in CPu; however, the mechanism by which the DAT interacts with Ca^{2+} handling at DA release sites remains unclear. As described in section 3.4.2, evidence of the relationship between DAT function and Ca^{2+} dynamics in other neurons and non-neuronal cell lines is mixed, with reports suggesting both increases and decreases in Ca^{2+} entry in response to DAT inhibition. Nonetheless, the findings described in Chapter 3 show that DAT inhibitors will increase the release-dependence of STP in CPu, disrupting the powerful release-independent STD that is observed under control conditions.

DAT inhibition also prevented relief of STD by a reduction in $[K^+]_o$, in both CPu and NAc, confirming that the DAT supports K^+-dependent gating. Direct control of K^+ channel function by the DAT has not been described, suggesting that this effect occurs indirectly. If K^+-dependent gating shapes DA release by influencing branch point conduction and Na_v channel activation, as described in section 6.1.1, the DAT might mask these effects through changes in membrane potential. Since the DAT mediates a depolarising current during DA uptake (Ingram et al. 2002), inhibition of the DAT is thought to be hyperpolarising. Hyperpolarisation may limit conduction failure and de-inactivate Na_v channels, increasing PPR and preventing further modulation of these factors by changes in $[K^+]_o$.

Taken together, these findings suggest that the DAT acts as a 'master regulator' of STP at DA release, governing the interaction of facilitation and depression processes to shape DA release. Regional differences in DAT expression will have implications for STP of DA release, which will be discussed in section 6.1.4. This suggests that drugs that inhibit the DAT could severely disrupt the patterns of STP that shape the conversion of presynaptic activity into DA release. When the DAT was inhibited, the dependence of PPR on IPI was reduced, and STD was partially relieved,

suggesting that DAT inhibitors might lead to aberrant signalling of lower-frequency firing in DA neurons *in vivo*.

6.1.4 Regional differences in the mechanistic hierarchy

DA signalling in different striatal regions is subject to distinct patterns of local regulation (Brown et al. 2011), and these differences might support the region-specific functions of DA signalling in behaviour (Everitt & Robbins 2013). Several key regional differences have been identified in previous work on STP of DA release (Platt 2012). Firstly, PPR is higher at short intervals in NAc than in CPu, which could indicate a stronger mechanism promoting STF. This might be attributable to higher expression of the fast Ca^{2+} buffer calbindin-D28k in DA neurons projecting to NAc (Haber et al. 1995; Greene et al. 2005; Chung et al. 2005), which could result in pseudo-facilitation due to buffer saturation, as has been previously described in cortical neurons (Blatow et al. 2003). Second, K^+-dependent gating of STP was more prevalent in CPu than in NAc. Since K^+-dependent gating is thought to arise from changes in excitability and AP conduction, this difference could be driven by the larger and more complex axonal arborisation of DA neurons projecting to CPu (Aransay et al. 2015), which might be more prone to conduction failures.

I have extended these findings by demonstrating the role of the DAT in maintaining the regional differences in presynaptic STP. When the DAT was inhibited, the dependence of STP on P_r in CPu was increased, and K^+-dependent gating was prevented in both regions. The regional differences in the hierarchy of mechanisms governing STP were therefore less pronounced during DAT inhibition. This may indicate that the DAT supports regional differences in STP, and that the extent and distribution of DAT expression could lead to adaptations of DA signalling within the axonal arbor.

An additional aspect of DA signalling that was not investigated in this thesis is the effects of striosome/matrix compartmentalisation on STP. Each compartment receives preferential input from different DA neurons (Gerfen et al. 1987; Matsuda et al. 2009), suggesting that the intrinsic

axonal factors governing STP may differ between the two compartments. Crucially, expression of the DAT is thought to be higher in striosomes than in matrix (Sgobio et al. 2017). Given the central role of the DAT in regulating STP of DA release, it seems feasible that this might lead to differential regulation of DA release, with implications for the effects of DA signalling between the striatal compartments. During collection of the data shown in Chapter 3, transgenic mice expressing fluorescent markers for striosome and matrix regions have become available (Crittenden et al. 2016), which should enable future experiments to investigate compartmental differences in STP.

6.1.5 Summary and Implications

In summary, presynaptic STP of DA release is governed by a region-specific combination of axonal mechanisms that are regulated by the DAT. This results in a characteristic pattern of STP that will shape the conversion of activity patterns in DA neurons to extracellular DA signals.

The geometric morphology of DA axons and their patterns of ion channel expression may represent an additional mechanism by which DA release is locally regulated. These properties may resolve an apparent contradiction in the structure and function of DA neurons. At the level of the midbrain, the diverse physiology of DA neurons enables a broad range of firing patterns, whereas in the striatum DA signalling is widely distributed, with individual DA neurons innervating large areas of striatal tissue. It may be that the structure of the DA axon is well-adapted to shape DA signalling by preferential conduction of APs to specific portions of the axonal arbor, as determined by axonal excitability.

The DAT could also contribute to the regional specialisation of STP. Since the DAT supports K^+-dependent gating and limits release-dependence of STP, higher levels of DAT expression could promote a pattern of STP that is more readily modulated by axonal conduction properties. Such a pattern of STP is observed in CPu, where DAT expression is thought to be greater. Drugs that inhibit the DAT may therefore produce a more regionally-homogeneous pattern of STP across the

striatum, altering DA signalling and consequently synaptic plasticity of excitatory inputs. Disruption of STD could enhance DA release in response to lower-frequency activity in DA neurons, promoting aberrant reinforcement of behaviour.

6.2 Enhancement of signal contrast by tonic activity in DA neurons

In Chapter 4, the effects of tonic background activity on the contrast of DA signals evoked by bursts of stimulation were investigated. Previous studies have identified that release in NAc is more sensitive to burst stimulation than in CPu, and that tonic stimulation can have different effects across striatal regions (Zhang et al. 2009). However, these studies are likely to have underestimated the contrast between release in response to single stimulations and in response to bursts due to activation of nAChRs, which promote powerful STD of DA release. Since phasic increases in DA neuron firing in response to rewards are thought to occur synchronously with pauses in ChI firing, it is important to determine how tonic background activity influences DA signal contrast in the absence of cholinergic signalling.

The findings described in Chapter 4 show that the contrast ratio between DA release in response to single stimulations and in response to bursts is increased following low-frequency tonic background activity, and that this effect is more prominent in NAc than CPu due to differences in Ca^{2+} handling and DAT function. The implications of these findings in the broader context of DA signalling will be discussed in this section.

6.2.1 Role of tonic firing is determined by frequency

Tonic firing in DA neurons has been observed at a range of frequencies up to approximately 10 Hz, typically in the range of 2-6 Hz. In Chapter 4, the effects of 2 Hz and 6 Hz tonic stimulation on burst contrast were compared to investigate the effects of changes in tonic firing frequency within this range. Tonic stimulation at 6 Hz appeared to enhance burst contrast to a lesser extent than stimulation at 2 Hz. However, opposite effects on steady-state $[DA]_o$ were observed; during

6 Hz tonic stimulation, steady-state $[DA]_o$ was higher than during 2 Hz tonic stimulation. This frequency-dependent effect of tonic firing on signal contrast was not simply due to altered basal $[DA]_o$ acting at D2 autoreceptors, since there was no correlation between average steady-state $[DA]_o$ during tonic background stimulation and contrast ratio of a 4 pulse burst.

This raises the possibility that fine-tuning of the tonic firing frequency of DA neurons in the 2-6 Hz range influences their role in DAergic signalling. DA neurons with a higher average firing frequency may contribute more to basal DA release in striatum, and increases in average firing across populations of DA neurons may drive slow changes in [DA] that are thought to encode motivation and/or reward proximity (Fiorillo et al. 2003; Howe et al. 2013). DA neurons with a lower firing frequency may contribute less to basal DA release, but instead be well-adapted for high-contrast signalling of high-frequency (25 Hz in this experiment) phasic events.

Basal firing frequencies in the SNc and VTA are thought to be similar (Clark & Chiodo 1988; Zhang et al. 2008; Panin et al. 2012). However, as described in Chapter 1, the mechanisms governing pacemaker frequency in midbrain DA neurons are diverse, segregating not just between functional regions but between biochemically-defined populations within the VTA and SNc. In certain populations, distinct pacemaker mechanisms in sub-populations of DA neurons may lead to differences in basal firing rate (Neuhoff et al. 2002), which could influence the control of basal $[DA]_o$ in striatum, and in the signal contrast of phasic DA release events. Regularity of basal firing, which also varies between DA neurons due to differences in expression of SK channels (Wolfart et al. 2001), may also affect the degree to which tonic activity can influence burst signal contrast.

However, it should be noted that the contribution to steady-state [DA] of DA release in response to low-frequency firing may be lower in a slice preparation than *in vivo.* In a physiological setting, temperature-sensitive processes such as DA uptake and recycling are likely to occur faster, which could result in less prominent depression of DA release at low frequencies. If this is the case, reporting of lower firing frequencies is likely to be enhanced, resulting in stronger regulation of

basal $[DA]_o$. Further experiments will be required to determine whether differential regulation of striatal $[DA]_o$ and burst signal contrast is preserved in more physiological conditions.

6.2.2 The DAT regulates effects of tonic firing and dependence of contrast on P_r

In Chapter 3, it was demonstrated that the DAT supports regional differences in STP, implying a central role in shaping the conversion of presynaptic activity to DA release. Consistent with this, the findings presented in Chapter 4 suggest that the DAT also governs the relationship between DA release in response to tonic background activity and to high-frequency bursts. In the presence of tonic background activity, DAT inhibition increased basal $[DA]_o$, but also enhanced signal contrast in response to stimulation at 25 Hz. This increase in signal contrast was more pronounced in CPu than in NAc, consistent with the stronger effect of DAT inhibition on PPR in CPu at this frequency in previous work (Platt 2012) and the higher maximal rate of DAT-mediated uptake in CPu than in NAc (Jones et al. 1995).

DAT inhibition also altered the effect of changes in P_r on signal contrast. In control conditions, reducing P_r by decreasing $[Ca^{2+}]_o$ increased signal contrast in CPu, but had no effect in NAc. When the DAT was inhibited with cocaine, decreasing P_r significantly increased signal contrast in both regions. The DAT can therefore limit signal contrast through effects on STP and extracellular summation of DA.

Taken together, these findings suggest that the DAT not only governs the pattern of STP at DA release sites, but also regulates signal contrast of DA release in response to bursts. Levels of DAT expression and function may therefore represent a mechanism by which DA neurons can control the presynaptic regulation of DA signalling. Trafficking of DAT protein to the axonal membrane is thought to be controlled by several activity-dependent factors. Activation of D2 autoreceptors is thought to promote DAT function since blockade or knock-down of D2 autoreceptors, or disruption of the physical interaction between D2 autoreceptors and the DAT, reduces DA uptake both *in vitro* and *in vivo* (Lee et al. 2007; Budygin et al. 2017; Benoit-Marand et al. 2011). This

process is thought to regulate DA uptake in response to changes in release (Mortensen & Amara 2003), but might also influence the additional functions of the DAT in shaping STP and signal contrast. Extracellular DA acting at D2 autoreceptors might therefore increase DAT expression at the axonal membrane over a timescale of minutes (Chen et al. 2013), promoting uptake and limiting sensitivity to bursts to maintain DA signalling within a limited dynamic range.

In non-neuronal cell cultures expressing DAT, localisation of DAT to the cell surface is increased by co-expression of α-synuclein (Hara et al. 2013) and DJ-1 (Luk et al. 2015), proteins implicated in familial forms of Parkinson's disease. Expression of the DAT, and therefore signal contrast of DA release events in response to bursts, may therefore be altered in certain disease states.

6.2.3 Regional differences in signal contrast

In these experiments, and as previously described (Zhang et al. 2009), DA release was more sensitive to high-frequency bursts of stimulation, and tonic background stimulation enhanced signal contrast to a greater extent in NAc than in CPu. This suggests that regional differences in uptake and STP may produce specialised patterns of signalling that are adapted to the differential roles of striatal regions in learning and behaviour.

Signal contrast was enhanced by tonic background activity to a greater extent in NAc than in CPu. This could occur due to pseudofacilitation in DA axons projecting to NAc, as described in Chapter 3. This will promote strong intracellular Ca^{2+} summation at NAc release sites, resulting in a higher steady-state $[DA]_o$ during background stimulation, and a greater sensitivity to burst length. At release sites in CPu, Ca^{2+} will be readily removed between stimulations due to minimal binding to buffers, limiting summation and therefore re-release of DA. DA release in NAc therefore appears to be better adapted for high-contrast signalling of burst events, with a high sensitivity to the number of spikes in a burst. This is, in turn, influenced by the strength of excitatory input to midbrain DA neurons (Overton & Clark 1997; Zhang et al. 2005), which is enhanced by stimuli

predictive of reward (Stuber et al. 2008), suggesting that Ca^{2+} dynamics in NAc DA release sites might promote reporting of the strength of synaptic inputs on DA neurons.

In CPu, steady-state $[DA]_o$ was greater during tonic background stimulation at 6 Hz compared to 2 Hz. However, release was relatively insensitive to burst length compared to NAc, even following tonic background stimulation. DA signalling in CPu therefore appears to be optimised for signalling of low-frequency changes in the tonic firing rate of DA neurons, driving continuous graded changes in $[DA]_o$. Furthermore, release in response to bursts was relatively insensitive to the number of spikes in the burst, suggesting that DA release in CPu is better adapted to report low-frequency changes in firing than short-term dynamic changes in synaptic inputs onto midbrain DA neurons.

The regional specialisation in signal contrast in response to bursts may reflect adaptations to different firing patterns in DA neurons projecting to the major functional regions of the striatum. A greater proportion of spikes occur in bursts in VTA neurons than in SNc (Clark & Chiodo 1988; Zhang et al. 2008), and bursts in VTA neurons contain more spikes on average (Tong et al. 1996). DA release in NAc might therefore be adapted to preferentially report these bursts and their duration as high contrast transients.

It should also be noted that, similar to the regional differences in mechanisms underlying STP described in Chapter 3, the regional specialisation of signal contrast appears to be supported by the DAT. When the DAT was inhibited, signal contrast in CPu became more sensitive to the number of pulses in a burst, similar to NAc. Conversely, DAT inhibition made signal contrast in NAc more sensitive to changes in P_r, similar to CPu. This further demonstrates the central role of the DAT in shaping DA signalling in the striatum.

6.2.4 Summary and Implications

Tonic background activity in DA axons promotes signal contrast of DA release in response to high frequency bursts. This effect is region-specific, with greater sensitivity to bursts and enhancement

of signal contrast in NAc than in CPu. Changes in the frequency of tonic background activity may have implications for DA signalling that extend beyond the determination of basal $[DA]_o$. This suggests that the conversion of high-frequency to presynaptic bursts does not occur through a static process, but may instead be determined on a millisecond timescale according to fluctuations in the rate and pattern of background activity. Long-term changes in tonic firing frequency might therefore influence the reporting of phasic increases in firing frequency. Furthermore, DA release sites in NAc may be adapted to report bursts as rapid $[DA]_o$ transients, while sites in CPu produce smaller release events that may summate in the extracellular space to drive gradual changes in basal $[DA]_o$. Firing patterns of DA neurons that have different projection targets or axonal characteristics should therefore be carefully interpreted in light of this region-specific specialisation of DA release.

Signal contrast was also regulated by the DAT, but not significantly by changes in P_r. This further demonstrates that the STP of DA signalling is not characterised by the high sensitivity to initial release that is observed at certain glutamatergic synapses. Instead, the DAT appeared to support the regional differences in signal contrast. Since trafficking of the DAT to axonal membranes is regulated by activity-dependent mechanisms, DAT function might represent a homeostatic mechanism that limits signal contrast in response to increases in DA release. Mutations and drugs that reduce DAT function might alter the properties of DA signalling by enhancing signal contrast, promoting aberrant DA transmission in response to reward-predicting cues.

Throughout Chapters 3 and 4, DA release has been studied in the absence of cholinergic input, due to pharmacological blockade of the β2-subunit-containing nicotinic acetylcholine receptors that mediate the powerful control of DA release by activity in striatal cholinergic interneurons (Rice & Cragg 2004). However, when considering the effects of presynaptic activity on DA release in the striatum, it is important to consider the effects of dynamic changes in ACh release. Cholinergic interneurons exhibit a stereotyped pause in response to salient sensory events, which

can coincide with phasic increases in DA neuron firing thought to signal reward value (Morris et al. 2004). Experiments that recreate the timing of this pause will be necessary to determine how burst signal contrast is influenced by tonic background activity during physiological patterns of ACh release in the striatum.

6.3 GABA release from DA neurons is not regulated by the DAT

DA neurons are capable of releasing GABA in slice preparations, which is thought to be co-packaged into DA vesicles and released in concert with DA (Tritsch et al. 2012; Tritsch et al. 2014; Kim et al. 2015). If GABA and DA are stored and released from the same vesicles, both should be regulated by the same presynaptic mechanisms. In Chapter 5, I explored the regulation of GABA release, to determine whether GABA released following selective stimulation of DA neurons is subject to presynaptic regulation by the DAT.

6.3.1 Co-released GABA may mediate tonic inhibition in SPNs

As described in section 5.4.1, the onset latency of the PSCs described in Chapter 5 was short (approximately 2 ms), while the decay kinetics were slow. This is consistent with the kinetics of PSCs evoked by stimulation of DA axons in previous work (Tritsch et al. 2012; Kim et al. 2015) and in contrast with the kinetics of currents evoked by stimulation of neighbouring SPNs or fast-spiking interneurons (Koos et al. 2004; Luo et al. 2013). Notably, the kinetics of PSCs evoked by co-released GABA were similar to those of PSCs evoked by activity in neuropeptide Y-neurogliaform neurons of the striatum, which are thought to be mediated by extrasynaptic $GABA_A$ receptors (Luo et al. 2013).

The slow kinetics of these currents might indicate that GABA release from DA neurons might mediate tonic inhibitory signalling at extrasynaptic receptors. In adult mice, SPNs express extrasynaptic and perisynaptic $GABA_A$ receptors containing α4 and δ subunits (Santhakumar et al. 2010), which are well-adapted for tonic signalling activated by GABA spillover due to their high

affinity for GABA and low degree of desensitisation (Wallner et al. 2003; Saxena & Macdonald 1994). In SPNs, extrasynaptic $GABA_A$ receptors mediate tonic inhibitory currents that are larger in D2-SPNs than in D1-SPNs during development (Janssen et al. 2009; Ade et al. 2008), but larger in D1-SPNs than in D2-SPNs in adult mice (Santhakumar et al. 2010), a developmental switch that is thought to occur due to changes in subunit composition (Luo et al. 2013). Since the D1- and D2-receptor expressing pathways are thought to mediate different aspects of learning and behaviour, a shift in tonic inhibition from D2-SPNs to D1-SPNs might mediate a change in the pattern of basal ganglia network activity during development. A role for GABA co-release in tonic inhibition could therefore represent an additional mechanism to modulate the postsynaptic effects on DA on striatal networks.

It might be argued that co-released GABA is unlikely to play a physiological role in the regulation of SPN excitability because tonic firing in DA neurons *in vivo* will result in rapid rundown of GABAergic PSCs. However, this rundown is less prominent where exogenous GABA is provided to maintain reuptake and recycling at release sites (Tritsch et al. 2014). This suggests that in the intact striatum, where uptake and synthesis of GABA would be expected to occur more rapidly, run-down of GABA PSCs might be less marked. Tonic firing might result in sufficient extracellular summation of small GABA transients to activate high-affinity extrasynaptic $GABA_A$ receptors, and mediate tonic inhibition of inputs to SPNs. Further experiments will be required to determine whether GABA co-release is maintained to this degree during normal DA neuron activity *in vivo*.

The effects of tonic inhibition on signalling are complex and variable depending on the properties of the postsynaptic neuron. In hippocampal pyramidal neurons, tonic activation of extrasynaptic $GABA_A$ receptors increases the threshold for excitatory inputs to drive AP generation (Pavlov et al. 2009) and decreases the membrane time constant, an important variable in regulating the timing of postsynaptic APs, by increasing membrane conductance (Wlodarczyk et al. 2013). In the rodent striatum, tonic $GABA_A$ conductance is required for a shift in the rules governing spike timing-

dependent plasticity at corticostriatal synapses during development (Valtcheva et al. 2017), although this does not depend on differential conductances in D1- and D2-SPNs in mice (Paille et al. 2013). If GABA release from DA neurons is sufficient to activate extrasynaptic receptors during tonic firing *in vivo*, it might therefore contribute to the gating of excitatory inputs to SPNs.

6.3.2 The DAT does not limit release of GABA

The DAT has been shown to limit release of DA, since inhibition of the DAT increases DA release in a manner that is dissociable from its effects on uptake (Lee et al. 2001; Stamford et al. 1989). This increase is thought to be driven by synapsin-dependent mobilisation of a reserve vesicle pool (Venton et al. 2006; Kile et al. 2010). If GABA and DA are co-stored and released from the same vesicles, DAT inhibition should increase GABA release in a similar manner to DA. However, the findings described in Chapter 5 suggest that inhibition of the DAT using cocaine does not increase the amplitude of PSCs detected at striatal SPNs, even where stimulation intensity is decreased to a sub-maximal level.

The lack of effect of cocaine on the amplitude or PPR of PSCs evoked by DA axon stimulation may indicate that co-released GABA is not regulated by the same presynaptic mechanisms as DA. Evidence exists in the literature that GABA co-release is dependent on the vesicular monoamine transporter (VMAT), which appears to transport GABA (Tritsch et al. 2012), and that GABA in TH-positive terminals in striatum is co-localised with synaptic vesicles that express VMAT (Stensrud et al. 2014). However, DAT inhibition, an intervention known to influence DA release through a mechanism involving synaptic vesicle mobilisation (Venton et al. 2006; Kile et al. 2010), does not appear to influence GABA release. These conflicting findings might be reconciled if GABA is co-released with DA from sites on DA axons that are distinct from those that release DA alone, or if GABA co-release occurs only in a sub-population of DA neurons that express synaptic machinery that is differentially regulated by the DAT. This is supported by the relatively low proportion of

TH-positive and VMAT-positive boutons in the striatum (approximately 11% and 13%, respectively) at which GABA storage has been detected (Stensrud et al. 2014).

Testing the possibility that GABA co-release is limited to specific DA neurons or release sites is likely to be challenging, however, since no genetic markers for GABA-releasing DA neurons, which could be used to selectively label or activate these cells, have yet been identified. Aldehyde dehydrogenase 1a1 (ALDH1a1) and plasma membrane GABA transporters (GAT1 and 4) are reportedly required to support GABA co-release, and these proteins are expressed in specific sub-populations of DA neurons in both VTA and SNc (Tritsch et al. 2014; Kim et al. 2015; La Manno et al. 2016). While the expression of GAT1/4 at DA axons has not been studied, ALDH1a1-positive fibres can selectively innervate specific regions of the striatum (Sgobio et al. 2017). ALDH1a1 and/or GAT1/4 may therefore represent suitable markers for GABA-releasing DA neurons in mice, but further studies will be required to confirm whether they are co-localised to a common sub-population of DA axons in the striatum, and whether intersectional optogenetic strategies (Fenno et al. 2014) can be used to evoke GABA release in DAT+/ALDH1a1+ but not DAT+/ALDH1a1- axons. If so, then this strategy could be used to independently study the regulation of DA and GABA release in each population.

It should be noted that comparisons between the presynaptic regulation of DA and co-released GABA are confounded by different detection methods. FCV provides a direct measurement of DA overflow in the extracellular space, and is therefore unaffected by postsynaptic receptor properties. In contrast, GABA release is detected by measuring $GABA_A$–mediated PSCs in SPNs. The amplitude and time course of GABA currents are therefore dependent on receptor sensitivity and kinetics. $GABA_A$ receptors can display rapid desensitisation (Jones & Westbrook 1995; Xu et al. 2016) that might limit their capacity to transduce increased extracellular GABA concentrations into larger postsynaptic currents. However, inhibitors of GABA uptake have been shown to prolong PSCs, presumably by increasing the lifetime of the extracellular GABA transient,

suggesting that these currents are not solely gated by receptor desensitisation. In a paired-pulse paradigm, receptor desensitisation at the second pulse might also limit PPR, and therefore prevent relief of STD by DAT inhibition, as is observed for DA release. Additional control experiments, such as changing laser intensity between pairs of pulses or applying drugs that are known to enhance neurotransmitter release, will be required to determine whether these negative results can be attributed to the effects of receptor desensitisation.

6.1.3 Summary and Implications

Selective activation of DA projections evokes GABA release in striatum, although a physiological role for this phenomenon has not yet been described. GABA release may be poorly-adapted for fast point-to-point signalling and direct modulation of membrane potential of SPNs, due to rapid rundown during repetitive stimulation. However, GABA release may be well suited to mediate shunting inhibition of excitatory inputs to SPNs through activation of high-affinity extrasynaptic $GABA_A$ receptors. These receptors are reported to be preferentially targeted by ethanol (Wallner et al. 2003). GABA co-release from DA neurons may therefore play a role in the development of alcohol addiction and represent a potential therapeutic target.

The amplitude of GABA-mediated PSCs was not altered by cocaine. This may indicate that GABA is not co-stored in DA vesicles, since inhibition of the DAT increases DA release through a mechanism related to vesicle mobilisation. However, drawing a firm conclusion regarding co-storage on the basis of this finding is difficult, since it is unclear how factors such as receptor desensitisation might influence the postsynaptic response to changes in GABA release. Further studies will be required to determine whether DA and GABA release are indeed differentially regulated at DA release sites. If the presynaptic regulation of each transmitter is different, this could indicate that GABA is released from specialised sites on DA axons, or by a specific sub-population of DA neurons that form projections throughout the striatum. The role of GABA co-release in striatal processing and behaviour remains unclear, but characterisation of GABA-

releasing sites or neurons could provide specific targets to investigate the contribution of this phenomenon to neurophysiology in healthy and diseased states.

6.4 Further work

The findings presented in this thesis raise a number of interesting questions that could be explored with existing experimental techniques. Firstly, electrical propagation in DAergic axons could be investigated using optical detection of either Ca^{2+} transients or changes in axonal membrane potential. Genetically-encoded voltage indicators (GEVI) could be used to examine the effects of changes in $[K^+]_o$ and DAT inhibition on axonal membrane potential and AP conduction. GEVI constructs can be conditionally expressed in a Cre-dependent manner, and can report individual action potentials in brain slices (Bayguinov et al. 2017), although it is unclear how these tools would perform in DA axons. Intracellular Ca^{2+} imaging tools have been employed in striatal DA axons *in vivo* (Howe & Dombeck 2016), and could be used in slice preparations to explore the interactions between DAT function and Ca^{2+} dynamics. Both techniques would necessarily require sparse transfection of midbrain DA neurons to resolve signalling in individual axons, given the high density of DA axons in the striatal neuropil (Howe & Dombeck 2016; Song et al. 2017).

Secondly, the effects of tonic background activity on DA release in response to bursts could be further explored *in vivo*. This approach would allow repetitive stimulation of DA axons under physiological conditions, to determine whether enhancement of signal contrast is a feasible function of tonic activity in intact dopaminergic projections. Furthermore, inhibitory opsins could be used to evoke time-locked pauses in cholinergic interneuron firing, to determine the effects of dynamic ACh release on burst signal contrast in slice preparations and *in vivo*.

Finally, considerable work remains to determine the properties of GABA signalling from intact DA neurons. Detection of GABA co-release in the intact organism is an important milestone is establishing whether this phenomenon plays a significant role in DA neuron function, but is likely

to require technically challenging *in vivo* patch-clamp experiments. Selective blockers and conditional genetic deletions of δ-subunit-containing $GABA_A$ receptors could be used to reveal the contribution of extrasynaptic receptors to PSCs evoked by selective stimulation of DA axons. Additional experiments could also determine the sensitivity of STP of GABA co-release to changes in axonal excitability and Ca^{2+} availability, to determine whether further differences from presynaptic regulation of DA release can be observed.

6.5 Conclusions

The findings presented in this thesis underscore the importance of presynaptic plasticity of DA release when considering the behavioural roles of DA neurotransmission. While an important and extensive body of work has examined the effects of behavioural and pharmacological interventions on firing patterns at DA neuron soma, the DA signal that acts on postsynaptic targets is additionally shaped by local regulation, including the intrinsic properties of DA axons that shape presynaptic plasticity. In this thesis, I have defined the region-specific relationships between presynaptic mechanisms underlying STP, confirming that DA release is shaped to a greater extent by axonal excitability and action potential propagation than by P_r, and that this idiosyncratic pattern of STP is maintained by the dopamine transporter. In the presence of tonic background stimulation designed to mimic activity patterns in DA neurons, these patterns of STP shape differential reporting of high-frequency bursts between striatal regions. However, the dopamine transporter does not appear to control release or plasticity of co-released GABA, raising questions about the origin of GABA release events within the extensive axonal projection of midbrain DA neurons. Further work is required to probe the role of conduction fidelity in STP of DA release, the effects of dynamic patterns of striatal ChI activity on burst signal contrast, and the specificity of GABA release to specific sub-populations of DA neurons.

Bibliography

Abbott, L.F. & Regehr, W.G., 2004. Synaptic computation. *Nature*, 431(7010), pp.796–803.

Abeliovich, A. et al., 2000. Mice Lacking α-Synuclein Display Functional Deficits in the Nigrostriatal Dopamine System. *Neuron*, 25(1), pp.239–252.

Abraham, W.C. et al., 2002. Induction and Experience-Dependent Consolidation of Stable Long-Term Potentiation Lasting Months in the Hippocampus. *Journal of Neuroscience*, 22(21).

Ade, K.K. et al., 2008. Differential Tonic GABA Conductances in Striatal Medium Spiny Neurons. *Journal of Neuroscience*, 28(5), pp.1185–1197.

Adler, E.M. et al., 1991. Alien intracellular calcium chelators attenuate neurotransmitter release at the squid giant synapse. *The Journal of neuroscience : the official journal of the Society for Neuroscience*, 11(6), pp.1496–507.

Adrover, M.F., Shin, J.H. & Alvarez, V.A., 2014. Glutamate and Dopamine Transmission from Midbrain Dopamine Neurons Share Similar Release Properties But Are Differentially Affected by Cocaine. *Journal of Neuroscience*, 34(9), pp.3183–3192.

Albin, R.L., Young, A.B. & Penney, J.B., 1989. The functional anatomy of basal ganglia disorders. *Trends in Neurosciences*, 12(10), pp.366–375.

Alcantara, A.A. et al., 2003. Localization of dopamine D2 receptors on cholinergic interneurons of the dorsal striatum and nucleus accumbens of the rat. *Brain Research*, 986(1–2), pp.22–29.

Alexander, G.E. & Crutcher, M.D., 1990. Functional architecture of basal ganglia circuits: neural substrates of parallel processing. *Trends in Neurosciences*, 13(7), pp.266–271.

Alle, H. & Geiger, J.R.P., 2006. Combined analog and action potential coding in hippocampal mossy fibers. *Science (New York, N.Y.)*, 311(5765), pp.1290–3.

Alle, H., Kubota, H. & Geiger, J.R.P., 2011. Sparse But Highly Efficient Kv3 Outpace BKCa Channels in Action Potential Repolarization at Hippocampal Mossy Fiber Boutons. *Journal of Neuroscience*, 31(22), pp.8001–8012.

Ammari, R. et al., 2009. A mouse juvenile or adult slice with preserved functional nigro-striatal dopaminergic neurons. *Neuroscience*, 159(1), pp.3–6.

Aperia, A. et al., 2000. Anatomical and physiological evidence for D1 and D2 dopamine receptor colocalization in neostriatal neurons. *Nature Neuroscience*, 3(3), pp.226–230.

Apicella, P., 2002. Tonically active neurons in the primate striatum and their role in the processing of information about motivationally relevant events. *European Journal of Neuroscience*, 16(11), pp.2017–2026.

Aransay, A. et al., 2015. Long-range projection neurons of the mouse ventral tegmental area: a single-cell axon tracing analysis. *Frontiers in Neuroanatomy*, 9, p.59.

Arbuthnott, G.W. & Wickens, J., 2007. Space, time and dopamine. *Trends in Neurosciences*, 30(2), pp.62–69.

Armstrong, C., Krook-Magnuson, E. & Soltesz, I., 2012. Neurogliaform and Ivy Cells: A Major Family of nNOS Expressing GABAergic Neurons. *Frontiers in neural circuits*, 6, p.23.

Armstrong, C.M. & Gilly, W.F., 1992. Access resistance and space clamp problems associated with whole-cell patch clamping. *Methods in Enzymology*, 207, pp.100–122.

Averbeck, B.B. et al., 2014. Estimates of projection overlap and zones of convergence within frontal-striatal circuits. *The Journal of neuroscience : the official journal of the Society for Neuroscience*, 34(29), pp.9497–505.

Avshalumov, M. V. et al., 2003. Glutamate-Dependent Inhibition of Dopamine Release in Striatum Is Mediated by a New Diffusible Messenger, H2O2. *J. Neurosci.*, 23(7), pp.2744–2750.

Bacaj, T. et al., 2013. Synaptotagmin-1 and Synaptotagmin-7 Trigger Synchronous and Asynchronous Phases of Neurotransmitter Release. *Neuron*, 80(4), pp.947–959.

Bäckman, C.M. et al., 2006. Characterization of a mouse strain expressing Cre recombinase from the 3' untranslated region of the dopamine transporter locus. *Genesis (New York, N.Y. : 2000)*, 44(8), pp.383–90.

Balestrino, M., Aitken, P.G. & Somjen, G.G., 1986. The effects of moderate changes of extracellular K+ and Ca2+ on synaptic and neural function in the CA1 region of the hippocampal slice. *Brain Research*, 377(2), pp.229–239.

Banks, M.I., White, J.A. & Pearce, R.A., 2000. Interactions between Distinct GABAA Circuits in Hippocampus. *Neuron*, 25(2), pp.449–457.

Bath, B.D. et al., 2000. Subsecond Adsorption and Desorption of Dopamine at Carbon-Fiber Microelectrodes. *Analytical Chemistry*, 72(24), pp.5994–6002.

Baukrowitz, T. & Yellen, G., 1995. Modulation of K+ current by frequency and external [K+]: A tale of two inactivation mechanisms. *Neuron*, 15(4), pp.951–960.

Baukrowitz, T. & Yellen, G., 1996. Use-dependent blockers and exit rate of the last ion from the multi-ion pore of a K+ channel. *Science (New York, N.Y.)*, 271(5249), pp.653–6.

Bayguinov, P.O. et al., 2017. Imaging Voltage in Genetically-Defined Neuronal Subpopulations with a Cre Recombinase-Targeted Hybrid Voltage Sensor. *The Journal of neuroscience : the official journal of the Society for Neuroscience*, 37(38), pp.9305–9319.

Beaulieu, J.-M. & Gainetdinov, R.R., 2011. The physiology, signaling, and pharmacology of dopamine receptors. *Pharmacological reviews*, 63(1), pp.182–217.

Beckstead, M.J. et al., 2004. Vesicular dopamine release elicits an inhibitory postsynaptic current in midbrain dopamine neurons. *Neuron*, 42(6), pp.939–46.

Beckstead, R.M., Domesick, V.B. & Nauta, W.J.H., 1979. Efferent connections of the substantia nigra and ventral tegmental area in the rat. *Brain Research*, 175(2), pp.191–217.

Bennett, B.D. & Wilson, C.J., 1999. Spontaneous activity of neostriatal cholinergic interneurons in vitro. *The Journal of neuroscience : the official journal of the Society for Neuroscience*, 19(13), pp.5586–96.

Benoit-Marand, M. et al., 2011. Inhibition of dopamine uptake by D2 antagonists: an in vivo study. *Journal of neurochemistry*, 116(3), pp.449–58.

Berendse, H.W. & Groenewegen, H.J., 1990. Organization of the thalamostriatal projections in the rat, with special emphasis on the ventral striatum. *The Journal of Comparative Neurology*, 299(2), pp.187–228.

Berrios, J. et al., 2016. Loss of UBE3A from TH-expressing neurons suppresses GABA co-release and enhances VTA-NAc optical self-stimulation. *Nature Communications*, 7, p.10702.

Bevan, M.D. et al., 1998. Selective innervation of neostriatal interneurons by a subclass of neuron

in the globus pallidus of the rat. *The Journal of neuroscience : the official journal of the Society for Neuroscience*, 18(22), pp.9438–52.

Bischofberger, J., Geiger, J.R.P. & Jonas, P., 2002. Timing and efficacy of Ca2+ channel activation in hippocampal mossy fiber boutons. *The Journal of neuroscience : the official journal of the Society for Neuroscience*, 22(24), pp.10593–602.

Björklund, A. & Dunnett, S.B., 2007. Dopamine neuron systems in the brain: an update. *Trends in Neurosciences*, 30(5), pp.194–202.

Blanchard, V. et al., 1994. Differential expression of tyrosine hydroxylase and membrane dopamine transporter genes in subpopulations of dopaminergic neurons of the rat mesencephalon. *Brain research. Molecular brain research*, 22(1–4), pp.29–38.

Blatow, M. et al., 2003. Ca2+ Buffer Saturation Underlies Paired Pulse Facilitation in Calbindin-D28k-Containing Terminals. *Neuron*, 38(1), pp.79–88.

Van Bockstaele, E.J. & Pickel, V.M., 1995. GABA-containing neurons in the ventral tegmental area project to the nucleus accumbens in rat brain. *Brain Research*, 682(1–2), pp.215–221.

Bogen, I.L. et al., 2006. Absence of synapsin I and II is accompanied by decreases in vesicular transport of specific neurotransmitters. *Journal of Neurochemistry*, 96(5), pp.1458–1466.

Bolam, J.P. & Pissadaki, E.K., 2012. Living on the edge with too many mouths to feed: Why dopamine neurons die. *Movement Disorders*, 27(12), pp.1478–1483.

Borre, L. et al., 2014. The second sodium site in the dopamine transporter controls cation permeation and is regulated by chloride. *The Journal of biological chemistry*, 289(37), pp.25764–73.

Borst, J.G.G. & Sakmann, B., 1996. Calcium influx and transmitter release in a fast CNS synapse. *Nature*, 383(6599), pp.431–434.

Branda, C.S. & Dymecki, S.M., 2004. Talking about a Revolution: The Impact of Site-Specific Recombinases on Genetic Analyses in Mice. *Developmental Cell*, 6(1), pp.7–28.

Brichta, L. & Greengard, P., 2014. Molecular determinants of selective dopaminergic vulnerability in Parkinson's disease: an update. *Frontiers in Neuroanatomy*, 8, p.152.

Brimblecombe, K.R. et al., 2015. Gating of dopamine transmission by calcium and axonal N-, Q-, T- and L-type voltage-gated calcium channels differs between striatal domains. *The Journal of physiology*, 593(4), pp.929–46.

Brimblecombe, K.R. & Cragg, S.J., 2015. Substance P Weights Striatal Dopamine Transmission Differently within the Striosome-Matrix Axis. *The Journal of neuroscience : the official journal of the Society for Neuroscience*, 35(24), pp.9017–23.

Brischoux, F. et al., 2009. Phasic excitation of dopamine neurons in ventral VTA by noxious stimuli. *Proceedings of the National Academy of Sciences of the United States of America*, 106(12), pp.4894–9.

Brody, D.L. & Yue, D.T., 2000. Release-Independent Short-Term Synaptic Depression in Cultured Hippocampal Neurons. *J. Neurosci.*, 20(7), pp.2480–2494.

Brown, H.D. et al., 2011. Primary food reward and reward-predictive stimuli evoke different patterns of phasic dopamine signaling throughout the striatum. *The European journal of neuroscience*, 34(12), pp.1997–2006.

Brown, M.T.C. et al., 2012. Ventral tegmental area GABA projections pause accumbal cholinergic interneurons to enhance associative learning. *Nature*, 492(7429), pp.452–6.

Bucher, D. & Goaillard, J.-M., 2011. Beyond faithful conduction: Short-term dynamics, neuromodulation, and long-term regulation of spike propagation in the axon. *Progress in Neurobiology*, 94(4), pp.307–346.

Budygin, E.A. et al., 2017. Acute Depletion of D2 Receptors from the Rat Substantia Nigra Alters Dopamine Kinetics in the Dorsal Striatum and Drug Responsivity. *Frontiers in Behavioral Neuroscience*, 10, p.248.

Bull, D.R. et al., 1990. Application of fast cyclic voltammetry to measurement of electrically evoked dopamine overflow from brain slices in vitro. *Journal of Neuroscience Methods*, 32(1), pp.37–44.

Bykhovskaia, M., 2011. Synapsin regulation of vesicle organization and functional pools. *Seminars in cell & developmental biology*, 22(4), pp.387–92.

Cachope, R. et al., 2012. Selective activation of cholinergic interneurons enhances accumbal phasic dopamine release: setting the tone for reward processing. *Cell reports*, 2(1), pp.33–41.

Calabresi, P. et al., 1997. Abnormal synaptic plasticity in the striatum of mice lacking dopamine D2 receptors. *The Journal of neuroscience : the official journal of the Society for Neuroscience*, 17(12), pp.4536–44.

Calabresi, P. et al., 2007. Dopamine-mediated regulation of corticostriatal synaptic plasticity. *Trends in Neurosciences*, 30(5), pp.211–219.

Cameron, K.N. et al., 2015. Amphetamine activates calcium channels through dopamine transporter-mediated depolarization. *Cell Calcium*, 58(5), pp.457–466.

Capogna, M. & Pearce, R.A., 2011. GABAA,slow: causes and consequences. *Trends in Neurosciences*, 34(2), pp.101–112.

Carr, D.B. et al., 2003. Transmitter modulation of slow, activity-dependent alterations in sodium channel availability endows neurons with a novel form of cellular plasticity. *Neuron*, 39(5), pp.793–806.

Carter, A.G., Soler-Llavina, G.J. & Sabatini, B.L., 2007. Timing and Location of Synaptic Inputs Determine Modes of Subthreshold Integration in Striatal Medium Spiny Neurons. *Journal of Neuroscience*, 27(33).

Carvelli, L. et al., 2004. Dopamine transporters depolarize neurons by a channel mechanism. *Proceedings of the National Academy of Sciences of the United States of America*, 101(45), pp.16046–51.

Carvelli, L., Blakely, R.D. & DeFelice, L.J., 2008. Dopamine transporter/syntaxin 1A interactions regulate transporter channel activity and dopaminergic synaptic transmission. *Proceedings of the National Academy of Sciences of the United States of America*, 105(37), pp.14192–7.

Cass, W.A. & Zahniser, N.R., 1991. Potassium Channel Blockers Inhibit D 2 Dopamine, but Not A 1 Adenosine, Receptor-Mediated Inhibition of Striatal Dopamine Release. *Journal of Neurochemistry*, 57(1), pp.147–152.

del Castillo, J. & Katz, B., 1954. Quantal components of the end-plate potential. *The Journal of physiology*, 124(3), pp.560–73.

Castle, M. et al., 2005. Thalamic innervation of the direct and indirect basal ganglia pathways in the rat: Ipsi- and contralateral projections. *The Journal of Comparative Neurology*, 483(2), pp.143–153.

Cebrian, C., Parent, A. & Prensa, L., 2005. Patterns of axonal branching of neurons of the substantia nigra pars reticulata and pars lateralis in the rat. *The Journal of Comparative Neurology*, 492(3), pp.349–369.

Cepeda, C. et al., 2008. Differential electrophysiological properties of dopamine D1 and D2 receptor-containing striatal medium-sized spiny neurons. *European Journal of Neuroscience*, 27(3), pp.671–682.

Chan, C.S. et al., 2007. "Rejuvenation" protects neurons in mouse models of Parkinson's disease. *Nature*, 447(7148), pp.1081–1086.

Chang, H.T. & Kita, H., 1992. Interneurons in the rat striatum: relationships between parvalbumin neurons and cholinergic neurons. *Brain Research*, 574(1–2), pp.307–311.

Chen, B.T. & Rice, M.E., 2001. Novel Ca2+ Dependence and Time Course of Somatodendritic Dopamine Release: Substantia Nigra versus Striatum. *J. Neurosci.*, 21(19), pp.7841–7847.

Chen, C. & Regehr, W.G., 1999. Contributions of residual calcium to fast synaptic transmission. *The Journal of neuroscience : the official journal of the Society for Neuroscience*, 19(15), pp.6257–66.

Chen, R. et al., 2013. Protein kinase Cβ is a modulator of the dopamine D2 autoreceptor-activated trafficking of the dopamine transporter. *Journal of Neurochemistry*, 125(5), pp.663–672.

Chergui, K., Akaoka, H., et al., 1994. Subthalamic nucleus modulates burst firing of nigral dopamine neurones via NMDA receptors. *Neuroreport*, 5(10), pp.1185–8.

Chergui, K., Suaud-Chagny, M.F. & Gonon, F., 1994. Nonlinear relationship between impulse flow, dopamine release and dopamine elimination in the rat brain in vivo. *Neuroscience*, 62(3), pp.641–645.

Chiodo, L.A. et al., 1980. Sensory stimuli alter discharge rate of dopamine (DA) neurons: evidence for two functional types of DA cells in the substantia nigra. *Brain Research*, 189(2), pp.544–549.

Chuhma, N. et al., 2009. Dopamine neuron glutamate cotransmission: frequency-dependent modulation in the mesoventromedial projection. *Neuroscience*, 164(3), pp.1068–1083.

Chuhma, N., 2004. Dopamine Neurons Mediate a Fast Excitatory Signal via Their Glutamatergic Synapses. *Journal of Neuroscience*, 24(4), pp.972–981.

Chung, C.Y. et al., 2005. Cell type-specific gene expression of midbrain dopaminergic neurons reveals molecules involved in their vulnerability and protection. *Human Molecular Genetics*, 14(13), pp.1709–1725.

Ciccarelli, A. et al., 2012. Organization of GABAergic synaptic circuits in the rat ventral tegmental area. *PloS one*, 7(10), p.e46250.

Clark, D. & Chiodo, L.A., 1988. Electrophysiological and pharmacological characterization of identified nigrostriatal and mesoaccumbens dopamine neurons in the rat. *Synapse*, 2(5), pp.474–485.

Cohen, J.Y. et al., 2012. Neuron-type-specific signals for reward and punishment in the ventral tegmental area. *Nature*, 482(7383), pp.85–8.

Collins, A.L. et al., 2016. Nucleus Accumbens Acetylcholine Receptors Modulate Dopamine and Motivation. *Neuropsychopharmacology*.

Congar, P., Bergevin, A. & Trudeau, L.-E., 2002. D2 Receptors Inhibit the Secretory Process Downstream From Calcium Influx in Dopaminergic Neurons: Implication of K+ Channels. *J Neurophysiol*, 87(2), pp.1046–1056.

Connor, J.A. & Stevens, C.F., 1971. Voltage clamp studies of a transient outward membrane current in gastropod neural somata. *The Journal of Physiology*, 213(1), pp.21–30.

Consolo, S. et al., 1999. Different sensitivity of in vivo acetylcholine transmission to D1 receptor stimulation in shell and core of nucleus accumbens. *Neuroscience*, 89(4), pp.1209–1217.

Contant, C. et al., 1996. Ultrastructural characterization of the acetylcholine innervation in adult rat neostriatum. *Neuroscience*, 71(4), pp.937–947.

Cooper, E.C. et al., 1998. Presynaptic Localization of Kv1.4-Containing A-Type Potassium Channels Near Excitatory Synapses in the Hippocampus. *J. Neurosci.*, 18(3), pp.965–974.

Costa, R.M., 2011. A selectionist account of de novo action learning. *Current Opinion in Neurobiology*, 21(4), pp.579–586.

Cragg, S.J., 2003. Variable Dopamine Release Probability and Short-Term Plasticity between Functional Domains of the Primate Striatum. *J. Neurosci.*, 23(10), pp.4378–4385.

Cragg, S.J. & Rice, M.E., 2004. DAncing past the DAT at a DA synapse. *Trends in Neurosciences*, 27(5), pp.270–277.

Creed, M. et al., 2016. Cocaine Exposure Enhances the Activity of Ventral Tegmental Area Dopamine Neurons via Calcium-Impermeable NMDARs. *Journal of Neuroscience*, 36(42), pp.10759–10768.

Crittenden, J.R. et al., 2016. Striosome-dendron bouquets highlight a unique striatonigral circuit targeting dopamine-containing neurons. *Proceedings of the National Academy of Sciences of the United States of America*, 113(40), pp.11318–11323.

Cui, G. et al., 2013. Concurrent activation of striatal direct and indirect pathways during action initiation. *Nature*, 494(7436), pp.238–42.

Cuttle, M.F. et al., 1998. Facilitation of the presynaptic calcium current at an auditory synapse in rat brainstem. *The Journal of physiology*, 512 (Pt 3)(Pt 3), pp.723–9.

Damsma, G. et al., 1991. Dopaminergic regulation of striatal acetylcholine release: importance of D1 and N-methyl-D-aspartate receptors. *Journal of Pharmacology and Experimental Therapeutics*, 259(3).

Danbolt, N.C., 2001. Glutamate uptake. *Progress in Neurobiology*, 65(1), pp.1–105.

Day, J.J. et al., 2007. Associative learning mediates dynamic shifts in dopamine signaling in the nucleus accumbens. *Nature Neuroscience*, 10(8), pp.1020–1028.

Debanne, D. et al., 1997. Action-potential propagation gated by an axonal IA-like K+ conductance in hippocampus. *Nature*, 389(6648), pp.286–289.

Debanne, D. et al., 1999. Gating of action potential propagation by an axonal A-like potassium conductance in the hippocampus: A new type of non-synaptic plasticity. *Journal of Physiology-Paris*, 93(4), pp.285–296.

Debanne, D., 2004. Information processing in the axon. *Nature reviews. Neuroscience*, 5(4),

pp.304–16.

Deisseroth, K., 2015. Optogenetics: 10 years of microbial opsins in neuroscience. *Nature Neuroscience*, 18(9), pp.1213–1225.

DeLong, M. & Wichmann, T., 2010. Changing Views of Basal Ganglia Circuits and Circuit Disorders. *Clinical EEG and Neuroscience*, 41(2), pp.61–67.

DeLong, M.R., 1990. Primate models of movement disorders of basal ganglia origin. *Trends in neurosciences*, 13(7), pp.281–5.

DeLong, M.R., Crutcher, M.D. & Georgopoulos, A.P., 1983. Relations between movement and single cell discharge in the substantia nigra of the behaving monkey. *The Journal of neuroscience : the official journal of the Society for Neuroscience*, 3(8), pp.1599–606.

Denker, A., Kröhnert, K. & Rizzoli, S.O., 2009. Revisiting synaptic vesicle pool localization in the Drosophila neuromuscular junction. *The Journal of Physiology*, 587(12), pp.2919–2926.

Descarries, L. et al., 1996. Dual character, asynaptic and synaptic, of the dopamine innervation in adult rat neostriatum: A quantitative autoradiographic and immunocytochemical analysis. *The Journal of Comparative Neurology*, 375(2), pp.167–186.

Descarries, L. et al., 2008. Glutamate in dopamine neurons: Synaptic versus diffuse transmission. *Brain Research Reviews*, 58(2), pp.290–302.

Descarries, L., Gisiger, V. & Steriade, M., 1997. Diffuse transmission by acetylcholine in the CNS. *Progress in Neurobiology*, 53(5), pp.603–625.

Ding, J.B. et al., 2010. Thalamic gating of corticostriatal signaling by cholinergic interneurons. *Neuron*, 67(2), pp.294–307.

Dobrunz, L.E. & Stevens, C.F., 1997. Heterogeneity of Release Probability, Facilitation, and Depletion at Central Synapses. *Neuron*, 18(6), pp.995–1008.

Dodson, P.D. et al., 2003. Presynaptic Rat Kv1.2 Channels Suppress Synaptic Terminal Hyperexcitability Following Action Potential Invasion. *The Journal of Physiology*, 550(1), pp.27–33.

Dodson, P.D. et al., 2016. Representation of spontaneous movement by dopaminergic neurons is cell-type selective and disrupted in parkinsonism. *Proceedings of the National Academy of Sciences of the United States of America*, 113(15), pp.E2180-8.

Dodson, P.D. & Forsythe, I.D., 2004. Presynaptic K+ channels: electrifying regulators of synaptic terminal excitability. *Trends in Neurosciences*, 27(4), pp.210–217.

Doig, N.M., Moss, J. & Bolam, J.P., 2010. Cortical and Thalamic Innervation of Direct and Indirect Pathway Medium-Sized Spiny Neurons in Mouse Striatum. *Journal of Neuroscience*, 30(44).

Drake, C.T. et al., 1997. GIRK1 immunoreactivity is present predominantly in dendrites, dendritic spines, and somata in the CA1 region of the hippocampus. *Proceedings of the National Academy of Sciences of the United States of America*, 94(3), pp.1007–12.

Dreyer, J.K. et al., 2010. Influence of Phasic and Tonic Dopamine Release on Receptor Activation. *Journal of Neuroscience*, 30(42), pp.14273–14283.

Dreyer, J.K. & Hounsgaard, J., 2013. Mathematical model of dopamine autoreceptors and uptake inhibitors and their influence on tonic and phasic dopamine signaling. *Journal of Neurophysiology*, 109(1).

Du, C. et al., 2006. Cocaine increases the intracellular calcium concentration in brain independently of its cerebrovascular effects. *The Journal of neuroscience : the official journal of the Society for Neuroscience*, 26(45), pp.11522–31.

Dubé, L., Smith, A.D. & Bolam, J.P., 1988. Identification of synaptic terminals of thalamic or cortical origin in contact with distinct medium-size spiny neurons in the rat neostriatum. *Journal of Comparative Neurology*, 267(4), pp.455–471.

Durieux, P.F., Schiffmann, S.N. & de Kerchove d'Exaerde, A., 2012. Differential regulation of motor control and response to dopaminergic drugs by D1R and D2R neurons in distinct dorsal striatum subregions. *The EMBO journal*, 31(3), pp.640–53.

Ehringer, H. & Hornykiewicz, O., 1960. Verteilung Von Noradrenalin Und Dopamin (3-Hydroxytyramin) Im Gehirn Des Menschen Und Ihr Verhalten Bei Erkrankungen Des Extrapyramidalen Systems. *Klinische Wochenschrift*, 38(24), pp.1236–1239.

Emptage, N.J., Reid, C.A. & Fine, A., 2001. Calcium Stores in Hippocampal Synaptic Boutons Mediate Short-Term Plasticity, Store-Operated Ca2+ Entry, and Spontaneous Transmitter Release. *Neuron*, 29(1), pp.197–208.

English, D.F. et al., 2011. GABAergic circuits mediate the reinforcement-related signals of striatal cholinergic interneurons. *Nature Neuroscience*, 15(1), pp.123–130.

Ertel, E.A. et al., 2000. Nomenclature of Voltage-Gated Calcium Channels. *Neuron*, 25(3), pp.533–535.

Everitt, B.J. & Robbins, T.W., 2013. From the ventral to the dorsal striatum: devolving views of their roles in drug addiction. *Neuroscience and biobehavioral reviews*, 37(9 Pt A), pp.1946–54.

Ewing, A.G., Bigelow, J.C. & Wightman, R.M., 1983. Direct in vivo monitoring of dopamine released from two striatal compartments in the rat. *Science (New York, N.Y.)*, 221(4606), pp.169–71.

Exley, R. et al., 2008. α6-Containing Nicotinic Acetylcholine Receptors Dominate the Nicotine Control of Dopamine Neurotransmission in Nucleus Accumbens. *Neuropsychopharmacology*, 33(9), pp.2158–2166.

Exley, R. & Cragg, S.J., 2008. Presynaptic nicotinic receptors: a dynamic and diverse cholinergic filter of striatal dopamine neurotransmission. *British journal of pharmacology*, 153 Suppl, pp.S283-97.

Fà, M. et al., 2003. Electrophysiological and pharmacological characteristics of nigral dopaminergic neurons in the conscious, head-restrained rat. *Synapse*, 48(1), pp.1–9.

Felmy, F., Neher, E. & Schneggenburger, R., 2003. Probing the Intracellular Calcium Sensitivity of Transmitter Release during Synaptic Facilitation. *Neuron*, 37(5), pp.801–811.

Fenno, L.E. et al., 2014. Targeting cells with single vectors using multiple-feature Boolean logic. *Nature Methods*, 11(7), pp.763–772.

Fernández-Alacid, L. et al., 2009. Subcellular compartment-specific molecular diversity of pre- and post-synaptic GABAB -activated GIRK channels in Purkinje cells. *Journal of Neurochemistry*, 110(4), pp.1363–1376.

Finkel, A.S. & Redman, S.J., 1985. Optimal Voltage Clamping with Single Electrode. In T. G. Smith et al., eds. *Voltage and Patch Clamping with Micorelectrodes*. New York, NY: Springer New York, pp. 95–120.

Fiorillo, C.D., 2013. Two Dimensions of Value: Dopamine Neurons Represent Reward But Not Aversiveness. *Science*, 341(6145).

Fiorillo, C.D., Song, M.R. & Yun, S.R., 2013. Multiphasic Temporal Dynamics in Responses of Midbrain Dopamine Neurons to Appetitive and Aversive Stimuli. *Journal of Neuroscience*, 33(11).

Fiorillo, C.D., Tobler, P.N. & Schultz, W., 2003. Discrete Coding of Reward Probability and Uncertainty by Dopamine Neurons. *Science*, 299(5614).

Fisher, S.D. et al., 2017. Reinforcement determines the timing dependence of corticostriatal synaptic plasticity in vivo. *Nature Communications*, 8(1), p.334.

Fleidervish, I.A., Friedman, A. & Gutnick, M.J., 1996. Slow inactivation of Na+ current and slow cumulative spike adaptation in mouse and guinea-pig neocortical neurones in slices. *The Journal of Physiology*, 493(1), pp.83–97.

Floresco, S.B. et al., 2003. Afferent modulation of dopamine neuron firing differentially regulates tonic and phasic dopamine transmission. *Nature Neuroscience*, 6(9), pp.968–973.

Forsythe, I.D. et al., 1998. Inactivation of Presynaptic Calcium Current Contributes to Synaptic Depression at a Fast Central Synapse. *Neuron*, 20(4), pp.797–807.

Foster, D.J. et al., 2014. M5 Receptor Activation Produces Opposing Physiological Outcomes in Dopamine Neurons Depending on the Receptor's Location. *Journal of Neuroscience*, 34(9).

Foust, A.J. et al., 2011. Somatic Membrane Potential and Kv1 Channels Control Spike Repolarization in Cortical Axon Collaterals and Presynaptic Boutons. *Journal of Neuroscience*, 31(43).

Franklin, K.B.J. & Paxinos, G., 2008. *The mouse brain in stereotaxic coordinates* 3rd ed., New York: Elsevier Academic Press.

Freeman, A.S., Meltzer, L.T. & Bunney, B.S., 1985. Firing properties of substantia nigra dopaminergic neurons in freely moving rats. *Life Sciences*, 36(20), pp.1983–1994.

Freeze, B.S. et al., 2013. Control of basal ganglia output by direct and indirect pathway projection neurons. *The Journal of neuroscience : the official journal of the Society for Neuroscience*, 33(47), pp.18531–9.

Fulton, S. et al., 2011. Contribution of Kv1.2 voltage-gated potassium channel to D2 autoreceptor regulation of axonal dopamine overflow. *The Journal of biological chemistry*, 286(11), pp.9360–72.

Garris, P.A. et al., 1994. Efflux of dopamine from the synaptic cleft in the nucleus accumbens of the rat brain. *The Journal of neuroscience : the official journal of the Society for Neuroscience*, 14(10), pp.6084–93.

Garris, P.A. et al., 1997. Real-Time Measurement of Electrically Evoked Extracellular Dopamine in the Striatum of Freely Moving Rats. *Journal of Neurochemistry*, 68(1), pp.152–161.

Gauthier, J. et al., 1999. The axonal arborization of single nigrostriatal neurons in rats. *Brain Research*, 834(1), pp.228–232.

Geiger, J.R.P. & Jonas, P., 2000. Dynamic Control of Presynaptic Ca2+ Inflow by Fast-Inactivating K+ Channels in Hippocampal Mossy Fiber Boutons. *Neuron*, 28(3), pp.927–939.

Gerfen, C. et al., 1990. D1 and D2 dopamine receptor-regulated gene expression of striatonigral

and striatopallidal neurons. *Science*, 250(4986).

Gerfen, C.R., 1985. The neostriatal mosaic. I. compartmental organization of projections from the striatum to the substantia nigra in the rat. *The Journal of Comparative Neurology*, 236(4), pp.454–476.

Gerfen, C.R. & Bolam, J.P., 2016. The Neuroanatomical Organization of the Basal Ganglia. In H. Steiner & K. Y. Tseng, eds. *Handbook of Basal Ganglia Structure and Function*. London: Academic Press, pp. 3–27.

Gerfen, C.R., Herkenham, M. & Thibault, J., 1987. The neostriatal mosaic: II. Patch- and matrix-directed mesostriatal dopaminergic and non-dopaminergic systems. *Journal of Neuroscience*, 7(12), pp.3915–3934.

Goldberg, E.M. et al., 2008. K+ Channels at the Axon Initial Segment Dampen Near-Threshold Excitability of Neocortical Fast-Spiking GABAergic Interneurons. *Neuron*, 58(3), pp.387–400.

Gonon, F. et al., 2000. Geometry and kinetics of dopaminergic transmission in the rat striatum and in mice lacking the dopamine transporter. *Progress in Brain Research*, 125, pp.291–302.

Grace, A.A. & Bunney, B.S., 1984a. The control of firing pattern in nigral dopamine neurons: burst firing. *The Journal of neuroscience : the official journal of the Society for Neuroscience*, 4(11), pp.2877–90.

Grace, A.A. & Bunney, B.S., 1984b. The control of firing pattern in nigral dopamine neurons: single spike firing. *The Journal of neuroscience : the official journal of the Society for Neuroscience*, 4(11), pp.2866–76.

Grace, A.A. & Onn, S.P., 1989. Morphology and electrophysiological properties of immunocytochemically identified rat dopamine neurons recorded in vitro. *The Journal of neuroscience : the official journal of the Society for Neuroscience*, 9(10), pp.3463–81.

Greene, J.G., Dingledine, R. & Greenamyre, J.T., 2005. Gene expression profiling of rat midbrain dopamine neurons: implications for selective vulnerability in parkinsonism. *Neurobiology of Disease*, 18(1), pp.19–31.

Greengard, P. et al., 1993. Synaptic vesicle phosphoproteins and regulation of synaptic function. *Science*, 259(5096), pp.780–785.

Grosse, G. et al., 2003. Axonal sorting of Kir3.3 defines a GABA-containing neuron in the CA3 region of rodent hippocampus. *Molecular and Cellular Neuroscience*, 24(3), pp.709–724.

Grossman, Y., Parnas, I. & Spira, M.E., 1979a. Differential conduction block in branches of a bifurcating axon. *The Journal of Physiology*, 295(1), pp.283–305.

Grossman, Y., Parnas, I. & Spira, M.E., 1979b. Mechanisms involved in differential conduction of potentials at high frequency in a branching axon. *The Journal of Physiology*, 295(1), pp.307–322.

Gu, H., Wall, S.C. & Rudnick, G., 1994. Stable expression of biogenic amine transporters reveals differences in inhibitor sensitivity, kinetics, and ion dependence. *The Journal of biological chemistry*, 269(10), pp.7124–30.

Guan, B., Chen, X. & Zhang, H., 2013. Two-Electrode Voltage Clamp. In N. Gamper, ed. *Ion Channels. Methods in Molecular Biology (Methods and Protocols)*. Totowa, NJ: Humana Press, pp. 79–89.

Gunaydin, L.A. et al., 2010. Ultrafast optogenetic control. *Nature Neuroscience*, 13(3), pp.387–

392.

Guo, Q. et al., 2015. Whole-brain mapping of inputs to projection neurons and cholinergic interneurons in the dorsal striatum. *PloS one*, 10(4), p.e0123381.

Gutman, G.A. et al., 2005. International Union of Pharmacology. LIII. Nomenclature and Molecular Relationships of Voltage-Gated Potassium Channels. *Pharmacological Reviews*, 57(4).

Guzmán, J.N. et al., 2003. Dopaminergic Modulation of Axon Collaterals Interconnecting Spiny Neurons of the Rat Striatum. *Journal of Neuroscience*, 23(26).

Haber, S.N. et al., 1995. Subsets of midbrain dopaminergic neurons in monkeys are distinguished by different levels of mRNA for the dopamine transporter: Comparison with the mRNA for the D2 receptor, tyrosine hydroxylase and calbindin immunoreactivity. *The Journal of Comparative Neurology*, 362(3), pp.400–410.

Hafizi, S., Kruk, Z.L. & Stamford, J.A., 1990. Fast cyclic voltammetry: improved sensitivity to dopamine with extended oxidation scan limits. *Journal of Neuroscience Methods*, 33(1), pp.41–49.

Hamid, A.A. et al., 2015. Mesolimbic dopamine signals the value of work. *Nature Neuroscience*, 19(1), pp.117–126.

Hamill, O.P. et al., 1981. Improved patch-clamp techniques for high-resolution current recording from cells and cell-free membrane patches. *Pflügers Archiv - European Journal of Physiology*, 391(2), pp.85–100.

Han, W. et al., 2002. Altered cocaine effects in mice lacking Cav2.3 (α1E) calcium channel. *Biochemical and Biophysical Research Communications*, 299(2), pp.299–304.

Hanson, D.C. et al., 1999. UK-78,282, a novel piperidine compound that potently blocks the Kv1.3 voltage-gated potassium channel and inhibits human T cell activation. *British Journal of Pharmacology*, 126(8), pp.1707–1716.

Hara, S. et al., 2013. Serine 129 phosphorylation of membrane-associated α-synuclein modulates dopamine transporter function in a G protein-coupled receptor kinase-dependent manner. *Molecular biology of the cell*, 24(11), pp.1649–60, S1-3.

Hartung, H., Threlfell, S. & Cragg, S.J., 2011. Nitric Oxide Donors Enhance the Frequency Dependence of Dopamine Release in Nucleus Accumbens. *Neuropsychopharmacology*, 36(9), pp.1811–1822.

Hatt, H. & Smith, D.O., 1976. Synaptic depression related to presynaptic axon conduction block. *The Journal of Physiology*, 259(2), pp.367–393.

He, Y., Zorumski, C.F. & Mennerick, S., 2002. Contribution of Presynaptic Na+ Channel Inactivation to Paired-Pulse Synaptic Depression in Cultured Hippocampal Neurons. *J Neurophysiol*, 87(2), pp.925–936.

Heien, M.L.A. V et al., 2003. Overoxidation of carbon-fiber microelectrodes enhances dopamine adsorption and increases sensitivity. *The Analyst*, 128(12), pp.1413–9.

Henselmans, J.M.L. & Stoof, J.C., 1991. Regional differences in the regulation of acetylcholine release upon D2 dopamine and N-methyl-d-aspartate receptor activation in rat nucleus accumbens and neostriatum. *Brain Research*, 566(1–2), pp.1–7.

Hermans, A. et al., 2008. Dopamine detection with fast-scan cyclic voltammetry used with analog background subtraction. *Analytical …*.

Hernandez-Lopez, S. et al., 2000. D2 dopamine receptors in striatal medium spiny neurons reduce L-type Ca2+ currents and excitability via a novel PLC[beta]1-IP3-calcineurin-signaling cascade. *The Journal of neuroscience : the official journal of the Society for Neuroscience*, 20(24), pp.8987–95.

Hernández-López, S. et al., 1997. D1 receptor activation enhances evoked discharge in neostriatal medium spiny neurons by modulating an L-type Ca2+ conductance. *The Journal of neuroscience : the official journal of the Society for Neuroscience*, 17(9), pp.3334–42.

Hersch, S.M. et al., 1997. Subcellular localization and molecular topology of the dopamine transporter in the striatum and substantia nigra. *The Journal of Comparative Neurology*, 388(2), pp.211–227.

Hilfiker, S. et al., 1998. Two sites of action for synapsin domain E in regulating neurotransmitter release. *Nature Neuroscience*, 1(1), pp.29–35.

Hjorth, J., Blackwell, K.T. & Kotaleski, J.H., 2009. Gap junctions between striatal fast-spiking interneurons regulate spiking activity and synchronization as a function of cortical activity. *The Journal of neuroscience : the official journal of the Society for Neuroscience*, 29(16), pp.5276–86.

Hnasko, T.S. et al., 2010. Vesicular glutamate transport promotes dopamine storage and glutamate corelease in vivo. *Neuron*, 65(5), pp.643–56.

Hochner, B., Parnas, H. & Parnas, I., 1991. Effects of intra-axonal injection of Ca2+ buffers on evoked release and on facilitation in the crayfish neuromuscular junction. *Neuroscience Letters*, 125(2), pp.215–218.

Hodgkin, A.L., Huxley, A.F. & Katz, B., 1952. Measurement of current-voltage relations in the membrane of the giant axon of Loligo. *The Journal of Physiology*, 116(4), pp.424–448.

Hoffman, A.F., Spivak, C.E. & Lupica, C.R., 2016. Enhanced Dopamine Release by Dopamine Transport Inhibitors Described by a Restricted Diffusion Model and Fast-Scan Cyclic Voltammetry. *ACS Chemical Neuroscience*, 7, pp.700–709.

Horvitz, J.C., Stewart, T. & Jacobs, B.L., 1997. Burst activity of ventral tegmental dopamine neurons is elicited by sensory stimuli in the awake cat. *Brain Research*, 759(2), pp.251–258.

Hoshi, T., Zagotta, W.N. & Aldrich, R.W., 1991. Two types of inactivation in Shaker K+ channels: Effects of alterations in the carboxy-terminal region. *Neuron*, 7(4), pp.547–556.

Houston, C.M. et al., 2009. Intracellular chloride ions regulate the time course of GABA-mediated inhibitory synaptic transmission. *The Journal of neuroscience : the official journal of the Society for Neuroscience*, 29(33), pp.10416–23.

Howe, M.W. et al., 2013. Prolonged dopamine signalling in striatum signals proximity and value of distant rewards. *Nature*, 500(7464), pp.575–9.

Howe, M.W. & Dombeck, D.A., 2016. Rapid signalling in distinct dopaminergic axons during locomotion and reward. *Nature*.

Hu, H. & Jonas, P., 2014. A supercritical density of Na+ channels ensures fast signaling in GABAergic interneuron axons. *Nature Neuroscience*, 17(5), pp.686–693.

Hyland, B.. et al., 2002. Firing modes of midbrain dopamine cells in the freely moving rat. *Neuroscience*, 114(2), pp.475–492.

Ibáñez-Sandoval, O. et al., 2011. A novel functionally distinct subtype of striatal neuropeptide Y

interneuron. *The Journal of neuroscience : the official journal of the Society for Neuroscience*, 31(46), pp.16757–69.

Imperato, A. et al., 1992. Cocaine releases limbic acetylcholine through endogenous dopamine action on D1 receptors. *European Journal of Pharmacology*, 229(2–3), pp.265–267.

Ingram, S.L., Prasad, B.M. & Amara, S.G., 2002. Dopamine transporter-mediated conductances increase excitability of midbrain dopamine neurons. *Nature neuroscience*, 5(10), pp.971–8.

Inokawa, H. et al., 2010. Juxtacellular labeling of tonically active neurons and phasically active neurons in the rat striatum. *Neuroscience*, 168(2), pp.395–404.

Iremonger, K.J. & Bains, J.S., 2007. Integration of asynchronously released quanta prolongs the postsynaptic spike window. *The Journal of neuroscience : the official journal of the Society for Neuroscience*, 27(25), pp.6684–91.

Isaacson, J.S., Solis, J.M. & Nicoll, R.A., 1993. Local and diffuse synaptic actions of GABA in the hippocampus. *Neuron*, 10(2), pp.165–175.

Ishikawa, T. et al., 2003. Distinct Roles of Kv1 and Kv3 Potassium Channels at the Calyx of Held Presynaptic Terminal. *Journal of Neuroscience*, 23(32).

Izzo, P.N. & Bolam, J.P., 1988. Cholinergic synaptic input to different parts of spiny striatonigral neurons in the rat. *The Journal of Comparative Neurology*, 269(2), pp.219–234.

Jackman, S.L. et al., 2014. Achieving high-frequency optical control of synaptic transmission. *The Journal of neuroscience : the official journal of the Society for Neuroscience*, 34(22), pp.7704–14.

Jackman, S.L. et al., 2016. The calcium sensor synaptotagmin 7 is required for synaptic facilitation. *Nature*, 529(7584), pp.88–91.

Jackson, M.B., Konnerth, A. & Augustine, G.J., 1991. Action potential broadening and frequency-dependent facilitation of calcium signals in pituitary nerve terminals. *Proceedings of the National Academy of Sciences*, 88(2), pp.380–384.

Janssen, M.J. et al., 2009. Dopamine modulation of GABA tonic conductance in striatal output neurons. *The Journal of neuroscience : the official journal of the Society for Neuroscience*, 29(16), pp.5116–26.

Jennings, K.A., Platt, N.J. & Cragg, S.J., 2015. The impact of a parkinsonian lesion on dynamic striatal dopamine transmission depends on nicotinic receptor activation. *Neurobiology of Disease*, 82, pp.262–268.

Jin, X. & Costa, R.M., 2010. Start/stop signals emerge in nigrostriatal circuits during sequence learning. *Nature*, 466(7305), pp.457–462.

Joel, D. & Weiner, I., 1994. The organization of the basal ganglia-thalamocortical circuits: Open interconnected rather than closed segregated. *Neuroscience*, 63(2), pp.363–379.

Johnson, S., Seutin, V. & North, R., 1992. Burst firing in dopamine neurons induced by N-methyl-D-aspartate: role of electrogenic sodium pump. *Science*, 258(5082).

Jones, I.W., Bolam, J.P. & Wonnacott, S., 2001. Presynaptic localisation of the nicotinic acetylcholine receptor beta2 subunit immunoreactivity in rat nigrostriatal dopaminergic neurones. *The Journal of comparative neurology*, 439(2), pp.235–47.

Jones, M. V. & Westbrook, G.L., 1995. Desensitized states prolong GABAA channel responses to

brief agonist pulses. *Neuron*, 15(1), pp.181–191.

Jones, S.R. et al., 1995. Comparison of Dopamine Uptake in the Basolateral Amygdaloid Nucleus, Caudate-Putamen, and Nucleus Accumbens of the Rat. *Journal of Neurochemistry*, 64(6), pp.2581–2589.

Joshua, M. et al., 2008. Midbrain dopaminergic neurons and striatal cholinergic interneurons encode the difference between reward and aversive events at different epochs of probabilistic classical conditioning trials. *The Journal of neuroscience : the official journal of the Society for Neuroscience*, 28(45), pp.11673–84.

Kalivas, P.W., Churchill, L. & Klitenick, M.A., 1993. GABA and enkephalin projection from the nucleus accumbens and ventral pallidum to the ventral tegmental area. *Neuroscience*, 57(4), pp.1047–1060.

Karayannis, T. et al., 2010. Slow GABA Transient and Receptor Desensitization Shape Synaptic Responses Evoked by Hippocampal Neurogliaform Cells. *Journal of Neuroscience*, 30(29).

Katz, B. & Miledi, R., 1968. The role of calcium in neuromuscular facilitation. *The Journal of Physiology*, 195(2), pp.481–492.

Kawaguchi, S. & Sakaba, T., 2015. Control of inhibitory synaptic outputs by low excitability of axon terminals revealed by direct recording. *Neuron*, 85(6), pp.1273–88.

Kawaguchi, Y., 1993. Physiological, morphological, and histochemical characterization of three classes of interneurons in rat neostriatum. *The Journal of neuroscience : the official journal of the Society for Neuroscience*, 13(11), pp.4908–23.

Kawano, M. et al., 2006. Particular subpopulations of midbrain and hypothalamic dopamine neurons express vesicular glutamate transporter 2 in the rat brain. *The Journal of Comparative Neurology*, 498(5), pp.581–592.

Keithley, R.B. et al., 2011. Higher sensitivity dopamine measurements with faster-scan cyclic voltammetry. *Analytical chemistry*, 83(9), pp.3563–71.

Khaliq, Z.M. & Bean, B.P., 2008. Dynamic, nonlinear feedback regulation of slow pacemaking by A-type potassium current in ventral tegmental area neurons. *The Journal of neuroscience : the official journal of the Society for Neuroscience*, 28(43), pp.10905–17.

Khaliq, Z.M. & Bean, B.P., 2010. Pacemaking in dopaminergic ventral tegmental area neurons: depolarizing drive from background and voltage-dependent sodium conductances. *The Journal of neuroscience : the official journal of the Society for Neuroscience*, 30(21), pp.7401–13.

Kile, B.M. et al., 2010. Synapsins differentially control dopamine and serotonin release. *The Journal of neuroscience : the official journal of the Society for Neuroscience*, 30(29), pp.9762–70.

Kim, J.-I. et al., 2015. Aldehyde dehydrogenase 1a1 mediates a GABA synthesis pathway in midbrain dopaminergic neurons. *Science*, 350(6256), pp.102–106.

Kirmse, K. et al., 2008. GABA transporter 1 tunes GABAergic synaptic transmission at output neurons of the mouse neostriatum. *The Journal of Physiology*, 586(23), pp.5665–5678.

Kita, H., Kosaka, T. & Heizmann, C.W., 1990. Parvalbumin-immunoreactive neurons in the rat neostriatum: a light and electron microscopic study. *Brain Research*, 536(1–2), pp.1–15.

Kiyatkin, E.A. & Rebec, G.V., 1998. Heterogeneity of ventral tegmental area neurons: Single-unit

recording and iontophoresis in awake, unrestrained rats. *Neuroscience*, 85(4), pp.1285–1309.

Kocsis, J.D., Malenka, R.C. & Waxman, S.G., 1983. Effects of extracellular potassium concentration on the excitability of the parallel fibres of the rat cerebellum. *The Journal of Physiology*, 334(1), pp.225–244.

Kole, M.H.P., Letzkus, J.J. & Stuart, G.J., 2007. Axon initial segment Kv1 channels control axonal action potential waveform and synaptic efficacy. *Neuron*, 55(4), pp.633–47.

Koós, T. & Tepper, J.M., 2002. Dual cholinergic control of fast-spiking interneurons in the neostriatum. *The Journal of neuroscience : the official journal of the Society for Neuroscience*, 22(2), pp.529–35.

Koos, T., Tepper, J.M. & Wilson, C.J., 2004. Comparison of IPSCs Evoked by Spiny and Fast-Spiking Neurons in the Neostriatum. *Journal of Neuroscience*, 24(36).

Kopysova, I.L. & Debanne, D., 1998. Critical role of axonal A-type K+ channels and axonal geometry in the gating of action potential propagation along CA3 pyramidal cell axons: a simulation study. *The Journal of neuroscience : the official journal of the Society for Neuroscience*, 18(18), pp.7436–51.

Kravitz, A. V et al., 2010. Regulation of parkinsonian motor behaviours by optogenetic control of basal ganglia circuitry. *Nature*, 466(7306), pp.622–6.

Kreitzer, A.C. & Malenka, R.C., 2007. Endocannabinoid-mediated rescue of striatal LTD and motor deficits in Parkinson's disease models. *Nature*, 445(7128), pp.643–647.

Kreitzer, A.C. & Malenka, R.C., 2008. Striatal plasticity and basal ganglia circuit function. *Neuron*, 60(4), pp.543–54.

Kress, G.J. et al., 2014. Fast phasic release properties of dopamine studied with a channel biosensor. *The Journal of neuroscience : the official journal of the Society for Neuroscience*, 34(35), pp.11792–802.

Kress, G.J. & Mennerick, S., 2009. Action potential initiation and propagation: Upstream influences on neurotransmission. *Neuroscience*, 158(1), pp.211–222.

Lacey, M.G., Mercuri, N.B. & North, R.A., 1988. On the potassium conductance increase activated by GABAB and dopamine D2 receptors in rat substantia nigra neurones. *The Journal of Physiology*, 401(1), pp.437–453.

Lacey, M.G., Mercuri, N.B. & North, R.A., 1989. Two Cell Types in Rat Substantia Nigra Zona Compacta Distinguished by Membrane Properties and the Actions of Dopamine and Opioids. *The Journal of Neuroscience*, 9(4), pp.1233–1241.

Lammel, S. et al., 2015. Diversity of Transgenic Mouse Models for Selective Targeting of Midbrain Dopamine Neurons. *Neuron*, 85(2), pp.429–438.

Lammel, S. et al., 2011. Projection-Specific Modulation of Dopamine Neuron Synapses by Aversive and Rewarding Stimuli. *Neuron*, 70(5), pp.855–862.

Lammel, S. et al., 2008. Unique Properties of Mesoprefrontal Neurons within a Dual Mesocorticolimbic Dopamine System. *Neuron*, 57(5), pp.760–773.

Lavoie, B. & Parent, A., 1991. Dopaminergic neurons expressing calbindin in normal and parkinsonian monkeys. *Neuroreport*, 2(10), pp.601–4.

Lavoie, B., Smith, Y. & Parent, A., 1989. Dopaminergic innervation of the basal ganglia in the squirrel monkey as revealed by tyrosine hydroxylase immunohistochemistry. *The Journal of Comparative Neurology*, 289(1), pp.36–52.

Lee, A. et al., 1999. Ca2+/calmodulin binds to and modulates P/Q-type calcium channels. *Nature*, 399(6732), pp.155–159.

Lee, F.J.S. et al., 2007. Dopamine transporter cell surface localization facilitated by a direct interaction with the dopamine D2 receptor. *The EMBO Journal*, 26(8), pp.2127–2136.

Lee, K.-H. et al., 2004. Syntaxin 1A and Receptor for Activated C Kinase Interact with the N-Terminal Region of Human Dopamine Transporter. *Neurochemical Research*, 29(7), pp.1405–1409.

Lee, S., Kim, K. & Zhou, Z.J., 2010. Role of ACh-GABA Cotransmission in Detecting Image Motion and Motion Direction. *Neuron*, 68(6), pp.1159–1172.

Lee, T.H. et al., 2001. Differential time-course profiles of dopamine release and uptake changes induced by three dopamine uptake inhibitors. *Synapse (New York, N.Y.)*, 41(4), pp.301–10.

Lerner, T.N. et al., 2015. Intact-Brain Analyses Reveal Distinct Information Carried by SNc Dopamine Subcircuits. *Cell*, 162(3), pp.635–647.

Liao, Y.J., Jan, Y.N. & Jan, L.Y., 1996. Heteromultimerization of G-Protein-Gated Inwardly Rectifying K+ Channel Proteins GIRK1 and GIRK2 and Their Altered Expression in weaver Brain. *J. Neurosci.*, 16(22), pp.7137–7150.

Liss, B. et al., 2001. Tuning pacemaker frequency of individual dopaminergic neurons by Kv4.3L and KChip3.1 transcription. *The EMBO Journal*, 20(20), pp.5715–5724.

Ljungberg, T., Apicella, P. & Schultz, W., 1992. Responses of monkey dopamine neurons during learning of behavioral reactions. *Journal of neurophysiology*, 67(1), pp.145–63.

Lokwan, S.J.A. et al., 1999. Stimulation of the pedunculopontine tegmental nucleus in the rat produces burst firing in A9 dopaminergic neurons. *Neuroscience*, 92(1), pp.245–254.

Luján, R. et al., 2003. Immunohistochemical localization of the voltage-gated potassium channel subunit Kv1.4 in the central nervous system of the adult rat. *Journal of Chemical Neuroanatomy*, 26(3), pp.209–224.

Luk, B. et al., 2015. A Physical Interaction between the Dopamine Transporter and DJ-1 Facilitates Increased Dopamine Reuptake L. Groc, ed. *PLOS ONE*, 10(8), p.e0136641.

Luo, R., Partridge, J.G. & Vicini, S., 2013. Distinct roles of synaptic and extrasynaptic GABAAreceptors in striatal inhibition dynamics. *Frontiers in Neural Circuits*, 7, p.186.

Lüscher, H.R. & Shiner, J.S., 1990. Computation of action potential propagation and presynaptic bouton activation in terminal arborizations of different geometries. *Biophysical Journal*, 58(6), pp.1377–1388.

Madisen, L. et al., 2012. A toolbox of Cre-dependent optogenetic transgenic mice for light-induced activation and silencing. *Nature Neuroscience*, 15(5), pp.793–802.

Maiya, R. et al., 2007. Defining the dopamine transporter proteome by convergent biochemical and in silico analyses. *Genes, brain, and behavior*, 6(1), pp.97–106.

Mameli-Engvall, M. et al., 2006. Hierarchical Control of Dopamine Neuron-Firing Patterns by Nicotinic Receptors. *Neuron*, 50(6), pp.911–921.

Mandikian, D. et al., 2014. Cell Type Specific Spatial and Functional Coupling Between Mammalian Brain Kv2.1 K+ Channels and Ryanodine Receptors. *The Journal of comparative neurology*, 522(15), p.3555.

La Manno, G. et al., 2016. Molecular Diversity of Midbrain Development in Mouse, Human, and Stem Cells. *Cell*, 167(2), p.566–580.e19.

Marcott, P.F., Mamaligas, A.A. & Ford, C.P., 2014. Phasic Dopamine Release Drives Rapid Activation of Striatal D2-Receptors. *Neuron*, 84(1), pp.164–176.

Margolis, E.B. et al., 2008. Midbrain Dopamine Neurons: Projection Target Determines Action Potential Duration and Dopamine D2 Receptor Inhibition. *Journal of Neuroscience*, 28(36).

Marinelli, M. & McCutcheon, J.E., 2014. Heterogeneity of dopamine neuron activity across traits and states. *Neuroscience*, 282C, pp.176–197.

Marsh, S.J. & Brown, D.A., 1991. Potassium currents contributing to action potential repolarization in dissociated cultured rat superior cervical sympathetic neurones. *Neuroscience Letters*, 133(2), pp.298–302.

Marshall, J.F. et al., 1990. Dopamine high-affinity transport site topography in rat brain: Major differences between dorsal and ventral striatum. *Neuroscience*, 37(1), pp.11–21.

Martel, P. et al., 2011. Role of Kv1 potassium channels in regulating dopamine release and presynaptic D2 receptor function. *PloS one*, 6(5), p.e20402.

Marty, A. & Neher, E., 1995. Tight-Seal Whole-Cell Recording. In B. Sakmann & E. Neher, eds. *Single-Channel Recording*. Boston, MA: Springer US, pp. 31–52.

Matamales, M. et al., 2016. Quantitative Imaging of Cholinergic Interneurons Reveals a Distinctive Spatial Organization and a Functional Gradient across the Mouse Striatum G. Fisone, ed. *PLOS ONE*, 11(6), p.e0157682.

Matsuda, W. et al., 2009. Single nigrostriatal dopaminergic neurons form widely spread and highly dense axonal arborizations in the neostriatum. *The Journal of neuroscience : the official journal of the Society for Neuroscience*, 29(2), pp.444–53.

Matsumoto, M. & Hikosaka, O., 2009. Two types of dopamine neuron distinctly convey positive and negative motivational signals. *Nature*, 459(7248), pp.837–841.

Maurice, N. et al., 2004. D2 Dopamine Receptor-Mediated Modulation of Voltage-Dependent Na+ Channels Reduces Autonomous Activity in Striatal Cholinergic Interneurons. *Journal of Neuroscience*, 24(46), pp.10289–10301.

McCaffery, P. & Dräger, U.C., 1994. High levels of a retinoic acid-generating dehydrogenase in the meso-telencephalic dopamine system. *Proceedings of the National Academy of Sciences of the United States of America*, 91(16), pp.7772–6.

McCutcheon, J.E. et al., 2012. Dopamine neurons in the ventral tegmental area fire faster in adolescent rats than in adults. *Journal of Neurophysiology*, 108(6).

McElvain, J.S. & Schenk, J.O., 1992. A multisubstrate mechanism of striatal dopamine uptake and its inhibition by cocaine. *Biochemical Pharmacology*, 43(10), pp.2189–2199.

McFarlane, C., Warner, D.S. & Dexter, F., 1995. Interactions between NMDA and AMPA glutamate receptor antagonists during halothane anesthesia in the rat. *Neuropharmacology*, 34(6), pp.659–663.

Melchior, J.R. et al., 2015. Optogenetic versus electrical stimulation of dopamine terminals in the nucleus accumbens reveals local modulation of presynaptic release. *Journal of neurochemistry*, 134(5), pp.833–44.

Mendez, J.A. et al., 2008. Developmental and Target-Dependent Regulation of Vesicular Glutamate Transporter Expression by Dopamine Neurons. *Journal of Neuroscience*, 28(25).

Mendez, J.A. et al., 2011. Somatodendritic Dopamine Release Requires Synaptotagmin 4 and 7 and the Participation of Voltage-gated Calcium Channels. *Journal of Biological Chemistry*, 286(27), pp.23928–23937.

Meneses, D. et al., 2016. KV1 and KV3 Potassium Channels Identified at Presynaptic Terminals of the Corticostriatal Synapses in Rat. *Neural plasticity*, 2016, p.8782518.

Mercuri, N.B. et al., 1994. Effects of dihydropyridine calcium antagonists on rat midbrain dopaminergic neurones. *British Journal of Pharmacology*, 113(3), pp.831–838.

Millar, J. et al., 1985. Electrochemical, pharmacological and electrophysiological evidence of rapid dopamine release and removal in the rat caudate nucleus following electrical stimulation of the median forebrain bundle. *European Journal of Pharmacology*, 109(3), pp.341–348.

Mingote, S. et al., 2015. Functional Connectome Analysis of Dopamine Neuron Glutamatergic Connections in Forebrain Regions. *Journal of Neuroscience*, 35(49).

Mirenowicz, J. & Schultz, W., 1994. Importance of unpredictability for reward responses in primate dopamine neurons. *Journal of Neurophysiology*, 72(2).

Miyashita, T. et al., 2013. Long-term channelrhodopsin-2 (ChR2) expression can induce abnormal axonal morphology and targeting in cerebral cortex. *Frontiers in neural circuits*, 7, p.8.

Mochida, S. et al., 2008. *Regulation of Presynaptic CaV2.1 Channels by Ca2+ Sensor Proteins Mediates Short-Term Synaptic Plasticity*,

Le Moine, C., Normand, E. & Bloch, B., 1991. Phenotypical characterization of the rat striatal neurons expressing the D1 dopamine receptor gene. *Proceedings of the National Academy of Sciences of the United States of America*, 88(10), pp.4205–9.

Montague, P., Dayan, P. & Sejnowski, T., 1996. A framework for mesencephalic dopamine systems based on predictive Hebbian learning. *Journal of Neuroscience*, 16(5).

Morris, G. et al., 2004. Coincident but distinct messages of midbrain dopamine and striatal tonically active neurons. *Neuron*, 43(1), pp.133–43.

Morris, R.G.M., 2003. Long-term potentiation and memory. *Philosophical Transactions of the Royal Society of London B: Biological Sciences*, 358(1432).

Mortensen, O. V. & Amara, S.G., 2003. Dynamic regulation of the dopamine transporter. *European Journal of Pharmacology*, 479(1–3), pp.159–170.

Muñoz-Cuevas, J., Vara, H. & Colino, A., 2004. Characterization of release-independent short-term depression in the juvenile rat hippocampus. *The Journal of physiology*, 558(Pt 2), pp.527–48.

Muñoz-Manchado, A.B. et al., 2014. Novel Striatal GABAergic Interneuron Populations Labeled in the 5HT3aEGFP Mouse. *Cerebral cortex (New York, N.Y. : 1991)*, p.bhu179-.

Nagel, G. et al., 2003. Channelrhodopsin-2, a directly light-gated cation-selective membrane channel. *Proceedings of the National Academy of Sciences of the United States of America*, 100(24), pp.13940–5.

Nagel, G. et al., 2005. Light Activation of Channelrhodopsin-2 in Excitable Cells of Caenorhabditis elegans Triggers Rapid Behavioral Responses. *Current Biology*, 15(24), pp.2279–2284.

Nair-Roberts, R.G. et al., 2008. Stereological estimates of dopaminergic, GABAergic and glutamatergic neurons in the ventral tegmental area, substantia nigra and retrorubral field in the rat. *Neuroscience*, 152(4), pp.1024–1031.

Nambu, A., Tokuno, H. & Takada, M., 2002. Functional significance of the cortico–subthalamo–pallidal "hyperdirect" pathway. *Neuroscience Research*, 43(2), pp.111–117.

Nanou, E. et al., 2016. Calcium sensor regulation of the CaV2.1 Ca2+ channel contributes to short-term synaptic plasticity in hippocampal neurons. *Proceedings of the National Academy of Sciences of the United States of America*, 113(4), pp.1062–7.

Naraghi, M. & Neher, E., 1997. Linearized buffered Ca2+ diffusion in microdomains and its implications for calculation of [Ca2+] at the mouth of a calcium channel. *The Journal of neuroscience : the official journal of the Society for Neuroscience*, 17(18), pp.6961–73.

Nauta, H.J.W., Pritz, M.B. & Lasek, R.J., 1974. Afferents to the rat caudoputamen studied with horseradish peroxidase. An evaluation of a retrograde neuroanatomical research method. *Brain Research*, 67(2), pp.219–238.

Nauta, W.J.H. et al., 1978. Efferent connections and nigral afferents of the nucleus accumbens septi in the rat. *Neuroscience*, 3(4), pp.385–401.

Nedergaard, S., 1999. Regulation of Action Potential Size and Excitability in Substantia Nigra Compacta Neurons: Sensitivity to 4-Aminopyridine. *Journal of Neurophysiology*, 82(6).

Neher, E., 1998. Usefulness and limitations of linear approximations to the understanding of Ca++ signals. *Cell Calcium*, 24(5–6), pp.345–357.

Neher, E., Sakmann, B. & Steinbach, J.H., 1978. The extracellular patch clamp: A method for resolving currents through individual open channels in biological membranes. *Pflügers Archiv European Journal of Physiology*, 375(2), pp.219–228.

Nelson, A.B. et al., 2014. Striatal cholinergic interneurons Drive GABA release from dopamine terminals. *Neuron*, 82(1), pp.63–70.

Nelson, A.B. & Kreitzer, A.C., 2014. Reassessing models of basal ganglia function and dysfunction. *Annual review of neuroscience*, 37, pp.117–35.

Neuhoff, H. et al., 2002. I(h) channels contribute to the different functional properties of identified dopaminergic subpopulations in the midbrain. *The Journal of neuroscience : the official journal of the Society for Neuroscience*, 22(4), pp.1290–302.

Neusch, C., Runde, D. & Moser, A., 2000. G Proteins Modulate D2 Receptor-Coupled K(ATP) Channels in Rat Dopaminergic Terminals. *Neurochemical Research*, 25(12), pp.1521–1526.

Nirenberg, M.J. et al., 1996. The dopamine transporter is localized to dendritic and axonal plasma membranes of nigrostriatal dopaminergic neurons. *The Journal of neuroscience : the official journal of the Society for Neuroscience*, 16(2), pp.436–47.

Nisenbaum, E. & Wilson, C., 1995. Potassium currents responsible for inward and outward rectification in rat neostriatal spiny projection neurons. *Journal of Neuroscience*, 15(6).

Obeso, J.A. et al., 2014. The expanding universe of disorders of the basal ganglia. *The Lancet*, 384(9942), pp.523–531.

Ofer, N., Shefi, O. & Yaari, G., 2017. Branching morphology determines signal propagation dynamics in neurons. *Scientific Reports*, 7(1), p.8877.

Ohana, O. & Sakmann, B., 1998. Transmitter release modulation in nerve terminals of rat neocortical pyramidal cells by intracellular calcium buffers. *The Journal of Physiology*, 513(1), pp.135–148.

Ohura, S. & Kamiya, H., 2016. Excitability tuning of axons in the central nervous system. *The Journal of Physiological Sciences*, 66(3), pp.189–196.

Oláh, S. et al., 2009. Regulation of cortical microcircuits by unitary GABA-mediated volume transmission. *Nature*, 461(7268), pp.1278–1281.

Overton, P.G. & Clark, D., 1997. Burst firing in midbrain dopaminergic neurons. *Brain Research Reviews*, 25(3), pp.312–334.

Owesson-White, C.A. et al., 2012. Sources contributing to the average extracellular concentration of dopamine in the nucleus accumbens. *Journal of Neurochemistry*, 121(2), pp.252–262.

Pacelli, C. et al., 2015. Elevated Mitochondrial Bioenergetics and Axonal Arborization Size Are Key Contributors to the Vulnerability of Dopamine Neurons. *Current Biology*, 25(18), pp.2349–2360.

Paille, V. et al., 2013. GABAergic circuits control spike-timing-dependent plasticity. *The Journal of neuroscience : the official journal of the Society for Neuroscience*, 33(22), pp.9353–63.

Pakhotin, P. & Bracci, E., 2007. Cholinergic interneurons control the excitatory input to the striatum. *The Journal of neuroscience : the official journal of the Society for Neuroscience*, 27(2), pp.391–400.

Pan, W.-X. et al., 2005. Dopamine Cells Respond to Predicted Events during Classical Conditioning: Evidence for Eligibility Traces in the Reward-Learning Network. *Journal of Neuroscience*, 25(26), pp.6235–6242.

Pancani, T. et al., 2014. M4 mAChR-Mediated Modulation of Glutamatergic Transmission at Corticostriatal Synapses. *ACS Chemical Neuroscience*, 5(4), pp.318–324.

Panin, F. et al., 2012. Coupled intracerebral microdialysis and electrophysiology for the assessment of dopamine neuron function in vivo. *Journal of pharmacological and toxicological methods*, 65(2), pp.83–92.

Pavlov, I. et al., 2009. Outwardly rectifying tonically active GABAA receptors in pyramidal cells modulate neuronal offset, not gain. *The Journal of neuroscience : the official journal of the Society for Neuroscience*, 29(48), pp.15341–50.

Pearce, R.A., 1993. Physiological evidence for two distinct GABAA responses in rat hippocampus. *Neuron*, 10(2), pp.189–200.

Pereira, D.B. et al., 2016. Fluorescent false neurotransmitter reveals functionally silent dopamine vesicle clusters in the striatum. *Nature Neuroscience*, 19(4), pp.578–586.

Perez, M.F., White, F.J. & Hu, X.-T., 2006. Dopamine D2 Receptor Modulation of K+ Channel Activity Regulates Excitability of Nucleus Accumbens Neurons at Different Membrane Potentials. *Journal of Neurophysiology*.

Phillips, P.E.M. et al., 2003. Subsecond dopamine release promotes cocaine seeking. *Nature*, 422(6932), pp.614–8.

Picconi, B. et al., 2003. Loss of bidirectional striatal synaptic plasticity in L-DOPA–induced dyskinesia. *Nature Neuroscience*, 6(5), pp.501–506.

Pieribone, V.A. et al., 1995. Distinct pools of synaptic vesicles in neurotransmitter release. *Nature*, 375(6531), pp.493–497.

Ping, H.X. & Shepard, P.D., 1996. Apamin-sensitive Ca2+-activated K+ channels regulate pacemaker activity in nigral dopamine neurons. *NeuroReport*, 7, pp.809–814.

Pissadaki, E.K. & Bolam, J.P., 2013. The energy cost of action potential propagation in dopamine neurons: clues to susceptibility in Parkinson's disease. *Frontiers in computational neuroscience*, 7, p.13.

Pistis, M. et al., 2004. Adolescent exposure to cannabinoids induces long-lasting changes in the response to drugs of abuse of rat midbrain dopamine neurons. *Biological Psychiatry*, 56(2), pp.86–94.

Pitman, K.A., Puil, E. & Borgland, S.L., 2014. GABA(B) modulation of dopamine release in the nucleus accumbens core. *The European journal of neuroscience*, 40(10), pp.3472–80.

Planert, H. et al., 2013. Membrane Properties of Striatal Direct and Indirect Pathway Neurons in Mouse and Rat Slices and Their Modulation by Dopamine J. T. Brown, ed. *PLoS ONE*, 8(3), p.e57054.

Platt, N.P., 2012. *Investigating the presynaptic control of striatal dopamine release (DPhil Thesis)*. University of Oxford.

Plotkin, J.L., Day, M. & Surmeier, D.J., 2011. Synaptically driven state transitions in distal dendrites of striatal spiny neurons. *Nature Neuroscience*, 14(7), pp.881–888.

Ponce, A. et al., 1996. G-protein-gated inward rectifier K+ channel proteins (GIRK1) are present in the soma and dendrites as well as in nerve terminals of specific neurons in the brain. *The Journal of neuroscience : the official journal of the Society for Neuroscience*, 16(6), pp.1990–2001.

Povlock, S.L. & Schenk, J.O., 2002. A Multisubstrate Kinetic Mechanism of Dopamine Transport in the Nucleus Accumbens and Its Inhibition by Cocaine. *Journal of Neurochemistry*, 69(3), pp.1093–1105.

Prakriya, M. & Mennerick, S., 2000. Selective Depression of Low–Release Probability Excitatory Synapses by Sodium Channel Blockers. *Neuron*, 26(3), pp.671–682.

Prensa, L. & Parent, A., 2001. The Nigrostriatal Pathway in the Rat: A Single-Axon Study of the Relationship between Dorsal and Ventral Tier Nigral Neurons and the Striosome/Matrix Striatal Compartments. *Journal of Neuroscience*, 21(18).

Puopolo, M., Raviola, E. & Bean, B.P., 2007. Roles of subthreshold calcium current and sodium current in spontaneous firing of mouse midbrain dopamine neurons. *The Journal of neuroscience : the official journal of the Society for Neuroscience*, 27(3), pp.645–56.

Rahman, S. & McBride, W.J., 2001. Feedback Control of Mesolimbic Somatodendritic Dopamine Release in Rat Brain. *Journal of Neurochemistry*, 74(2), pp.684–692.

Rama, S. et al., 2017. The role of axonal Kv1 channels in CA3 pyramidal cell excitability. *Scientific reports*, 7(1), p.315.

Ramanathan, S. et al., 2002. Synaptic convergence of motor and somatosensory cortical afferents onto GABAergic interneurons in the rat striatum. *The Journal of neuroscience : the official*

journal of the Society for Neuroscience, 22(18), pp.8158–69.

Redgrave, P., Gurney, K. & Reynolds, J., 2008. What is reinforced by phasic dopamine signals? *Brain Research Reviews*, 58(2), pp.322–339.

Redgrave, P., Vautrelle, N. & Reynolds, J.N.J., 2011. Functional properties of the basal ganglia's re-entrant loop architecture: selection and reinforcement. *Neuroscience*, 198, pp.138–51.

Regehr, W.G., Delaney, K.R. & Tank, D.W., 1994. The role of presynaptic calcium in short-term enhancement at the hippocampal mossy fiber synapse. *The Journal of neuroscience : the official journal of the Society for Neuroscience*, 14(2), pp.523–37.

Rettig, J. & Neher, E., 2002. Emerging roles of presynaptic proteins in Ca++-triggered exocytosis. *Science (New York, N.Y.)*, 298(5594), pp.781–5.

Reynolds, J.N.. & Wickens, J.R., 2002. Dopamine-dependent plasticity of corticostriatal synapses. *Neural Networks*, 15(4–6), pp.507–521.

Reynolds, J.N.J., Hyland, B.I. & Wickens, J.R., 2001. A cellular mechanism of reward-related learning. *Nature*, 413(6851), pp.67–70.

Rhodes, K.J. et al., 1997. Association and Colocalization of the Kvβ1 and Kvβ2 β-Subunits with Kv1 α-Subunits in Mammalian Brain K+Channel Complexes. *Journal of Neuroscience*, 17(21).

Rice, M.E. & Cragg, S.J., 2004. Nicotine amplifies reward-related dopamine signals in striatum. *Nature neuroscience*, 7(6), pp.583–4.

Rice, M.E., Patel, J.C. & Cragg, S.J., 2011. Dopamine release in the basal ganglia. *Neuroscience*, 198, pp.112–137.

Rivera, A. et al., 2002. Molecular phenotype of rat striatal neurons expressing the dopamine D5 receptor subtype. *European Journal of Neuroscience*, 16(11), pp.2049–2058.

Rizzoli, S.O. & Betz, W.J., 2005. Synaptic vesicle pools. *Nature Reviews Neuroscience*, 6(1), pp.57–69.

Roitman, M.F. et al., 2004. Dopamine Operates as a Subsecond Modulator of Food Seeking. *Journal of Neuroscience*, 24(6).

Romo, R. & Schultz, W., 1990. Dopamine neurons of the monkey midbrain: contingencies of responses to active touch during self-initiated arm movements. *Journal of Neurophysiology*, 63(3).

Rooney, K.E. & Wallace, L.J., 2015. Computational modeling of extracellular dopamine kinetics suggests low probability of neurotransmitter release. *Synapse*, 69(11), pp.515–525.

Rowan, M.J.M. et al., 2016. Synapse-Level Determination of Action Potential Duration by K+ Channel Clustering in Axons. *Neuron*, 91(2), pp.370–383.

Rowan, M.J.M., Tranquil, E. & Christie, J.M., 2014. Distinct Kv Channel Subtypes Contribute to Differences in Spike Signaling Properties in the Axon Initial Segment and Presynaptic Boutons of Cerebellar Interneurons. *Journal of Neuroscience*, 34(19), pp.6611–6623.

Rozov, A. et al., 2001. Transmitter release modulation by intracellular Ca2+ buffers in facilitating and depressing nerve terminals of pyramidal cells in layer 2/3 of the rat neocortex indicates a target cell-specific difference in presynaptic calcium dynamics. *The Journal of Physiology*, 531(3), pp.807–826.

Rudy, B. & McBain, C.J., 2001. Kv3 channels: voltage-gated K+ channels designed for high-

frequency repetitive firing. *Trends in Neurosciences*, 24(9), pp.517–526.

Runnels, P.L. et al., 1999. Effect of pH and Surface Functionalities on the Cyclic Voltammetric Responses of Carbon-Fiber Microelectrodes. *Analytical Chemistry*, 71(14), pp.2782–2789.

Sabatini, B.L. & Regehr, W.G., 1997. Control of neurotransmitter release by presynaptic waveform at the granule cell to Purkinje cell synapse. *The Journal of neuroscience : the official journal of the Society for Neuroscience*, 17(10), pp.3425–35.

Sabatini, B.L. & Regehr, W.G., 1996. Timing of neurotransmission at fast synapses in the mammalian brain. *Nature*, 384(6605), pp.170–172.

Salinas, A.G. et al., 2016. Dopamine dynamics and cocaine sensitivity differ between striosome and matrix compartments of the striatum. *Neuropharmacology*, 108, pp.275–283.

Santhakumar, V., Jones, R.T. & Mody, I., 2010. Developmental regulation and neuroprotective effects of striatal tonic GABAA currents. *Neuroscience*, 167(3), pp.644–655.

Sasaki, T., Matsuki, N. & Ikegaya, Y., 2012. Targeted axon-attached recording with fluorescent patch-clamp pipettes in brain slices. *Nature Protocols*, 7(6), pp.1228–1234.

Saunders, A., Huang, K.W. & Sabatini, B.L., 2016. Globus Pallidus Externus Neurons Expressing Parvalbumin Interconnect the Subthalamic Nucleus and Striatal Interneurons D. I. Finkelstein, ed. *PLOS ONE*, 11(2), p.e0149798.

Saviane, C., Mohajerani, M.H. & Cherubini, E., 2003. An ID-like current that is downregulated by Ca2+ modulates information coding at CA3-CA3 synapses in the rat hippocampus. *The Journal of physiology*, 552(Pt 2), pp.513–24.

Saxena, N.C. & Macdonald, R.L., 1994. Assembly of GABAA receptor subunits: role of the delta subunit. *The Journal of neuroscience : the official journal of the Society for Neuroscience*, 14(11 Pt 2), pp.7077–86.

Schiemann, J. et al., 2012. K-ATP channels in dopamine substantia nigra neurons control bursting and novelty-induced exploration. *Nature Neuroscience*, 15(9), pp.1272–1280.

Schlösser, B. et al., 1995. δ, μ, and κ opioid receptor agonists inhibit dopamine overflow in rat neostriatal slices. *Neuroscience Letters*, 191(1–2), pp.126–130.

Schmitz, Y., Schmauss, C. & Sulzer, D., 2002. Altered dopamine release and uptake kinetics in mice lacking D2 receptors. *The Journal of neuroscience : the official journal of the Society for Neuroscience*, 22(18), pp.8002–9.

Schneggenburger, R. & Neher, E., 2000. Intracellular calcium dependence of transmitter release rates at a fastcentral synapse. *Nature*, 406(6798), pp.889–893.

Schultz, W., 2016. Dopamine reward prediction-error signalling: a two-component response. *Nature Reviews Neuroscience*, 17(3), pp.183–195.

Schultz, W., 1986. Responses of midbrain dopamine neurons to behavioral trigger stimuli in the monkey. *Journal of neurophysiology*, 56(5), pp.1439–61.

Schultz, W., Dayan, P. & Montague, P.R., 1997. A Neural Substrate of Prediction and Reward. *Science*, 275(5306).

Schultz, W. & Romo, R., 1990. Dopamine neurons of the monkey midbrain: contingencies of responses to stimuli eliciting immediate behavioral reactions. *Journal of Neurophysiology*, 63(3).

Schultz, W., Ruffieux, A. & Aebischer, P., 1983. The activity of pars compacta neurons of the monkey substantia nigra in relation to motor activation. *Experimental Brain Research*, 51(3), pp.377–387.

Schulz, J.M. & Reynolds, J.N.J., 2013. Pause and rebound: sensory control of cholinergic signaling in the striatum. *Trends in neurosciences*, 36(1), pp.41–50.

Seal, R. & Edwards, R., 2006. Functional implications of neurotransmitter co-release: glutamate and GABA share the load. *Current Opinion in Pharmacology*, 6(1), pp.114–119.

Seutin, V. et al., 2001. Evidence for a modulatory role of I(h) on the firing of a subgroup of midbrain dopamine neurons. *NeuroReport*, 12(12), pp.959–4965.

Sgobio, C. et al., 2017. Aldehyde dehydrogenase 1–positive nigrostriatal dopaminergic fibers exhibit distinct projection pattern and dopamine release dynamics at mouse dorsal striatum. *Scientific Reports*, 7(1), p.5283.

Sheng, M. et al., 1994. Contrasting Subcellular Localization of the Kv1.2 K+ Channel Subunit in Different Neurons of Rat Brain. *The Journal of Neuroscience*, 74(4), pp.2408–2417.

Sheng, M. et al., 1992. Subcellular segregation of two A-type K+ channel proteins in rat central neurons. *Neuron*, 9(2), pp.271–284.

Sherman, A.J., Shrier, A. & Cooper, E., 1999. Series Resistance Compensation for Whole-Cell Patch-Clamp Studies Using a Membrane State Estimator. *Biophysical Journal*, 77(5), pp.2590–2601.

Shin, J.H. et al., 2015. Muscarinic regulation of dopamine and glutamate transmission in the nucleus accumbens. *Proceedings of the National Academy of Sciences of the United States of America*, 112(26), pp.8124–9.

Shu, Y. et al., 2007. Selective control of cortical axonal spikes by a slowly inactivating K+ current. *Proceedings of the National Academy of Sciences of the United States of America*, 104(27), pp.11453–8.

Sigworth, F.J., 1995. Electronic Design of the Patch Clamp. In B. Sakmann & E. Neher, eds. *Single-Channel Recording*. Boston, MA: Springer US, pp. 95–127.

Smith, D.O., 1980. Mechanisms of action potential propagation failure at sites of axon branching in the crayfish. *The Journal of physiology*, 301, pp.243–59.

Smith, I.D. & Grace, A.A., 1992. Role of the subthalamic nucleus in the regulation of nigral dopamine neuron activity. *Synapse*, 12(4), pp.287–303.

Smith, Y. et al., 1994. Synaptic relationships between dopaminergic afferents and cortical or thalamic input in the sensorimotor territory of the striatum in monkey. *The Journal of Comparative Neurology*, 344(1), pp.1–19.

Smith, Y. et al., 2004. The thalamostriatal system: a highly specific network of the basal ganglia circuitry. *Trends in Neurosciences*, 27(9), pp.520–527.

Sombers, L.A. et al., 2009. Synaptic overflow of dopamine in the nucleus accumbens arises from neuronal activity in the ventral tegmental area. *The Journal of neuroscience : the official journal of the Society for Neuroscience*, 29(6), pp.1735–42.

Somogyi, P., Bolam, J.P. & Smith, A.D., 1981. Monosynaptic cortical input and local axon collaterals of identified striatonigral neurons. A light and electron microscopic study using the golgi-peroxidase transport-degeneration procedure. *The Journal of Comparative*

Neurology, 195(4), pp.567–584.

Sonders, M.S. et al., 1997. Multiple Ionic Conductances of the Human Dopamine Transporter: The Actions of Dopamine and Psychostimulants. *J. Neurosci.*, 17(3), pp.960–974.

Song, C. et al., 2017. Transgenic Strategies for Sparse but Strong Expression of Genetically Encoded Voltage and Calcium Indicators. *International Journal of Molecular Sciences*, 18(7), p.1461.

Specht, C.G. & Schoepfer, R., 2001. Deletion of the alpha-synuclein locus in a subpopulation of C57BL/6J inbred mice. *BMC Neuroscience*, 2(1), p.11.

Stamford, J.A., Kruk, Z.L. & Millar, J., 1989. Dissociation of the actions of uptake blockers upon dopamine overflow and uptake in the rat nucleus accumbens: In vivo voltammetric data. *Neuropharmacology*, 28(12), pp.1383–1388.

Steinberg, E.E. et al., 2013. A causal link between prediction errors, dopamine neurons and learning. *Nature neuroscience*, 16(7), pp.966–73.

Stensrud, M.J. et al., 2013. Vesicular glutamate transporter-3 in the rodent brain: vesicular colocalization with vesicular γ-aminobutyric acid transporter. *The Journal of comparative neurology*, 521(13), pp.3042–56.

Stensrud, M.J., Puchades, M. & Gundersen, V., 2014. GABA is localized in dopaminergic synaptic vesicles in the rodent striatum. *Brain structure & function*, 219(6), pp.1901–12.

Stoof, J.C., Verheijden, P.F.H.M. & Leysen, J.E., 1987. Stimulation of D2-receptors in rat nucleus accumbens slices inhibits dopamine and acetylcholine release but not cyclic AMP formation. *Brain Research*, 423(1–2), pp.364–368.

Stopper, C.M. et al., 2014. Overriding Phasic Dopamine Signals Redirects Action Selection during Risk/Reward Decision Making. *Neuron*, 84(1), pp.177–189.

Storm, J.F., 1990. Potassium currents in hippocampal pyramidal cells. *Progress in brain research*, 83, pp.161–87.

Strata, P. & Harvey, R., 1999. Dale's principle. *Brain Research Bulletin*, 50(5), pp.349–350.

Straub, C. et al., 2014. Multiphasic modulation of cholinergic interneurons by nigrostriatal afferents. *The Journal of neuroscience : the official journal of the Society for Neuroscience*, 34(25), pp.8557–69.

Stuber, G.D. et al., 2010. Dopaminergic Terminals in the Nucleus Accumbens But Not the Dorsal Striatum Corelease Glutamate. *Journal of Neuroscience*, 30(24), pp.8229–8233.

Stuber, G.D. et al., 2008. Reward-Predictive Cues Enhance Excitatory Synaptic Strength onto Midbrain Dopamine Neurons. *Science*, 321(5896).

Suaud-Chagny, M.F. et al., 1992. Relationship between dopamine release in the rat nucleus accumbens and the discharge activity of dopaminergic neurons during local in vivo application of amino acids in the ventral tegmental area. *Neuroscience*, 49(1), pp.63–72.

Sudhof, T.C., 2012. Calcium Control of Neurotransmitter Release. *Cold Spring Harbor Perspectives in Biology*, 4(1), pp.a011353–a011353.

Sulzer, D., Cragg, S.J. & Rice, M.E., 2016. Striatal dopamine neurotransmission: Regulation of release and uptake. *Basal Ganglia*, 6(3), pp.123–148.

Surmeier, D.J. et al., 1992. Dopamine receptor subtypes colocalize in rat striatonigral neurons.

Proceedings of the National Academy of Sciences of the United States of America, 89(21), pp.10178–82.

Surmeier, D.J., Mercer, J.N. & Chan, C.S., 2005. Autonomous pacemakers in the basal ganglia: who needs excitatory synapses anyway? *Current Opinion in Neurobiology*, 15(3), pp.312–318.

Surmeier, D.J., Song, W.J. & Yan, Z., 1996. Coordinated expression of dopamine receptors in neostriatal medium spiny neurons. *The Journal of neuroscience : the official journal of the Society for Neuroscience*, 16(20), pp.6579–91.

Swadlow, H.A., Kocsis, J.D. & Waxman, S.G., 1980. Modulation of Impulse Conduction Along the Axonal Tree. *Annual Review of Biophysics and Bioengineering*, 9(1), pp.143–179.

Szabadics, J., Tamás, G. & Soltesz, I., 2007. Different transmitter transients underlie presynaptic cell type specificity of GABAA,slow and GABAA,fast. *Proceedings of the National Academy of Sciences of the United States of America*, 104(37), pp.14831–6.

Tan, K.R. et al., 2012. GABA Neurons of the VTA Drive Conditioned Place Aversion. *Neuron*, 73(6), pp.1173–1183.

Tanaka, T. et al., 1995. *The role of ATP-sensitive potassium channels in striatal dopamine release: An in vivo microdialysis study*,

Tecuapetla, F. et al., 2010. Glutamatergic signaling by mesolimbic dopamine neurons in the nucleus accumbens. *The Journal of neuroscience : the official journal of the Society for Neuroscience*, 30(20), pp.7105–10.

Tepper, J., Sawyer, S. & Groves, P., 1987. Electrophysiologically identified nigral dopaminergic neurons intracellularly labeled with HRP: light-microscopic analysis. *Journal of Neuroscience*, 7(9).

Tepper, J.M. & Bolam, J.P., 2004. Functional diversity and specificity of neostriatal interneurons. *Current opinion in neurobiology*, 14(6), pp.685–92.

Tepper, J.M. & Koós, T., 1999. Inhibitory control of neostriatal projection neurons by GABAergic interneurons. *Nature Neuroscience*, 2(5), pp.467–472.

Thivierge, J.-P., Rivest, F. & Monchi, O., 2007. Spiking neurons, dopamine, and plasticity: Timing is everything, but concentration also matters. *Synapse*, 61(6), pp.375–390.

Thomson, A.M., 2000. Molecular frequency filters at central synapses. *Progress in Neurobiology*, 62(2), pp.159–196.

Threlfell, S. et al., 2012. Striatal dopamine release is triggered by synchronized activity in cholinergic interneurons. *Neuron*, 75(1), pp.58–64.

Threlfell, S. et al., 2010. Striatal muscarinic receptors promote activity dependence of dopamine transmission via distinct receptor subtypes on cholinergic interneurons in ventral versus dorsal striatum. *The Journal of neuroscience : the official journal of the Society for Neuroscience*, 30(9), pp.3398–408.

Threlfell, S. & Cragg, S.J., 2011. Dopamine signaling in dorsal versus ventral striatum: the dynamic role of cholinergic interneurons. *Frontiers in systems neuroscience*, 5, p.11.

Tobler, P.N., Fiorillo, C.D. & Schultz, W., 2005. Adaptive coding of reward value by dopamine neurons. *Science (New York, N.Y.)*, 307(5715), pp.1642–5.

Tong, Z.-Y., Overton, P.G. & Clark, D., 1996. Stimulation of the prefrontal cortex in the rat induces

patterns of activity in midbrain dopaminergic neurons which resemble natural burst events. *Synapse*, 22(3), pp.195–208.

Trimmer, J.S. et al., 2015. Subcellular localization of K+ channels in mammalian brain neurons: remarkable precision in the midst of extraordinary complexity. *Neuron*, 85(2), pp.238–56.

Tritsch, N.X. et al., 2014. Midbrain dopamine neurons sustain inhibitory transmission using plasma membrane uptake of GABA, not synthesis. *eLife*, 3, p.e01936.

Tritsch, N.X., Ding, J.B. & Sabatini, B.L., 2012. Dopaminergic neurons inhibit striatal output through non-canonical release of GABA. *Nature*, 490(7419), pp.262–6.

Tritsch, N.X., Granger, A.J. & Sabatini, B.L., 2016. Mechanisms and functions of GABA co-release. *Nature reviews. Neuroscience*, 17(3), pp.139–45.

Tritsch, N.X. & Sabatini, B.L., 2012. Dopaminergic modulation of synaptic transmission in cortex and striatum. *Neuron*, 76(1), pp.33–50.

Tsai, H.-C. et al., 2009. Phasic Firing in Dopaminergic Neurons Is Sufficient for Behavioral Conditioning. *Science*, 324(5930).

Tunstall, M.J. et al., 2002. Inhibitory Interactions Between Spiny Projection Neurons in the Rat Striatum. *Journal of Neurophysiology*, 88(3).

Turrigiano, G., 2012. Homeostatic synaptic plasticity: local and global mechanisms for stabilizing neuronal function. *Cold Spring Harbor perspectives in biology*, 4(1), p.a005736.

Ungerstedt, U., 1971. Stereotaxic Mapping of the Monoamine Pathways in the Rat Brain. *Acta Physiologica Scandinavica*, 82(S367), pp.1–48.

Ungless, M.A., Magill, P.J. & Bolam, J.P., 2004. Uniform Inhibition of Dopamine Neurons in the Ventral Tegmental Area by Aversive Stimuli. *Science*, 303(5666).

Usiello, A. et al., 2000. Distinct functions of the two isoforms of dopamine D2 receptors. *Nature*, 408(6809), pp.199–203.

Vaaga, C.E., Borisovska, M. & Westbrook, G.L., 2014. Dual-transmitter neurons: functional implications of co-release and co-transmission. *Current Opinion in Neurobiology*, 29, pp.25–32.

Vaarmann, A. et al., 2010. Novel pathway for an old neurotransmitter: Dopamine-induced neuronal calcium signalling via receptor-independent mechanisms. *Cell Calcium*, 48(2–3), pp.176–182.

Valtcheva, S. et al., 2017. Developmental control of spike-timing-dependent plasticity by tonic GABAergic signaling in striatum. *Neuropharmacology*, 121, pp.261–277.

Venton, B.J. et al., 2006. Cocaine Increases Dopamine Release by Mobilization of a Synapsin-Dependent Reserve Pool. *Journal of Neuroscience*, 26(12), pp.3206–3209.

Vergara, R. et al., 2003. Spontaneous voltage oscillations in striatal projection neurons in a rat corticostriatal slice. *The Journal of physiology*, 553(Pt 1), pp.169–82.

Vilaro, M.T., Palacios, J.M. & Mengod, G., 1990. Localization of m5 muscarinic receptor mRNA in rat brain examined by in situ hybridization histochemistry. *Neuroscience Letters*, 114(2), pp.154–159.

Voorn, P. et al., 2004. Putting a spin on the dorsal–ventral divide of the striatum. *Trends in Neurosciences*, 27(8), pp.468–474.

Wall, N.R. et al., 2013. Differential Innervation of Direct- and Indirect-Pathway Striatal Projection Neurons. *Neuron*, 79(2), pp.347–360.

Wallner, M., Hanchar, H.J. & Olsen, R.W., 2003. Ethanol enhances alpha 4 beta 3 delta and alpha 6 beta 3 delta gamma-aminobutyric acid type A receptors at low concentrations known to affect humans. *Proceedings of the National Academy of Sciences of the United States of America*, 100(25), pp.15218–23.

Wang, L. et al., 2014. Modulation of dopamine release in the striatum by physiologically relevant levels of nicotine. *Nature communications*, 5, p.3925.

Wang, Z. et al., 2006. Dopaminergic control of corticostriatal long-term synaptic depression in medium spiny neurons is mediated by cholinergic interneurons. *Neuron*, 50(3), pp.443–52.

Watabe-Uchida, M. et al., 2012. Whole-Brain Mapping of Direct Inputs to Midbrain Dopamine Neurons. *Neuron*, 74(5), pp.858–873.

Weiner, D.M., Levey, A.I. & Brann, M.R., 1990. Expression of muscarinic acetylcholine and dopamine receptor mRNAs in rat basal ganglia. *Proceedings of the National Academy of Sciences of the United States of America*, 87(18), pp.7050–4.

Wichmann, T. & Delong, M.R., 2007. Anatomy and physiology of the basal ganglia: relevance to Parkinson's disease and related disorders. *Handbook of clinical neurology*, 83, pp.1–18.

Wilson, C. & Kawaguchi, Y., 1996. The origins of two-state spontaneous membrane potential fluctuations of neostriatal spiny neurons. *Journal of Neuroscience*, 16(7).

Wilson, C.J., 1995. Dynamic modification of dendritic cable properties and synaptic transmission by voltage-gated potassium channels. *Journal of Computational Neuroscience*, 2(2), pp.91–115.

Wilson, C.J. & Groves, P.M., 1981. *Spontaneous firing patterns of identified spiny neurons in the rat neostriatum*,

Wlodarczyk, A.I. et al., 2013. Tonic GABAA conductance decreases membrane time constant and increases EPSP-spike precision in hippocampal pyramidal neurons. *Frontiers in Neural Circuits*, 7, p.205.

Wolfart, J. et al., 2001. Differential Expression of the Small-Conductance, Calcium-Activated Potassium Channel SK3 Is Critical for Pacemaker Control in Dopaminergic Midbrain Neurons. *Journal of Neuroscience*, 21(10).

Wu, L. & Saggau, P., 1994. Presynaptic calcium is increased during normal synaptic transmission and paired-pulse facilitation, but not in long-term potentiation in area CA1 of hippocampus. *Journal of Neuroscience*, 14(2).

Wulff, H. & Zhorov, B.S., 2008. K+ Channel Modulators for the Treatment of Neurological Disorders and Autoimmune Diseases. *Chemical Reviews*, 108(5), pp.1744–1773.

Wykes, R.C.E. et al., 2007. Differential Regulation of Endogenous N- and P/Q-Type Ca2+ Channel Inactivation by Ca2+/Calmodulin Impacts on Their Ability to Support Exocytosis in Chromaffin Cells. *Journal of Neuroscience*, 27(19), pp.5236–5248.

Xia, Y. et al., 2011. Nucleus Accumbens Medium Spiny Neurons Target Non-Dopaminergic Neurons in the Ventral Tegmental Area. *Journal of Neuroscience*, 31(21).

Xu, J., Mashimo, T. & Südhof, T.C., 2007. Synaptotagmin-1, -2, and -9: Ca(2+) sensors for fast release that specify distinct presynaptic properties in subsets of neurons. *Neuron*, 54(4),

pp.567–81.

Xu, J. & Wu, L.-G., 2005. The decrease in the presynaptic calcium current is a major cause of short-term depression at a calyx-type synapse. *Neuron*, 46(4), pp.633–45.

Xu, X. et al., 2016. Competitive antagonists facilitate the recovery from desensitization of α1β2γ2 GABAA receptors expressed in Xenopus oocytes. *Acta Pharmacologica Sinica*, 37(8), pp.1020–1030.

Xu, Z.C., Wilson, C.J. & Emson, P.C., 1989. Restoration of the corticostriatal projection in rat neostriatal grafts: electron microscopic analysis. *Neuroscience*, 29(3), pp.539–50.

Yamada, T. et al., 1990. Relative sparing in Parkinson's disease of substantia nigra dopamine neurons containing calbindin-D28K. *Brain Research*, 526(2), pp.303–307.

Yan, Z. et al., 1997. D2 dopamine receptors reduce N-type Ca2+ currents in rat neostriatal cholinergic interneurons through a membrane-delimited, protein-kinase-C-insensitive pathway. *Journal of neurophysiology*, 77(2), pp.1003–15.

Yan, Z. & Surmeier, D.J., 1997. D5 Dopamine Receptors Enhance Zn2+-Sensitive GABAA Currents in Striatal Cholinergic Interneurons through a PKA/PP1 Cascade. *Neuron*, 19(5), pp.1115–1126.

Yang, J. et al., 2013. Dopaminergic modulation of axonal potassium channels and action potential waveform in pyramidal neurons of prefrontal cortex. *The Journal of physiology*, 591(13), pp.3233–51.

Yeomans, J.S., Maidment, N.T. & Bunney, B.S., 1988. Excitability properties of medial forebrain bundle axons of A9 and A10 dopamine cells. *Brain Research*, 450(1), pp.86–93.

Yetnikoff, L. et al., 2014. An update on the connections of the ventral mesencephalic dopaminergic complex. *Neuroscience*, 282C, pp.23–48.

Yim, M.Y. et al., 2011. Significance of Input Correlations in Striatal Function O. Sporns, ed. *PLoS Computational Biology*, 7(11), p.e1002254.

Yin, H.H. et al., 2009. Dynamic reorganization of striatal circuits during the acquisition and consolidation of a skill. *Nature neuroscience*, 12(3), pp.333–41.

Yorgason, J.T., Zeppenfeld, D.M. & Williams, J.T., 2017. Cholinergic Interneurons Underlie Spontaneous Dopamine Release in Nucleus Accumbens. *The Journal of neuroscience : the official journal of the Society for Neuroscience*, 37(8), pp.2086–2096.

Zaltieri, M. et al., 2015. α-synuclein and synapsin III cooperatively regulate synaptic function in dopamine neurons. *Journal of cell science*, 128(13), pp.2231–43.

van Zessen, R. et al., 2012. Activation of VTA GABA Neurons Disrupts Reward Consumption. *Neuron*, 73(6), pp.1184–1194.

Zhang, D. et al., 2008. Oscillatory firing of dopamine neurons: Differences between cells in the substantia nigra and ventral tegmental area. *Synapse*, 62(3), pp.169–175.

Zhang, F. et al., 2011. The Microbial Opsin Family of Optogenetic Tools. *Cell*, 147(7), pp.1446–1457.

Zhang, H. & Sulzer, D., 2004. Frequency-dependent modulation of dopamine release by nicotine. *Nature neuroscience*, 7(6), pp.581–2.

Zhang, L. et al., 2009. Controls of Tonic and Phasic Dopamine Transmission in the Dorsal and

Ventral Striatum. *Molecular Pharmacology*, 76(2).

Zhang, L., Liu, Y. & Chen, X., 2005. Carbachol induces burst firing of dopamine cells in the ventral tegmental area by promoting calcium entry through L-type channels in the rat. *The Journal of Physiology*, 568(2), pp.469–481.

Zhang, S. et al., 2015. Dopaminergic and glutamatergic microdomains in a subset of rodent mesoaccumbens axons. *Nature neuroscience*, 18(3), pp.386–92.

Zheng, T. & Wilson, C.J., 2002. Corticostriatal Combinatorics: The Implications of Corticostriatal Axonal Arborizations. *Journal of Neurophysiology*, 87(2).

Zhou, F.-M., Liang, Y. & Dani, J.A., 2001. Endogenous nicotinic cholinergic activity regulates dopamine release in the striatum. *Nature neuroscience*, 4(12), pp.1224–1229.

Zucker, R.S. & Regehr, W.G., 2002. Short-term synaptic plasticity. *Annual review of physiology*, 64, pp.355–405.

Zweifel, L.S. et al., 2009. Disruption of NMDAR-dependent burst firing by dopamine neurons provides selective assessment of phasic dopamine-dependent behavior. *Proceedings of the National Academy of Sciences of the United States of America*, 106(18), pp.7281–8.